AD-A152 237 A MULTIPOLE MODEL OF THE OBSERVED CEREBRAL CORTEX MAGNETIC FIELD(U) AIR FORCE INST OF TECH WRIGHT-PATTERSON AFB OH SCHOOL OF ENGINEERING 1/2

UNCLASSIFIED P J DE REGO DEC 84 AFIT/GE/ENG/84D-23 F/G 6/16 NL

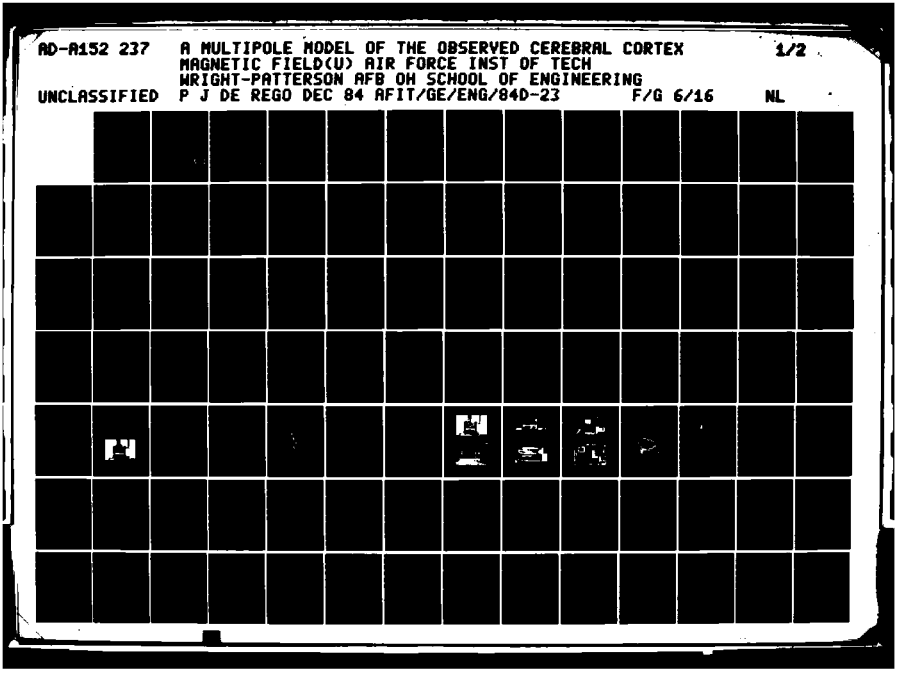

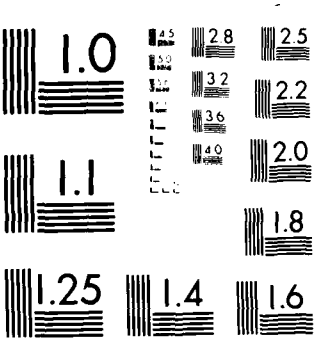

A MULTIPOLE MODEL OF THE OBSERVED CEREBRAL CORTEX MAGNETIC FIELD

THESIS

Paul J. De Rego
First Lieutenant, USAF

AFIT/GE/ENG/84D-23

DEPARTMENT OF THE AIR FORCE
AIR UNIVERSITY
AIR FORCE INSTITUTE OF TECHNOLOGY

Wright-Patterson Air Force Base, Ohio

AFIT/GE/ENG/84D-23

A MULTIPOLE MODEL OF THE OBSERVED CEREBRAL CORTEX MAGNETIC FIELD

THESIS

Paul J. De Rego
First Lieutenant, USAF

AFIT/GE/ENG/84D-23

AFIT/GE/ENG/84D-23

A MULTIPOLE MODEL OF THE OBSERVED CEREBRAL CORTEX MAGNETIC FIELD

THESIS

Presented to the Faculty of the School of Engineering
of the Air Force Institute of Technology
Air University
In Partial Fulfillment of the
Requirements for the Degree of
Master of Science in Electrical Engineering

Paul J. De Rego, B.S.
First Lieutenant, USAF

December 1984

Preface

The study described in this thesis was stimulated by the need for a working multipolar model of brain activity. Many investigators are presently studying the magnetic fields emmitted by cerebral cortex sources, but few of these studies are aimed at modeling the observed field. My strong interest in biological systems of communication, computation, and control has led me to study both biological system operation and modern estimation and control techniques.

A degree of uncertainty, caused by inaccurate measurements, random occurances, and vague descriptions will naturally corrupt any attempt to estimate biological states. Fortunately, these uncertainties may be reduced through deterministic, stochastic, and fuzzy variable methods respectively. A priliminary step required before the estimation of any real world event is the development of proper models. Although these concepts have been refined in applications of flight control, interplanetary navigation, etc, models of our own cerebral cortex are still in their infancy. This thesis study was therefore oriented to expand our knowledge in properly modeling the observed activity of the brain.

The model developed considers two or three dipoles located in a conducting sphere. Since both a software model and an actual conducting sphere experiment were desired, time allowed only five dipole combinations to be investigated. Although the study was limited to only a few

cases, the results are of significant value and an expansion of the model should definitely be considered.

The task of completing the software and experimentation could not have been accomplished without the help of others. Enormous credit must go to my faculty advisor, Dr. Matthew Kabrisky, for his continual support in keeping the project moving in the right direction. Special thanks must also go to Dr. Charles Hatsell, whose knowledge and deep interest in this study helped me hurdle every threatening barrier. The list of credits would certainly be incomplete without thanking each person in the HEG laboratory and the AMRL computer center for providing the most pleasant working environment and contributing to the project without hesitation.

I am most grateful for the continuous and unbounded moral support given to me by my mother, father, and entire family. Special thanks must also be given to my roommate and dear friend William Kahea Aiu for his moral strength, home grown hospitality, and "ono" cooking that made the endurance of the AFIT program and thesis project possible.

As true with all my work, this project is dedicated to the Father, Son, and Holy Spirit who I am eternally grateful for His support and guidance in helping me fulfill His will.

Aloha ke Akua,

Paul J. De Rego

Table of Contents

List of Figures

Abstract

A Multipole model of magnetic field sources in the cerebral cortex was developed as an expansion of Grynszpan's single dipole in a conducting sphere model. Both computer simulation and actual conducting sphere experiments were used to generate field plots in five separate dipole configurations. These include one case of a single dipole, three cases of three dipoles on a single radial, and one case of two dipoles on independent radials.

The results show that dipoles oriented on a single radial do not produce multiple flux peaks, but rather a twisted version of the single dipole field. Sufficiently distant dipoles on independent radials, however, do produce multiple peaks. The largest field distortions occurred when nonconducting masses were in close proximity to the active dipoles.

I. Introduction

The human central nervous system (CNS) is probably the most complex operating network known to man, capable of manufacturing its own environment and even evaluating its own sensory perception. Besides higher intellect, man displays the ability to consciously control precise muscle movements, a quality also shared with other animals. In mammals, the structure responsible for such movements is the cerebral cortex. Fortunately, the cortex can be effectively studied because of its highly organized nature and the close correspondence of its basic elements to evolutionary precursors. This characteristic behavior of both simple and complex biological systems has contributed greatly in understanding at least some aspects of the organic computing process. Here, a review of fundamental neurology would prove advantageous in the interest of developing a useful model of the observed electro-magnetic activity.

Basic Electrophysiology (1,2:104-120)

The basic active element of the nervous system is the neuron, or nerve cell. Unlike other cells in the body, the neuron has the ability to output a sizeable electrical pulse in response to multiple inputs. The output pulse, called an action potential (AP), is the result of an electro-chemical process. Although the neuron is a very special cell, its operation stems from basic electrophysiology found in all cells of the body.

Over the millions of years of evolution, Earth creatures, including the human animal, have retained a fundamental foundation of a cell immersed in salt water. The primary ions of interest are Sodium (Na+), Chloride (Cl-), and Potassium (K+). A cell's semi-permeable membrane allows a restricted flow of these ions from the inside of the cell to the outside, and vice versa. The result is a controlled potential difference across the cell's membrane, the foundation for sustained electrical activity. Figure I-1 depicts the relative concentrations of Na+, Cl-, and K+ with respect to a neuron.

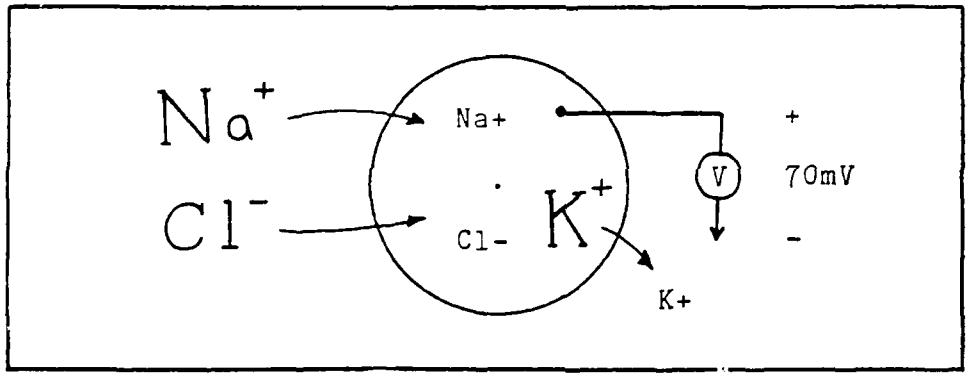

Figure I-1. Relative Concentrations of Intra and Extra Cellular Ions. The large symbols represent a high concentration and the arrows represent diffusion.

Communication from neurons to other neurons, muscle fibers, or glands is primarily accomplished via action potentials (AP). With the application of sufficient stimulus, an affected section of membrane experiences a sudden rise of Na+ permeability. The rapid influx of Na+ results in a localized breakdown of membrane potential called

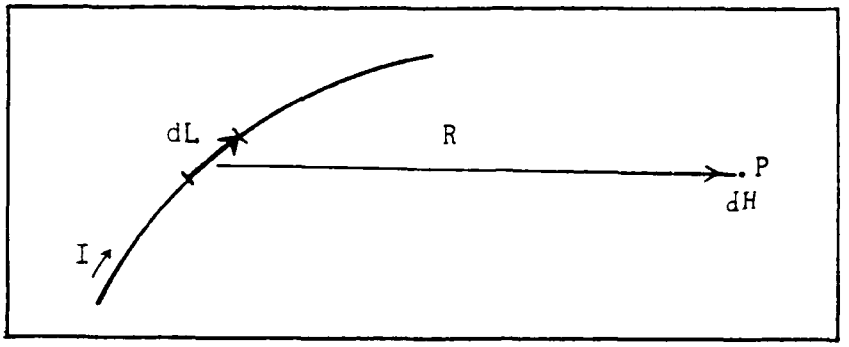

Figure II-1. The Biot-Savart Law (5:233).

The magnetic field intensity is derived by considering the generated force per current element along the path length. The conducting length dL with a current I has a "current moment" given by: IdL = current x length = current moment. The Magnetic Flux Density B is defined as the force per current moment (14:146): B = dF/IdL. The magnetic flux density thus has the units of newton per ampere-meter. These units are equivalent to the units weber per meter squared, 10,000 gauss, or the International System of units, Tesla (5:260).

The magnetic flux density conceptually refers to the number of magnetic flux lines passing through a unit area. It is related to the magnetic field intensity through the properties of the medium involved (7:29):

II. Field Measurement Theory

Basic Electromagnetics

The theory relating to magnetic fields generated by current flow is based upon the Biot-Savart law. As noted in the introduction, this law states that at any measuring point, the magnitude of the magnetic field intensity is proportional to the dipole current, length, and the angle between the dipole and the measuring point (5:232). To avoid any generalities, the exact law should include differential dipole lengths and vector parameters. Equation (1) describes the magnetic field intensity generated by a differential dipole length:

$$dH = \frac{IdL \times a}{4\pi R^2} \tag{1}$$

where

dH = infinitesimal magnetic field intensity
dL = infinitesimal path length
I = current
a = unit vector from path to measuring point
R = distance between path and measuring point

("x" denotes the vector cross product)

Figure II-1 depicts how the differential length of equation (1) contributes to the magnetic field intensity measured at point P. Integration of dH along the entire current path yields the generated field.

The remaining five chapters of this report will cover existing magnetic field measurement theory, the multipole model developement, experimental procedure, discussion, and conclusions.

Chapter II includes some basic electromagnetics and fundamentals in SQUID technology.

In chapter III a multipole model is developed as a direct extension of Grynszpan's single dipole model. The method of using meridians and parallels to navigate the sphere is also explained, as well as the software used to develop magnetic contour maps.

Chapter IV is a detailed discription of the experimental equipment and procedure. This includes the particular 2nd order SQUID gradiometer used, the gimbaled sphere mount, support equipment, and the procedure of collecting data.

The results are presented in chapter V. A comparison is made between the theoretical and the experimental plots.

The discussion is given in chapter VI. A suggestion of how an array of such dipole stacks can be used as an estimator is also presented. Finally, the conclusion will include an overview of the project and some recommendations for continuing studies.

Scope And General Assumptions

The multipole model developed consists of three current dipoles within a saline filled pyrex sphere. Three primary assumptions exist in this model. First, the skull is assumed to closely resemble a non-conducting spherical shell. Secondly, this spherical shell contains a homogeneous conducting fluid. And thirdly, the source of interest consists of a tight group of localized dipoles. The first two assumptions eliminate the complexity associated with the true shape and consistency of the head. Although the head is not perfectly spherical, many investigators accept the spherical model as reasonable for most areas of interest (10:27). The inhomogeneties of the midbrain, cerebral cortex, cerebral spinal fluid, meninges, skull, etc, will distort and attenuate the detected field. Reputable investigators, however, claim that these effects do not seriously disrupt source localization (10:27).

Once a source is localized, a multipole model can be adjusted to best represent the distortions found in the observed field. Two cases are investigated. In the first, the dipoles comprise a single stack alligned on a radial and are oriented in variable directions perpendicular to the radial. The second case considers tangential dipoles lying on different radials. A comparison will be made between computer generated isofield maps and actual isofield maps detected by a second order SQUID gradiometer.

application of the effecting stimulus. The model developed in this thesis, however, represents an isolated source of cortical activity. Whereas averaging is currently necessary in actual brain studies, it will not be necessary in a model with deterministic inputs.

The problem statement motivating the model will be discussed next and a detailed description of the theory and model developement will follow in subsequent chapters.

Problem Statement

Many researchers of today who are studying the characteristics of evoked responses in the cerebral cortex isolate the source of activity by assuming a model of a single current dipole. The dipole is located between the positive and negative flux density peaks and at an easily determined depth and orientation (7:130-131). However, the observed two dimensional isofield maps resemble distorted dipole fields and usually exhibit several flux density peaks. The departure from circular fields indicates various boundary conditions and together with multiple peaks suggests that more than just one dipole should model the isolated source. In 1983, Katila and Karp published a multipole expansion of cardiac magnetic fields seeking to find the "simplest description of an equivalent source that accounts for the observed field pattern" (7:252-254). This thesis will apply a similar thought process in modeling the observed field of isolated cerebral cortex sources.

locked responses, a technique also used on EEG and MEG data to eliminate noise and localize dipole sources.

Each of the three data aquisition methods mentioned have advantages and disadvantages, and in the interest of studying the human cerebral cortex, these qualities must be evaluated. The microelectrode histograms can be eliminated immediately since real time analysis is impossible and sticking electrodes into the cortex of human subjects is out of the question. Although the pros and cons between magneto-encephalography and electro-encephalography deserve more attention, the particular application of this thesis favor the MEG's advantages over those of the EEG. Basicly, the four deciding characteristics are:

(1) The SQUID gradiometer detects only field components of sources close to the sensor (9:230).

(2) The predominant fields sensed are due to the intracellular currents with little effect from the extracellular volume currents (9:237).

(3) The magnetic field is not affected by insulating layers, which minimizes the effects of the non-computing meninges, skull, and skin.

(4) The MEG is a non-invasive method of obtaining brain waves without the added complexity of reference electrodes.

From this point forward, reference to data aquisition will be in terms of magneto-encephalography.

The best known method of determining the location of a dipole source and observing its activity is through averaging. Because of the physical characteristics of chemical transmitters and propagating action potentials, at least some neural responses are time-locked to the

The recording of continuous magnetic fields above the surface of the head is termed magneto-encephalography (MEG). Since the first known MEG recording by David Cohen in 1967 at the Massachusetts Institute of Technology (6:784-786), the magneto-encephalography technique has been substantially improved. The present day MEG is obtained using a Superconducting Quantum Interference Device, commonly referred to as a SQUID. In the interest of eliminating distant noises of large magnitude, contemporary SQUIDs are constructed as first and second order gradiometers. The multiloop gradiometer operating at approximately 4.2 degrees Kelvin (7:69) allows the SQUID to detect extremely weak magnetic fields (on the order of 10exp(-15) Tesla) uncorrupted by large fields such as room lights, power supplies, etc. The penalty paid for the reduction in noise is a reduction in sensitivity for each additional flux detecting loop. This penalty is considered relatively small when there is a need to operarate a SQUID in the noisy environments of unshielded laboratories and hospitals, hence the use of a "second order gradiometer" is advised (7:92-93). Concepts about SQUID and second order gradiometer operation will be covered in chapters II and III respectively.

As discussed above, the low frequency waves containing information about the on-going brain activity can be detected through EEG or MEG methods. Frank R. Ervin has even detected these same low frequency "brain waves" by constructing histograms of microelectrode data from single cortical neurons (8:35-51). Ervin's data is the average of many time-

electric fields" (4:21). The resultant summation wave of this electrical activity yields a view of the general brain state. Interpretation of the EEG requires a thorough evaluation of the wave frequency, amplitude, form, periodicity, and also of the electrode locations. The detected brain wave frequencies are relatively low and are classified into four broad bands (4:50):

alfa -------- 8 through 13 hertz
beta ------- 14 and above hertz
theta ------- 4 through 8 hertz
delta ----- 0.5 through 3 hertz

The amplitude of scalp potentials is on the order of microvolts and evaluated as relative peaks and troughs. Patterns described by the above criteria have been studied in both normal and abnormal brains and form the basis for clinical determination of neural abnormalities. Reference 4:131-236 for a clinical evaluation of various EEG patterns.

Electrical brain activity and current flow also create distinctive magnetic fields reflecting the source of activity. If the sources are modelled as simple dipoles (two equal but oppositely charged particles separated in space), then the detected magnetic field is directly related to the dipole source current by the Biot-Savart law. This law, first proposed in 1820, will be discussed further in subsequent chapters. In short, the law states that at any measuring point, the magnitude of the magnetic field intensity is proportional to the dipole current, length, and the angle between an equivalent dipole and the measuring point (5:232).

dipoles contribute significantly to the magnetic field outside the head, assuming the head can be approximated as a conducting sphere. This result stems from Grynszpans dipole model which will be discussed in chapter III. Note that magnetic field studies will be expected to localize cerebral activity in the columns found in the cortical folds.

Although the cerebral cortex's general use of the columns is still being debated in scientific circles, the most promising theory is that of two dimensional Fourier analysis described by Kabrisky in 1966 (18). However, before the actual mathematical computations performed by the network of cortical columns can be studied non-evasively through epidermal detectors, the instrumentation and models for such detectors must be refined.

Encephalography

Electrical activity implies current flow. Recall that the CNS has been shown to have a communications network based upon a transmembrane flow of ions and propagating action potentials. With the intense activity of propagating action potentials, an induced current flows throughout the body fluid. The induced current can be subdivided into the two classes of (1) intracellular currents and (2) extracellular volume currents. The well known electro-encephalogram (EEG) provides information about brain activity by detecting surface potentials created from induced extracellular volume currents. In 1853 H. Helmholtz noted that a detected surface potential may represent an "infinite variety of internal

In 1963 David Hubel published a very interesting discovery that he and his partner, Wiesel, made while doing stimulus orientation experiments with micro-electrodes in the visual cortex of a cat. They found that the cortex is functionally organized into a honey-comb type structure of tiny cortical columns (17:61). These columns, not defined by any anatomical wall, range from about 50 to 500 microns in diameter. It is presently accepted by most investigators that the cortex does indeed consist of functional cortical columns, each responsible of some parameter common to all its cells (17:267).

Note that the cortical columns consisting of primarily pyramidal cells, as shown in figure I-5, generate vertical dipolar activity on the brain surface and horizontal activity in the cortical folds. It turns out that only the horizontal

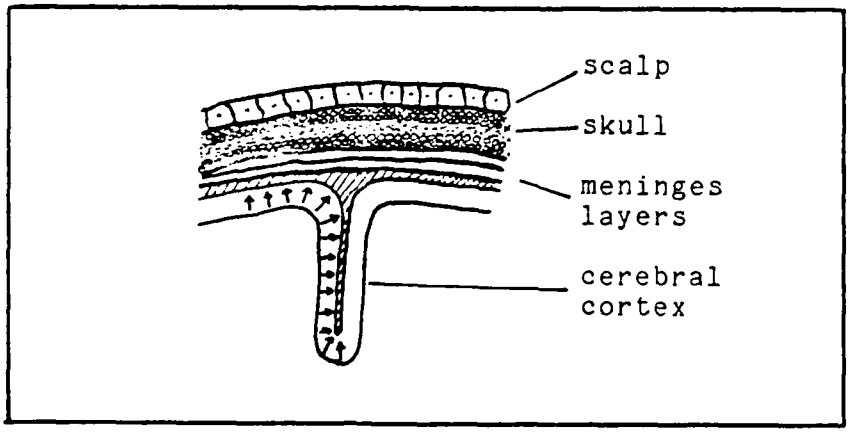

Figure I-6. Cortical Column Dipoles. (Reference 7:403-405).

The axon of most pyramidal cells extends out of the cortex to connect to other cortex areas or subcortical areas. Thus, while the stellate cells are primarily cortical interconnecting neurons, the pyramidal cells act as the primary output neurons.

Anatomists have defined six cortical layers by the density of various occuppying cell types. However, some areas such as the motor cortex have many vertical pyramidal cells and few stellate or other type cells. Similarily, other areas such as the sensory cortex, are primarily horizontal interconnecting stellate cells. Although the six layers in these cortical regions are hard to distinguish, their near homogeneous anatomical structures are an aid to electromagnetic source modeling. Figure I-5 shows a section of mouse cortex stained by the Golgi technique. Note the highly vertical orientation in this region of cortex.

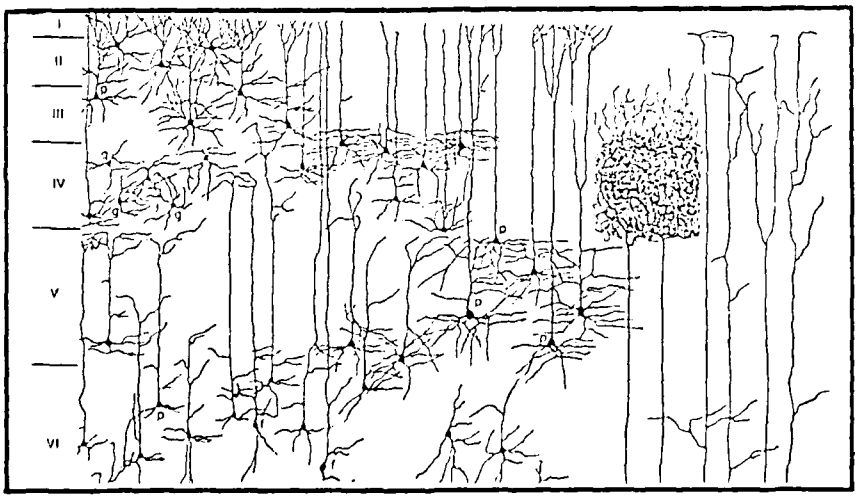

Figure I-5. Cerebral Cortex. (From Lorente de No'; Reprinted in reference 16:263).

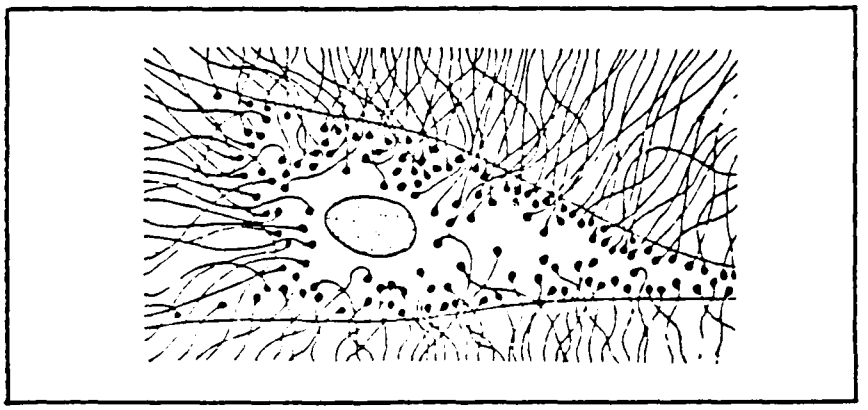

Figure I-4. A Neuron with Many Synaptic Junctions (3:247)

The Cerebral Cortex

The cerebral cortex is the most recent addition to the complex neurological systems found in mammals. In humans, this sheet of neurons, interconnections, and glial cells is about 2.5 square feet in area and about 2 or 3 millimeters thick.

Because of its late apearance in the evolutionary chain, the primary areas of the cortex are called the neocortical cortex. The neocortex consist of two principle cell types:

1. Stellate cells.
2. Pyramidal cells.

The stellate cells are small and have short axons that stay within the local cortex area. The pyramidal cells, however, have long "apical" dendrites that extend to the surface of the cortex, and "basal" dendrites that spread horizontally.

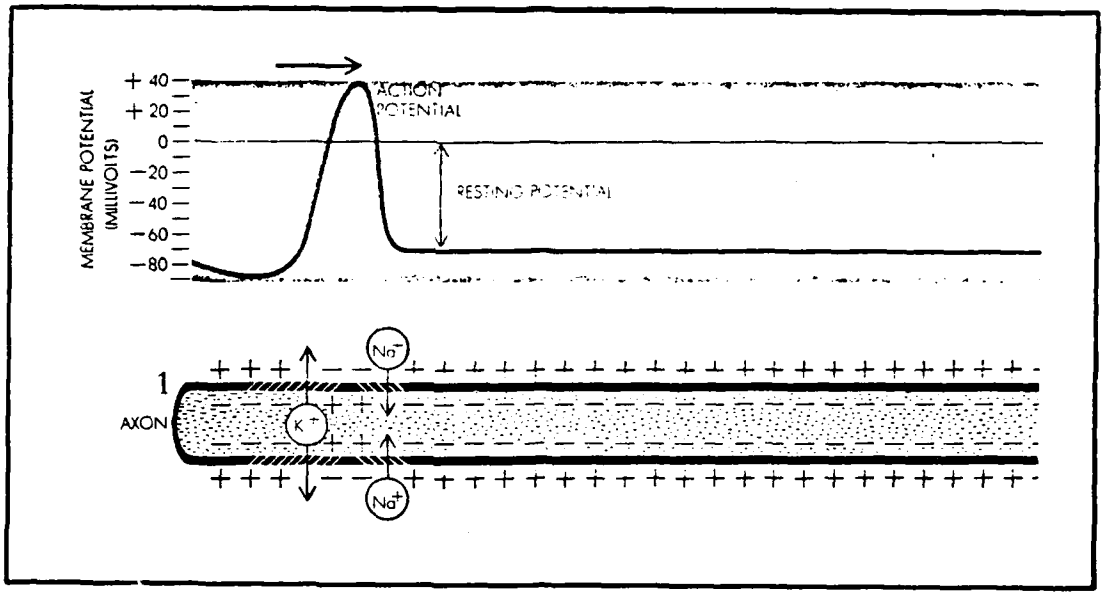

Figure I-2. A Propagating Axonal Action Potential (3:251)

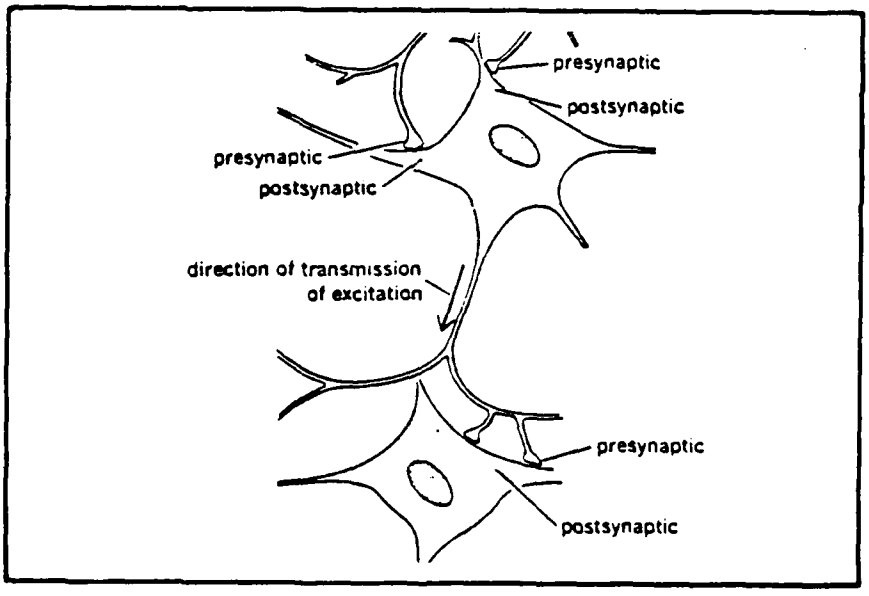

Figure I-3. Synaptic Junctions between Neurons

depolarization. Within milliseconds the membrane is repolarized by a lowering of Na+ permeability and an increase of K+ permeability. The activity at one section of membrane provides sufficient stimulus to trigger adjacent membrane sections. Thus, the AP propagates the length of the neuron without attenuation.

Although many inputs may be applied, each neuron is equipped with only one output channel, called an "axon". The terminating end of the axon is called a "synapse" and forms a synaptic junction with the receiving cell. An axon may have more than one synapse. Upon receipt of an AP, vesicles within the synapse release chemical transmitters which excite (produce an EPSP-excitatory post synaptic potential) or inhibit (produce an IPSP-inhibitory post synaptic potential) the receiving cell. A multitude of EPSPs and IPSPs will summate both temporally and spatially within a receiving neuron. The neuron will then fire (initiate an AP) only if the graded summation exceeds a fixed threshold. Thus, a system for computation and communication can be achieved via a network of functional neurons. A propagating AP is diagrammed in figure I-2. Figure I-3 depicts presynaptic neurons synapsing with postsynaptic neurons. Figure I-4 shows how a neuron may have a multitude of inputs, but only one output.

$$B = u_o(H + M) \qquad (2)$$

where

H = magnetic field intensity
L = path length
M = magnetization: the response of a material when subject to a magnetic field.

u_o = permeability of free space ($4\pi \times 10^{-7}$ Hen/m)

Note from equation (2) that the mere presence of a material causes an increase in flux density over that of free space.

This thesis is only concerned with the single radial componemt of the magnetic field vector. In this case, where B and M are parallel to H, equation (2) reduces to its scaler form. A further simplification can be made if the medium involved is considered to have properties similar to that of free space, i.e, M=0.

SQUID Technology

When the interest of measuring extremely small magnetic fields developed, investigators discovered that the quantum effects of superconducting currents is related to the magnetic flux density passing through a superconducting current loop. This phenomenon forms the basis of the SQUID gradiometer described in chapter I. An overview of the concepts will be given in the following paragraphs. A more indepth discussion can be found in chapter 4 of reference 7.

At temperatures close to absolute zero, as required for superconductivity, the attractive force between electrons

becomes more important than disordering thermal effects. As a result, the electrons bind together in pairs which appear to have the same quantum state. With a large number of electrons behaving in the same manner, a superconducting metal exhibits some unusual properties. The quantum effect on the wavelike properties of the superconducting electrons made the development of the SQUID possible.

In 1960 Giaever discovered a tunneling effect of superconducting electrons through an insulating barrier separating a superconductor and a normal metal or two superconductors (15:3,4). Because of the quantum behavior of the electrons, their wavelike properties can not drop abruptly to zero at the barrier. Such an abrupt drop of wave amplitude, according to quantum theory, would cause a gigantic particle kinetic energy. Instead, the "electron wave-like properties" penetrate the barrier and decay smoothly to zero. Penetration of the barrier from both sides allows the electrons to "tunnel" from one side to the other. In 1962 Josephson predicted an interesting occurance if the two superconductors were separated by a very thin insulating barrier. The tunneling electrons, according to Josephson, would set up a supercurrent through the insulator, i.e, current would flow through the insulator without any voltage drop. A superconducting barrier is thus called a Josephson junction.

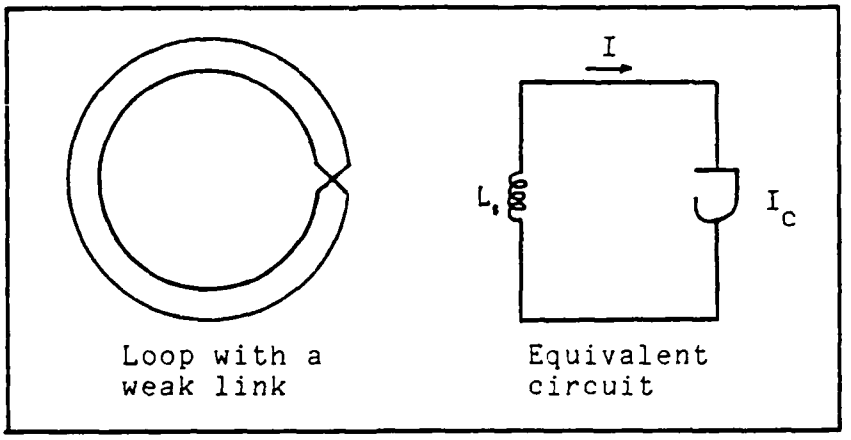

Figure II-2. A Superconducting Loop with a Josephson Junction Weak Link.

In addition, Josephson showed that the superconducting current is described by (7:74):

$$I = I_C \sin \phi \tag{3}$$

where

I = superconducting current

I_C = critical current value: If the junction is forced to carry a current greater than I_C, a voltage drop must appear. This additional current flows across the junction in the normal fashion (with resistance).

ϕ = phase difference between the electron wave functions on either side of the junction.

At the Bell Telephone Laboratories Rowell and Anderson were the first to experimentally varify this theory (15:66). The phase difference ϕ is free to adjust itself to allow any current to flow up to the critical current value. This property is called the "DC Josephson effect" and equation (3) is called the "DC Josephson equation".

If a voltage V is present across the Josephson junction, it turns out to be proportional to the rate of change of the electron waves' phase difference O (7:74):

$$V = \frac{h}{4e} \frac{d\phi}{dt}$$

$$V = \frac{\Phi_o}{2} \frac{d\phi}{dt} \qquad (4)$$

where

h = Plank's constant = 6.63×10^{-34} J*s
$2e$ = charge on the electron pair
Φ_o = flux quantum = $h/2e = 2.07 \times 10^{-7}$ Weber

Note that a voltage appearing across the junction will cause the phase difference to change with time. Putting this into equation (2) sets up an alternating current and is thus called the "AC Josephson effect".

When a flux density is applied to a superconducting loop containing a Josephson juction, the induced voltage alters the properties of the junction and a non-linear relationship is established between the applied magnetic field and the current flowing around the loop. The sensitivity of a Josephson junction will be on the order of a flux quantum.

There are two primary methods of measuring the effects the applied flux has on the Josephson junction loop. Both methods use the instrumentation concept of "Parametric Amplification". The signal detecting circuit is driven by a "pump" voltage or current source. How the pump source

affects the detecting circuit and vice-versa is governed by a reactive component. The method of signal detection is based on the fact that the capacitance or inductance of this component is controlled by the input signal.

The first of the two systems is the "DC-SQUID". This method requires only a DC pump current since the reactance affecting AC current is produced by the "AC Josephson effect". A circuit diagram of DC-SQUID is shown in figure II-3. Note that two Josephson junctions are required. If just one junction was used, the current (which must be larger than the critical current to assure the AC Josephson effect) would take the path of least resistance and flow around the junction.

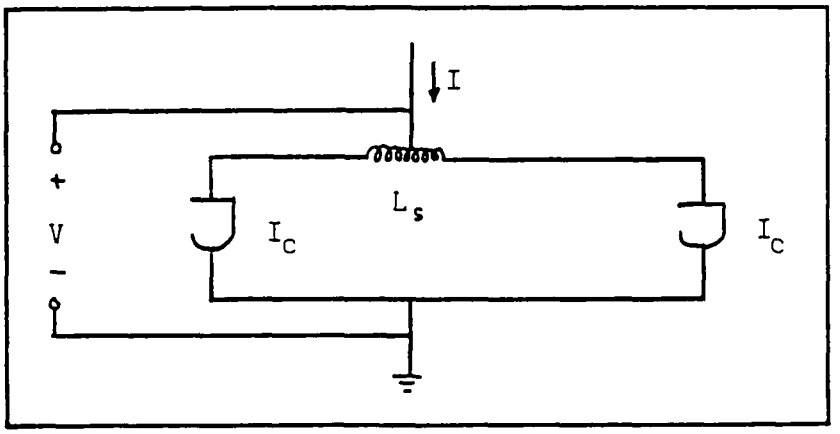

Figure II-3. Circuit Diagram of a DC-SQUID (7:79).

If the pump current is greater than the sum of the two critical currents, then both junctions will be driven into the "AC Josephson" state. An input flux to the coil will alter the SQUID loop inductance L_S which in turn alters the voltage V measured across the SQUID.

The more commonly used flux detection system is the RF-SQUID. Unlike the the DC system described above, the RF-SQUID requires only one Josephson junction. A circuit diagram is shown in figure II-4.

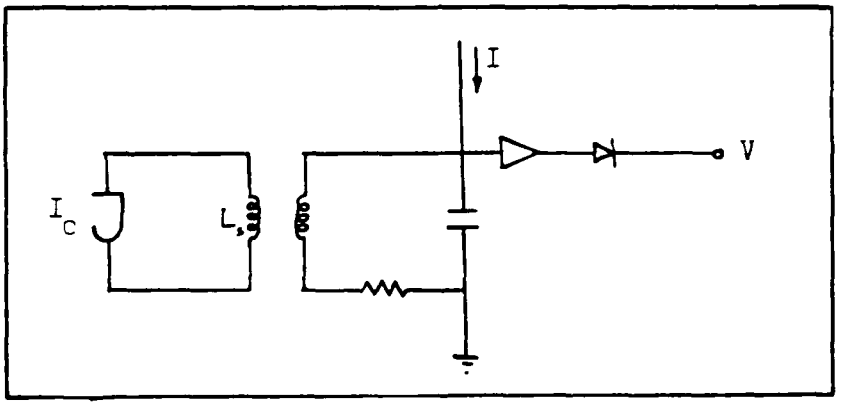

Figure II-4. Circuit Diagram of a RF-SQUID (7:77).

In the RF method, the loop inductance of the SQUID circuit is inductively coupled to a resonant tank circuit which is driven by a radio frequency pumping current. After resonation is set up in the resonant tank circuit, the current flowing between the capacitor and inductor (see figure II-4) will exceed the RF pumping current by the

quality factor "Q". The resulting voltage across the parallel capacitor-inductor circuit is amplified and rectified to give the measured output voltage.

Since the SQUID loop will oscillate at the "Josephson frequency" given by f = 2e/h = 483 MHz/uV (7:74), inductive coupling is best achieved at radio frequencies. The coupling between the tank and SQUID circuits allows the RF pumping current to drive the Josephson junction into its AC Josephson state. When flux density is applied to the SQUID loop, the SQUID inductance is altered, which then alters the resonant circuit coupled to it. Changes in the resonant tank circuit are then detected at the output voltage V .

In both the DC and the RF systems, the output voltage is a non-linear function of input flux density, and periodic with the period given by the flux quantum. Since it is desireable to compensate for the non-linearities and avoid the periodicity of the SQUID output, investigators have designed a simple closed feedback loop, from which the nulling signal is picked off as the output measurement. Because the second order gradiometer used in this thesis consists of a RF-SQUID and the feedback loop described above, the combined system will be described further.

Recall the RF-SQUID shown in figure II-4. Figure II-5 shows the same circuit, only this time it is embedded in a flux feedback loop.

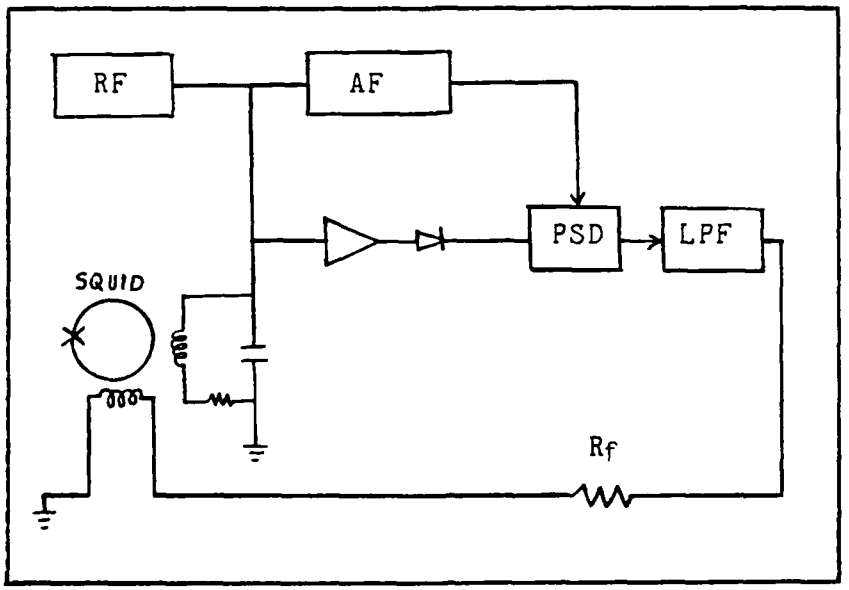

Figure II-5. SQUID Feedback Loop (7:81).

To gain an understanding of the operation of the feedback loop, one can start at the feedback resistor R and go around the loop. On the feedback line there will be a modulation frequency that originated from the audio frequency generator AF . This modulation frequency introduces a flux to the SQUID loop. Since the SQUID signal will be riding on the AF, the AF must be chosen to have an appropiately large enough bandwidth, usually about 50KHz (7:81). After passing through an amplifier and a RF-amplitude modulation detector(diode), the audio frequency modulated signal goes into a "lock in" amplifier which is locked in on the audio frequency. The "lock in" amplifier simply consists of a Phase-Sensitive Detector and a low pass filter. The

modulated signal, which represents the SQUID detected input flux, then passes through the feedback resistor. The coil after the feedback resistor is wound such that the flux signal introduced cancels with the flux present in the SQUID loop. The negative feedback loop is thus closed. The null current can be detected by measuring the voltage across the feedback resistor. When there is no input flux to the SQUID coil, the negative feedback signal perfectly cancels the present SQUID flux, and the null current is zero. Similarly, when an input flux is applied, the feedback system attempts to compensate for it, and a null current is generated. It turns out that the null current is linearly related to the input flux. The system is called a "flux locked loop".

Flux Polarity and Sinusoidal Phase Shift

Most investigative studies use a sinusoidal input to stimulate cerebral or mid brain dipoles of interest. At any instant of time, magnetic flux lines will exit the scalp surface on one side of the dipole and enter on the other. See figure II-6. This is in accordance with the right hand rule, which lets the right hand thumb represent current direction and the curl of the fingers represent magnetic flux flow. The accepted convention lets the exiting (upward) flux be positive and the entering (downward) flux be negative. Assuming no transmission line delays or reactance, the generated dipole flux will track the input voltage.

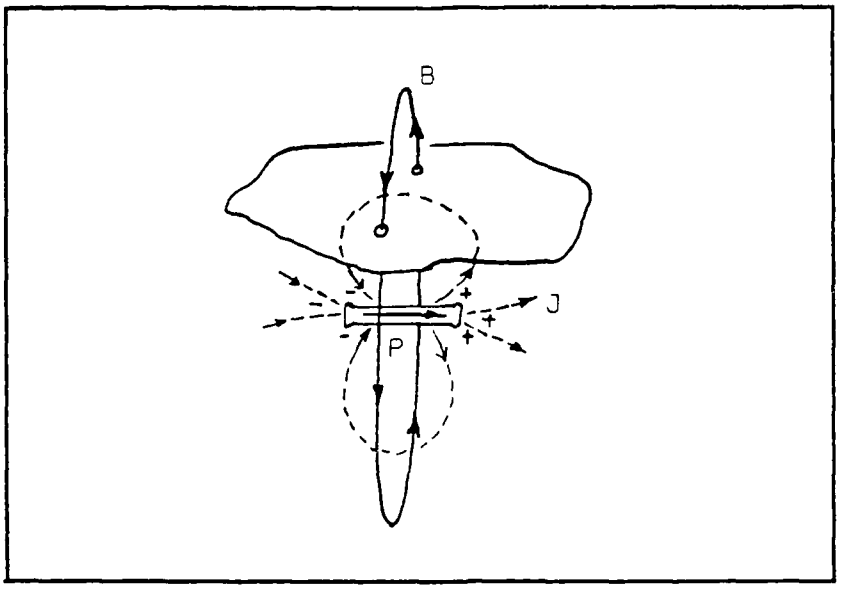

Figure II-6. Magnetic Flux Flow (Ref 9:226). P = Dipole moment, B = Magnetic flux density, J = induced extracellular volume current.

Recall that the SQUID detection system depends on flux linkages. The electromotive force (emf) generated by magnetic flux passing through a coil is given by Faraday's law of induction:

$$emf = - N \frac{d\Phi}{dt} \qquad (5)$$

where,

Φ = Magnetic flux
N = # of turns in the coil.

Note that a sinusoidal input flux to a coil will result in a sinusoidal emf with a 90 degree phase shift. Using equation (5) and assuming negligible flux leakage, it can be shown that the voltage (emf) across a secondary transformer coil is directly proportional to the voltage across the primary coil:

$$v_2 = \frac{N_1}{N_2} v_1 \qquad (6)$$

where,

v_2 = voltage across secondary coil
v_1 = voltage across primary coil
N_1 = # of turns in first coil
N_2 = # of turns in second coil

Figure II-7 illustrates the inductive coupling and phase relations found in a RF SQUID.

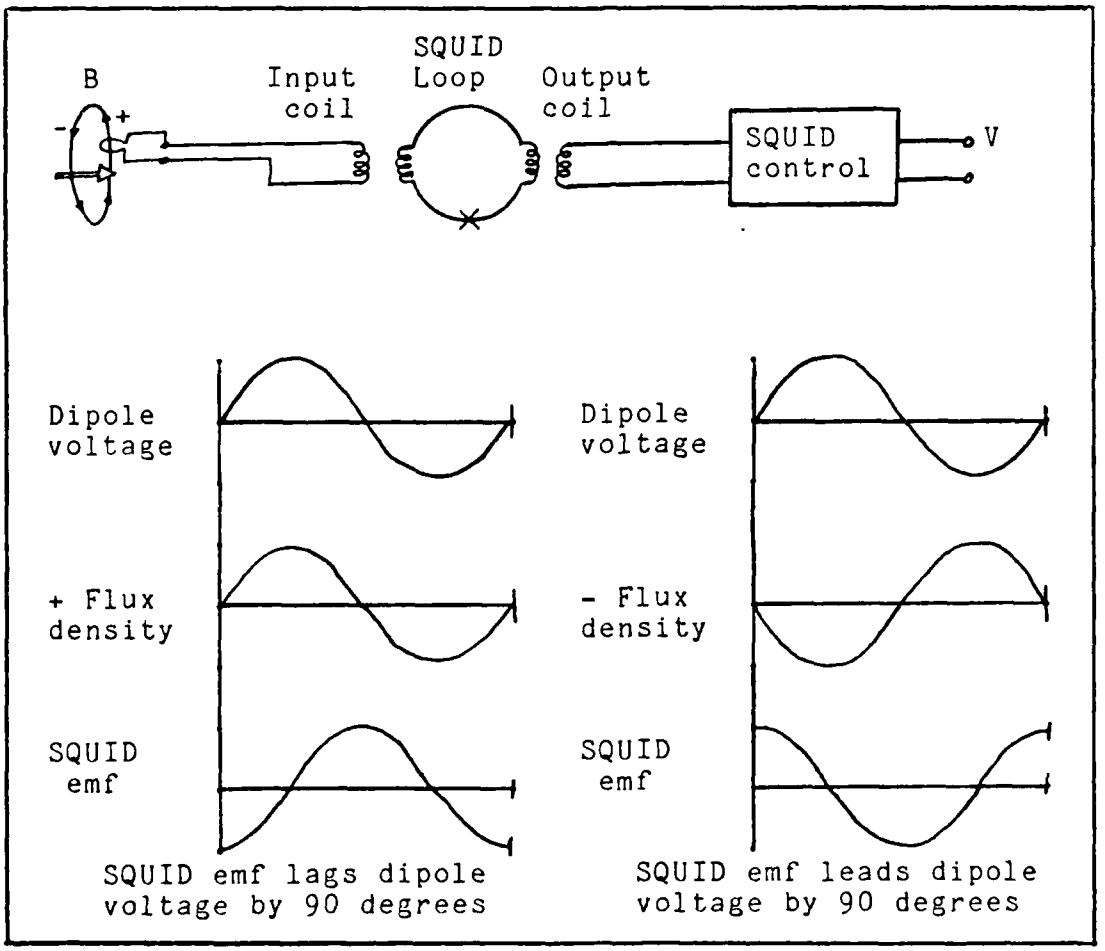

Figure II-7. Phase Relation Between Dipole Voltage and Induced SQUID Electromotive Force (emf).

A sinusoidal flux input to the detection coil results in a 90 degree lagging sinusoid induced across the input coil and correspondently in the SQUID loop. The signal is embedded in the nonlinear characteristics of the SQUID, and then relinearized through the feedback SQUID control circuit. Although the induced emf in the SQUID loop lags the input flux by a known 90 degrees, reactances within the rest of the control circuitry, signal processing amplifiers, and filters will cause additional phase shifts.

Since the reactances will shift sinusoids of a given frequency by the same amount, the 180 degree phase difference between the +Flux induced emf and the -Flux induced emf is preserved. This characteristic is used to determine the detected flux's polarity by recording the phase difference between the input stimulus and the processed output signal. The output associated with +Flux will be 180 degrees out of phase with the output associated with -Flux.

III. Model Development and Plotting

Expansion of Grynszpan's Model

In a dissertation published in 1971 (11:26-32), Grynszpan developed equations describing the magnetic field produced by a single dipole in a sphere. Cuffin and Cohen outlined these results while evaluating the magnetic fields outside various volume conductor shapes (12:374-375). The equation of interest is the radial component of the magnetic field strength. In spherical coordinants, this component is the magnitude of the magnetic field vector, and hence the magnetic strength detected by a SQUID.

Grynszpan used a spherical coordinant system with the origin coinciding with the sphere's origin. The dipole was fixed at X=Y=0 and variable on the z-axis. The dipole orientation was fixed in the positive X direction and parallel to the XY-plane. Figure III-1 depicts this arrangement. The calculated radial component is given by:

$$H = \frac{P\ a\ \mathrm{Sin}\ \phi\ \mathrm{Sin}\ \theta}{4\pi\ R^2\ \gamma^{3/2}} \qquad (7)$$

where

$$\gamma = 1 - \frac{2\ a\ \mathrm{Cos}\ \theta}{R} + \left(\frac{a}{R}\right)^2$$

P = Dipole Moment
a = Dipole location on the z-axis
π = 3.14159
R = Field Location in Spherical Coordinants

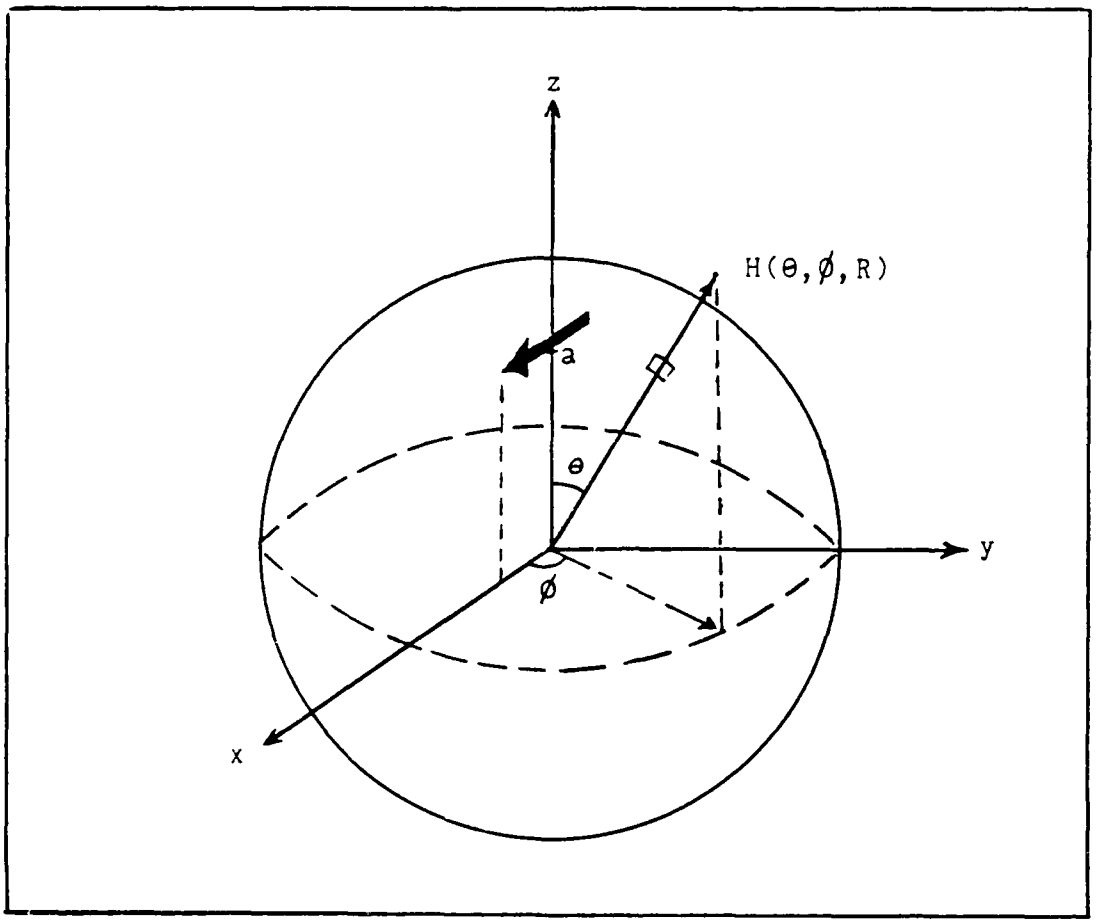

Figure III-1. Grynszpan's Dipole Model. The dipole is represented by the heavy arrow at z=a and $H(\theta,\emptyset,R)$ is the calculated radial field component.

Note that Grynszpan's model considers only one tangential dipole which has strict orientation constraints. It also includes all derivatives in the Taylor series expansion. Since the multipole model intended for this thesis requires various tangential dipole positions, and the 2nd order SQUID gradiometer does not detect the 0th and 1st order derivatives, certain modifications were made to the calculated radial field component.

A super insulated fiberglass dewar houses the BMP probe and its liquid helium bath. The gradiometer coils are positioned in a thin neck pertruding from the bottom of the dewar. This allows the gradiometer to be placed close to the magnetic field source.

Recall the RF SQUID and feedback system described in chapter II (see figure II-5). The S.H.E system is a similar RF SQUID with the exception that the feedback path is fed directly into the BMP probe output instead of being inductively coupled to the SQUID loop. Conceptual circuit operation, however, is the same. The output of the BMP probe is fed into a S.H.E. model 300X RF head unit mounted on the top of the dewar. The RF head connects to the S.H.E. model 30X control unit. Together the system is called the S.H.E 330X and is diagrammed in figure IV-2.

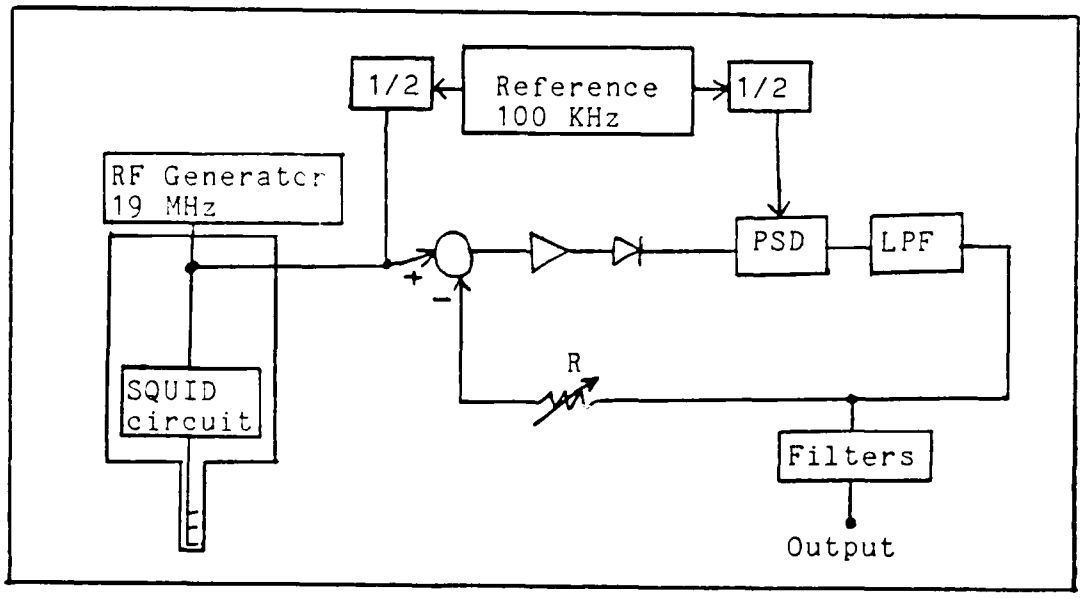

Figure IV-2. S.H.E. Model 330X SQUID System.

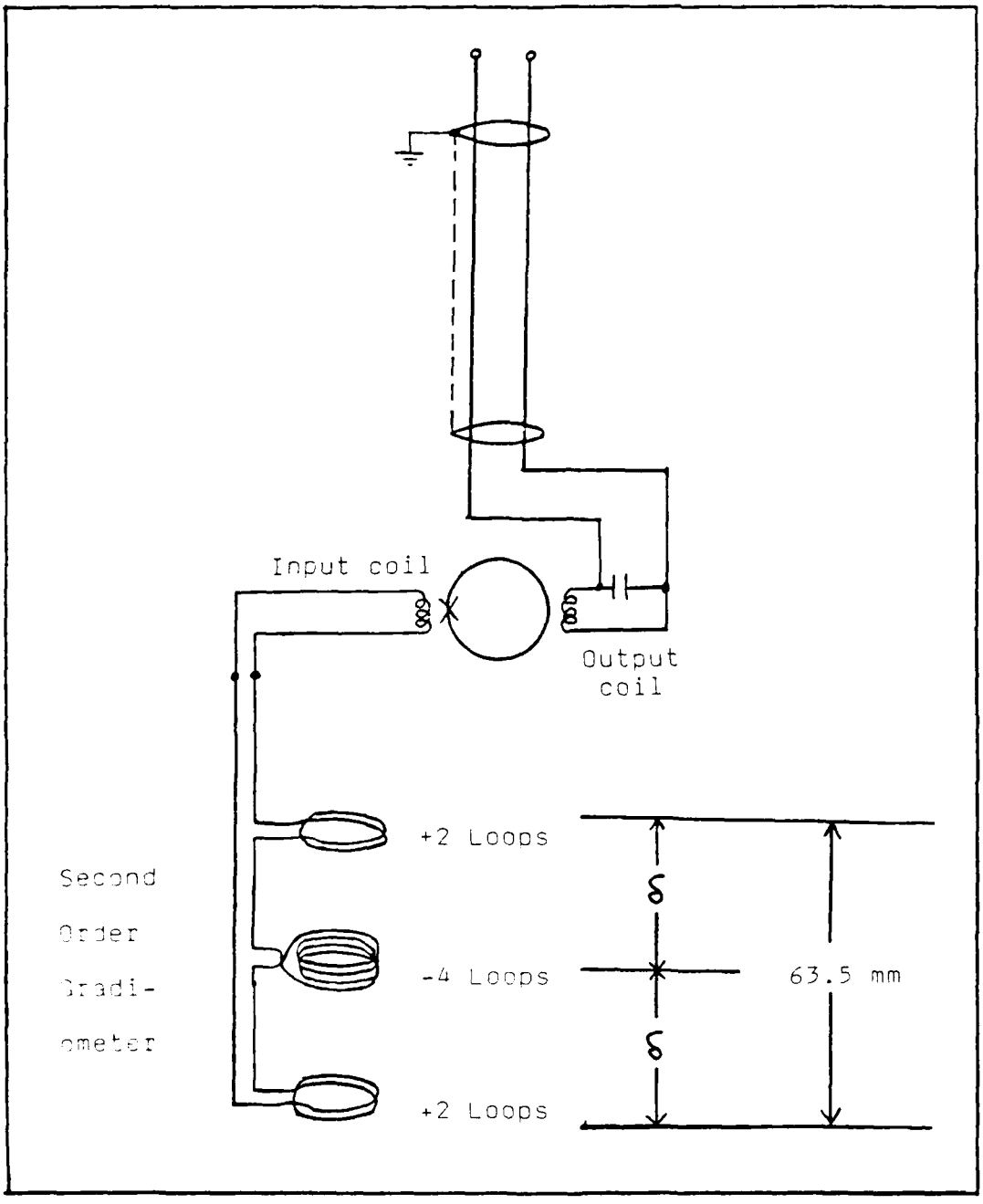

Figure IV-1. S.H.E. Model BMP Biomagnetic Probe (Reference 19 and 20).

IV. The Multipole in a Sphere Experiment

Five dipole configurations were examined. The first run consisted of a single dipole located on the z-axis and oriented in the positive x direction as described by Grynszpan's original model (see figure III-1). This configuration povided a reference for the behavior of a single dipole within a conducting sphere. The second run extended to a three dipole stack on the z-axis. The dipoles were all oriented in the positive x direction but located at different z-axis positions. In the third and fourth runs, the the lower two dipoles of the stack were rotated. A fifth experiment was also conducted which considered two dipoles located on different radians (both off the z-axis) and oriented in different directions.

The Second Order SQUID Gradiometer

The magnetic fields generated by the dipoles were detected with a SQUID system biult by the S.H.E. Corporation. The detecting probe (model BMP) consists of single weak link niobium superconducting loop inductively coupled to a niobium input coil. Two niobium screws provide a superconducting connection between the input coil and the second order gradiometer loops. The output coil is part of a R.F. resonant tank circuit. The BMP probe, as diagrammed in figure IV-1, is supercooled in a liquid Helium bath to 4.2 degrees Kelvin.

magnetic field as it exists on the upper half of the measurement sphere.

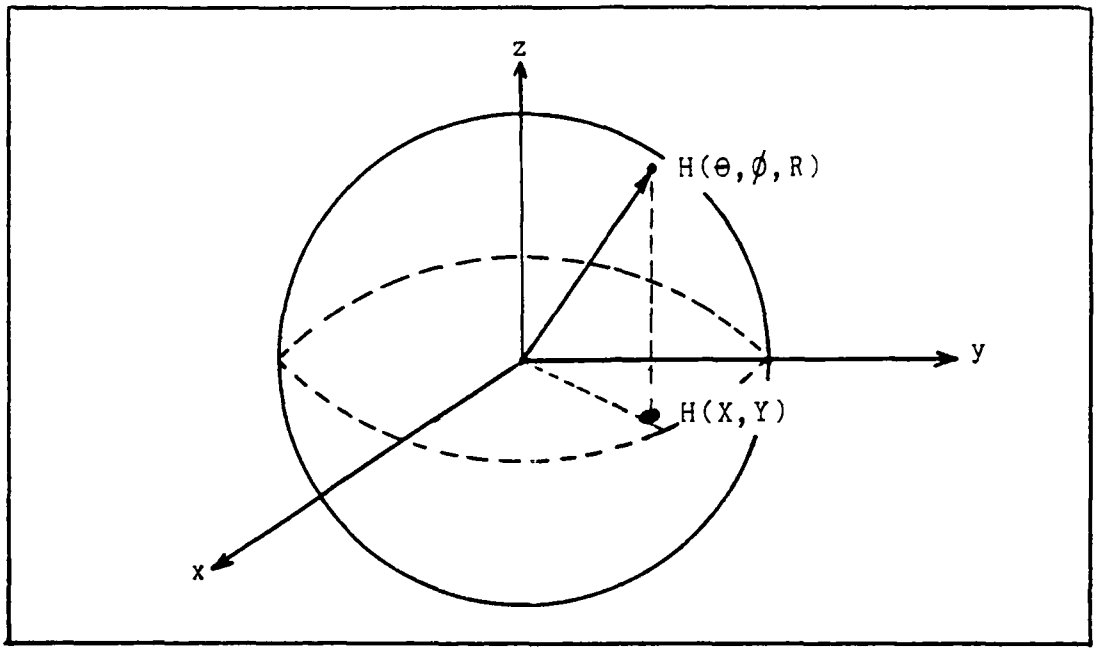

Figure III-5. The XY plotted Data. The data in the upper hemisphere is projected onto the XY-plane. The resulting contour plot is an overhead view of the detected field on the upper measurement hemisphere.

Because the dipoles were all located in the upper hemisphere, the overhead XY view provided a sufficient discription of the various field patterns and the XZ view was not necessary. The IBM control language used to run the "System II" software is given in Appendix B.

The blank spaces shown in the file names above correspond to the run# which the user enters interactively when the program is executed. The program, titled MAGCAL2, and its control language can be found in Appendix A.

Plotting the Data

The data from both the simulation runs and the actual conducting sphere experiments were plotted via a sofeware package called "Surface II Graphics System" (13). The software was designed to display spatially distributed data in the form of a contour map. Although originally created for the purpose of studying geological formations, the software can be effectively used to plot any planer distributed data. The primary constraints are that the data must lie on a plane, be single valued, and have locations described by two orthogonal coordinants.

Because the Surface II software requires the data to be located in a plane, only two dimensional views of the measurement sphere were plotted. Recall that the Magcal program calculates the detected magnetic field in spherical coordinants and then converts to cartesian coordinants. In order to project the spherical data onto a plane without being double valued, only one hemisphere can be plotted. Figure III-5 depicts how the upper hemisphere is projected onto the XY-plane. Magcal accomplishes this by printing into file XYPL___ only data with a Z component greater than or equal to zero. The resulting plot is an overhead view of the

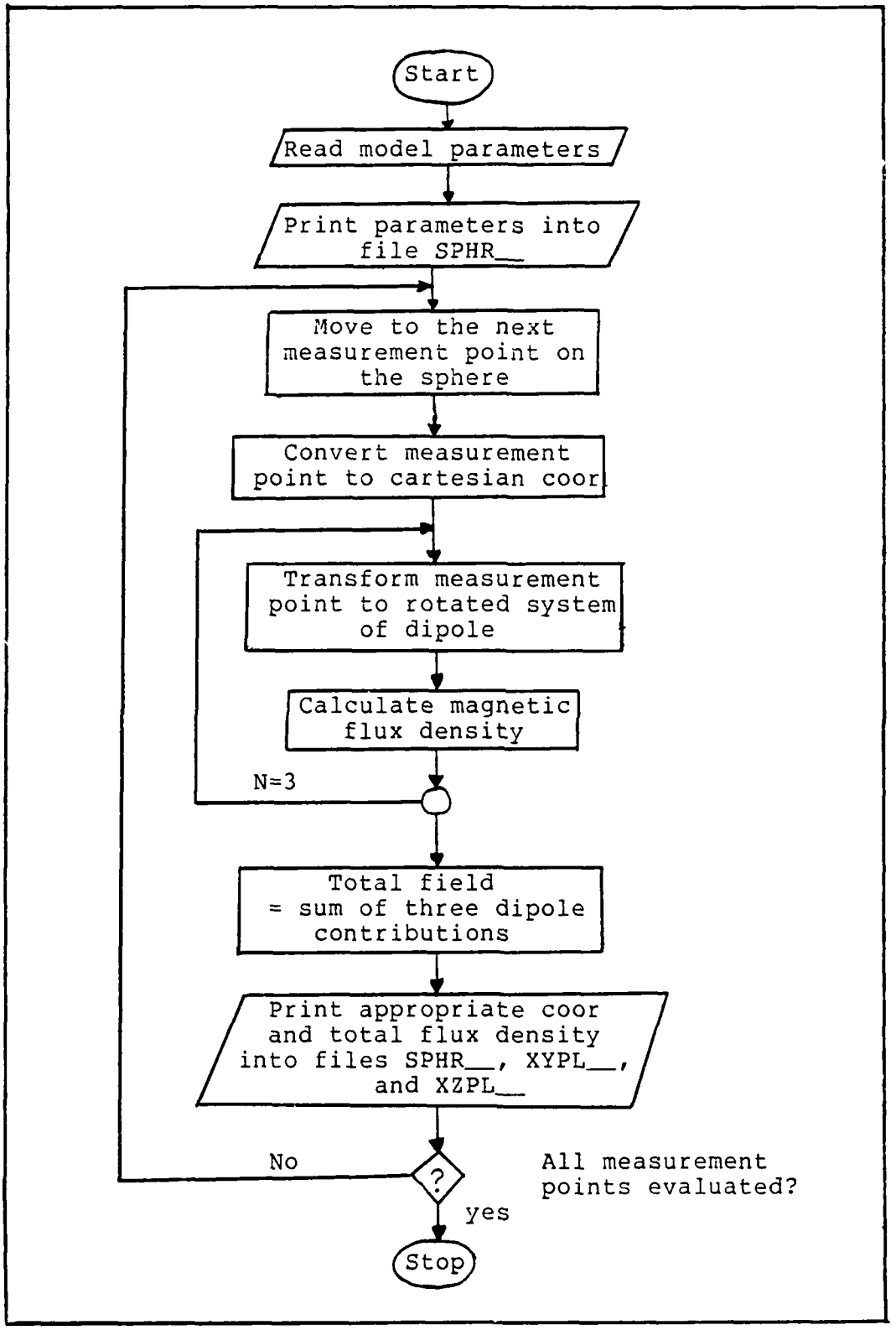

Figure III-4. Flowchart of program MAGCAL2

to the position of the first set of gradiometer coils (recall equation (10)). It will be shown in chapter IV that this radius, R, is equal to 10.98 centimeters.

The computer simulation of the detected field required a systematic method of encompassing the sphere. Naturally, a spherical coordinate system was chosen. The equator of the sphere was divided into 28 equal units. The number of radians between each unit is therefore:

$$\frac{2\pi \text{ radians}}{28} = 0.2244 \text{ radians} \qquad (15)$$

As a result, a grid of 28 meridians and 28 parallels was used in the simulation.

The simulation program consisted of a Fortran 77 routine which was run on an IBM 30/30 digital computer. The routine interactively obtained the simulation parameters peculiar to each individual run and then entered a loop that accomplished the following tasks:

1) Move to a measurement position on the sphere.
2) Convert the measurement point to cartesian coordinants.
3) Calculate the magnetic flux density by using the transformation of equation (8) and the flux density of equation (14).
4) Print input and output data into file SPHR___.
5) Print upper hemis. XY coor. and data into file XYPL___.
6) Print lat. " (Y+)XZ " XZPL___.

$$B = \sum_{m=1}^{3} \mathcal{J}_m \left[P_m a_m \sin \phi_m \sin \theta_m \sum_{n=1}^{3} \frac{K_n}{r_n f_m^{3/2}(r_n)} \right] x10^{-7}$$

where, (14)

B = Magnetic flux density.....TESLA
P = Dipole moment.....AMP*METER
a = Dipole distance from origin.....METER
$\mathcal{J}$ = Coordinant rotation transformation

r_1 = R = origin to 1st set of coils.....METER
r_2 = R+δ = origin to 2nd set of coils.....METER
r_3 = R+2δ = origin to 3rd set of coils.....METER

K_1 = 2 = positve loops in 1st set of coils
K_2 = -4 = negative loops in 2nd set of coils
K_3 = 2 = positive loops in 3rd set of coils

$$f_m(r) = 1 - \frac{2 a_m \cos \theta_m}{r} + \left(\frac{a_m}{r}\right)^2$$

Generating the Computer Simulation Data

The pyrex sphere used in the experiments has a radius of 9.1 centimeters. Note from equation (14), that the detected flux density is independent of the radius of the conducting sphere. Grynzspan's derivations achieve this result based on an expansion that is valid only for the field outside the conducting sphere (outside the source region) (11:22,26-29). Since all the field measurements, both simulated and experimental, were taken outside the conducting sphere, its radius is not a parameter in the simulated data.

The computer generated fields are represented by equi-flux density cotours plotted on an imaginary measurement sphere. The radius of the "measurement sphere" corresponds

By inspection, the first two components of equation (12) are seen to go to zero. However, algebraic expansion shows that the same is not true for the 2nd and higher order components. Because of the factorial division found in the Taylor series expansion, the higher order gradients quickly become more and more insignificant. Although all gradients higher than the first order will be detected by the gradiometer of figure III-3, the 2nd order is most prominent and hence the name "second order gradiometer" is given.

It is now desireable to apply the 2nd order gradiometer concepts to the expanded 3-dipole Grynszpan model. Since the model considers only a single scaler component, and assuming the model has similar magnetic characteristics of free space, the relation between the magnetic field strength(H) and the magnetic flux density(B) is given by the scaler equation (5:260):

$$B = u_o H \tag{13}$$

where

u_o = permeability of free space

$= 4\pi \times 10^{-7}$ HENRY/METER

Recalling the multipole magnetic field strength of equation (9), the detected flux density of equation (11), and the relation given in equation (13), the flux density detected by the 2nd order gradiometer is:

The total flux detected is the sum of the three flux density and the loop area products:

$$\Phi = 2B(R)A - 4B(R+\delta)A + 2B(R+2\delta)A \qquad (10)$$

where

$B(r)$ = Magnetic flux density w.r.t. position
R = Radial distance to first coil
A = Area of each coil
δ = Distance between each set of coils

Since each coil has the same area, the total detected flux density is:

$$B = 2B(R) - 4B(R+\delta) + 2B(R+2\delta) \qquad (11)$$

To show how the spacial discriminating gradiometer does not detect the constant and the 1st gradient of equation (11), perform a Taylor series expansion about the point q:

$$B = B(q) + B'(q)(R-q) + \frac{B''(q)(R-q)^2}{2!} + \ldots + \frac{B^{n}(q)(R-q)^{n}}{n!}$$

$$= B(q)\left[2 - 4 + 2\right]$$
$$+ B'(q)\left[2(R-q) - 4(R+\delta-q) + 2(R+2\delta-q)\right]$$
$$+ \frac{B''(q)}{2!}\left[2(R-q)^2 - 4(R+\delta-q)^2 + 2(R+2\delta-q)^2\right]$$
$$\vdots$$
$$+ \frac{B^{n}(q)}{n!}\left[2(R-q)^{n} - 4(R+\delta-q)^{n} + 2(R+2\delta-q)^{n}\right] \qquad (12)$$

The Field Detected by a 2nd Order Gradiometer

The 2nd order gradiometer consists of a single wire wound into three sets of coils. The center set has twice the number of turns and is wound in the opposite sense of the other two sets. Figure III-3 illustrates how a 2nd order gradiometer will detect the magnetic field at three locations corresponding to the three loops. The magnetic field component normal to the loops will be spacially discriminated in the 0th and 1st order derivatives. In other words, constant fields and linearly changing fields (with respect to distance) perpendicular to the 2nd order gradiometer are not detected. This can be shown by considering the total flux detected by the three magnetometers.

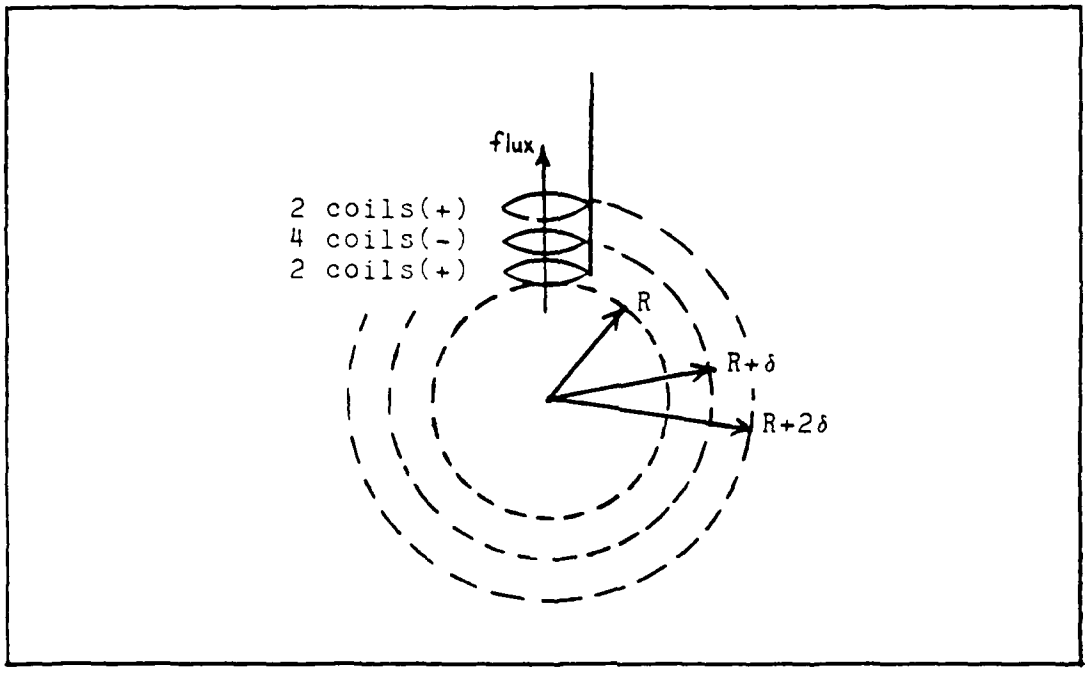

Figure III-3. A Second Order Gradiometer.

Now consider three dipoles located anywhere in the sphere. As long as each dipole is tangential to the sphere surface, it can be fit to a Grynzspan model rotated with respect to the standard cartesian coordinant system. With a given measurement point, each model identifies the point in its own coordinant system and calculates its respective field contribution. The resultant radial field is the scaler sum:

$$H = \sum_{m=1}^{3} \mathcal{J}_m \left[\frac{P_m \, a_m \, \text{Sin} \, \phi_m \text{Sin} \, \theta_m}{4\pi R^2 \quad \gamma_m^{3/2}} \right] \tag{9}$$

where

$$\gamma = 1 - \frac{2 \, a_m \, \text{Cos} \, \theta_m}{R} + \left(\frac{a_m}{R} \right)^2$$

P = Dipole Moment
a = Tangential dipole's distance from origin
π = 3.1416
R = Field distance from origin
$\mathcal{J}$ = Coordinant rotation transformation.

Note that the output of interest is given in the standard coordinant system. It must also be described in the rotated system if the rotated dipole contribution is to be calculated correctly. This is accomplished through a linear transformation (21:397-398):

$$\begin{bmatrix} x^* \\ y^* \\ z^* \end{bmatrix} = \begin{bmatrix} C1 & C2 & C3 \\ C4 & C5 & C6 \\ C7 & C8 & C9 \end{bmatrix} \begin{bmatrix} x \\ y \\ z \end{bmatrix} \qquad (8)$$

where,

coefficients C1-C9 are given by the dot product between the six axis:

C1 = cos(angle between x* and x)
C2 = cos(angle between x* and y)
C3 = cos(angle between x* and z)

C4 = cos(angle between y* and x)
C5 = cos(angle between y* and y)
C6 = cos(angle between y* and z)

C7 = cos(angle between z* and x)
C8 = cos(angle between z* and y)
C9 = cos(angle between z* and z).

Recall from equation (5) that Grynzspan solved his model in spherical coordinants. Transforming:

$$R = \sqrt{x^{*2} + y^{*2} + z^{*2}}$$

$$\theta = \arccos(z^*/R)$$

$$\phi = \arctan(y^*/x^*)$$

Consider a second Grynzspan dipole model occupying the same sphere, but belonging to a rotated coordinant system. This is illustrated in figure III-2. The resulting field generated by the two dipoles at some point P(x,y,z) will be the vector sum of H(x,y,z) and H(x^*,y^*,z^*).

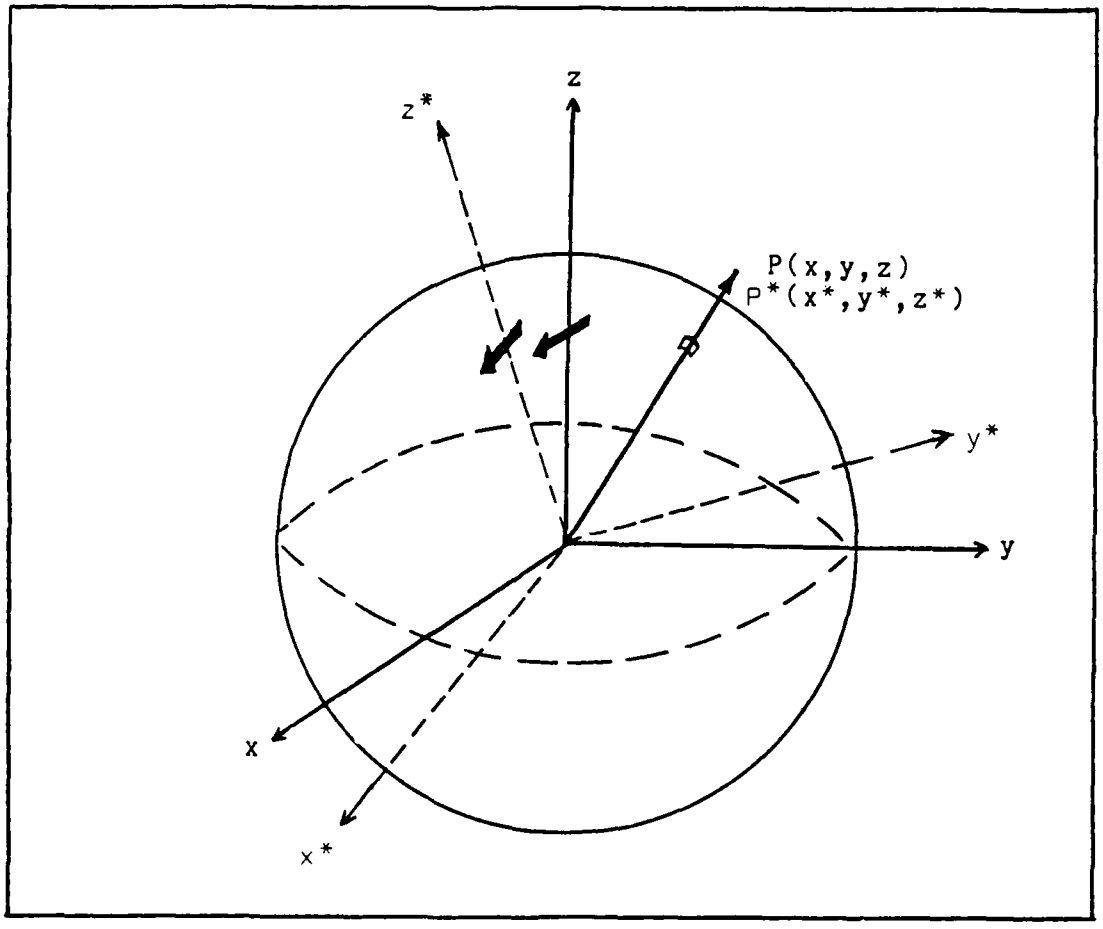

Figure III-2. A Two Dipole Model. The Second dipole belongs to a rotated Grynzspan coordinate system. The resulting field will be H(x,y,z) + H (x^*,y^*,z^*).

The Pyrex Sphere and Mount

In collecting the experimental magnetic field data, the SQUID was fixed. Therefore, the conducting sphere was mounted on a two axis gimbal capable of systematic positioning.

The conducting sphere was simply a 3000 milliliter spherical Pyrex flask filled with 0.9% saline solution. The sphere had a single openning. The dipoles' mount and wires entered through a #10 rubber stopper.

The gimbaled sphere mount was constucted entirely of wood and plastic. The sphere sat firmly in a rubber lined wooden bowl. The sphere neck passed through the bottom of the bowl and through a tight fitting plastic sleave. The sphere- bowl-sleave assembly moved together as a unit. This assembly was mounted on a swing. A short plastic pipe through the seat of the swing provided a snug bearing for the sphere assembly. A plastic ring with three nylon set screws clamped tightly to the length of the neck protruding through the bottom of the swing. Thus the sphere assembly was allowed snug rotation but restricted from backing out of the swing.

The swing assembly was supported by two vertical members. The hinges consisted of nylon bolts passing through nylon bearings and fastened with plastic nuts. The axis of swing corresponded to the horizontal axis of the Pyrex sphere. The vertical members supporting the swing assembly attached to a heavy circular base with a 14 inch diameter.

A plastic 360 degree protractor was mounted on each of the two axis. One protractor attached to the swing seat and measured sphere rotation about the z-axis. A pointer protruding from the wooden bowl assembly indicated the corresponding angle ϕ. The second protractor was attached to one side of the swing. The protractor moved with the swing and measured rotation about the horizontal axis. A pointer fixed to the vertical member supporting the swing indicated the corresponding spherical coordinant parameter θ. The conducting sphere and mount is shown in figure IV-3.

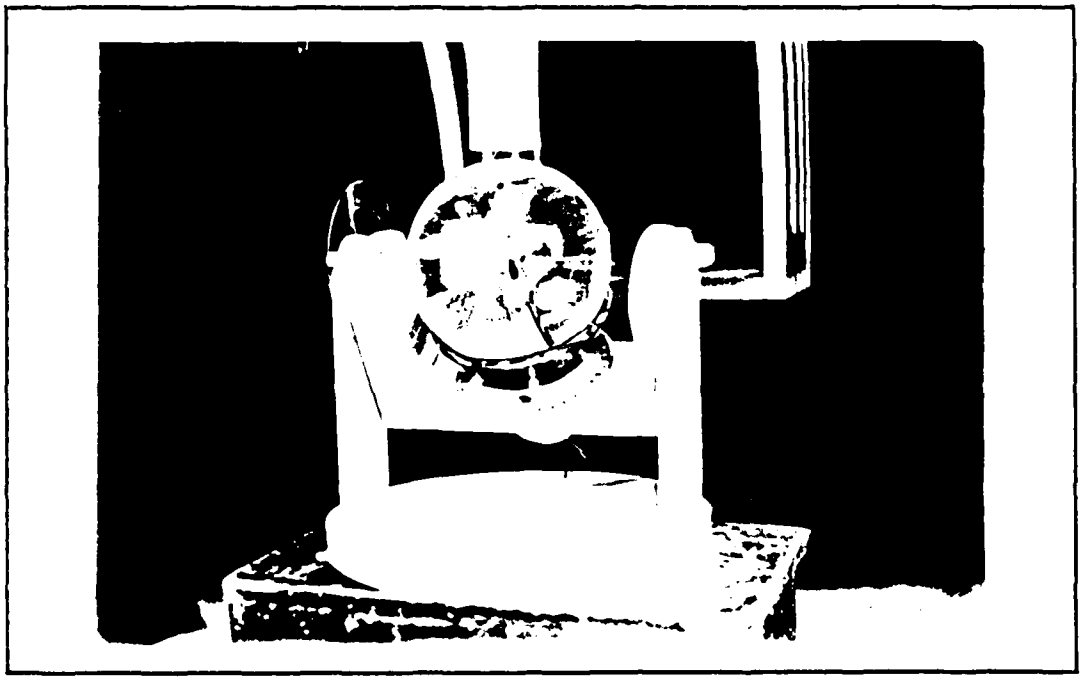

Figure IV-3. The Conducting Sphere and Mount.

The Dipole Support Mount

Each current dipole was made from a single conductor shielded cable (M17/119-RG MIL-C17E 77314 Plastoid Corp). With the shield rolled back to give the appropriate dipole length, a small ball of solder was applied to both the end of the single conductor and the rolled back shield. In this way, current flowed through the saline solution to produce an effective current dipole.

For the experiments, the dipoles had to be rigidly fixed at a known position and orientation. A plexiglass mount capable of holding three dipoles on a radial stack was built. Each dipole could be rotated independently about the z-axis and clamped in position. Figure IV-4 is an expanded drawing of the dipole mount. Because of their negligible magnetic properties, a stainless steel screw and a brass anchor were used to clamp the mount together.

The stem of the dipole mount was placed through a nylon disk designed to fit snugly in the spherical flask's neck. Together with a #10 size rubber stopper, the dipole mount could be rigidly positioned within the conducting sphere. The mount stem and the flask lip were marked to insure proper dipole depth and orientation.

During the experiments, the SQUID was fixed and the conducting sphere was rotated about the origin. Recall from chapter III (see figure III-3) that the measurement sphere radius must be defined by the location of the SQUID's flux detecting loops. With the bottom of the SQUID dewar placed

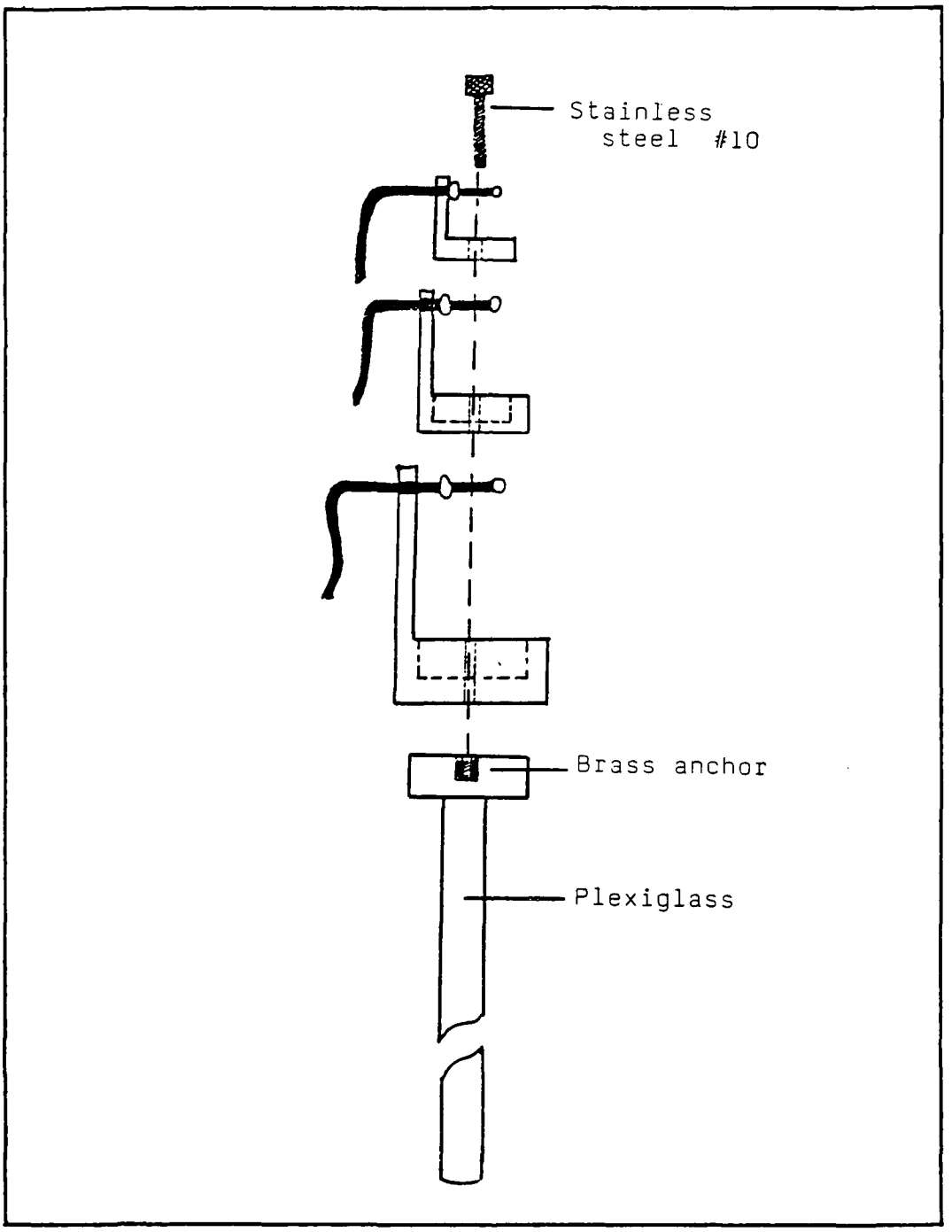

Figure IV-4. The Dipole Support Mount

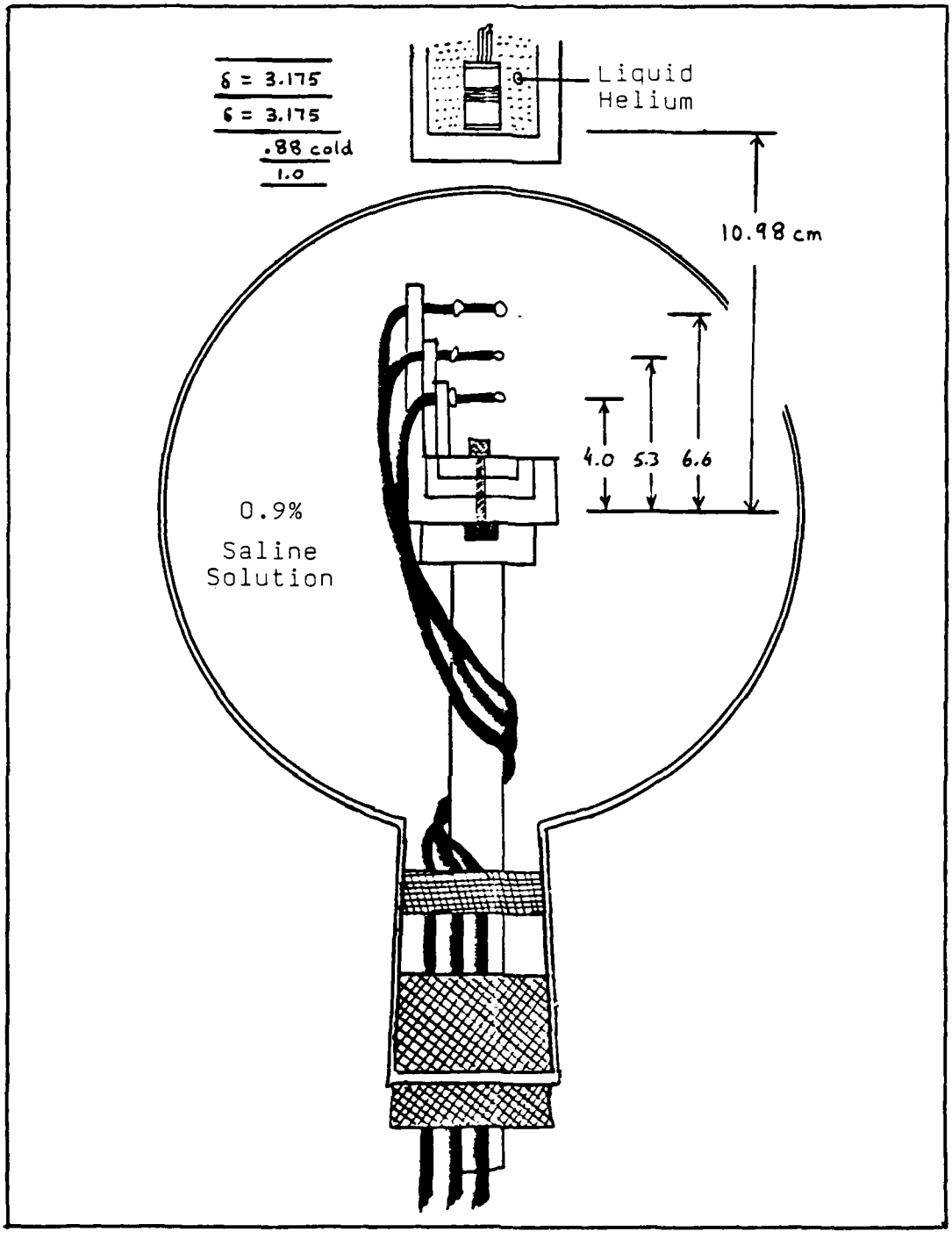

Figure IV-5. Dipole Stack Within Conducting Sphere and the SQUID detection Coils.

one centimeter above the sphere surface, the bottom detection coils are 10.98 centimeters from the origin. Figure IV-5 shows the relation between the SQUID detection coils, the conducting sphere, and the dipoles.

The Experimental Setup

The SQUID sensor hangs from an aluminum and plexiglass mount supported by wooden beams. The entire SQUID support frame sits on a concrete floor in a corner of the AFAMRL/MEG laboratory.

The support equipment used in the experiment include:

Waveform Generator	Wavetek 175
Oscilloscope	Tektronix 7623A
Comb Filter	60 Hz, by SRL
Amplifier	Grass MOD.P511H
Dual Channel FFT Analyzer	Nicolet 660B

A 25 hertz sinewave of 1.41 VAC (RMS) was simutaneously sent to each dipole lead. To prevent short circuit accidents and to determine the current flow, a 1000 ohm resistor was put in series with each dipole. The sphere mount sat on top a base constucted of wood and cement blocks, and the SQUID was positioned one centimeter vertically overhead as shown in figure IV-5 and figure IV-7.

The signal detected by the SQUID passed through the RF Head, the SQUID controller, an amplifier, a 60Hz comb filter, viewed by an oscilloscope, and finally to channel B of a spectrum analyzer. The 1.41 VAC dipole input signal provided a reference to channel A of the spectrum analyzer. This setup is shown in figure IV-6.

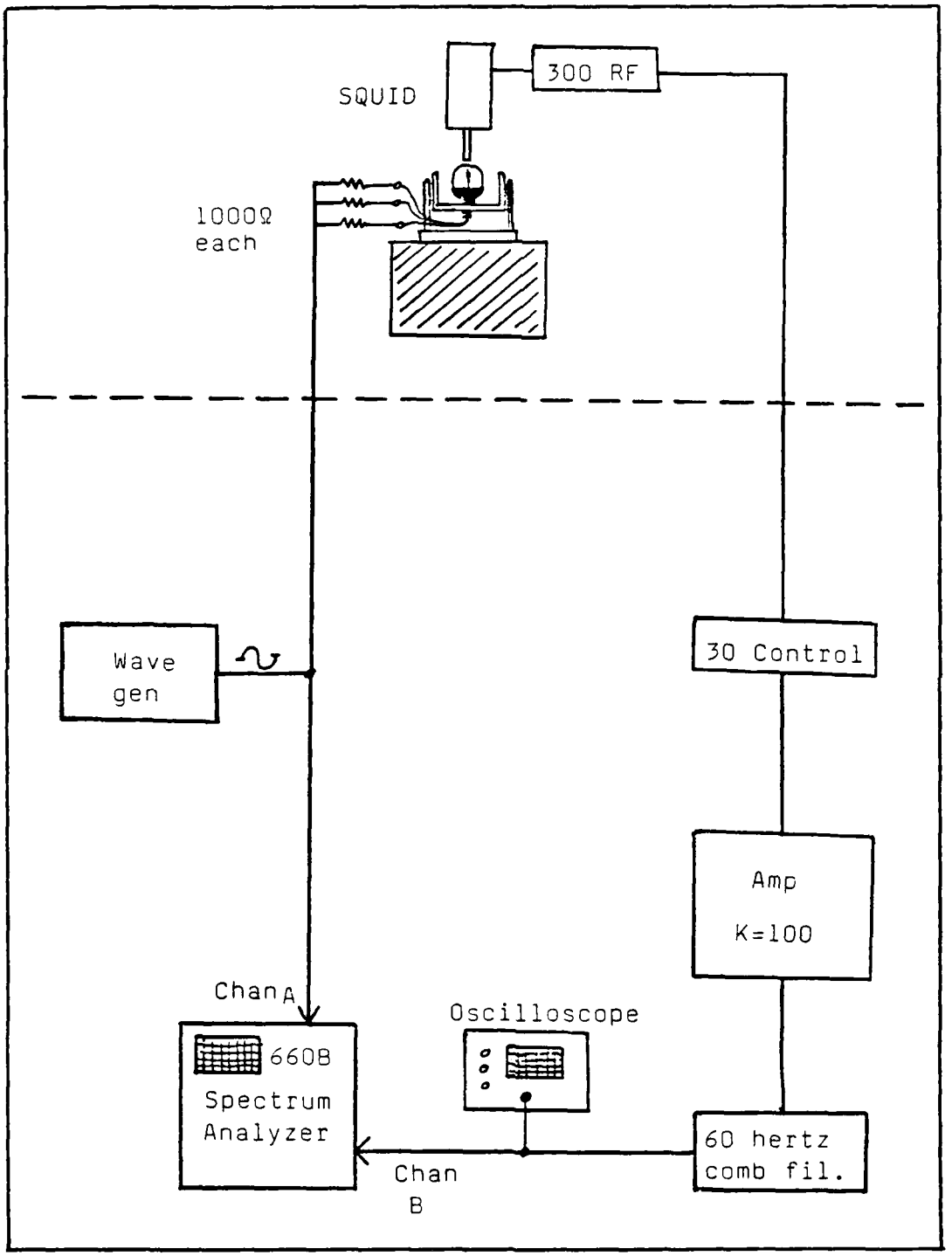

Figure IV-6. The Experimental Setup.

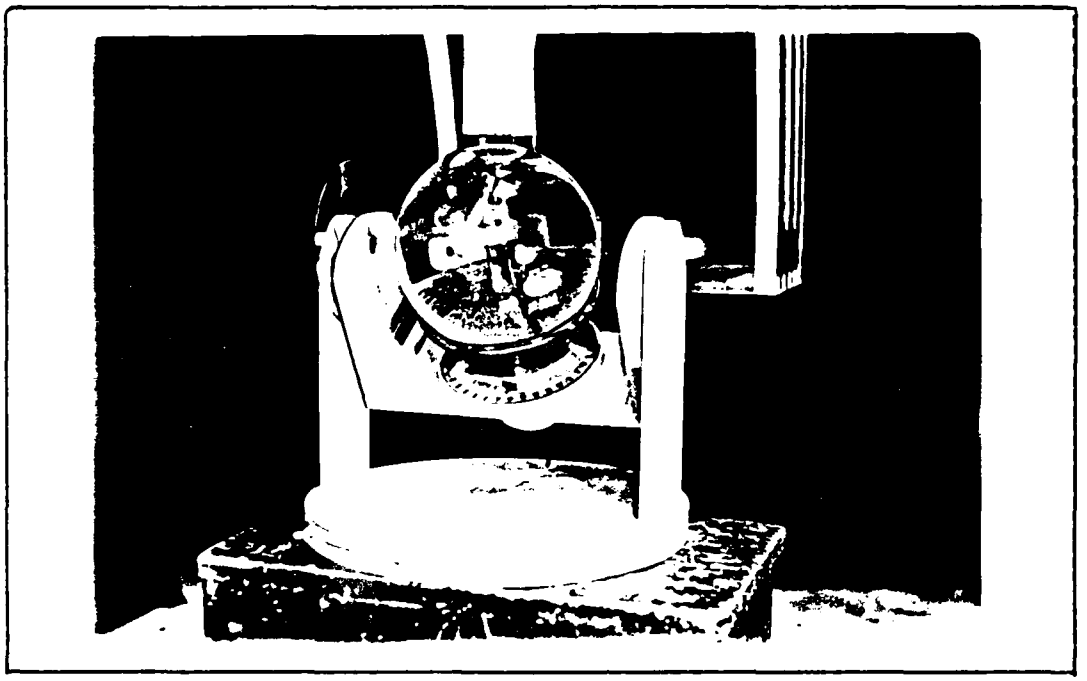

Figure IV-7. The Conducting Sphere and Mount.

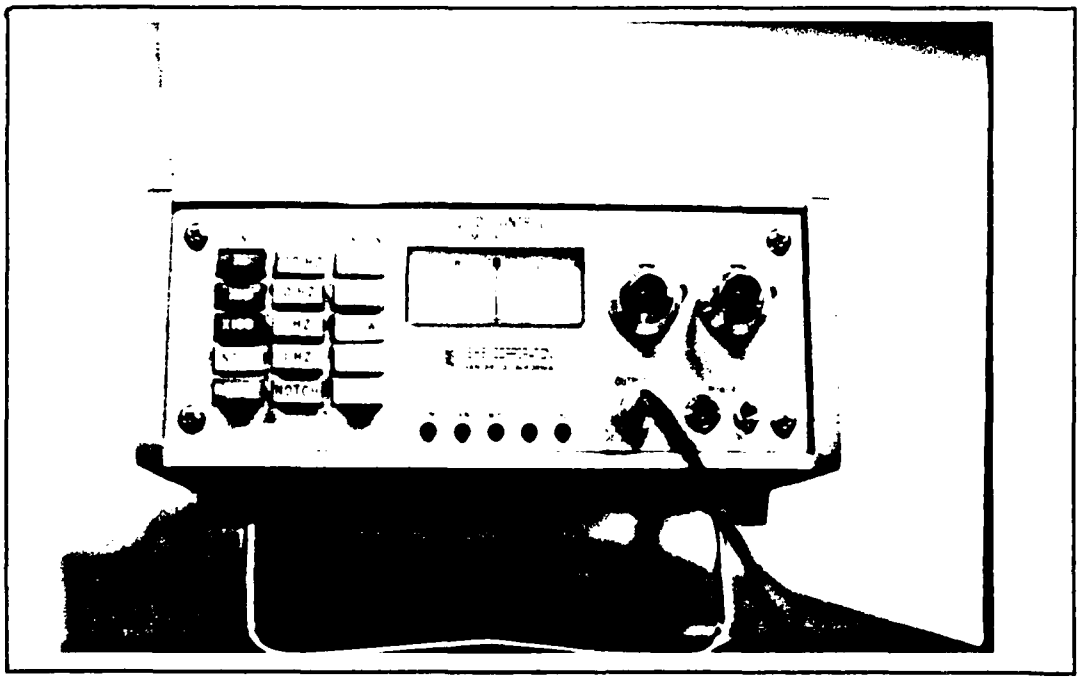

Figure IV-8. The 30X SQUID Controller.

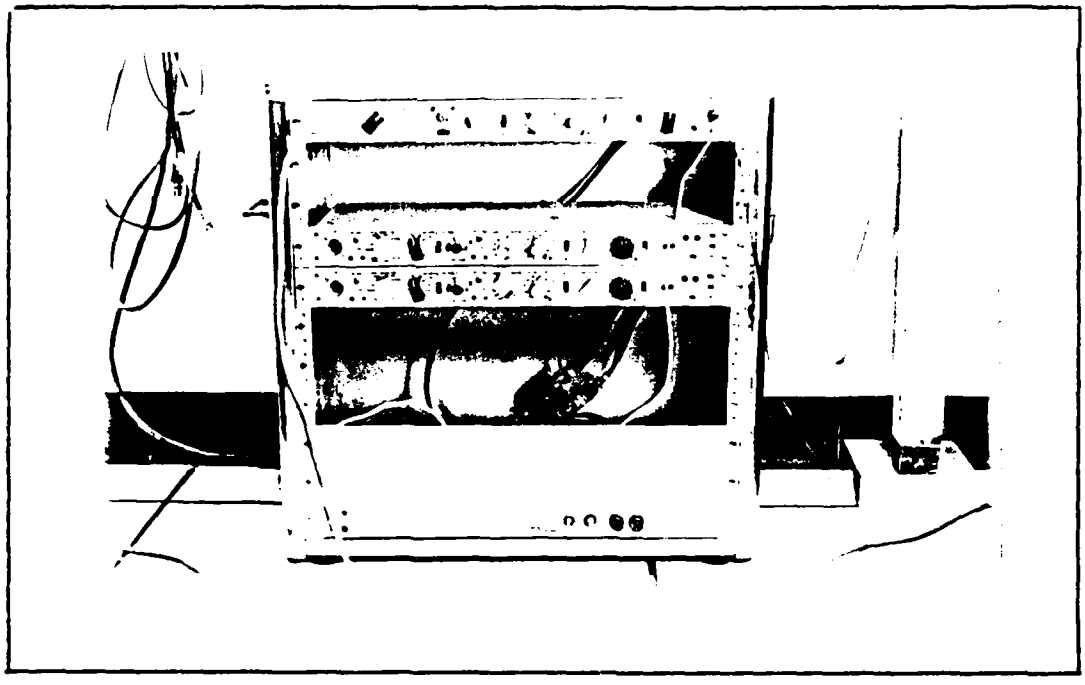

Figure IV-9. MOD.P511H Amplifier.

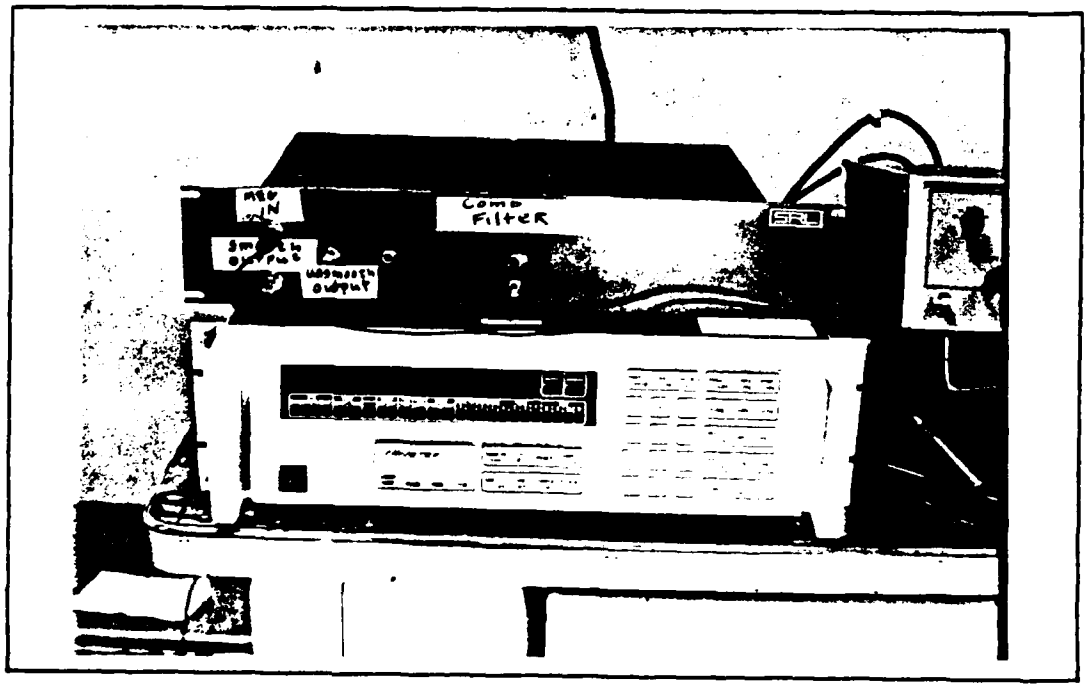

Figure IV-10. Comb Filter and Wavetek 175 Generator.

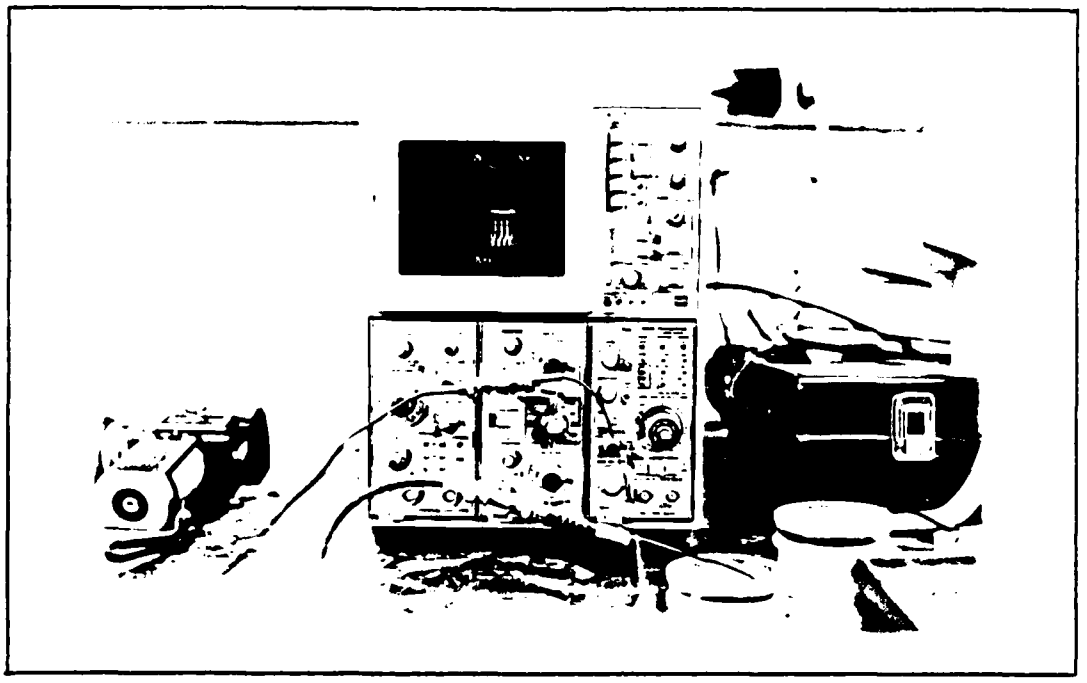

Figure IV-11. Tektronix 7623A Oscilloscope.

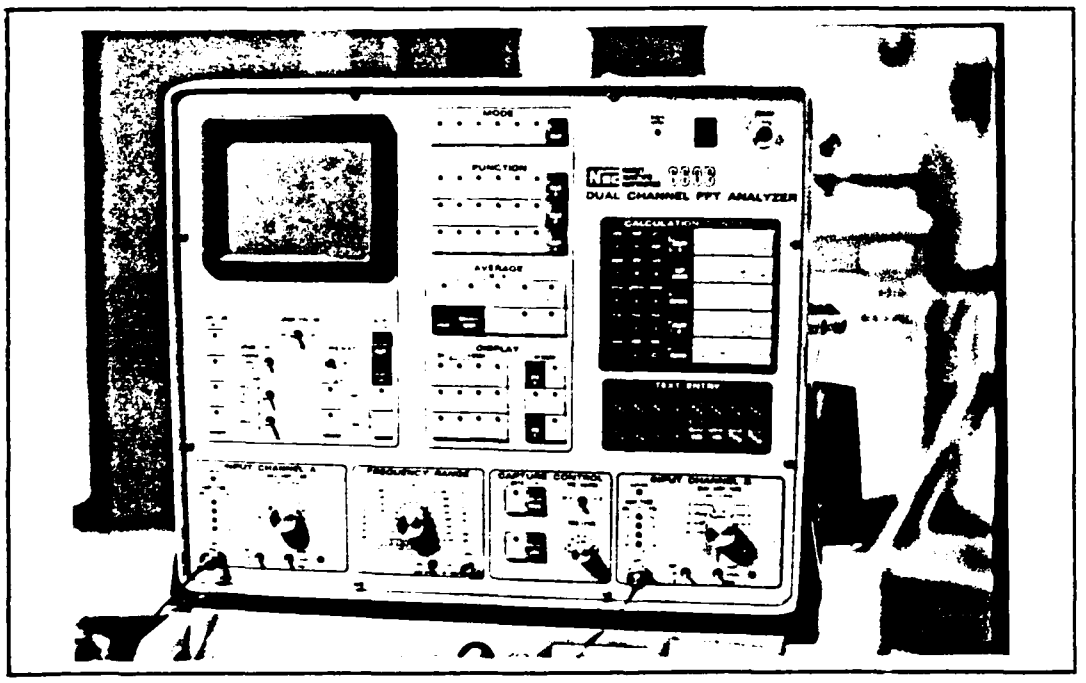

Figure IV-12. Nicolet 660B Dual Channel FFT Analyzer.

Collecting the Data

In the first four experiments, the dipole stack mount was set and clamped to the appropiate orientations. The fifth experiment did not consist of a dipole stack and hence a separate means of supporting the dipoles was used. Figures IV-13 and IV-14 show the dipole mount for the first four and the fifth experiments respectively. Figures IV-15 through IV-19 illustrate the five multipole models examined.

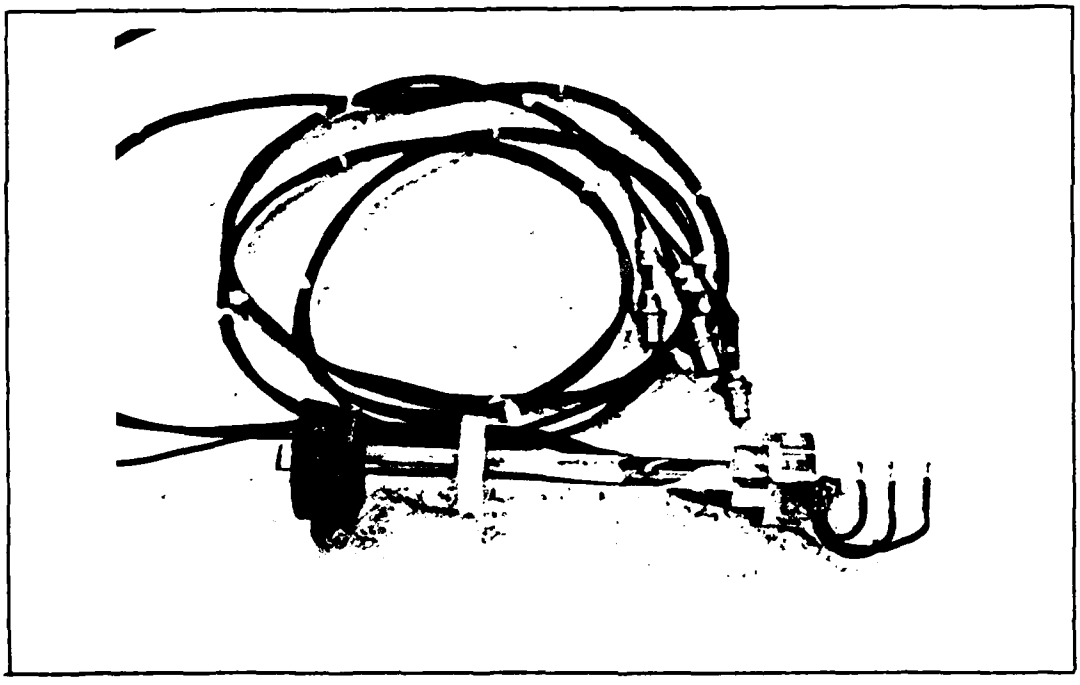

Figure IV-13. The Dipole Mount used in Experiments #1-4.

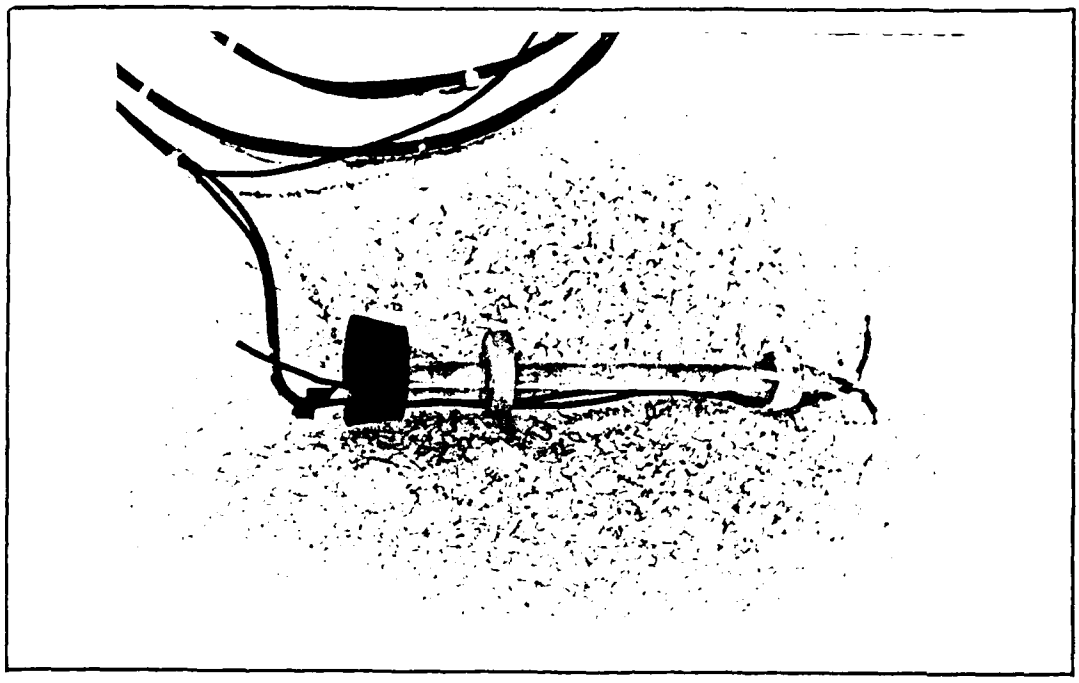

Figure IV-14. The Dipole Mount used in Experiment #5.

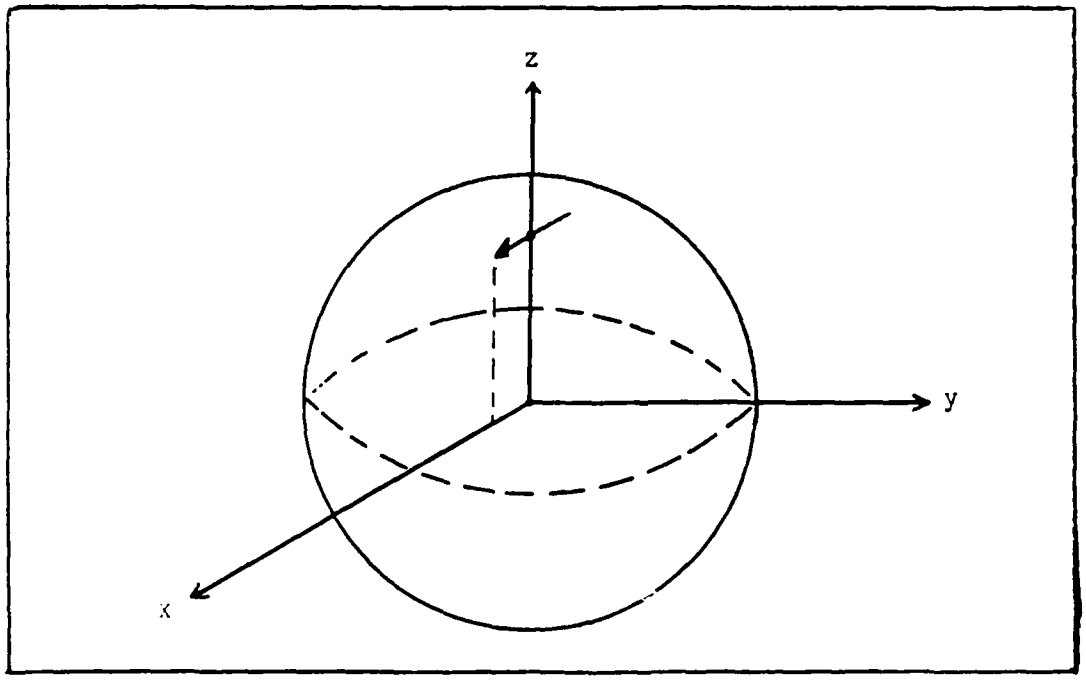

Figure IV-15. Experiment #1 Model.

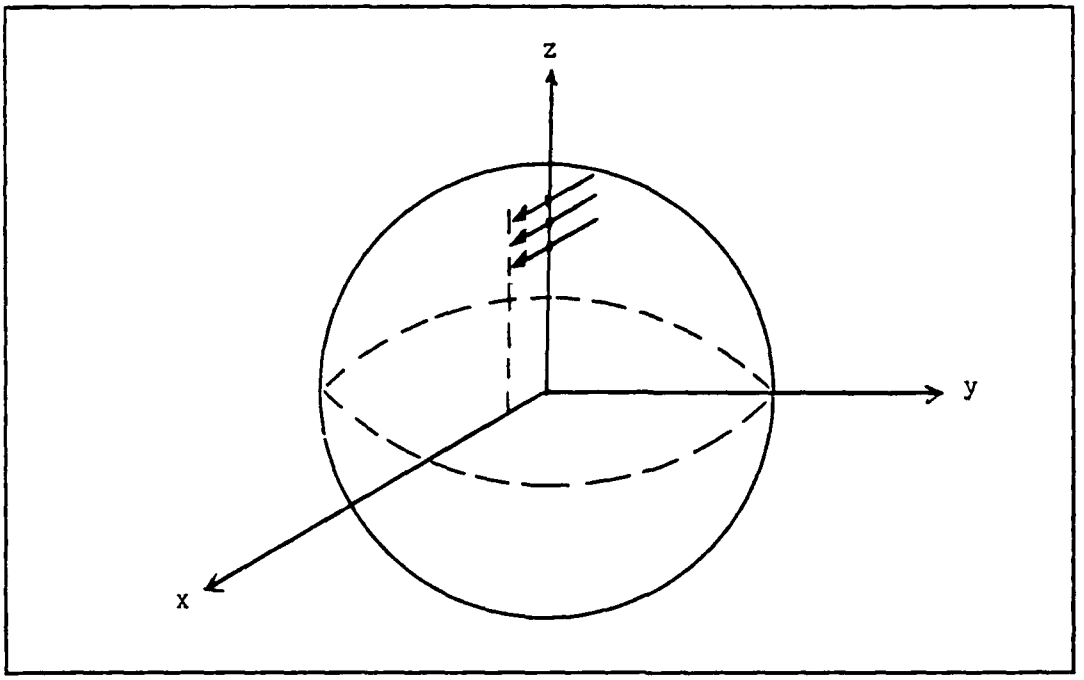

Figure IV-16. Experiment #2 Model.

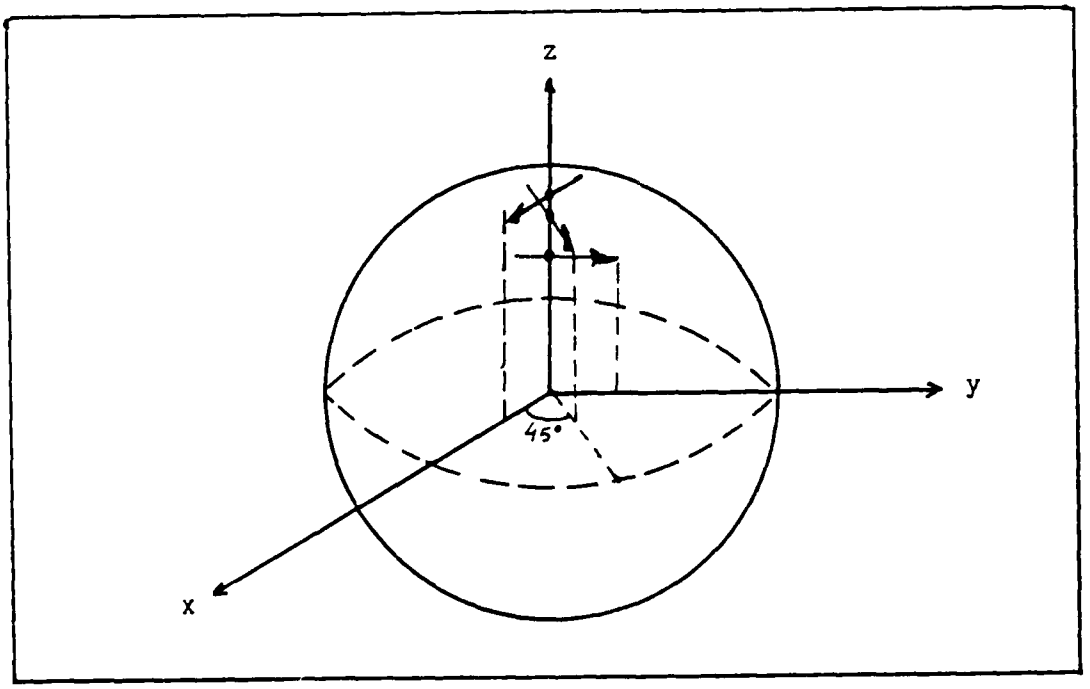

Figure IV-17. Experiment # 3 Model.

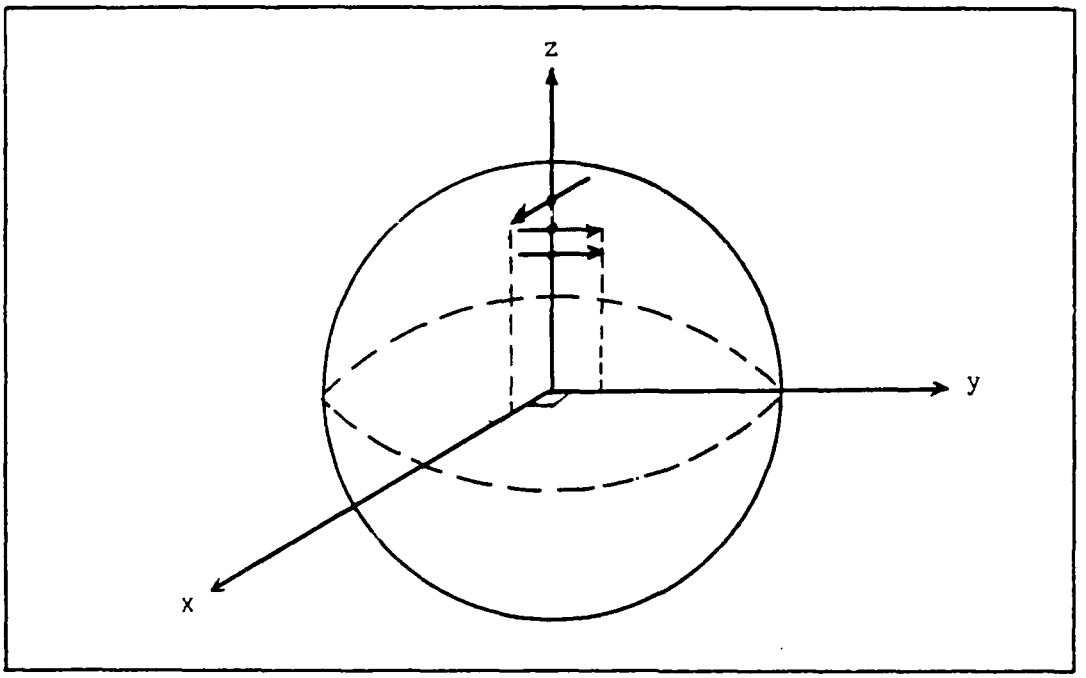

Figure IV-18. Experiment #4 Model.

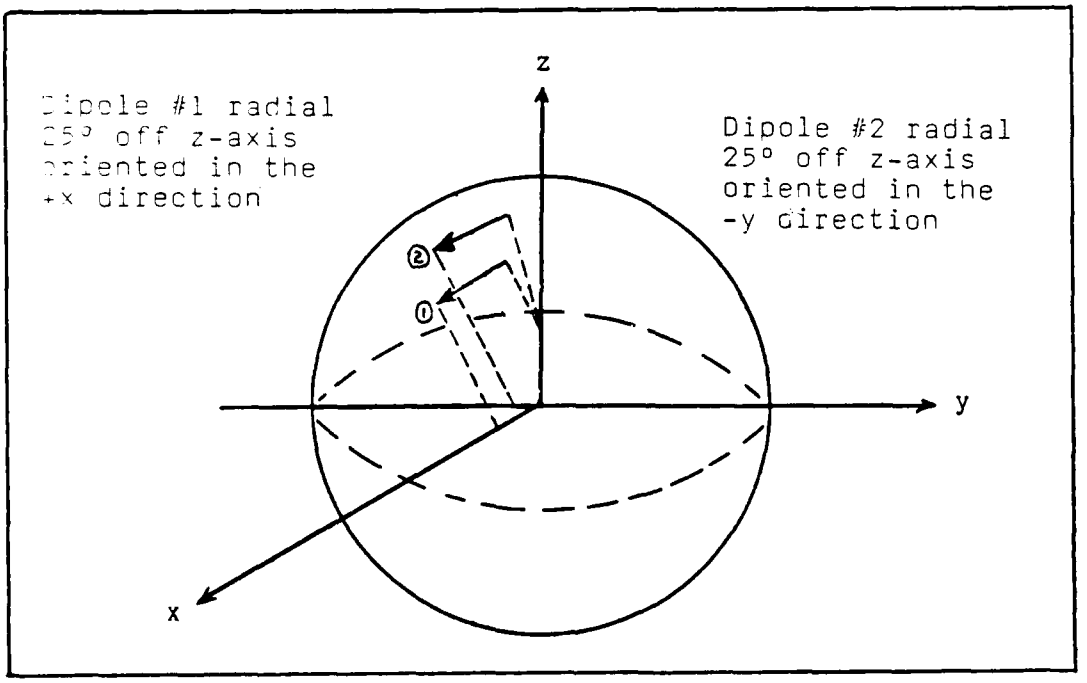

Figure IV-19. Experiment #5 Model.

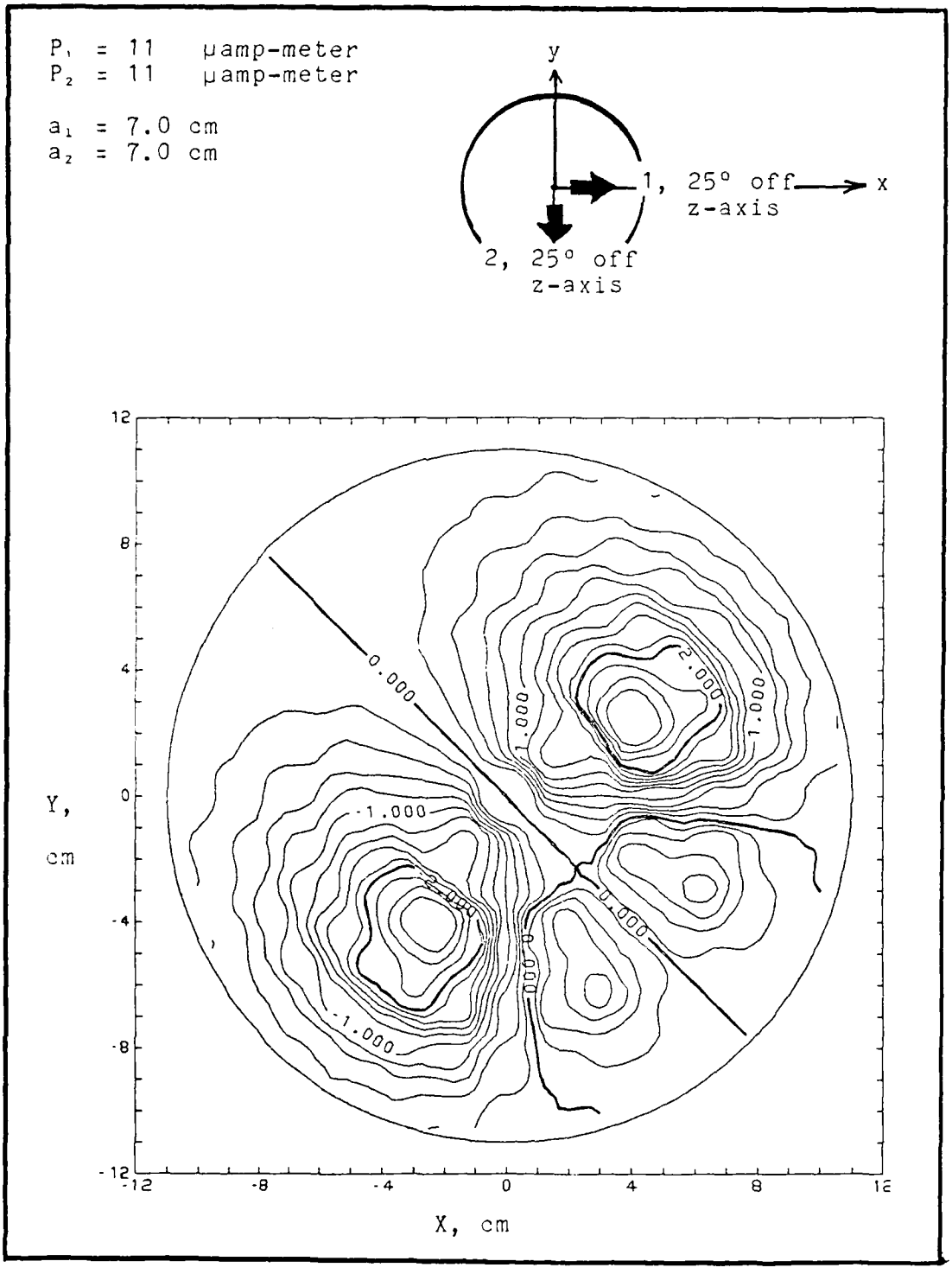

Figure V-9. Calculated Field for Model #5. The measurement sphere radius is 10.98 cm. Magnitudes are given in Tesla XEE-11.

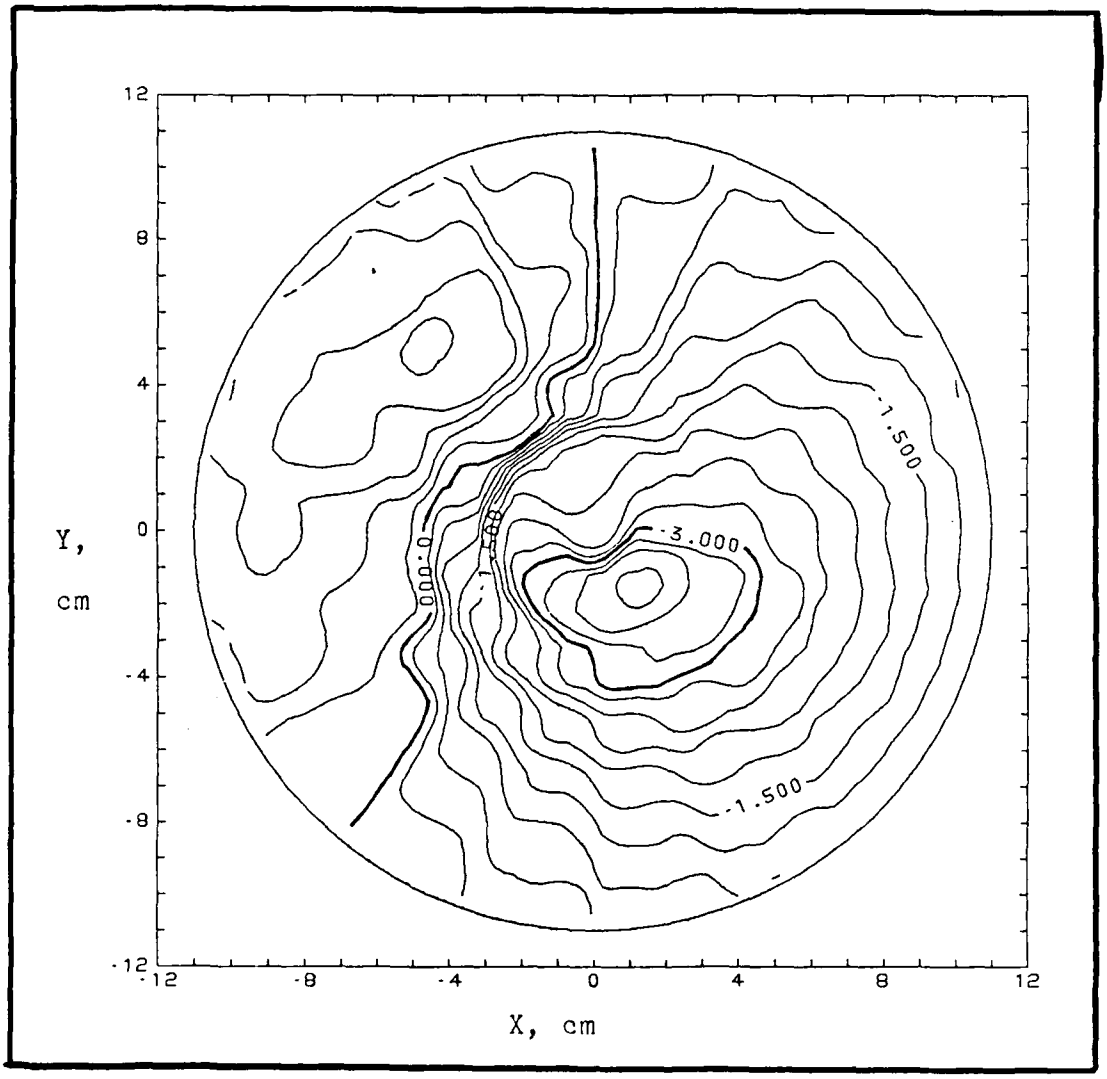

Figure V-8. Experiment Field for Model #4. The measurement sphere radius is 10.98 cm. Magnitudes are given in Tesla XEE-11.

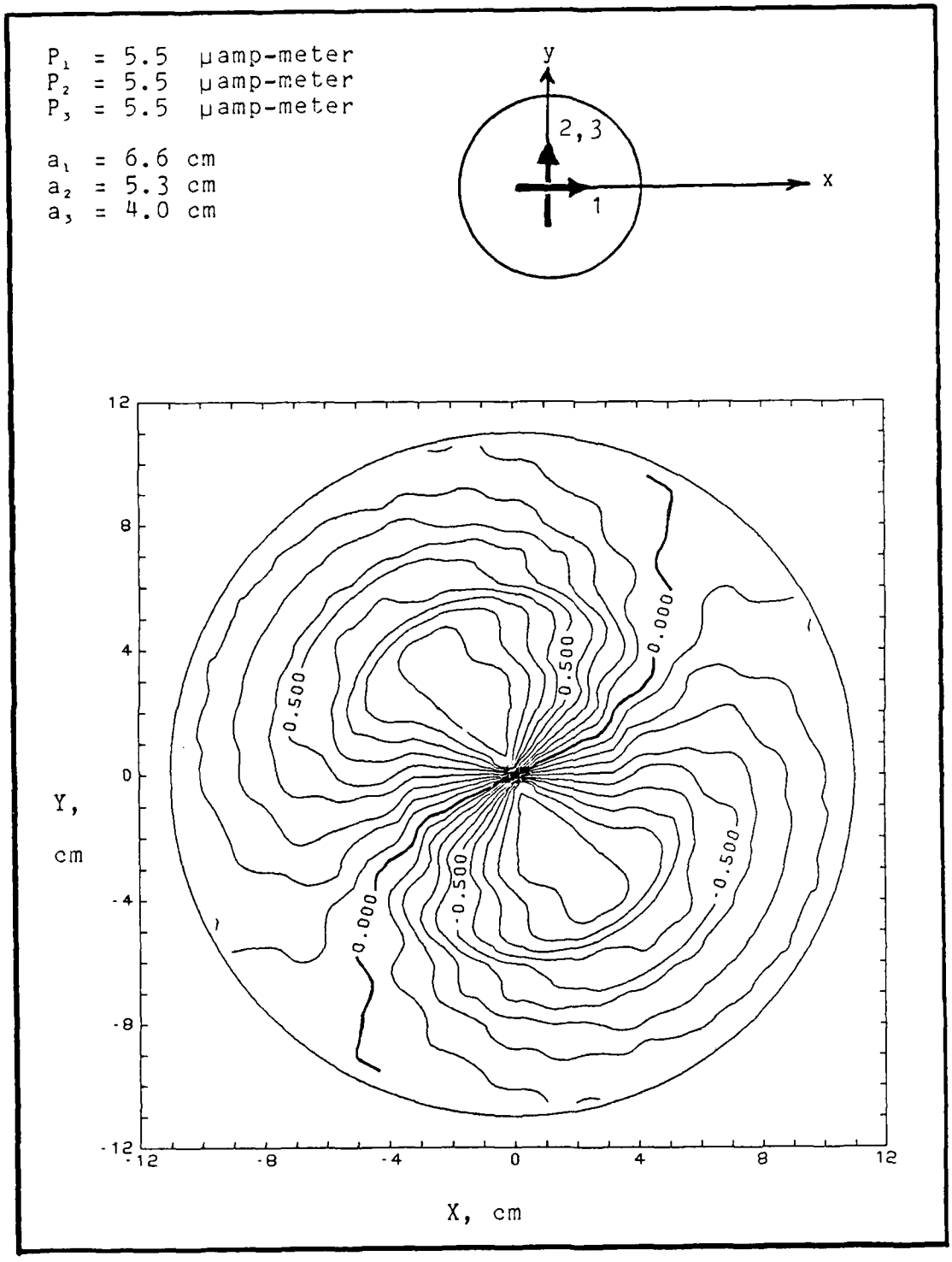

Figure V-7. Calculated Field for Model #4. The measurement sphere radius is 10.98 cm. Magnitudes are given in Tesla XEE-11.

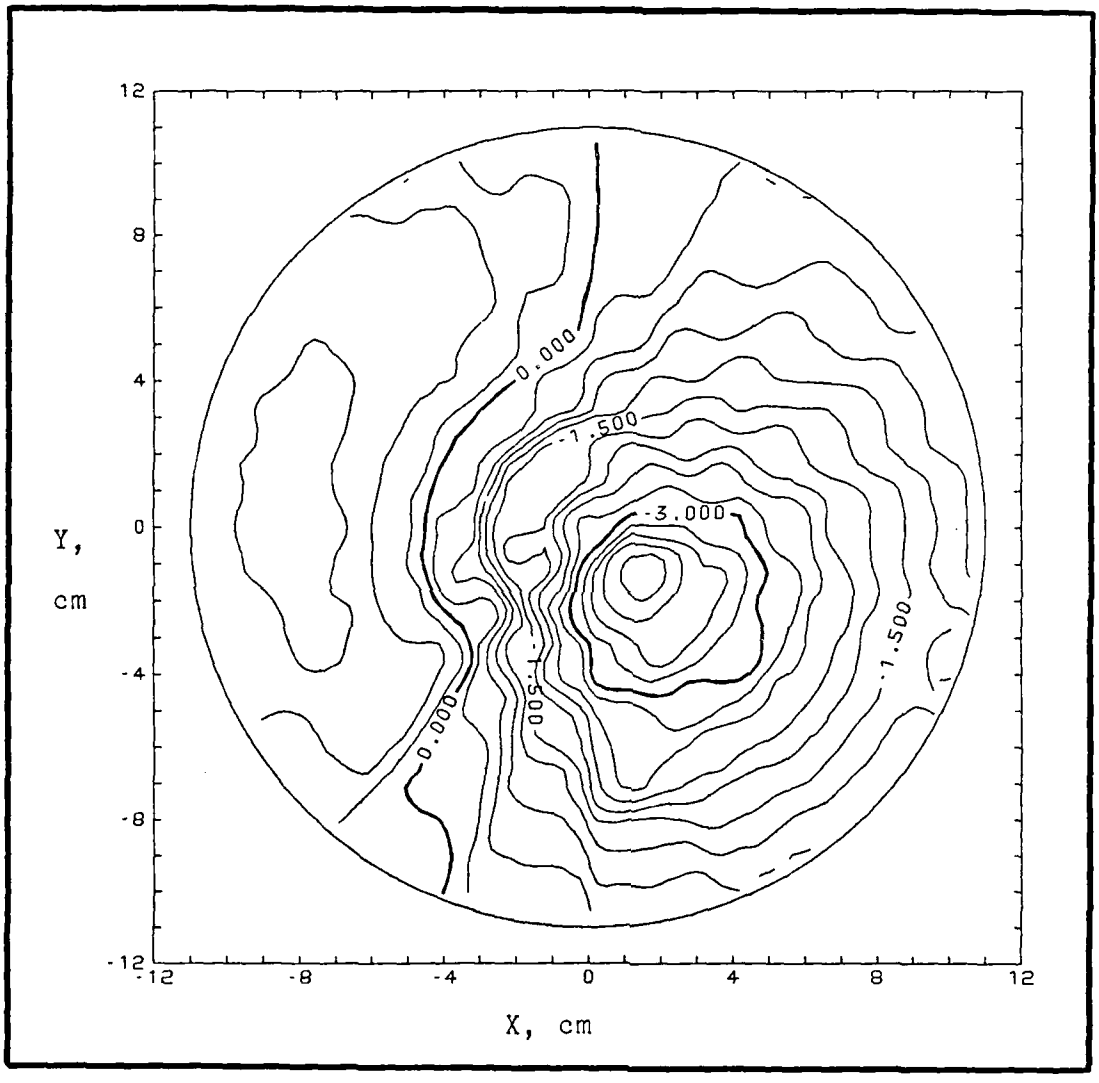

Figure V-6. Experiment Field for Model #3. The measurement sphere radius is 10.98 cm. Magnitudes are given in Tesla XEE-11.

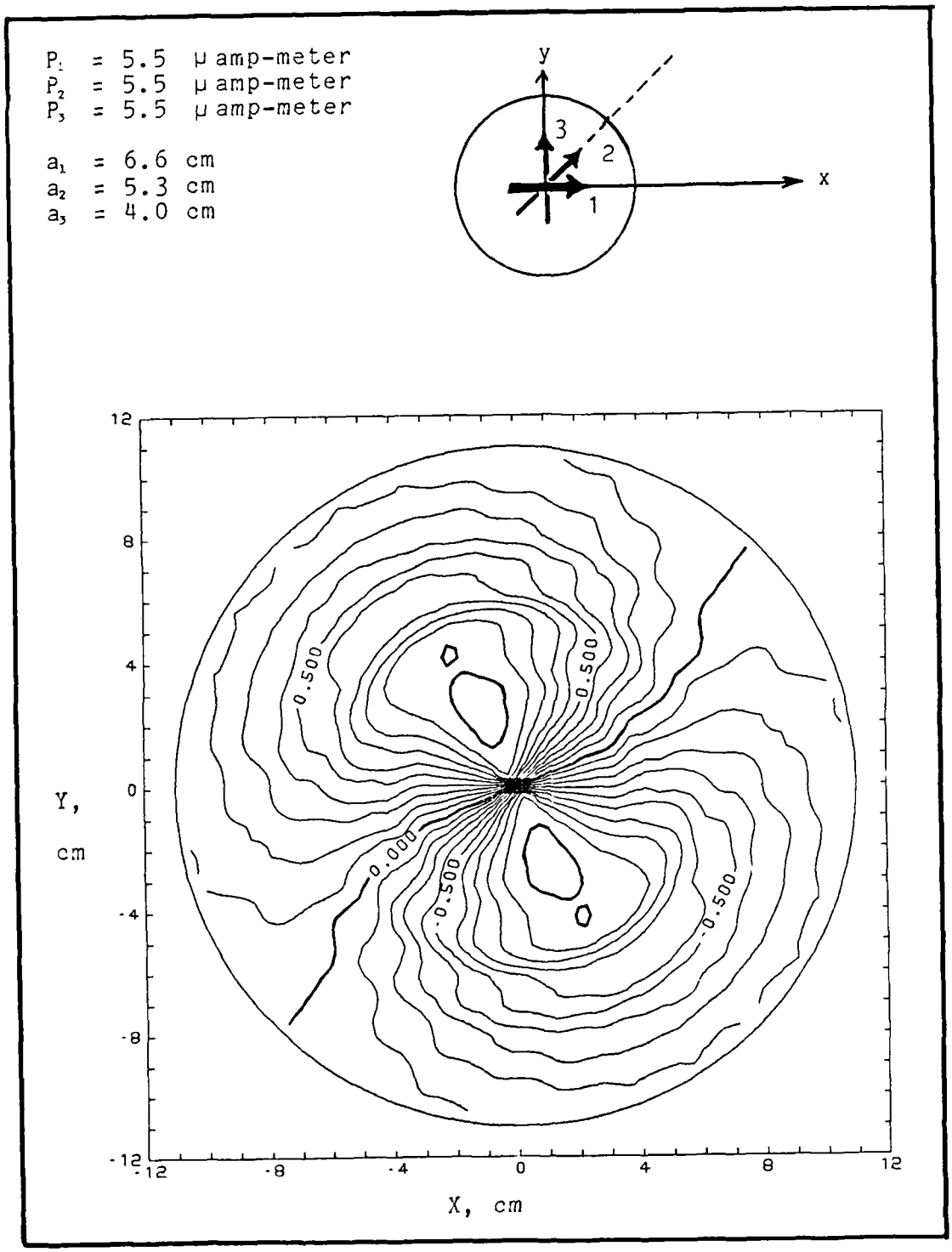

Figure V-5. Calculated Field for Model #3. The measurement sphere radius is 10.98 cm. Magnitudes are given in Tesla XEE-11.

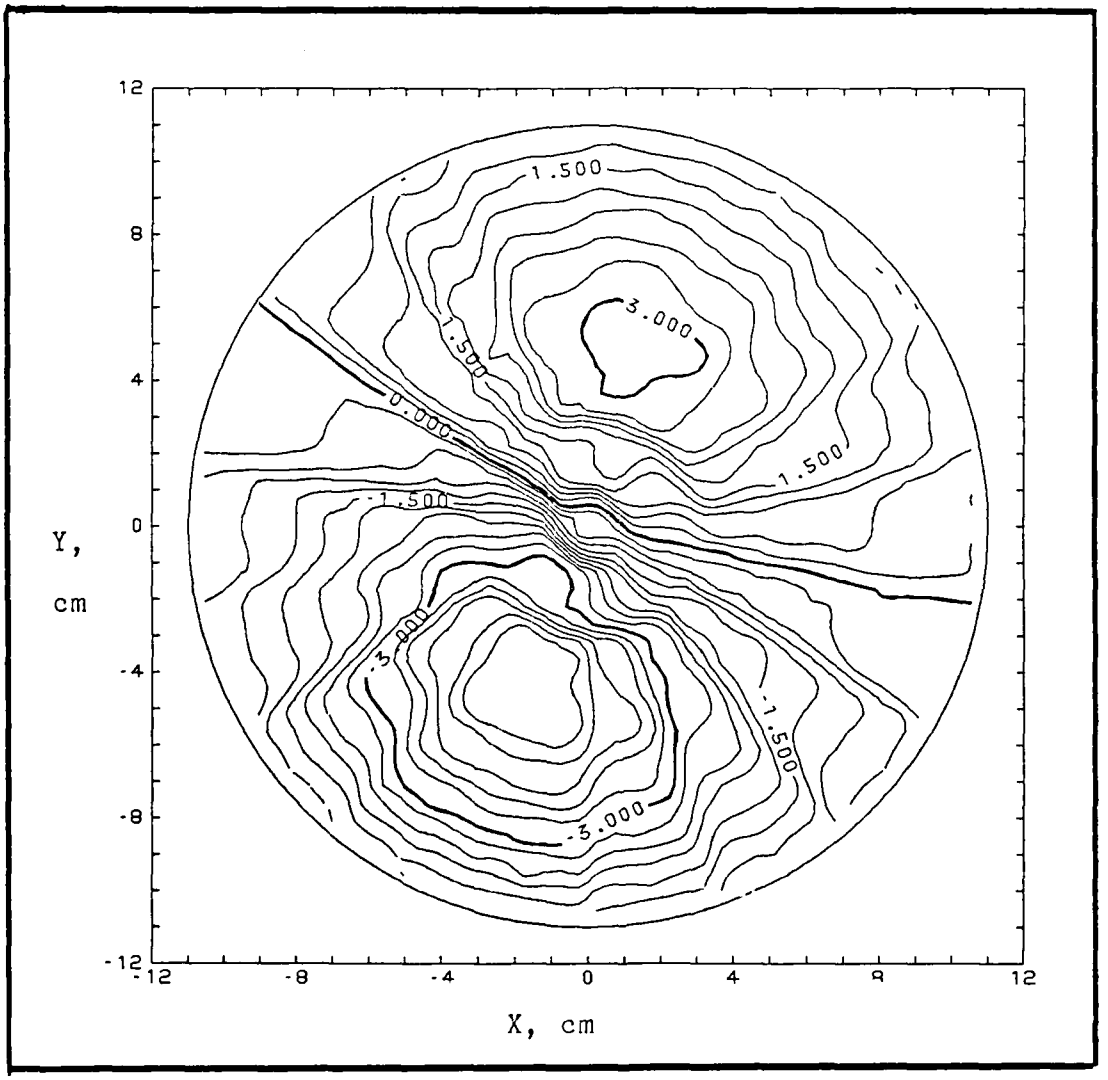

Figure V-4. Experiment Field for Model #2. The measurement sphere radius is 10.98 cm. Magnitudes are given in Tesla XEE-11.

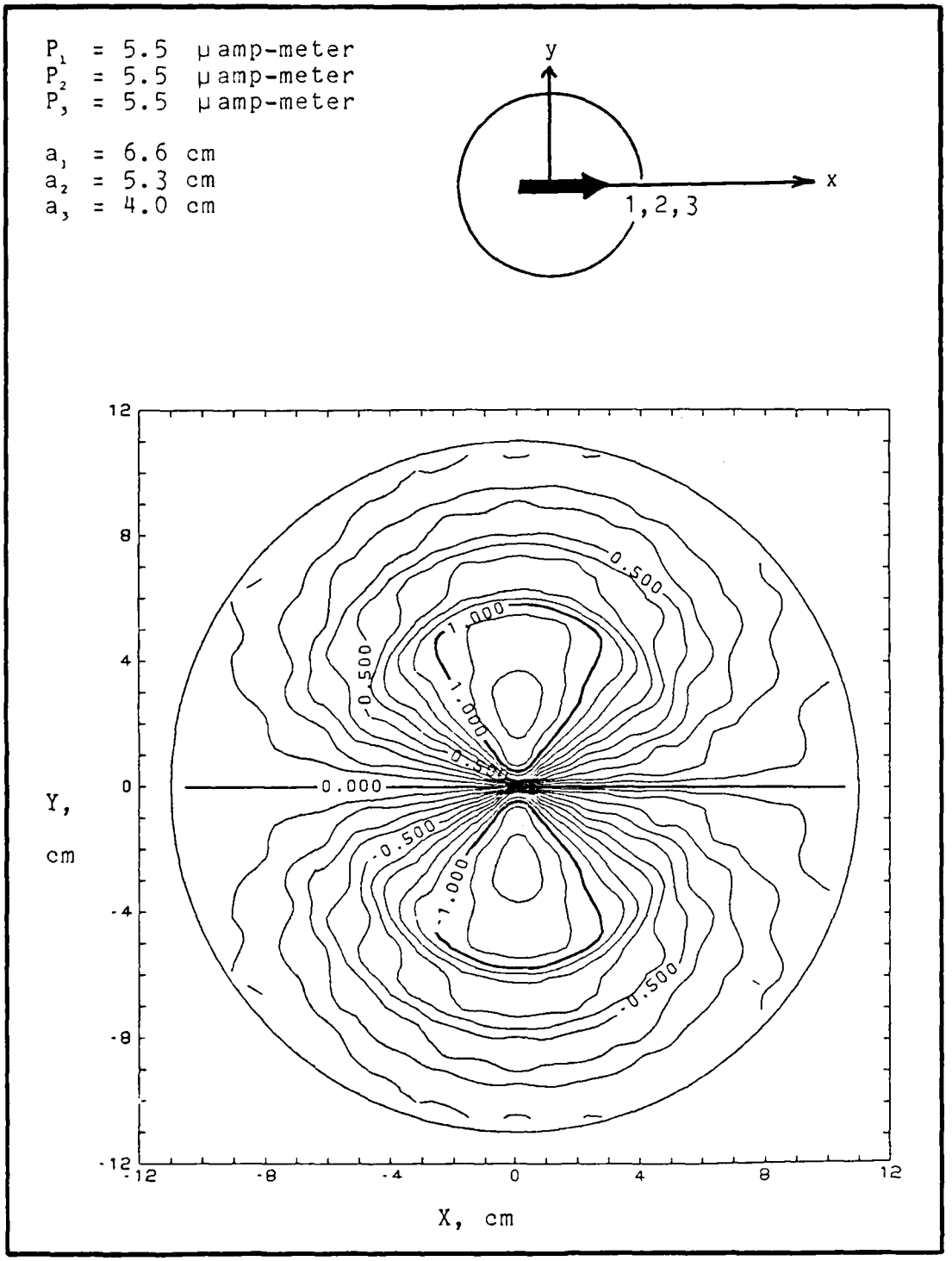

Figure V-3. Calculated Field for Model #2. The measurement sphere radius is 10.98 cm. Magnitudes are given in Tesla XEE-11.

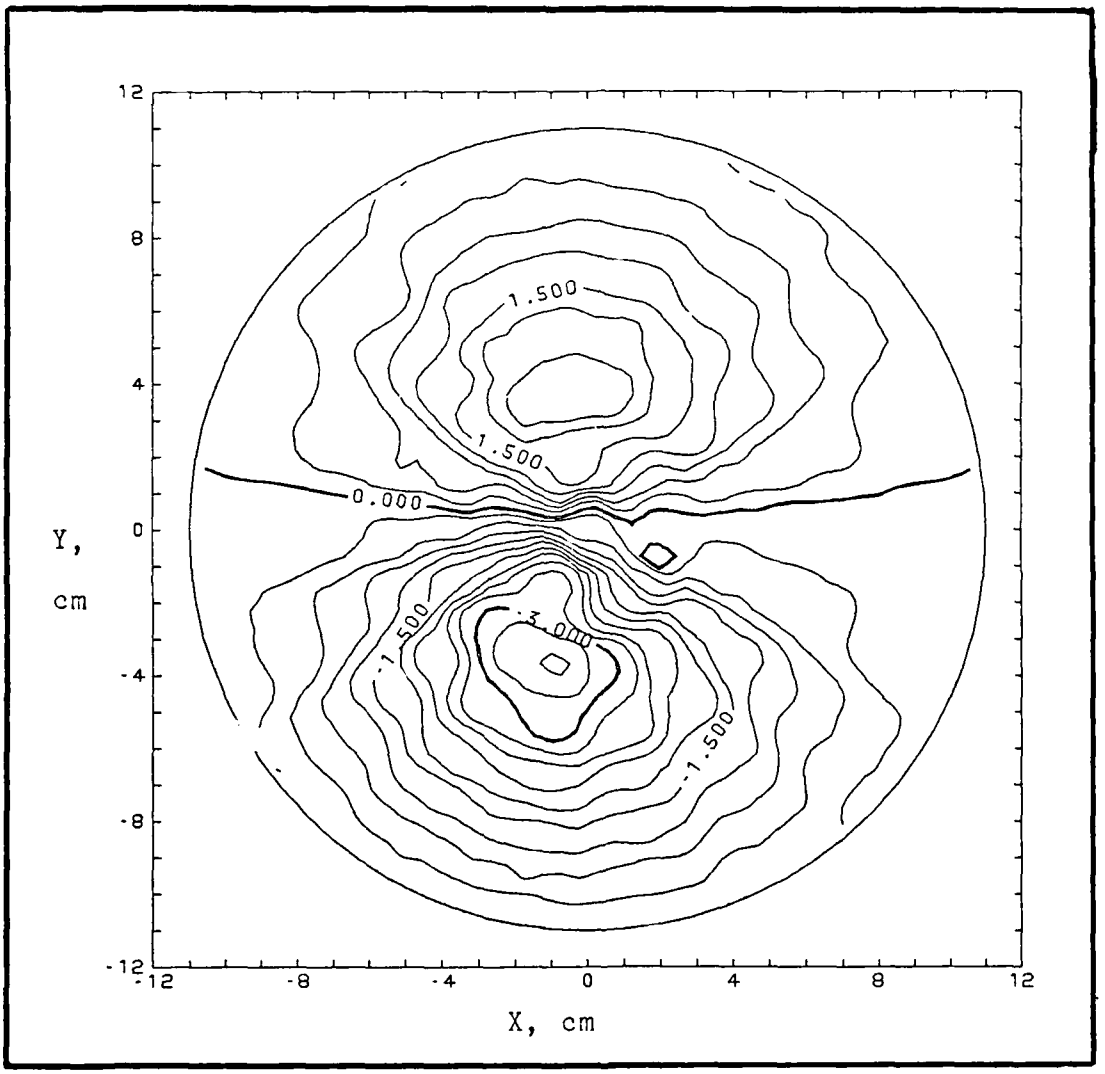

Figure V-2. Experiment Field for Model #1. The measurement sphere radius is 10.98 cm. Magnitudes are given in Tesla XEE-11.

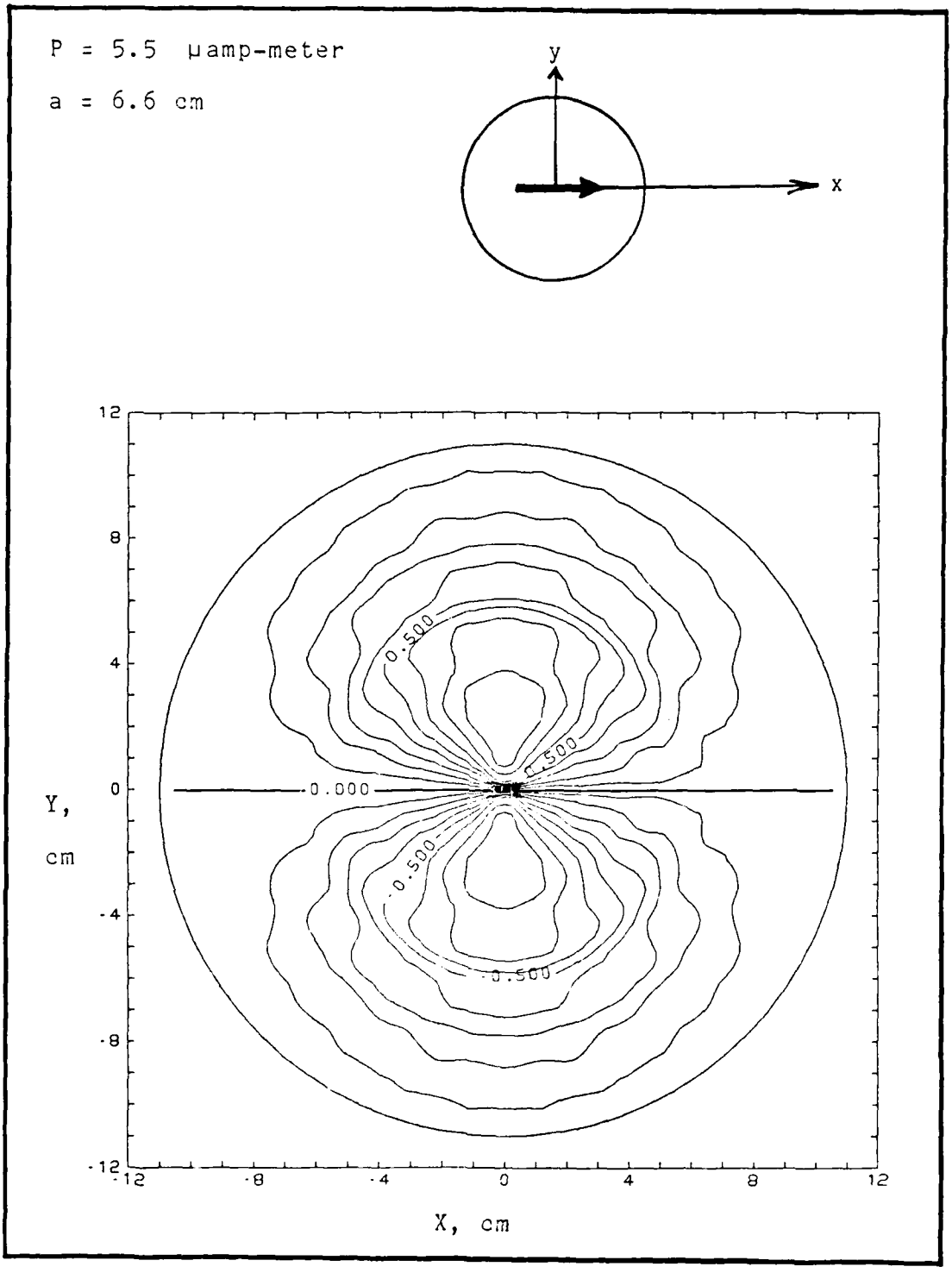

Figure V-1. Calculated Field for Model #1. The measurement sphere radius is 10.98 cm. Magnitudes are given in Tesla XEE-11.

When model #5 was evaluated in the conducting sphere experiment, the "primary null + branches" field did not completely form. Note from figure V-10 that the positive flux peak belonging to the -y oriented dipole did not appear. However, the contour lines in the vacinity do indicate the peak's presence. By inspecting the calculated field of figure V-9, it is apparent that this missing peak should have appeared at the coordinant (-5,4). It is believed that imperfections in the experimental model plus sphere inhomogenetıes resulted in the positive peak being swallowed up by the neighboring negative peaks.

The data used to plot the computer generated fields and the actual fields measured with the second order SQUID gradiometer are given in appendixes C and D respectively.

the fields took on a twisted appearance as compared to the first two models. The null line favors the shallow dipole at field points directly above the dipole stack, and favors the deeper dipoles at field points away from the dipole stack.

The fields plotted for the first four experiment models are highly distorted. The primary cause for this distortion is believed to be related to the dipole mount. The 3rd and 4th experiments show more distortion since the rotated mounts interfere to a higher degree with the current densities. The dipoles in the 5th experiment were held in place by a far less bulky mount and thus caused the least distortion.

The 5th model considers the field generated by two dipoles located on different radials. The calculated field was found to have a branched null line. The primary null followed the average direction of the contributing dipoles with the branches extending from the primary null and passing over the vacinity of respective dipoles. See figure V-9. An additional computer generated plot (not included in this report) showed that as the dipoles of model #5 were moved closer to the sphere origin, the null branches moved closer to the primary null. For deep model #5 dipoles, the branches fused with the primary null, thus eliminating the two close proximity density peaks and resulting in a plot resembling that of a dipole stack. This result is expected since the dipoles will meet in the limit of reaching the origin.

V. Results

Recall the five models shown in figures VI-15 through VI-19. Two plots were drawn for each of the five models:

1. Calculated field
2. Experiment field

Each plot is an overhead view of the equi-magnitude magnetic flux density contours that encompass the measurement sphere. An overhead diagram with the parameters describing the various dipole locations and orientations is included with the calculated field plot. See figures V-1 through V-10.

When comparing the computer generated field with the conducting sphere experiment field, both similarities and discrepancies are noticed. In each model, first note the similarity of the general form of the two fields. A null contour separates the positve flux densities from the negative flux densities and maximum density peaks appear within an expected region.

The data of the experiment plots are on the same order of magnitude but about three times larger than the calculated data. This result indicates that the measurement sphere radius used in the calculated fields may have been too small. This is a real possibility since the actual radius was difficult to measure and the magnetic field varies as the square of the distance. Since this factor remains consistent throughout the data, important contour shape information is preserved.

As the dipoles were rotated in the 3rd and 4th models,

The polarity of the detected flux with respect to the input voltage was determined by the phase shift between the dipole input voltage and the SQUID output voltage. Recall from chapter II that the output voltage lags the input voltage for positive flux (w.r.t. input) and leads for negative flux (w.r.t. input). For each measurement point, the 660B also calculated the transfer fuction of the output/input. In the collection of the data, corresponding phase shifts where primarily clustered into two groups approximately 180 degrees apart. Phase shifts that deviated from the rule greatly were associated with very low signals and were assumed to be near the null contour. Using the right hand rule as a guide, positive phases were assigned negative flux densities and negative phases were assigned positive flux densities.

In each of the five experiments, the conducting sphere was placed one centimeter directly beneath the SQUID dewar. With both sphere orientation angles set to zero, the linear axis of the SQUID was set to coincide with the z-axis of the sphere.

Data collection was accomplished by systematically rotating the gimbal mounted sphere to spherical grid points defined by the horizontal and vertical protractors. The grid consisted of 163 points in the northern hemisphere only. The measurement points were converted to cartesian coordinants and their resulting x-y values are given in the experimental data listings of appendix D.

For each point, the 660B spectrum analyzer averaged 5 output voltage measurements over a span of 20 seconds. The following factors were used to convert the detected RMS voltage to magnetic flux density (Ref 22):

SQUID sensitivity on x10 scale ..	1.74×10^{-7} gaus/volt	
Grass amplifier	x100,	+134 shift @ 25 Hz
60 Hz Comb filter	x1,	+2 shift @ 25 Hz

$$1.74 \times 10^{-5} \text{ gaus/v}_1 \quad X \quad 10^{-4} \text{tesla/gaus} \quad X \quad \frac{1v_1}{100v_2}$$

$$= \boxed{1.74 \times 10^{-11} \text{tesla/v}_2} \qquad (16)$$

where,

v_1 = output of 330X control unit
v_2 = output of Grass amplifier

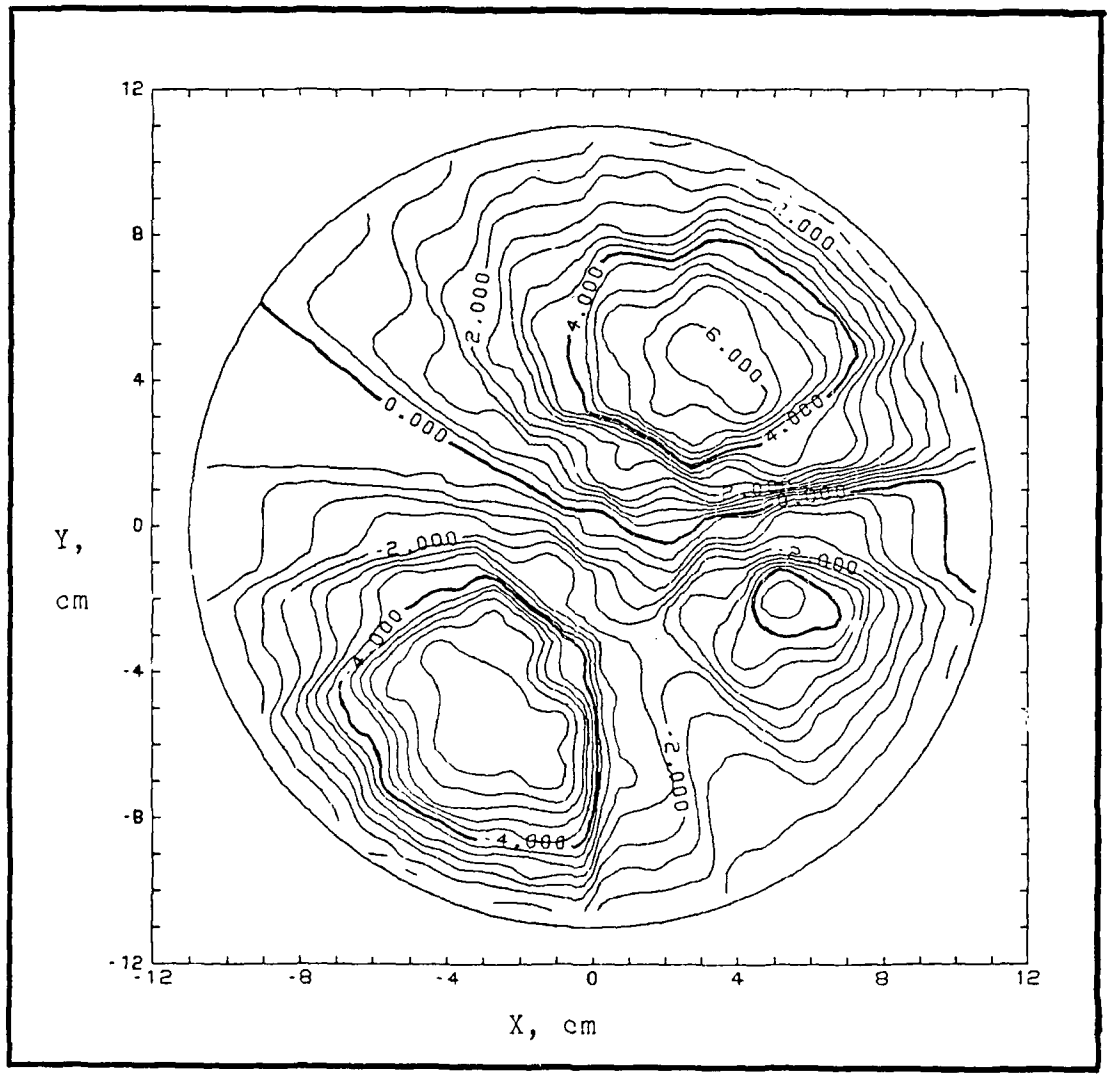

Figure V-10. Experiment Field for Model #5. The measurement sphere radius is 10.98 cm. Magnitudes are given in Tesla XEE-11.

VI. Discussion and Conclusions

The model developed in this study considers the simple case of a homogeneous conducting sphere. The external radial magnetic field component existing outside the sphere results from the dipole currents alone. Cuffin and Cohen (12:374-375, 381) showed that the volume currents have negligible or zero contribution.

The perfect homogeneous sphere, however, could not be replicated in the actual conducting sphere experiments. The presence of the dipole wires, mount, etc, does not allow the volume currents to symmetrically cancel. This was most prominent in the cases where a large mass of nonconducting material was present near the active dipoles. As a result, the unsymmetric volume currents did contribute substantially to the detected field and warped it with respect to the homogeneous model. Here, it should be noted that the degree of field warping is dependent on the proximity of gross inhomogeneties to the active dipoles.

Multipole Array Field Estimator

Recall that the desired goal of modeling the magnetic field activity of the cerebral cortex is to find the simplest description of the sources that produce the observed field pattern. This may be achieved by modeling the cortex as an array of stacks containing one, two, or three dipoles each. Cortical folds rich in pyramidal cells tangential to the head surface would be expected to have a larger stack than surface

cortex and thus have a greater contribution to the detected field.

The parameters required to describe each dipole must include dipole moment, distance from the origin, and a 3X3 transformation matrix defining dipole orientation. With 11 parameters required for each dipole, the number of model variables can grow to an enormous size. Since this size can be reduced when modeling isolated sources by setting most of the dipoles to zero, the overall cerebral cortex model may be developed from the summed effects of the reduced models.

Of course the complete functional computations of the cortex are far too complex to consider presently. It is, however, reasonable to develop models of observed fields with the dipole parameters describing isolated brain states. If a given state can be modeled reliably, it may be possible to apply stochastic estimation techniques successfully.

For example, consider the estimation of 2 states within the motor cortex corresponding to the flexion and extension of the index finger. Each state must be described by several parameters indicating all pertinent dipole contributions. Although isolated state fields may be obtained through repetitive averaging experiments, specific dipole locations are difficult to determine in the case of a multipolar source. State dynamics and noise characteristics also need to be fully understood.

The uncertain model parameters may be estimated through maximum likelihood techniques. The likelihood is a function of the parameters to be estimated and the measured data. The

goal is to find the value of the parameter vector that maximizes the likelihood function. These techniques are covered in detail in chapter 10 of reference 23.

At this point it is not even known if state and parameter estimation is possible. Many experiments need to be accomplished before the models may even be considered an adaquate representation.

Recommendations for Continuing Studies

Data collection using a single second order SQUID requires hours of work before a field plot can be generated. If just one SQUID is available, it is suggested to automate data collection with a digital computer. This could be done by using the output ports of the 660B spectrum analyzer to transmit magnitude and phase data directly to a plot file. Although the conducting sphere, or subject, would have to be manually placed, the plot turnaround time could be significantly reduced.

The most desirable system would allow all data points to be taken simutaneously. A multi-array SQUID would surely enhance these experiments. In the interest of studying real time cerebral fields, the desired magneto-encephalography analyzer should include an array of at least 100 semiconductor SQUIDs.

Conclusion

This project took Grynszpan's dipole in a sphere model and expanded it to include any combination of three

tangential dipoles. The results show that dipoles oriented on a stack do not produce multiple peaks, but rather a twisted version of a single dipole field. Dipoles located on different radials will produce multiple peaks provided the dipoles are separated by a measurable distance.

The experiments using an actual conducting sphere support the model results. The pyrex mount used to support the dipoles caused a disturbance in the volume currents. It was found that the greatest field distortion occured when large masses of the nonconducting pyrex were near the active dipoles.

Mathematical modeling of cerebral cortex activity is still in its infancy. The rapid advancement of multiarray SQUID technology is necessary to develop experiments needed to determine model adaquacy.

Appendix A

This section contains the Fortran 77 routine and the IBM 30/30 control language used to generate the calculated field data. Also included is an example execution of the program.

Job Control Language for MAGCAL2

```
00010 PROC 1 SERIES
00020 CFREE ATTR(XXX) FI(FT11F001,FT12F001,FT14F001)
00030 ATTR XXX RECFM(F B) LRECL(80) BLKSIZE(12960)
00040 ALLOC FI(FT11F001) DA(SPHR&SERIES.) NEW TRACK SP(2,2) USING(XXX)
00050 ALLOC FI(FT12F001) DA(XYPL&SERIES.) NEW TRACK SP(2,2) USING(XXX)
00060 ALLOC FI(FT14F001) DA(XZPL&SERIES.) NEW TRACK SP(2,2) USING(XXX)
00070 CALL (MAGCAL2)
END OF DATA
```

CLIST Data to Control MAGCAL2

```
00010 //HETPJD2 JOB   HET,DEREGO,NOTIFY=HETPJD,TIME=(2),MSGCLASS=Z
00020 // EXEC FORTVCL
00030 //SYSPRINT   DD SYSOUT=Z
00040 //FORT.SYSIN DD DSN=HETPJD.FORT(MAGCAL2),DISP=SHR
00050 //LKED.SYSLMOD DD DSN=HETPJD.LOAD(MAGCAL2),DISP=(NEW,CATLG),
00060 //  UNIT=DISK,VOL=SER=PACK01,SPACE=(TRK,(10,10,2)),
00070 //  DCB=SYS1.LINKLIB
END OF DATA
```

Program MAGCAL2

```
C                    MULTIDIPOLE IN A SPHERE
C
C                       1LT PAUL J. DE REGO
C                       AFIT, WPAFB, OHIO
C                       OCTOBER 30, 1984
C
C      THE PROGRAM CALCULATES THE MAGNETIC FLUX
C     DENSITY, AT A UNIFORM RADIUS, DETECTED BY THE AFMRL
C     SQUID GRADIOMETER OUTSIDE A CONDUCTING SPHERE CON-
C     TAINING 3 CURRENT DIPOLES.
C
C      THE CALCULATIONS USED ARE BASED ON GRYNSZPAN'S
C     RADIAL FIELD EQUATION.  REVISIONS INCLUDE AN EXPAN-
C     SION TO INCLUDE THREE TANGENTIAL DIPOLES POSITIONED
C     ANYWHERE IN THE CONDUCTING SPHERE.
C
C      CONCEPTIONALLY, THE GRYNSZPAN MODEL IS ROTATED.
C     COMPUTATIONALLY, THIS IS DONE BY DESCRIBING THE
C     MEASUREMENT POINT OF THE STANDARD CARTESIAN COORDINATE
C     SYSTEM IN THE ROTATED CARTESIAN COORDINATE SYSTEM.
C     THE POINT IS TRANSFORMED TO SPHERICAL COORDINATES
C     W.R.T. THE ROTATED SYSTEM AND THEN THE FIELD IS CAL-
C     CULATED USING GRYNSZPAN'S EQUATION.
C
C      THE MEASURING POINT IS TRANSFORMED FOR EACH DIPOLE
C     SEPARATELY.  THE RESULTS ARE SUMMED AND STORED AS THE
C     FIELD OF THE POINT W.R.T. THE STANDARD SYSTEM IN BOTH
C     SPHERICAL AND CARTESIAN COORDINATES.
C        THE INPUT AND OUTPUT DATA ARE RECORDED IN A
C     SINGLE FILE.  FROM THE DATA TWO ADDITIONAL FILES,
C     FIELD ABOVE XY PLANE AND FIELD ABOVE XZ PLANE,
C     ARE CREATED. THESE TWO FILES ARE COMPATIBLE
C     WITH THE SURFACE II CONTOUR PROGRAM.
C
C     VARIABLE KEY
C        INPUT:
C     P = DIPOLE MOMENT                                    (AMP-M)
C     A = DISTANCE BETWEEN TANGENTIAL DIPOLE & ORIGIN      (M)
C     R = MEASUREMENT SPHERE RADIUS (1ST GRAD COILS)       (M)
C     C1-C9 ..... 3X3 TRANSFORMATION MATRIX
C
C        OUTPUT:
C     1. MEASUREMENT SPHERE FILE
C     2. XY PLANE PROJECTION FILE
C     3. XZ PLANE PROJECTION FILE
```

```
C
C           BD .....2ND ORDER DETECTED FLUX DENS.....(TESLA)
C
C           R  .....SPHER COOR PARAMETER.............(M)
C           T+B, F+B ..SPHER COOR PARAMETERS..........(RADIANS)
C
C           X, Y, Z  ..CART COOR PARAMETERS..........(CM)
C
C ------------------------------------------------------------
      INTEGER T,F,I
      REAL P(3),A(3),R,C1(3),C2(3),C3(3),C4(3),C5(3),C6(3),
     +C7(3),C8(3),C9(3)
C ------------------------------------------------------------
C
      DO 20 I=1,3
      PRINT *,'ENTER DIPOLE #',I,'MOMENT:  X.XXE XX (AMP*M)'
      READ (5,10)P(I)
10    FORMAT(E8.2)
20    CONTINUE
C
      DO 30 I=1,3

      PRINT *,'ENTER DIPOLE #',I,'LOCN: X.X (M FROM ORIGIN)'
      READ(5,60)A(I)
60    FORMAT(F6.4)
30    CONTINUE
C
      DO 40 I=1,3
      PRINT *,'TRANSFORMATION MATRIX FOR DIPOLE#',I
      PRINT *,' '
      PRINT *,'     C1   C2   C3   '
      PRINT *,'     C4   C5   C6   '
      PRINT *,'     C7   C8   C9   '
      PRINT *,' '
      PRINT *,'ENTER THE FIRST ROW, C1 C2 C3, IN THIS FORMAT:'
      PRINT *,'  X.XXX  X.XXX  X.XXX'
      READ(5,70)C1(I),C2(I),C3(I)
      PRINT *,'ENTER THE SECOND ROW, C4 C5 C6, IN THIS FORMAT:'
      PRINT *,'  X.XXX  X.XXX  X.XXX'
      READ(5,70)C4(I),C5(I),C6(I)
      PRINT *,'ENTER THE THIRD ROW, C7 C8 C9, IN THIS FORMAT:'
      PRINT *,'  X.XXX  X.XXX  X.XXX'
      READ(5,70)C7(I),C8(I),C9(I)
70    FORMAT(3F7.3)
```

```
00890 40    CONTINUE
00900 C
00910       PRINT *,'ENTER THE MEAS RADIUS (1ST GRAD COIL): X.X (M)'
00920       READ(5,600)R
00930 C
00940 C -------------------                              -------------
00950       OPEN(11)
00960       OPEN(12)
00970       OPEN(14)
00980 C
00990       WRITE(11,1112)
01000       WRITE(11,2010)
01010       WRITE(11,2020)P(1),P(2),P(3)
01020       WRITE(11,2030)A(1),A(2),A(3)
01030       WRITE(11,1112)
01040       WRITE(11,2040)C1(1),C2(1),C3(1),C1(2),C2(2),C3(2),
01050      +C1(3),C2(3),C3(3)
01060       WRITE(11,2041)C4(1),C5(1),C6(1),C4(2),C5(2),C6(2),
01070      +C4(3),C5(3),C6(3)
01080       WRITE(11,2042)C7(1),C8(1),C9(1),C7(2),C8(2),C9(2),
01090      +C7(3),C8(3),C9(3)
01100       WRITE(11,1112)

01110       WRITE(11,2050)R
01120       WRITE(11,1112)
01130       WRITE(11,1110)
01140       WRITE(11,1112)
01150       WRITE(11,1111)
01160       WRITE(11,1112)
01170 1110  FORMAT('','SPHER DATA POINTS: THETA=T+0.2244; PHI=F+0.2244')
01180 2010  FORMAT(11X,'DIPOLE#1',12X,'DIPOLE#2',12X,'DIPOLE#3')
01190 2020  FORMAT('MOMENT',6X,E8.2,12X,E8.2,12X,E8.2,3X,'(AMP*M)')
01200 2030  FORMAT('LOCATN',4X,F7.3,13X,F7.3,13X,F7.3,6X,'(M FR ORN)')
01210 2040  FORMAT('TRANS ',5X,3F6.3,2X,3F6.3,2X,3F6.3)
01220 2041  FORMAT('MATRIX',5X,3F6.3,2X,3F6.3,2X,3F6.3)
01230 2042  FORMAT('       ',5X,3F6.3,2X,3F6.3,2X,3F6.3)
01240 2050  FORMAT('THE MEAS SPHERE RADIUS IS',2X,F6.4,2X,'M')
01250 1111  FORMAT(4X,'BD(T,F,R)',10X,'X',7X,'Y',7X,'Z',6X,
01260      +       'FLUX DENS. XEE-11 TESLA')
01270 1112  FORMAT('')
01280 C
01290 C -------------------------------------------------------
01300 C
01310 C     ***UPPER POLE***
01320       F=0
```

```
01330         T=0
01340         CALL FIELD(T,F,R,A,P,C1,C2,C3,C4,C5,C6,C7,C8,C9)
01350 C
01360 C       ***PARALLELS AND MERIDIANS***
01370         DO 1121     T=1,14
01380         DO 1120     F=0,2
01390         CALL FIELD(T,F,R,A,P,C1,C2,C3,C4,C5,C6,C7,C8,C9)
01400 1120    CONTINUE
01410 1121    CONTINUE
01420 C
01430 C       ***LOWER POLE***
01440         F=0
01450         T=14
01460         CALL FIELD(T,F,R,A,P,C1,C2,C3,C4,C5,C6,C7,C8,C9)
01470         CLOSE(11)
01480         CLOSE(12)
01490         CLOSE(14)
01500 C -------------------------------------------------------------
01510         STOP
01520         END
01530 C -------------------------------------------------------------
01540 C

01550         SUBROUTINE FIELD(T,F,R,A,P,C1,C2,C3,C4,C5,C6,C7,C8,C9)
01560         INTEGER T,F,M,N,I
01570         REAL R,A(3),P(3),B,D,RD(3),K(3),FR(3),SUM1,SUM2,
01580        +  S1(3),S2(3),BD,X,Y,Z,C1(3),C2(3),C3(3),C4(3),C5(3),C6(3),
01590        +  C7(3),C8(3),C9(3),XX,YY,ZZ,TT,FF
01600 C
01610 C       RADIANS BETWEEN ALL PARALLELS AND MERIDIANS
01620         B=.2244
01630 C
01640 C       DISTANCE BETWEEN GRADIOMETER COILS (METERS)
01650         D = .03175
01660 C
01670         K(1)=   2
01680         K(2)= (-4)
01690         K(3)=   2
01700 C
01710 C       TRANSFORM MEASUREMENT POINT TO CARTESIAN
01720         X = R * COS(F*B) * SIN(T*B)
01730         Y = R * SIN(F*B) * SIN(T*B)
01740         Z = R * COS(T*B)
01750 C
01760         DO 1127    M=1,3
```

```
01720 C
01730       TRANSFORM MEASUREMENT POINT TO ROTATED SYSTEM
01740       XX = P1(M)*X + P2(M)*Y + P3(M)*Z
01800       YY = P4(M)*X + P5(M)*Y + P6(M)*Z
01810       ZZ = P7(M)*X + P8(M)*Y + P9(M)*Z
01820
01830 C     TRANSFORM TO SPHERICAL COOR W.R.T. ROTATED SYSTEM
01840       TT = ACOS(ZZ/R)
01850       IF (XX.EQ.0.0 .AND. YY.EQ.0.0) THEN
01860       FF = 0
01870       ELSE
01880       FF = ATAN2(YY,XX)
01890       END IF
01900 C
01910 C     THE SECOND ORDER GRADIOMETER EFFECT
01920       DO 1128    N=1,3
01930       RD(N) = R + D*(N-1)
01940       FR(N) = 1 - 2*A(M)*COS(TT)/RD(N) + (A(M)/RD(N))**2
01950       S1(N) = K(N)/ (RD(N)**2 *FR(N)**1.5)
01960 1128  CONTINUE
01970       SUM1 = S1(1) + S1(2) + S1(3)
01980 C

01990       S2(M) = P(M) * A(M)  * SIN(TT) * SIN(FF) * SUM1
02000 1127  CONTINUE
02010       BD = S2(1) + S2(2) + S2(3)
02020 C
02030 C     RECALL THAT THE CALCULATED RESULT, BD, HAS EE-7 TACKED
02040 C     ONTO IT.  THIS FACTOR WAS CARRIED THROUGH FROM THE
02050 C     PERMEABILITY CONSTANT.
02060 C
02070       BD = BD * 10000
02080 C     TO MAKE PLOTTING LESS DIFFICULT, BD IS SCALED ANOTHER 4
02090 C     ORDERS OF MAGNITUDE.  THE SCALING FACTOR IS ADJUSTED TO
02100 C     EE-11.  SINCE THIS FACTOR IS ALSO THE SAME ORDER OF MAG
02110 C     AS THE EXPERIMENT SENSITIVITY, DATA COMPARISON IS EASIER.
02120 C
02130 C     THE CARTESIAN COORDINATES ARE PLOTTED IN CENTIMETERS:
02140       X = X * 100
02150       Y = Y * 100
02160       Z = Z * 100
02170 C
02180 C     SPHERICAL DATA
02190       WRITE(11,1129),T,F,R,X,Y,Z,BD
02200 1129  FORMAT(2X,'BD(',I2,',',I2,',',F6.4,')',3F8.3,4X,E15.8)
02210 C
02220 C     XY PLANE PROJECTION
02230       IF(Z.GE.0) THEN
02240       WRITE(12,1130),X,Y,BD
02250       END IF
02260 C
02270 C     XZ PLANE PROJECTION
02280       I=0
02290       IF(Y.GE.0) THEN
02300       I=1
02310       END IF
02320       IF(Z.GE.0) THEN
02330       I=I+1
02340       END IF
02350       IF(I.EQ.2) THEN
02360       WRITE(14,1130),X,Z,BD
02370       END IF
02380 C
02390 1130  FORMAT(2F8.3,5X,E15.8)
02400 C
02410       END
END OF DATA
```

Example Execution of MAGCAL2

The job control language JCL(MAGCAL2), control file CLIST(MAGCAL2), and the routine FORT(MAGCAL2) are compiled by submitting JCL(MAGCAL2). Once the program has been compiled, it can be executed. The program will prompt the user for input data. The position parameter series indicates the particular run #. For example, the parameter series 05 will create and store the calculated data in files SPHR05, XYPL05, and XZPL05.

```
EX 'MAGCAL2'
ENTER POSITIONAL PARAMETER SERIES -
05
ENTER DIPOLE #          1 MOMENT:  X.XXE XX (AMP*M)
1.10 E-05
ENTER DIPOLE #          2 MOMENT:  X.XXE XX (AMP*M)
1.10 E-05
ENTER DIPOLE #          3 MOMENT:  X.XXE XX (AMP*M)
0
ENTER DIPOLE #          1 LOCN: X.X (M FROM ORIGIN)
0.070
ENTER DIPOLE #          2 LOCN: X.X (M FROM ORIGIN)
0.070
ENTER DIPOLE #          3 LOCN: X.X (M FROM ORIGIN)
0
TRANSFORMATION MATRIX FOR DIPOLE#          1

    C1  C2  C3
    C4  C5  C6
    C7  C8  C9

ENTER THE FIRST ROW, C1 C2 C3, IN THIS FORMAT:
  X.XXX  X.XXX  X.XXX
  0.906  0.000 -0.423
ENTER THE SECOND ROW, C4 C5 C6, IN THIS FORMAT:
  X.XXX  X.XXX  X.XXX
  0.000  1.000  0.000
ENTER THE THIRD ROW, C7 C8 C9, IN THIS FORMAT:
  X.XXX  X.XXX  X.XXX
  0.423  0.000  0.906
```

```
TRAMSFORMATION MATRIX FOR DIPOLE#          2

    C1   C2   C3
    C4   C5   C6
    C7   C8   C9

ENTER THE FIRST ROW, C1 C2 C3, IN THIS FORMAT:
  X.XXX  X.XXX  X.XXX
  0.000 -0.906 -0.423
ENTER THE SECOND ROW, C4 C5 C6, IN THIS FORMAT:
  X.XXX  X.XXX  X.XXX
  1.000  0.000  0.000
ENTER THE THIRD ROW, C7 C8 C9, IN THIS FORMAT:
  X.XXX  X.XXX  X.XXX
  0.000 -0.423  0.906
TRANSFORMATION MATRIX FOR DIPOLE#          3

    C1   C2   C3
    C4   C5   C6
    C7   C8   C9

ENTER THE FIRST ROW, C1 C2 C3, IN THIS FORMAT:
  X.XXX  X.XXX  X.XXX
  1.000  0.000  0.000
ENTER THE SECOND ROW, C4 C5 C6, IN THIS FORMAT:
  X.XXX  X.XXX  X.XXX
  0.000  1.000  0.000
ENTER THE THIRD ROW, C7 C8 C9, IN THIS FORMAT:
  X.XXX  X.XXX  X.XXX
  0.000  0.000  1.000
ENTER THE MEAS RADIUS (1ST GRAD COIL): X.X (M)
0.1098
READY
```

Appendix B

This section contains the IBM 30/30 control language used to run the Surface II Graphics plot program. The software consists of a variety of routines. A desired plot can be formed by listing the pertinent routines and specifying their required parameters in a parameter file. A detailed explanation of the capabilities of each routine and how to specify their parameters is given in reference 13.

Job Control Language for XYPLOT

```
[illegible] [illegible] DEREJA.MSGCLASS=A,NOTIFY=HETPJD,TIME=(2),CLASS=F
[illegible]
//STEPLIB      DD DSN=[illegible].SURF2.[illegible].DISP=SHR
//FT01F001 DD DSN=[illegible]TEMP1,UNIT=DISK,SPACE=(TRK,(50,30))
//FT02F001 DD DSN=&TEMP2,UNIT=DISK,SPACE=(TRK,(50,30))
//FT03F001 DD DSN=&TEMP3,UNIT=DISK,SPACE=(TRK,(50,30))
//FT05F001 DD DSN=HETPJD.[illegible](XYPLOT),DISP=SHR
//FT06F001 DD SYSOUT=A
//FT07F001 DD SYSOUT=A
//FT11F001 DD DSN=HETPJD.XYPLOS,DISP=SHR
//FT12F001 DD DSN=HETPJD.PLOT(OUTLINE),DISP=SHR
//FT15F001 DD DSN=&&SRFOUT1,UNIT=DISK,SPACE=(TRK,(2,2))
//FT20F001 DD DSN=&&SRFOUT2,UNIT=DISK,SPACE=(TRK,(2,2))
//FT42F001 DD SYSOUT=A
//FT43F001 DD SYSOUT=A
//FT31F001 DD SYSOUT=A
//*FT31F001 DD DSN=JCORJGJ.SRFOUT3.DATA,UNIT=DISK,SPACE=(TRK,(1,1)),
//*  DISP=(,KEEP),DCB=(BLKSIZE=800,LRECL=800,RECFM=U)
//PLOTLOG     DD SYSOUT=A
//VECTR1      DD DSN=HEGBP.DSG.VECTR1,UNIT=DISK,SPACE=(TRK,(2,2)),
//      DISP=(OLD,KEEP)
//VECTR2      DD DSN=HEGBP.DSG.VECTR2,UNIT=DISK,SPACE=(TRK,(2,2)),
//      DISP=(OLD,KEEP)
//PLOTPARM    DD DSN=HETPJD.PLOTPARM.DATA(PLOTDSG1),DISP=SHR
//
END OF DATA
```

AD-A152 237 A MULTIPOLE MODEL OF THE OBSERVED CEREBRAL CORTEX MAGNETIC FIELD(U) AIR FORCE INST OF TECH WRIGHT-PATTERSON AFB OH SCHOOL OF ENGINEERING 2/2

UNCLASSIFIED P J DE REGO DEC 84 AFIT/GE/ENG/84D-23 F/G 6/16 NL

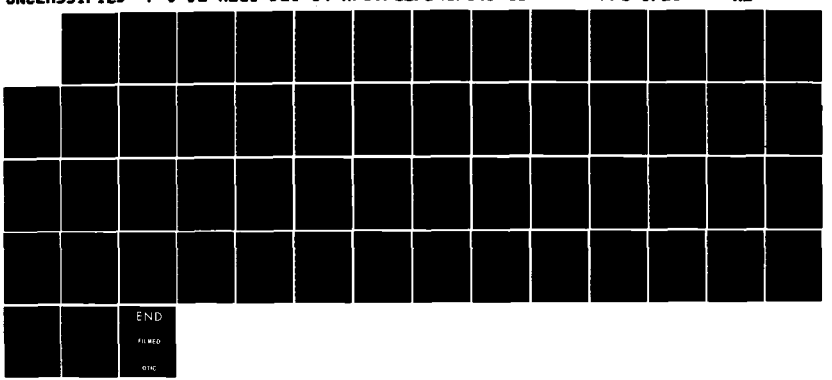

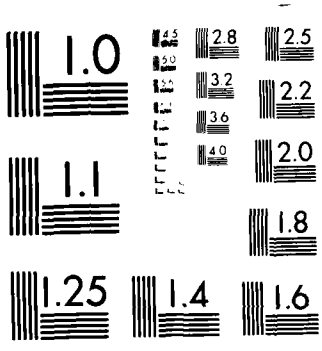

Parameter File CMD(XYPLOT)

```
00010 TITLE          MAGCAL - CONTOUR PLOT USING CALCULATED DATA-SPHROS
00020 DEVICE         6,'LT DE REGO'
00030 IDXY           170,11,3,1,2,3,-1,0,1,0,'(2F8.3,5X,E15.8)'
00040 ROUTLINE       12,1,'(10X,2F10.2)'
00050 ECHO
00060 GRID           0,50,50,0,0,0,0
00070 EXTREMES      -12,12,-12,12
00080 BLANK
00100 CONTOUR
00110 CINTERVAL      0.0,0.2,0.5,0.1,3,0.1,10
00120 POUTLINE
00130 SIZCONTOUR     1,6,6
00140 BOX            1,4,1,4,0,0,0,1,0,1
00150 PERFORM
00160 STOP
END OF DATA
```

Job Control Language for PLot Program PLOTDSG2

```
00010 //HETPJD3 JOB  HET,DEREGO,NOTIFY=HETPJD,TIME=(2),MSGCLASS=A,
00015 //   CLASS=D
00020 //PLOT     EXEC PGM=VTPLOT,COND=(0,LT)
00030 //STEPLIB     DD DSN=VTEC.PLOTLIB,DISP=SHR
00040 //PLOTLOG     DD SYSOUT=A
00050 //VECTR1      DD DSN=HEGBP.DSG.VECTR1,DISP=(OLD,KEEP)
00060 //VECTR2      DD DSN=HEGBP.DSG.VECTR2,DISP=(OLD,KEEP)
00070 //SYSVECTR    DD UNIT=CEE,DCB=(BLKSIZE=133,LRECL=133,RECFM=FA)
00080 //
END OF DATA
```

Appendix C

This section contains the data generated by the program MAGCAL2 for each of the five models. The same dipole parameters were used in the actual experiments. The data collected from the experiments is given in appendix D.

Calculated Data for Model #1

	[illegible]	DIPOLE #2	[illegible]	
MOMENT	[illegible]	0.00E+00	0.00E+00	AMP-M
LOCATN	[illegible]	0.050	0.040	(M FR ORIG)

ROTO	1.000 0.000 0.000	1.000 0.000 0.000	1.000 0.000 0.000
MATRIX	0.000 1.000 0.000	0.000 1.000 0.000	0.000 1.000 0.000
	0.000 0.000 1.000	0.000 0.000 1.000	0.000 0.000 1.000

THE MEAS SPHERE RADIUS IS 0.1038 M

SPHER DATA POINTS: THETA=T+0.2244: PHI=P+0.2244

BD(T,P,R)	X	Y	Z	FLUX DENS. XEE-11 TESLA
BD(0. 0.0.1038)	0.380	0.000	10.380	0.00000000E+00
BD(1. 0.0.1038)	2.443	0.000	10.705	0.00000000E+00
BD(1. 1.0.1038)	2.382	0.544	10.705	0.19933736E+00
BD(1. 2.0.1038)	2.201	1.060	10.705	0.38867944E+00
BD(1. 3.0.1038)	1.910	1.523	10.705	0.55853128E+00
BD(1. 4.0.1038)	1.523	1.910	10.705	0.70037536E+00
BD(1. 5.0.1038)	1.060	2.201	10.705	0.80709982E+00
BD(1. 6.0.1038)	0.544	2.382	10.705	0.87335312E+00
BD(1. 7.0.1038)	-0.000	2.443	10.705	0.89581299E+00
BD(1. 8.0.1038)	-0.544	2.382	10.705	0.87335181E+00
BD(1. 9.0.1038)	-1.060	2.201	10.705	0.80709720E+00
BD(1.10.0.1038)	-1.523	1.910	10.705	0.70037156E+00
BD(1.11.0.1038)	-1.910	1.523	10.705	0.55852675E+00
BD(1.12.0.1038)	-2.201	1.060	10.705	0.38867378E+00
BD(1.13.0.1038)	-2.382	0.544	10.705	0.19933182E+00
BD(1.14.0.1038)	-2.443	-0.000	10.705	-0.65426748E-05
BD(1.15.0.1038)	-2.382	-0.544	10.705	-0.19934344E+00
BD(1.16.0.1038)	-2.201	-1.060	10.705	-0.38868541E+00
BD(1.17.0.1038)	-1.910	-1.523	10.705	-0.55853552E+00
BD(1.18.0.1038)	-1.523	-1.910	10.705	-0.70037913E+00
BD(1.19.0.1038)	-1.060	-2.201	10.705	-0.80710286E+00
BD(1.20.0.1038)	-0.544	-2.382	10.705	-0.87335426E+00
BD(1.21.0.1038)	0.000	-2.443	10.705	-0.89581299E+00
BD(1.22.0.1038)	0.544	-2.382	10.705	-0.87335050E+00
BD(1.23.0.1038)	1.060	-2.201	10.705	-0.80709416E+00
BD(1.24.0.1038)	1.523	-1.910	10.705	-0.70036781E+00
BD(1.25.0.1038)	1.910	-1.523	10.705	-0.55852181E+00
BD(1.26.0.1038)	2.201	-1.060	10.705	-0.38866812E+00
BD(1.27.0.1038)	2.382	-0.544	10.705	-0.19932556E+00

```
BD(  2,  0,0.1098)    4.764    0.000    9.893     0.00000000E+00
BD(  2,  1,0.1098)    4.645    1.066    9.893     0.16937536E+00
BD(  2,  2,0.1098)    4.292    2.067    9.893     0.33025771E+00
BD(  2,  3,0.1098)    3.725    2.970    9.893     0.47457939E+00
BD(  2,  4,0.1098)    2.970    3.725    9.893     0.59510344E+00
BD(  2,  5,0.1098)    2.067    4.292    9.893     0.68578660E+00
BD(  2,  6,0.1098)    1.060    4.645    9.893     0.74208146E+00
BD(  2,  7,0.1098)   -0.000    4.764    9.893     0.76116508E+00
BD(  2,  8,0.1098)   -1.060    4.645    9.893     0.74208027E+00
BD(  2,  9,0.1098)   -2.067    4.292    9.893     0.68578428E+00
BD(  2, 10,0.1098)   -2.970    3.725    9.893     0.59510040E+00
BD(  2, 11,0.1098)   -3.725    2.970    9.893     0.47457564E+00
BD(  2, 12,0.1098)   -4.292    2.067    9.893     0.33025306E+00
BD(  2, 13,0.1098)   -4.645    1.066    9.893     0.16937071E+00
BD(  2, 14,0.1098)   -4.764   -0.000    9.893    -0.55532545E-05
BD(  2, 15,0.1098)   -4.645   -1.066    9.893    -0.16938061E+00
BD(  2, 16,0.1098)   -4.292   -2.067    9.893    -0.33026266E+00
BD(  2, 17,0.1098)   -3.725   -2.970    9.893    -0.47456303E+00
BD(  2, 18,0.1098)   -2.970   -3.725    9.893    -0.59510678E+00
BD(  2, 19,0.1098)   -2.067   -4.292    9.893    -0.68578881E+00
BD(  2, 20,0.1098)   -1.060   -4.645    9.893    -0.74208260E+00
BD(  2, 21,0.1098)    0.000   -4.764    9.893    -0.76116508E+00

BD(  2, 22,0.1098)    1.060   -4.645    9.893    -0.74207926E+00
BD(  2, 23,0.1098)    2.067   -4.292    9.893    -0.68578166E+00
BD(  2, 24,0.1098)    2.970   -3.725    9.893    -0.59509718E+00
BD(  2, 25,0.1098)    3.725   -2.970    9.893    -0.47457153E+00
BD(  2, 26,0.1098)    4.292   -2.067    9.893    -0.33024812E+00
BD(  2, 27,0.1098)    4.645   -1.060    9.893    -0.16936535E+00
BD(  3,  0,0.1098)    6.346    0.000    8.584     0.00000000E+00
BD(  3,  1,0.1098)    6.674    1.523    8.584     0.93098104E-01
BD(  3,  2,0.1098)    6.168    2.970    8.584     0.18152785E+00
BD(  3,  3,0.1098)    5.352    4.268    8.584     0.26085496E+00
BD(  3,  4,0.1098)    4.268    5.352    8.584     0.32710159E+00
BD(  3,  5,0.1098)    2.970    6.168    8.584     0.37694597E+00
BD(  3,  6,0.1098)    1.523    6.674    8.584     0.40788871E+00
BD(  3,  7,0.1098)   -0.000    6.846    8.584     0.41837829E+00
BD(  3,  8,0.1098)   -1.523    6.674    8.584     0.40788823E+00
BD(  3,  9,0.1098)   -2.970    6.168    8.584     0.37694490E+00
BD(  3, 10,0.1098)   -4.268    5.352    8.584     0.32710010E+00
BD(  3, 11,0.1098)   -5.352    4.268    8.584     0.26085293E+00
BD(  3, 12,0.1098)   -6.168    2.970    8.584     0.18152523E+00
BD(  3, 13,0.1098)   -6.674    1.523    8.584     0.93095481E-01
BD(  3, 14,0.1098)   -6.846   -0.000    8.584    -0.30556730E-05
BD(  3, 15,0.1098)   -6.674   -1.523    8.584    -0.93100905E-01

BD(  3, 16,0.1098)   -6.168   -2.970    8.584    -0.18153059E+00
BD(  3, 17,0.1098)   -5.352   -4.268    8.584    -0.26085705E+00
BD(  3, 18,0.1098)   -4.268   -5.352    8.584    -0.32710344E+00
BD(  3, 19,0.1098)   -2.970   -6.168    8.584    -0.37694740E+00
BD(  3, 20,0.1098)   -1.523   -6.674    8.584    -0.40788943E+00
BD(  3, 21,0.1098)    0.000   -6.846    8.584    -0.41837829E+00
BD(  3, 22,0.1098)    1.523   -6.674    8.584    -0.40788752E+00
BD(  3, 23,0.1098)    2.970   -6.168    8.584    -0.37694347E+00
BD(  3, 24,0.1098)    4.268   -5.352    8.584    -0.32709819E+00
BD(  3, 25,0.1098)    5.352   -4.268    8.584    -0.26085061E+00
BD(  3, 26,0.1098)    6.168   -2.970    8.584    -0.18152261E+00
BD(  3, 27,0.1098)    6.674   -1.523    8.584    -0.93093561E-01
BD(  4,  0,0.1098)    8.585    0.000    6.846     0.00000000E+00
BD(  4,  1,0.1098)    8.369    1.910    6.846     0.47029614E-01
BD(  4,  2,0.1098)    7.734    3.725    6.846     0.91700971E-01
BD(  4,  3,0.1098)    6.713    5.352    6.846     0.13177407E+00
```

BD(4, 4,0.1098)	5.352	6.712	6.846	0.16523927E+00
BD(4, 5,0.1098)	3.725	7.734	6.846	0.19041878E+00
BD(4, 6,0.1098)	1.910	8.369	6.846	0.20604998E+00
BD(4, 7,0.1098)	-0.000	8.585	6.846	0.21134877E+00
BD(4, 8,0.1098)	-1.910	8.369	6.846	0.20604968E+00
BD(4, 9,0.1098)	-3.725	7.734	6.846	0.19041818E+00
BD(4,10,0.1098)	-5.352	6.712	6.846	0.16523856E+00
BD(4,11,0.1098)	-6.712	5.352	6.846	0.13177295E+00
BD(4,12,0.1098)	-7.734	3.725	6.846	0.91699839E-01
BD(4,13,0.1098)	-8.369	1.910	6.846	0.47028303E-01
BD(4,14,0.1098)	-8.585	-0.000	6.846	-0.15436108E-05
BD(4,15,0.1098)	-8.369	-1.910	6.846	-0.47031052E-01
BD(4,16,0.1098)	-7.734	-3.725	6.846	-0.91702402E-01
BD(4,17,0.1098)	-6.712	-5.352	6.846	-0.13177526E+00
BD(4,18,0.1098)	-5.352	-6.712	6.846	-0.16524017E+00
BD(4,19,0.1098)	-3.725	-7.734	6.846	-0.19041938E+00
BD(4,20,0.1098)	-1.910	-8.369	6.846	-0.20605028E+00
BD(4,21,0.1098)	0.000	-8.585	6.846	-0.21134877E+00
BD(4,22,0.1098)	1.910	-8.369	6.846	-0.20604926E+00
BD(4,23,0.1098)	3.725	-7.734	6.846	-0.19041747E+00
BD(4,24,0.1098)	5.352	-6.712	6.846	-0.16523755E+00
BD(4,25,0.1098)	6.712	-5.352	6.846	-0.13177186E+00
BD(4,26,0.1098)	7.734	-3.725	6.846	-0.91698408E-01
BD(4,27,0.1098)	8.369	-1.910	6.846	-0.47026820E-01
BD(5, 0,0.1098)	9.893	0.000	4.764	0.00000000E+00
BD(5, 1,0.1098)	9.645	2.201	4.764	0.24553016E-01
BD(5, 2,0.1098)	8.913	4.292	4.764	0.47874872E-01
BD(5, 3,0.1098)	7.734	6.168	4.764	0.68796039E-01
BD(5, 4,0.1098)	6.168	7.734	4.764	0.86267412E-01
BD(5, 5,0.1098)	4.292	8.913	4.764	0.99412978E-01
BD(5, 6,0.1098)	2.201	9.645	4.764	0.10757363E+00
BD(5, 7,0.1098)	-0.000	9.893	4.764	0.11034006E+00
BD(5, 8,0.1098)	-2.201	9.645	4.764	0.10757345E+00
BD(5, 9,0.1098)	-4.292	8.913	4.764	0.99412680E-01
BD(5,10,0.1098)	-6.168	7.734	4.764	0.86266935E-01
BD(5,11,0.1098)	-7.734	6.168	4.764	0.68795443E-01
BD(5,12,0.1098)	-8.913	4.292	4.764	0.47874164E-01
BD(5,13,0.1098)	-9.645	2.201	4.764	0.24552308E-01
BD(5,14,0.1098)	-9.893	-0.000	4.764	-0.80588143E-06
BD(5,15,0.1098)	-9.645	-2.201	4.764	-0.24553746E-01
BD(5,16,0.1098)	-8.913	-4.292	4.764	-0.47875579E-01
BD(5,17,0.1098)	-7.734	-6.168	4.764	-0.68796575E-01
BD(5,18,0.1098)	-6.168	-7.734	4.764	-0.86267829E-01
BD(5,19,0.1098)	-4.292	-8.913	4.764	-0.99413335E-01
BD(5,20,0.1098)	-2.201	-9.645	4.764	-0.10757381E+00
BD(5,21,0.1098)	0.000	-9.893	4.764	-0.11034006E+00
BD(5,22,0.1098)	2.201	-9.645	4.764	-0.10757327E+00
BD(5,23,0.1098)	4.292	-8.913	4.764	-0.99412322E-01
BD(5,24,0.1098)	6.168	-7.734	4.764	-0.86266458E-01
BD(5,25,0.1098)	7.734	-6.168	4.764	-0.68794847E-01
BD(5,26,0.1098)	8.913	-4.292	4.764	-0.47873471E-01
BD(5,27,0.1098)	9.645	-2.201	4.764	-0.24551544E-01
BD(6, 0,0.1098)	10.705	0.000	2.443	0.00000000E+00
BD(6, 1,0.1098)	10.436	2.382	2.443	0.13718124E-01
BD(6, 2,0.1098)	9.645	4.645	2.443	0.26748382E-01
BD(6, 3,0.1098)	8.369	6.674	2.443	0.38437311E-01
BD(6, 4,0.1098)	6.674	8.369	2.443	0.48198853E-01
BD(6, 5,0.1098)	4.645	9.645	2.443	0.55543493E-01
BD(6, 6,0.1098)	2.382	10.436	2.443	0.60102955E-01
BD(6, 7,0.1098)	-0.000	10.705	2.443	0.61648585E-01

```
BD( 6, 8,0.1098)  -2.382  10.436   2.443     0.60102865E-01
BD( 6, 9,0.1098)  -4.645   9.645   2.443     0.55543322E-01
BD( 6,10,0.1098)  -6.674   8.369   2.443     0.48198652E-01
BD( 6,11,0.1098)  -8.369   6.674   2.443     0.38437016E-01
BD( 6,12,0.1098)  -9.645   4.645   2.443     0.26747983E-01
BD( 6,13,0.1098) -10.436   2.382   2.443     0.13717733E-01
BD( 6,14,0.1098) -10.705  -0.000   2.443    -0.45025757E-06
BD( 6,15,0.1098) -10.436  -2.382   2.443    -0.13718527E-01
BD( 6,16,0.1098)  -9.645  -4.645   2.443    -0.26748773E-01
BD( 6,17,0.1098)  -8.369  -6.674   2.443    -0.38437627E-01
BD( 6,18,0.1098)  -6.674  -8.369   2.443    -0.48199143E-01
BD( 6,19,0.1098)  -4.645  -9.645   2.443    -0.55543657E-01

BD( 6,20,0.1098)  -2.382 -10.436   2.443    -0.60103029E-01
BD( 6,21,0.1098)   0.000 -10.705   2.443    -0.61648585E-01
BD( 6,22,0.1098)   2.382 -10.436   2.443    -0.60102765E-01
BD( 6,23,0.1098)   4.645  -9.645   2.443    -0.55543102E-01
BD( 6,24,0.1098)   6.674  -8.369   2.443    -0.48198342E-01
BD( 6,25,0.1098)   8.369  -6.674   2.443    -0.38436681E-01
BD( 6,26,0.1098)   9.645  -4.644   2.443    -0.26747599E-01
BD( 6,27,0.1098)  10.436  -2.382   2.443    -0.13717297E-01
BD( 7, 0,0.1098)  10.980   0.000  -0.000     0.00000000E+00
BD( 7, 1,0.1098)  10.705   2.443  -0.000     0.82161427E-02
BD( 7, 2,0.1098)   9.893   4.764  -0.000     0.16020294E-01
BD( 7, 3,0.1098)   8.584   6.846  -0.000     0.23021121E-01
BD( 7, 4,0.1098)   6.846   8.585  -0.000     0.28867550E-01
BD( 7, 5,0.1098)   4.764   9.893  -0.000     0.33266451E-01
BD( 7, 6,0.1098)   2.443  10.705  -0.000     0.35997227E-01
BD( 7, 7,0.1098)  -0.000  10.980  -0.000     0.36922947E-01
BD( 7, 8,0.1098)  -2.443  10.705  -0.000     0.35997178E-01
BD( 7, 9,0.1098)  -4.764   9.893  -0.000     0.33266351E-01
BD( 7,10,0.1098)  -6.846   8.584  -0.000     0.28867416E-01
BD( 7,11,0.1098)  -8.585   6.846  -0.000     0.23020938E-01
BD( 7,12,0.1098)  -9.893   4.764  -0.000     0.16020067E-01
BD( 7,13,0.1098) -10.705   2.443  -0.000     0.82159117E-02

BD( 7,14,0.1098) -10.980  -0.000  -0.000    -0.26967109E-06
BD( 7,15,0.1098) -10.705  -2.443  -0.000    -0.82163885E-02
BD( 7,16,0.1098)  -9.893  -4.764  -0.000    -0.16020536E-01
BD( 7,17,0.1098)  -8.584  -6.846  -0.000    -0.23021292E-01
BD( 7,18,0.1098)  -6.846  -8.585  -0.000    -0.28867714E-01
BD( 7,19,0.1098)  -4.764  -9.893  -0.000    -0.33266567E-01
BD( 7,20,0.1098)  -2.443 -10.705  -0.000    -0.35997290E-01
BD( 7,21,0.1098)   0.000 -10.980  -0.000    -0.36922947E-01
BD( 7,22,0.1098)   2.443 -10.705  -0.000    -0.35997126E-01
BD( 7,23,0.1098)   4.764  -9.893  -0.000    -0.33266220E-01
BD( 7,24,0.1098)   6.846  -8.584  -0.000    -0.28867241E-01
BD( 7,25,0.1098)   8.585  -6.846  -0.000    -0.23020729E-01
BD( 7,26,0.1098)   9.893  -4.764  -0.000    -0.16019829E-01
BD( 7,27,0.1098)  10.705  -2.443  -0.000    -0.82156546E-02
BD( 8, 0,0.1098)  10.705   0.000  -2.443     0.00000000E+00
BD( 8, 1,0.1098)  10.436   2.382  -2.443     0.52107647E-02
BD( 8, 2,0.1098)   9.645   4.645  -2.443     0.10160238E-01
BD( 8, 3,0.1098)   8.369   6.674  -2.443     0.14600236E-01
BD( 8, 4,0.1098)   6.674   8.369  -2.443     0.18308107E-01
BD( 8, 5,0.1098)   4.645   9.645  -2.443     0.21057928E-01
BD( 8, 6,0.1098)   2.382  10.436  -2.443     0.22829823E-01
BD( 8, 7,0.1098)  -0.000  10.705  -2.443     0.23416921E-01
```

BD(8, 8,0,1098)	-2.382	10.436	-2.443	0.22829790E-01
BD(8, 9,0,1098)	-4.645	9.645	-2.443	0.21097865E-01
BD(8,10,0,1098)	-6.674	8.369	-2.443	0.18308017E-01
BD(8,11,0,1098)	-8.369	6.674	-2.443	0.14600117E-01
BD(8,12,0,1098)	-9.645	4.645	-2.443	0.10160092E-01
BD(8,13,0,1098)	-10.436	2.382	-2.443	0.52106157E-02
BD(8,14,0,1098)	-10.705	-0.000	-2.443	-0.17102815E-06
BD(8,15,0,1098)	-10.436	-2.382	-2.443	-0.52109212E-02
BD(8,16,0,1098)	-9.645	-4.645	-2.443	-0.10160390E-01
BD(8,17,0,1098)	-8.369	-6.674	-2.443	-0.14600344E-01
BD(8,18,0,1098)	-6.674	-8.369	-2.443	-0.18308219E-01
BD(8,19,0,1098)	-4.645	-9.645	-2.443	-0.21096010E-01
BD(8,20,0,1098)	-2.382	-10.436	-2.443	-0.22829860E-01
BD(8,21,0,1098)	0.000	-10.705	-2.443	-0.23416921E-01
BD(8,22,0,1098)	2.382	-10.436	-2.443	-0.22829752E-01
BD(8,23,0,1098)	4.645	-9.645	-2.443	-0.21097783E-01
BD(8,24,0,1098)	6.674	-8.369	-2.443	-0.18307909E-01
BD(8,25,0,1098)	8.369	-6.674	-2.443	-0.14599990E-01
BD(8,26,0,1098)	9.645	-4.644	-2.443	-0.10159947E-01
BD(8,27,0,1098)	10.436	-2.382	-2.443	-0.52104555E-02
BD(9, 0,0,1098)	9.893	0.000	-4.764	0.00000000E+00
BD(9, 1,0,1098)	9.645	2.201	-4.764	0.34354615E-02
BD(9, 2,0,1098)	8.913	4.292	-4.764	0.66986568E-02
BD(9, 3,0,1098)	7.734	6.168	-4.764	0.96259452E-02
BD(9, 4,0,1098)	6.168	7.734	-4.764	0.12070548E-01
BD(9, 5,0,1098)	4.292	8.913	-4.764	0.13909884E-01
BD(9, 6,0,1098)	2.201	9.645	-4.764	0.15051719E-01
BD(9, 7,0,1098)	-0.000	9.893	-4.764	0.15438788E-01
BD(9, 8,0,1098)	-2.201	9.645	-4.764	0.15051700E-01
BD(9, 9,0,1098)	-4.292	8.913	-4.764	0.13909828E-01
BD(9,10,0,1098)	-6.168	7.734	-4.764	0.12070484E-01
BD(9,11,0,1098)	-7.734	6.168	-4.764	0.96258633E-02
BD(9,12,0,1098)	-8.913	4.292	-4.764	0.66985600E-02
BD(9,13,0,1098)	-9.645	2.201	-4.764	0.34353649E-02
BD(9,14,0,1098)	-9.893	-0.000	-4.764	-0.11275904E-06
BD(9,15,0,1098)	-9.645	-2.201	-4.764	-0.34355661E-02
BD(9,16,0,1098)	-8.913	-4.292	-4.764	-0.66987574E-02
BD(9,17,0,1098)	-7.734	-6.168	-4.764	-0.96260272E-02
BD(9,18,0,1098)	-6.168	-7.734	-4.764	-0.12070604E-01
BD(9,19,0,1098)	-4.292	-8.913	-4.764	-0.13909921E-01
BD(9,20,0,1098)	-2.201	-9.645	-4.764	-0.15051734E-01
BD(9,21,0,1098)	0.000	-9.893	-4.764	-0.15438788E-01
BD(9,22,0,1098)	2.201	-9.645	-4.764	-0.15051670E-01
BD(9,23,0,1098)	4.292	-8.913	-4.764	-0.13909783E-01
BD(9,24,0,1098)	6.168	-7.734	-4.764	-0.12070421E-01
BD(9,25,0,1098)	7.734	-6.168	-4.764	-0.96257813E-02
BD(9,26,0,1098)	8.913	-4.292	-4.764	-0.66984631E-02
BD(9,27,0,1098)	9.645	-2.201	-4.764	-0.34352574E-02
BD(10, 0,0,1098)	8.584	0.000	-6.846	0.00000000E+00
BD(10, 1,0,1098)	8.369	1.910	-6.846	0.23007514E-02
BD(10, 2,0,1098)	7.734	3.725	-6.846	0.44861324E-02
BD(10, 3,0,1098)	6.712	5.352	-6.846	0.64465627E-02
BD(10, 4,0,1098)	5.352	6.712	-6.846	0.80837272E-02
BD(10, 5,0,1098)	3.725	7.734	-6.846	0.93155429E-02
BD(10, 6,0,1098)	1.910	8.369	-6.846	0.10080229E-01
BD(10, 7,0,1098)	-0.000	8.584	-6.846	0.10339461E-01

BD(10, 8,0.1098)	-1.910	8.369	-6.846	0.10080218E-01
BD(10, 9,0.1098)	-3.725	7.734	-6.846	0.93155093E-02
BD(10,10,0.1098)	-5.352	6.712	-6.846	0.80836862E-02
BD(10,11,0.1098)	-6.712	5.352	-6.846	0.64465106E-02
BD(10,12,0.1098)	-7.734	3.725	-6.846	0.44860691E-02
BD(10,13,0.1098)	-8.369	1.910	-6.846	0.23006871E-02
BD(10,14,0.1098)	-8.584	-0.000	-6.846	-0.75515459E-07
BD(10,15,0.1098)	-8.369	-1.910	-6.846	-0.23006196E-02
BD(10,16,0.1098)	-7.734	-3.725	-6.846	-0.44862032E-02
BD(10,17,0.1098)	-6.712	-5.352	-6.846	-0.64466186E-02
BD(10,18,0.1098)	-5.352	-6.712	-6.846	-0.80837756E-02
BD(10,19,0.1098)	-3.725	-7.734	-6.846	-0.93155727E-02
BD(10,20,0.1098)	-1.910	-8.369	-6.846	-0.10080244E-01
BD(10,21,0.1098)	0.000	-8.584	-6.846	-0.10339461E-01
BD(10,22,0.1098)	1.910	-8.369	-6.846	-0.10080200E-01
BD(10,23,0.1098)	3.725	-7.734	-6.846	-0.93154795E-02
BD(10,24,0.1098)	5.352	-6.712	-6.846	-0.80836415E-02
BD(10,25,0.1098)	6.712	-5.352	-6.846	-0.64464547E-02
BD(10,26,0.1098)	7.734	-3.725	-6.846	-0.44860058E-02
BD(10,27,0.1098)	8.369	-1.910	-6.846	-0.23006145E-02
BD(11, 0,0.1098)	6.846	0.000	-8.585	0.00000000E+00
BD(11, 1,0.1098)	6.674	1.523	-8.585	0.15153158E-02
BD(11, 2,0.1098)	6.168	2.970	-8.585	0.29546469E-02
BD(11, 3,0.1098)	5.352	4.268	-8.585	0.42458177E-02
BD(11, 4,0.1098)	4.268	5.352	-8.585	0.53240843E-02
BD(11, 5,0.1098)	2.970	6.168	-8.585	0.61353780E-02
BD(11, 6,0.1098)	1.523	6.674	-8.585	0.66390187E-02
BD(11, 7,0.1098)	-0.000	6.846	-8.585	0.68097524E-02
BD(11, 8,0.1098)	-1.523	6.674	-8.585	0.66390112E-02
BD(11, 9,0.1098)	-2.970	6.168	-8.585	0.61353594E-02
BD(11,10,0.1098)	-4.268	5.352	-8.585	0.53240582E-02
BD(11,11,0.1098)	-5.352	4.268	-8.585	0.42457841E-02
BD(11,12,0.1098)	-6.168	2.970	-8.585	0.29546043E-02
BD(11,13,0.1098)	-6.674	1.523	-8.585	0.15152725E-02
BD(11,14,0.1098)	-6.846	-0.000	-8.585	-0.49735821E-07
BD(11,15,0.1098)	-6.674	-1.523	-8.585	-0.15153612E-02
BD(11,16,0.1098)	-6.168	-2.970	-8.585	-0.29546912E-02
BD(11,17,0.1098)	-5.352	-4.268	-8.585	-0.42458512E-02
BD(11,18,0.1098)	-4.268	-5.352	-8.585	-0.53241141E-02
BD(11,19,0.1098)	-2.970	-6.168	-8.585	-0.61354004E-02
BD(11,20,0.1098)	-1.523	-6.674	-8.585	-0.66390298E-02
BD(11,21,0.1098)	0.000	-6.846	-8.585	-0.68097524E-02
BD(11,22,0.1098)	1.523	-6.674	-8.585	-0.66390000E-02
BD(11,23,0.1098)	2.970	-6.168	-8.585	-0.61353371E-02
BD(11,24,0.1098)	4.268	-5.352	-8.585	-0.53240284E-02
BD(11,25,0.1098)	5.352	-4.268	-8.585	-0.42457469E-02
BD(11,26,0.1098)	6.168	-2.970	-8.585	-0.29545617E-02
BD(11,27,0.1098)	6.674	-1.523	-8.585	-0.15152248E-02
BD(12, 0,0.1098)	4.754	0.000	-9.893	0.00000000E+00
BD(12, 1,0.1098)	4.649	1.060	-9.893	0.92463871E-03
BD(12, 2,0.1098)	4.292	2.067	-9.893	0.18029111E-02
BD(12, 3,0.1098)	3.725	2.970	-9.893	0.25907785E-02
BD(12, 4,0.1098)	2.970	3.725	-9.893	0.32487332E-02
BD(12, 5,0.1098)	2.067	4.292	-9.893	0.37437808E-02

```
BD(12, 6,0.1098)   1.060   4.645  -9.893     0.40510967E-02
BD(12, 7,0.1098)  -0.000   4.764  -9.893     0.41552782E-02
BD(12, 8,0.1098)  -1.060   4.645  -9.893     0.40510930E-02
BD(12, 9,0.1098)  -2.067   4.292  -9.893     0.37437701E-02
BD(12,10,0.1098)  -2.970   3.725  -9.893     0.32487167E-02
BD(12,11,0.1098)  -3.725   2.970  -9.893     0.25907592E-02
BD(12,12,0.1098)  -4.292   2.067  -9.893     0.18028854E-02
BD(12,13,0.1098)  -4.645   1.060  -9.893     0.92461263E-03
BD(12,14,0.1098)  -4.764  -0.000  -9.893    -0.30348570E-07
BD(12,15,0.1098)  -4.645  -1.060  -9.893    -0.92466665E-03
BD(12,16,0.1098)  -4.292  -2.067  -9.893    -0.18029395E-02
BD(12,17,0.1098)  -3.725  -2.970  -9.893    -0.25907985E-02
BD(12,18,0.1098)  -2.970  -3.725  -9.893    -0.32487507E-02
BD(12,19,0.1098)  -2.067  -4.292  -9.893    -0.37437938E-02
BD(12,20,0.1098)  -1.060  -4.645  -9.893    -0.40511042E-02
BD(12,21,0.1098)   0.000  -4.764  -9.893    -0.41552782E-02
BD(12,22,0.1098)   1.060  -4.645  -9.893    -0.40510893E-02
BD(12,23,0.1098)   2.067  -4.292  -9.893    -0.37437563E-02
BD(12,24,0.1098)   2.970  -3.725  -9.893    -0.32486985E-02
BD(12,25,0.1098)   3.725  -2.970  -9.893    -0.25907354E-02
BD(12,26,0.1098)   4.292  -2.067  -9.893    -0.18028589E-02
BD(12,27,0.1098)   4.645  -1.060  -9.893    -0.92458306E-03

BD(13, 0,0.1098)   2.443   0.000 -10.705     0.00000000E+00
BD(13, 1,0.1098)   2.382   0.544 -10.705     0.43913885E-03
BD(13, 2,0.1098)   2.201   1.060 -10.705     0.85625798E-03
BD(13, 3,0.1098)   1.910   1.523 -10.705     0.12304399E-02
BD(13, 4,0.1098)   1.523   1.910 -10.705     0.15429212E-02
BD(13, 5,0.1098)   1.060   2.201 -10.705     0.17780347E-02
BD(13, 6,0.1098)   0.544   2.382 -10.705     0.19239904E-02
BD(13, 7,0.1098)  -0.000   2.443 -10.705     0.19734693E-02
BD(13, 8,0.1098)  -0.544   2.382 -10.705     0.19239876E-02
BD(13, 9,0.1098)  -1.060   2.201 -10.705     0.17780303E-02
BD(13,10,0.1098)  -1.523   1.910 -10.705     0.15429144E-02
BD(13,11,0.1098)  -1.910   1.523 -10.705     0.12304303E-02
BD(13,12,0.1098)  -2.201   1.060 -10.705     0.85624540E-03
BD(13,13,0.1098)  -2.382   0.544 -10.705     0.43912674E-03
BD(13,14,0.1098)  -2.443  -0.000 -10.705    -0.14413459E-07
BD(13,15,0.1098)  -2.382  -0.544 -10.705    -0.43915235E-03
BD(13,16,0.1098)  -2.201  -1.060 -10.705    -0.85627101E-03
BD(13,17,0.1098)  -1.910  -1.523 -10.705    -0.12304496E-02
BD(13,18,0.1098)  -1.523  -1.910 -10.705    -0.15429310E-02
BD(13,19,0.1098)  -1.060  -2.201 -10.705    -0.17780415E-02
BD(13,20,0.1098)  -0.544  -2.382 -10.705    -0.19239928E-02
BD(13,21,0.1098)   0.000  -2.443 -10.705    -0.19734693E-02

BD(13,22,0.1098)   0.544  -2.382 -10.705    -0.19239848E-02
BD(13,23,0.1098)   1.060  -2.201 -10.705    -0.17780222E-02
BD(13,24,0.1098)   1.523  -1.910 -10.705    -0.15429049E-02
BD(13,25,0.1098)   1.910  -1.523 -10.705    -0.12304194E-02
BD(13,26,0.1098)   2.201  -1.060 -10.705    -0.85623283E-03
BD(13,27,0.1098)   2.382  -0.544 -10.705    -0.43911254E-03
BD(14, 0,0.1098)  -0.000   0.000 -10.980     0.91717680E-15
END OF DATA
```

Calculated Data for Model #2

	DIPOLE #1	DIPOLE #2	DIPOLE #3	
MOMENT	0.55E-05	0.55E-05	0.55E-05	(AMP-M
LOCATN	0.0,0.	0.0,0.	0.040	(M FR
UNAMS	1.000 0.000 0.000	1.000 0.000 0.000	1.000 0.000 0.000	
MATRIX	0.000 1.000 0.000	0.000 1.000 0.000	0.000 1.000 0.000	
	0.000 0.000 1.000	0.000 0.000 1.000	1.000 0.000 0.000	

THE MEAN SPHERE RADIUS IS 0.1098 M

THETA = DATA POINTS: PHI=F+0.2244; PHI=F+0.2244

BDY(I,J)	X	Y	Z	FLUX DENS. XEE-11 TO (A
BDY(1, 0,0.1098)	0.000	0.000	10.380	0.00000000E+00
BDY(1, 1,0.1098)	2.443	0.000	10.705	0.00000000E+00
BDY(1, 1,0.1098)	2.382	0.544	10.705	0.28366572E+00
BDY(1, 2,0.1098)	2.201	1.060	10.705	0.55235910E+00
BDY(1, 3,0.1098)	1.910	1.523	10.705	0.79206884E+00
BDY(1, 4,0.1098)	1.523	1.910	10.705	0.99058157E+00
BDY(1, 5,0.1098)	1.060	2.201	10.705	0.11381159E+01
BDY(1, 5,0.1098)	0.544	2.382	10.705	0.12277231E+01
BDY(1, 7,0.1098)	-0.000	2.443	10.705	0.12554846E+01
BDY(1, 8,0.1098)	-0.544	2.382	10.705	0.12205734E+01
BDY(1, 9,0.1098)	-1.060	2.201	10.705	0.11251841E+01
BDY(1,10,0.1098)	-1.523	1.910	10.705	0.97436494E+00
BDY(1,11,0.1098)	-1.910	1.523	10.705	0.77575052E+00
BDY(1,12,0.1098)	-2.201	1.060	10.705	0.53919804E+00
BDY(1,13,0.1098)	-2.382	0.544	10.705	0.27633065E+00
BDY(1,14,0.1098)	-2.443	-0.000	10.705	-0.90678488E-05
BDY(1,15,0.1098)	-2.382	-0.544	10.705	-0.27634680E+00
BDY(1,16,0.1098)	-2.201	-1.060	10.705	-0.53921407E+00
BDY(1,17,0.1098)	-1.910	-1.523	10.705	-0.77576286E+00
BDY(1,18,0.1098)	-1.523	-1.910	10.705	-0.97437525E+00
BDY(1,19,0.1098)	-1.060	-2.201	10.705	-0.11251926E+01
BDY(1,20,0.1098)	-0.544	-2.382	10.705	-0.12205772E+01
BDY(1,21,0.1098)	0.000	-2.443	10.705	-0.12554855E+01
BDY(1,22,0.1098)	0.544	-2.382	10.705	-0.12277193E+01
BDY(1,23,0.1098)	1.060	-2.201	10.705	-0.11381092E+01
BDY(1,24,0.1098)	1.523	-1.910	10.705	-0.99057108E+00
BDY(1,25,0.1098)	1.910	-1.523	10.705	-0.79205531E+00
BDY(1,26,0.1098)	2.201	-1.060	10.705	-0.55234307E+00
BDY(1,27,0.1098)	2.382	-0.544	10.705	-0.28364897E+00
BDY(2, 0,0.1098)	4.764	0.000	9.893	0.00000000E+00
BDY(2, 1,0.1098)	4.649	1.066	9.893	0.27320643E+00
BDY(2, 2,0.1098)	4.292	2.067	9.893	0.53076887E+00
BDY(2, 3,0.1098)	3.725	2.976	9.893	0.75827289E+00
BDY(2, 4,0.1098)	2.976	3.725	9.893	0.94417930E+00
BDY(2, 5,0.1098)	2.067	4.292	9.893	0.10799923E+01
BDY(2, 6,0.1098)	1.060	4.645	9.893	0.11602716E+01
BDY(2, 7,0.1098)	-0.000	4.764	9.893	0.11823807E+01
BDY(2, 8,0.1098)	-1.060	4.645	9.893	0.11462793E+01
BDY(2, 9,0.1098)	-2.067	4.292	9.893	0.10544090E+01
BDY(2,10,0.1098)	-2.970	3.725	9.893	0.91160643E+00
BDY(2,11,0.1098)	-3.725	2.976	9.893	0.72494918E+00
BDY(2,12,0.1098)	-4.292	2.067	9.893	0.50349987E+00
BDY(2,13,0.1098)	-4.649	1.060	9.893	0.25792176E+00
BDY(2,14,0.1098)	-4.764	-0.000	9.893	-0.84625235E-05

BD(2,14,0.1098)	-4.764	-0.000	9.893	-0.84625235E-05
BD(2,15,0.1098)	-4.645	-1.060	9.893	-0.25793672E+00
BD(2,16,0.1098)	-4.292	-2.067	9.893	-0.50351459E+00
BD(2,17,0.1098)	-3.725	-2.970	9.893	-0.72496068E+00
BD(2,18,0.1098)	-2.970	-3.725	9.893	-0.91161633E+00
BD(2,19,0.1098)	-2.067	-4.292	9.893	-0.10544167E+01
BD(2,20,0.1098)	-1.060	-4.645	9.893	-0.11462831E+01
BD(2,21,0.1098)	0.000	-4.764	9.893	-0.11823816E+01
BD(2,22,0.1098)	1.060	-4.645	9.893	-0.11802678E+01
BD(2,23,0.1098)	2.067	-4.292	9.893	-0.10799847E+01
BD(2,24,0.1098)	2.970	-3.725	9.893	-0.94416970E+00
BD(2,25,0.1098)	3.725	-2.970	9.893	-0.75826055E+00
BD(2,26,0.1098)	4.292	-2.067	9.893	-0.53075373E+00
BD(2,27,0.1098)	4.645	-1.060	9.893	-0.27325028E+00
BD(3, 0,0.1098)	6.846	0.000	8.584	0.00000000E+00
BD(3, 1,0.1098)	6.674	1.523	8.584	0.18418664E+00
BD(3, 2,0.1098)	6.168	2.970	8.584	0.35526085E+00
BD(3, 3,0.1098)	5.352	4.268	8.584	0.50222510E+00
BD(3, 4,0.1098)	4.268	5.352	8.584	0.61771917E+00
BD(3, 5,0.1098)	2.970	6.168	8.584	0.69803381E+00
BD(3, 6,0.1098)	1.523	6.674	8.584	0.74192619E+00
BD(3, 7,0.1098)	-0.000	6.846	8.584	0.74949068E+00
BD(3, 8,0.1098)	-1.523	6.674	8.584	0.72170919E+00
BD(3, 9,0.1098)	-2.970	6.168	8.584	0.66050106E+00
BD(3,10,0.1098)	-4.268	5.352	8.584	0.56890941E+00
BD(3,11,0.1098)	-5.352	4.268	8.584	0.45119959E+00
BD(3,12,0.1098)	-6.168	2.970	8.584	0.31279147E+00
BD(3,13,0.1098)	-6.674	1.523	8.584	0.16065433E+00
BD(3,14,0.1098)	-6.846	-0.000	8.584	-0.52495334E-05
BD(3,15,0.1098)	-6.674	-1.523	8.584	-0.16066362E+00
BD(3,16,0.1098)	-6.168	-2.970	8.584	-0.31280082E+00
BD(3,17,0.1098)	-5.352	-4.268	8.584	-0.45126656E+00
BD(3,18,0.1098)	-4.268	-5.352	8.584	-0.56891584E+00
BD(3,19,0.1098)	-2.970	-6.168	8.584	-0.66050559E+00
BD(3,20,0.1098)	-1.523	-6.674	8.584	-0.72171152E+00
BD(3,21,0.1098)	0.000	-6.846	8.584	-0.74949127E+00
BD(3,22,0.1098)	1.523	-6.674	8.584	-0.74192381E+00
BD(3,23,0.1098)	2.970	-6.168	8.584	-0.69802988E+00
BD(3,24,0.1098)	4.268	-5.352	8.584	-0.61771351E+00
BD(3,25,0.1098)	5.352	-4.268	8.584	-0.50221741E+00
BD(3,26,0.1098)	6.168	-2.970	8.584	-0.35525119E+00
BD(3,27,0.1098)	6.674	-1.523	8.584	-0.18417578E+00
BD(4, 0,0.1098)	8.585	0.000	6.846	0.00000000E+00
BD(4, 1,0.1098)	8.369	1.910	6.846	0.12255067E+00
BD(4, 2,0.1098)	7.734	3.725	6.846	0.23400450E+00
BD(4, 3,0.1098)	6.712	5.352	6.846	0.32437348E+00
BD(4, 4,0.1098)	5.352	6.712	6.846	0.38884884E+00
BD(4, 5,0.1098)	3.725	7.734	6.846	0.42808050E+00
BD(4, 6,0.1098)	1.910	8.369	6.846	0.44479442E+00
BD(4, 7,0.1098)	-0.000	8.585	6.846	0.44134152E+00
BD(4, 8,0.1098)	-1.910	8.369	6.846	0.41928818E+00
BD(4, 9,0.1098)	-3.725	7.734	6.846	0.37993348E+00

```
BD( 4,10,0.1098)   -5.352    6.712    6.846     0.32486743E+00
BD( 4,11,0.1098)   -6.712    5.352    6.846     0.25627136E+00
BD( 4,12,0.1098)   -7.734    3.725    6.846     0.17697734E+00
BD( 4,13,0.1098)   -8.369    1.910    6.846     0.9034019?E-01
BD( 4,14,0.1098)   -8.585   -0.000    6.846    -0.29605271E-05
BD( 4,15,0.1098)   -8.369   -1.910    6.846    -0.9034550.E-01
BD( 4,16,0.1098)   -7.734   -3.725    6.846    -0.17698228E+00
BD( 4,17,0.1098)   -6.712   -5.352    6.846    -0.25627565E+00
BD( 4,18,0.1098)   -5.352   -6.712    6.846    -0.32487106E+00
BD( 4,19,0.1098)   -3.725   -7.734    6.846    -0.3799362?E+00
BD( 4,20,0.1098)   -1.910   -8.369    6.846    -0.41928941E+00
BD( 4,21,0.1098)    0.000   -8.585    6.846    -0.44134241E+00
BD( 4,22,0.1098)    1.910   -8.369    6.846    -0.44479394E+00
BD( 4,23,0.1098)    3.725   -7.734    6.846    -0.42867877E+00
BD( 4,24,0.1098)    5.352   -6.712    6.846    -0.38884604E+00
BD( 4,25,0.1098)    6.712   -5.352    6.846    -0.32436872E+00
BD( 4,26,0.1098)    7.734   -3.725    6.846    -0.23399842E+00
BD( 4,27,0.1098)    8.369   -1.910    6.846    -0.12254351E+00
BD( 5, 0,0.1098)    9.893    0.000    4.764     0.00000000E+00
BD( 5, 1,0.1098)    9.645    2.201    4.764     0.86975396E-01
BD( 5, 2,0.1098)    8.913    4.292    4.764     0.16814840E+00
BD( 5, 3,0.1098)    7.734    6.168    4.764     0.22953035E+00

BD( 5, 4,0.1098)    6.168    7.734    4.764     0.26539707E+00
BD( 5, 5,0.1098)    4.292    8.913    4.764     0.28026271E+00
BD( 5, 6,0.1098)    2.201    9.645    4.764     0.28051043E+00
BD( 5, 7,0.1098)   -0.000    9.893    4.764     0.27015424E+00
BD( 5, 8,0.1098)   -2.201    9.645    4.764     0.25095505E+00
BD( 5, 9,0.1098)   -4.292    8.913    4.764     0.22365242E+00
BD( 5,10,0.1098)   -6.168    7.734    4.764     0.18887687E+00
BD( 5,11,0.1098)   -7.734    6.168    4.764     0.14758426E+00
BD( 5,12,0.1098)   -8.913    4.292    4.764     0.10116762E+00
BD( 5,13,0.1098)   -9.645    2.201    4.764     0.51369261E-01
BD( 5,14,0.1098)   -9.893   -0.000    4.764    -0.16799022E-05
BD( 5,15,0.1098)   -9.645   -2.201    4.764    -0.51372316E-01
BD( 5,16,0.1098)   -8.913   -4.292    4.764    -0.10117066E+00
BD( 5,17,0.1098)   -7.734   -6.168    4.764    -0.14758694E+00
BD( 5,18,0.1098)   -6.168   -7.734    4.764    -0.18887889E+00
BD( 5,19,0.1098)   -4.292   -8.913    4.764    -0.22365403E+00
BD( 5,20,0.1098)   -2.201   -9.645    4.764    -0.25095618E+00
BD( 5,21,0.1098)    0.000   -9.893    4.764    -0.27015465E+00
BD( 5,22,0.1098)    2.201   -9.645    4.764    -0.28051054E+00
BD( 5,23,0.1098)    4.292   -8.913    4.764    -0.28026229E+00
BD( 5,24,0.1098)    6.168   -7.734    4.764    -0.26539564E+00
BD( 5,25,0.1098)    7.734   -6.168    4.764    -0.22952735E+00

BD( 5,26,0.1098)    8.913   -4.292    4.764    -0.16814387E+00
BD( 5,27,0.1098)    9.645   -2.201    4.764    -0.86970031E-01
BD( 6, 0,0.1098)   10.705    0.000    2.443     0.00000000E+00
BD( 6, 1,0.1098)   10.436    2.382    2.443     0.60829788E-01
BD( 6, 2,0.1098)    9.645    4.645    2.443     0.12995464E+00
BD( 6, 3,0.1098)    8.369    6.674    2.443     0.17969024E+00
BD( 6, 4,0.1098)    6.674    8.369    2.443     0.20096236E+00
BD( 6, 5,0.1098)    4.645    9.645    2.443     0.20224088E+00
BD( 6, 6,0.1098)    2.382   10.436    2.443     0.19313401E+00
BD( 6, 7,0.1098)   -0.000   10.705    2.443     0.17880517E+00
BD( 6, 8,0.1098)   -2.382   10.436    2.443     0.16103059E+00
BD( 6, 9,0.1098)   -4.645    9.645    2.443     0.14014053E+00
BD( 6,10,0.1098)   -6.674    8.369    2.443     0.11618876E+00
BD( 6,11,0.1098)   -8.369    6.674    2.443     0.89445055E-01
BD( 6,12,0.1098)   -9.645    4.645    2.443     0.60529798E-01
BD( 6,13,0.1098)  -10.436    2.382    2.443     0.30379631E-01
BD( 6,14,0.1098)  -10.705   -0.000    2.443    -0.98706823E-06
BD( 6,15,0.1098)  -10.436   -2.382    2.443    -0.3038142?E-01
BD( 6,16,0.1098)   -9.645   -4.645    2.443    -0.60531683E-01
BD( 6,17,0.1098)   -8.369   -6.674    2.443    -0.89446723E-01
BD( 6,18,0.1098)   -6.674   -8.369    2.443    -0.11619014E+00
BD( 6,19,0.1098)   -4.645   -9.645    2.443    -0.14014196E+00
```

```
BD(  6,20,0.1098)   -2.382  -10.436    2.443     -0.161031E0E+00
BD(  6,21,0.1098)    0.000  -10.705    2.443     -0.178866078+00
BD(  6,22,0.1098)    2.382  -10.436    2.443     -0.193134618+00
BD(  6,23,0.1098)    4.645   -9.645    2.443     -0.202241188+00
BD(  6,24,0.1098)    6.674   -8.369    2.443     -0.200961358+00
BD(  6,25,0.1098)    8.369   -6.674    2.443     -0.179683048+00
BD(  6,26,0.1098)    9.645   -4.644    2.443     -0.129950648+00
BD(  6,27,0.1098)   10.436   -2.382    2.443     -0.608255578-01
BD(  7, 0,0.1098)   10.930    0.000   -0.000      0.000000008+00
BD(  7, 1,0.1098)   10.705    2.443   -0.000      0.429931248-01
BD(  7, 2,0.1098)    9.893    4.764   -0.000      0.106368888+00
BD(  7, 3,0.1098)    8.584    6.846   -0.000      0.150659268+00
BD(  7, 4,0.1098)    6.846    8.585   -0.000      0.164292098+00
BD(  7, 5,0.1098)    4.764    9.893   -0.000      0.156620018+00
BD(  7, 6,0.1098)    2.443   10.705   -0.000      0.144999138+00
BD(  7, 7,0.1098)   -0.000   10.986   -0.000      0.128774768+00
BD(  7, 8,0.1098)   -2.443   10.705   -0.000      0.111965608+00
BD(  7, 9,0.1098)   -4.764    9.893   -0.000      0.946644548-01
BD(  7,10,0.1098)   -6.846    8.584   -0.000      0.766525278-01
BD(  7,11,0.1098)   -8.585    6.846   -0.000      0.578493758-01
BD(  7,12,0.1098)   -9.893    4.764   -0.000      0.384547348-01
BD(  7,13,0.1098)  -10.705    2.443   -0.000      0.189098908-01

BD(  7,14,0.1098)  -10.980   -0.000   -0.000     -0.598152858-06
BD(  7,15,0.1098)  -10.705   -2.443   -0.000     -0.189410348-01
BD(  7,16,0.1098)   -9.893   -4.764   -0.000     -0.384560088-01
BD(  7,17,0.1098)   -8.584   -6.846   -0.000     -0.578503808-01
BD(  7,18,0.1098)   -6.846   -8.585   -0.000     -0.766536008-01
BD(  7,19,0.1098)   -4.764   -9.893   -0.000     -0.946655878-01
BD(  7,20,0.1098)   -2.443  -10.705   -0.000     -0.111986738+00
BD(  7,21,0.1098)    0.000  -10.980   -0.000     -0.128775668+00
BD(  7,22,0.1098)    2.443  -10.705   -0.000     -0.144940148+00
BD(  7,23,0.1098)    4.764   -9.893   -0.000     -0.158670258+00
BD(  7,24,0.1098)    6.846   -8.584   -0.000     -0.164293118+00
BD(  7,25,0.1098)    8.585   -6.846   -0.000     -0.150657598+00
BD(  7,26,0.1098)    9.893   -4.764   -0.000     -0.106965608+00
BD(  7,27,0.1098)   10.705   -2.443   -0.000     -0.429892768-01
BD(  8, 0,0.1098)   10.705    0.000   -2.443      0.000000008+00
BD(  8, 1,0.1098)   10.486    2.382   -2.443      0.432511368-01
BD(  8, 2,0.1098)    9.645    4.645   -2.443      0.957370408-01
BD(  8, 3,0.1098)    8.369    6.674   -2.443      0.130513058+00
BD(  8, 4,0.1098)    6.674    8.369   -2.443      0.139304[8E+00
BD(  8, 5,0.1098)    4.645    9.645   -2.443      0.131137028+00
BD(  8, 6,0.1098)    2.382   10.436   -2.443      0.116247538+00
BD(  8, 7,0.1098)   -0.000   10.705   -2.443      0.993413[5E-01

BD(  8, 8,0.1098)   -2.382   10.436   -2.443      0.841441758-01
BD(  8, 9,0.1098)   -4.645    9.645   -2.443      0.6[8837[2E-01
BD(  8,10,0.1098)   -6.674    8.369   -2.443      0.545307258-01
BD(  8,11,0.1098)   -8.369    6.674   -2.443      0.402747[2E-01
BD(  8,12,0.1098)   -9.645    4.645   -2.443      0.263125[5E-01
BD(  8,13,0.1098)  -10.436    2.382   -2.443      0.123312[8E-01
BD(  8,14,0.1098)  -10.705   -0.000   -2.443     -0.411072[5E-06
BD(  8,15,0.1098)  -10.436   -2.382   -2.443     -0.128[[060E-01
BD(  8,16,0.1098)   -9.645   -4.645   -2.443     -0.263133[1E-01
BD(  8,17,0.1098)   -8.369   -6.674   -2.443     -0.402753[7E-01
BD(  8,18,0.1098)   -6.674   -8.369   -2.443     -0.545[[[[2E-01
BD(  8,19,0.1098)   -4.645   -9.645   -2.443     -0.6[[[[[2E-01
BD(  8,20,0.1098)   -2.382  -10.436   -2.443     -0.841[[[[9E-01
BD(  8,21,0.1098)    0.000  -10.705   -2.443      0.[[[[[[[E-01
BD(  8,22,0.1098)    2.382  -10.436   -2.443     -0.11[[[[[E+00
BD(  8,23,0.1098)    4.645   -9.645   -2.443     -0.1[[[[[[E+00
BD(  8,24,0.1098)    6.674   -8.369   -2.443     -0.1[[[[[[E+00
BD(  8,25,0.1098)    8.369   -6.674   -2.443     -0.1[[[[[[E+00
BD(  8,26,0.1098)    9.645   -4.644   -2.443     -0.95[[[[[[E-01
BD(  8,27,0.1098)   10.436   -2.382   -2.443     -0.43[[[[[[E-01
BD(  9, 0,0.1098)    9.893    0.000   -4.764      0.000000008+00
BD(  9, 1,0.1098)    9.645    2.381   -4.764      0.451760248-01
```

```
BD( 6,20,0.1098)   -2.382 -10.436    2.443     -0.29608089E-01
BD( 6,21,0.1098)    0.000 -10.705    2.443     -0.61649971E-01
BD( 6,22,0.1098)    2.382 -10.436    2.443     -0.90600371E-01
BD( 6,23,0.1098)    4.645  -9.645    2.443     -0.11560764E+00
BD( 6,24,0.1098)    6.674  -8.369    2.443     -0.13364780E+00
BD( 6,25,0.1098)    8.369  -6.674    2.443     -0.14558637E+00
BD( 6,26,0.1098)    9.645  -4.644    2.443     -0.15022463E+00
BD( 6,27,0.1098)   10.436  -2.382    2.443     -0.14732993E+00
BD( 7, 0,0.1098)   10.980   0.000   -0.000     -0.91851771E-01
BD( 7, 1,0.1098)   10.705   2.443   -0.000     -0.81332684E-01
BD( 7, 2,0.1098)    9.893   4.764   -0.000     -0.66735268E-01
BD( 7, 3,0.1098)    8.584   6.846   -0.000     -0.48791405E-01
BD( 7, 4,0.1098)    6.846   8.585   -0.000     -0.28400972E-01
BD( 7, 5,0.1098)    4.764   9.893   -0.000     -0.65863505E-02
BD( 7, 6,0.1098)    2.443  10.705   -0.000      0.15558507E-01
BD( 7, 7,0.1098)   -0.000  10.980   -0.000      0.36923263E-01
BD( 7, 8,0.1098)   -2.443  10.705   -0.000      0.56436427E-01
BD( 7, 9,0.1098)   -4.764   9.893   -0.000      0.73119640E-01
BD( 7,10,0.1098)   -6.846   8.584   -0.000      0.86136341E-01
BD( 7,11,0.1098)   -8.585   6.846   -0.000      0.94833791E-01
BD( 7,12,0.1098)   -9.893   4.764   -0.000      0.98775864E-01
BD( 7,13,0.1098)  -10.705   2.443   -0.000      0.97764909E-01

BD( 7,14,0.1098)  -10.980  -0.000   -0.000      0.91851532E-01
BD( 7,15,0.1098)  -10.705  -2.443   -0.000      0.81332326E-01
BD( 7,16,0.1098)   -9.893  -4.764   -0.000      0.66734672E-01
BD( 7,17,0.1098)   -8.584  -6.846   -0.000      0.48790850E-01
BD( 7,18,0.1098)   -6.846  -8.585   -0.000      0.28400317E-01
BD( 7,19,0.1098)   -4.764  -9.893   -0.000      0.65857023E-02
BD( 7,20,0.1098)   -2.443 -10.705   -0.000     -0.15559223E-01
BD( 7,21,0.1098)    0.000 -10.980   -0.000     -0.36923874E-01
BD( 7,22,0.1098)    2.443 -10.705   -0.000     -0.56436982E-01
BD( 7,23,0.1098)    4.764  -9.893   -0.000     -0.73120177E-01
BD( 7,24,0.1098)    6.846  -8.584   -0.000     -0.86136699E-01
BD( 7,25,0.1098)    8.585  -6.846   -0.000     -0.94834030E-01
BD( 7,26,0.1098)    9.893  -4.764   -0.000     -0.98775864E-01
BD( 7,27,0.1098)   10.705  -2.443   -0.000     -0.97764730E-01
BD( 8, 0,0.1098)   10.705   0.000   -2.443     -0.62594891E-01
BD( 8, 1,0.1098)   10.436   2.382   -2.443     -0.55814750E-01
BD( 8, 2,0.1098)    9.645   4.645   -2.443     -0.46235800E-01
BD( 8, 3,0.1098)    8.369   6.674   -2.443     -0.34338370E-01
BD( 8, 4,0.1098)    6.674   8.369   -2.443     -0.20719070E-01
BD( 8, 5,0.1098)    4.645   9.645   -2.443     -0.60608536E-02
BD( 8, 6,0.1098)    2.382  10.436   -2.443      0.89012869E-02
BD( 8, 7,0.1098)   -0.000  10.705   -2.443      0.23417130E-01
BD( 8, 8,0.1098)   -2.382  10.436   -2.443      0.36758680E-01
BD( 8, 9,0.1098)   -4.645   9.645   -2.443      0.48256997E-01
BD( 8,10,0.1098)   -6.674   8.369   -2.443      0.57335500E-01
BD( 8,11,0.1098)   -8.369   6.674   -2.443      0.63538909E-01
BD( 8,12,0.1098)   -9.645   4.645   -2.443      0.66556275E-01
BD( 8,13,0.1098)  -10.436   2.382   -2.443      0.66236198E-01
BD( 8,14,0.1098)  -10.705  -0.000   -2.443      0.62594712E-01
BD( 8,15,0.1098)  -10.436  -2.382   -2.443      0.55814505E-01
BD( 8,16,0.1098)   -9.645  -4.645   -2.443      0.46235427E-01
BD( 8,17,0.1098)   -8.369  -6.674   -2.443      0.34337930E-01
BD( 8,18,0.1098)   -6.674  -8.369   -2.443      0.20718542E-01
BD( 8,19,0.1098)   -4.645  -9.645   -2.443      0.60603991E-02
BD( 8,20,0.1098)   -2.382 -10.436   -2.443     -0.89017786E-02
BD( 8,21,0.1098)    0.000 -10.705   -2.443     -0.23417551E-01
BD( 8,22,0.1098)    2.382 -10.436   -2.443     -0.36753108E-01
BD( 8,23,0.1098)    4.645  -9.645   -2.443     -0.48257388E-01
BD( 8,24,0.1098)    6.674  -8.369   -2.443     -0.57335790E-01
BD( 8,25,0.1098)    8.369  -6.674   -2.443     -0.63539088E-01
BD( 8,26,0.1098)    9.645  -4.644   -2.443     -0.66556275E-01
BD( 8,27,0.1098)   10.436  -2.382   -2.443     -0.66236138E-01
BD( 9, 0,0.1098)    9.893   0.000   -4.764     -0.43139141E-01
BD( 9, 1,0.1098)    9.645   2.201   -4.764     -0.38622074E-01
```

BD(4,10,0.1098)	-5.352	6.712	6.846	0.35936677E+00
BD(4,11,0.1098)	-6.712	5.352	6.846	0.37520176E+00
BD(4,12,0.1098)	-7.734	3.725	6.846	0.37222254E+00
BD(4,13,0.1098)	-8.369	1.910	6.846	0.35057831E+00
BD(4,14,0.1098)	-8.585	-0.000	6.846	0.31135452E+00
BD(4,15,0.1098)	-8.369	-1.910	6.846	0.25651795E+00
BD(4,16,0.1098)	-7.734	-3.725	6.846	0.18881834E+00
BD(4,17,0.1098)	-6.712	-5.352	6.846	0.11165106E+00
BD(4,18,0.1098)	-5.352	-6.712	6.846	0.28885048E-01
BD(4,19,0.1098)	-3.725	-7.734	6.846	-0.55329453E-01
BD(4,20,0.1098)	-1.910	-8.369	6.846	-0.13676989E+00
BD(4,21,0.1098)	0.000	-8.585	6.846	-0.21135169E+00
BD(4,22,0.1098)	1.910	-8.369	6.846	-0.27533543E+00
BD(4,23,0.1098)	3.725	-7.734	6.846	-0.32551324E+00
BD(4,24,0.1098)	5.352	-6.712	6.846	-0.35936779E+00
BD(4,25,0.1098)	6.712	-5.352	6.846	-0.37520206E+00
BD(4,26,0.1098)	7.734	-3.725	6.846	-0.37222195E+00
BD(4,27,0.1098)	8.369	-1.910	6.846	-0.35057712E+00
BD(5, 0,0.1098)	9.893	0.000	4.764	-0.20714957E+00
BD(5, 1,0.1098)	9.645	2.201	4.764	-0.17740279E+00
BD(5, 2,0.1098)	8.913	4.292	4.764	-0.13876027E+00
BD(5, 3,0.1098)	7.734	6.168	4.764	-0.93159795E-01
BD(5, 4,0.1098)	6.168	7.734	4.764	-0.42887986E-01
BD(5, 5,0.1098)	4.292	8.913	4.764	0.95345415E-02
BD(5, 6,0.1098)	2.201	9.645	4.764	0.61479010E-01
BD(5, 7,0.1098)	-0.000	9.893	4.764	0.11034077E+00
BD(5, 8,0.1098)	-2.201	9.645	4.764	0.15366924E+00
BD(5, 9,0.1098)	-4.292	8.913	4.764	0.18929213E+00
BD(5,10,0.1098)	-6.168	7.734	4.764	0.21542317E+00
BD(5,11,0.1098)	-7.734	6.168	4.764	0.23075187E+00
BD(5,12,0.1098)	-8.913	4.292	4.764	0.23450989E+00
BD(5,13,0.1098)	-9.645	2.201	4.764	0.22650838E+00
BD(5,14,0.1098)	-9.893	-0.000	4.764	0.20714879E+00
BD(5,15,0.1098)	-9.645	-2.201	4.764	0.17740178E+00
BD(5,16,0.1098)	-8.913	-4.292	4.764	0.13875896E+00
BD(5,17,0.1098)	-7.734	-6.168	4.764	0.93158364E-01
BD(5,18,0.1098)	-6.168	-7.734	4.764	0.42886604E-01
BD(5,19,0.1098)	-4.292	-8.913	4.764	-0.95361397E-02
BD(5,20,0.1098)	-2.201	-9.645	4.764	-0.61480667E-01
BD(5,21,0.1098)	0.000	-9.893	4.764	-0.11034214E+00
BD(5,22,0.1098)	2.201	-9.645	4.764	-0.15367037E+00
BD(5,23,0.1098)	4.292	-8.913	4.764	-0.18929332E+00
BD(5,24,0.1098)	6.168	-7.734	4.764	-0.21542388E+00
BD(5,25,0.1098)	7.734	-6.168	4.764	-0.23075229E+00
BD(5,26,0.1098)	8.913	-4.292	4.764	-0.23450977E+00
BD(5,27,0.1098)	9.645	-2.201	4.764	-0.22650796E+00
BD(6, 0,0.1098)	10.705	0.000	2.443	-0.13704842E+00
BD(6, 1,0.1098)	10.436	2.382	2.443	-0.11989415E+00
BD(6, 2,0.1098)	9.645	4.645	2.443	-0.96727848E-01
BD(6, 3,0.1098)	8.369	6.674	2.443	-0.68711281E-01
BD(6, 4,0.1098)	6.674	8.369	2.443	-0.37249252E-01
BD(6, 5,0.1098)	4.645	9.645	2.443	-0.39192922E-02
BD(6, 6,0.1098)	2.382	10.436	2.443	0.29607162E-01
BD(6, 7,0.1098)	-0.000	10.705	2.443	0.61649058E-01
BD(6, 8,0.1098)	-2.382	10.436	2.443	0.90599418E-01
BD(6, 9,0.1098)	-4.645	9.645	2.443	0.11500686E+00
BD(6,10,0.1098)	-6.674	8.369	2.443	0.13364732E+00
BD(6,11,0.1098)	-8.369	6.674	2.443	0.14556613E+00
BD(6,12,0.1098)	-9.645	4.645	2.443	0.15022463E+00
BD(6,13,0.1098)	-10.436	2.382	2.443	0.14730022E+00
BD(6,14,0.1098)	-10.705	-0.000	2.443	0.13704795E+00
BD(6,15,0.1098)	-10.436	-2.382	2.443	0.11989355E+00
BD(6,16,0.1098)	-9.645	-4.645	2.443	0.96726354E-01
BD(6,17,0.1098)	-8.369	-6.674	2.443	0.68710446E-01
BD(6,18,0.1098)	-6.674	-8.369	2.443	0.37248190E-01
BD(6,19,0.1098)	-4.645	-9.645	2.443	0.39192139E-02

```
BD( 2,15,0.1098)   -4.645   -1.060    9.893     0.35608387E+00
BD( 2,16,0.1098)   -4.292   -2.067    9.893     0.15533835E+00
BD( 2,17,0.1098)   -3.725   -2.970    9.893    -0.53195253E-01
BD( 2,18,0.1098)   -2.970   -3.725    9.893    -0.25906265E+00
BD( 2,19,0.1098)   -2.067   -4.292    9.893    -0.45193881E+00
BD( 2,20,0.1098)   -1.060   -4.645    9.893    -0.62215358E+00
BD( 2,21,0.1098)    0.000   -4.764    9.893    -0.76117051E+00

BD( 2,22,0.1098)    1.060   -4.645    9.893    -0.86201847E+00
BD( 2,23,0.1098)    2.067   -4.292    9.893    -0.91964173E+00
BD( 2,24,0.1098)    2.970   -3.725    9.893    -0.93114984E+00
BD( 2,25,0.1098)    3.725   -2.970    9.893    -0.89596587E+00
BD( 2,26,0.1098)    4.292   -2.067    9.893    -0.81585395E+00
BD( 2,27,0.1098)    4.645   -1.060    9.893    -0.69483227E+00
BD( 3, 0,0.1098)    6.846    0.000    8.584    -0.44397569E+00
BD( 3, 1,0.1098)    6.674    1.523    8.584    -0.33974600E+00
BD( 3, 2,0.1098)    6.168    2.970    8.584    -0.21848011E+00
BD( 3, 3,0.1098)    5.352    4.268    8.584    -0.86258650E-01
BD( 3, 4,0.1098)    4.268    5.352    8.584     0.50287962E-01
BD( 3, 5,0.1098)    2.970    6.168    8.584     0.18431294E+00
BD( 3, 6,0.1098)    1.523    6.674    8.584     0.30909562E+00
BD( 3, 7,0.1098)   -0.000    6.846    8.584     0.41837960E+00
BD( 3, 8,0.1098)   -1.523    6.674    8.584     0.50668353E+00
BD( 3, 9,0.1098)   -2.970    6.168    8.584     0.56958026E+00
BD( 3,10,0.1098)   -4.268    5.352    8.584     0.60391593E+00
BD( 3,11,0.1098)   -5.352    4.268    8.584     0.60796839E+00
BD( 3,12,0.1098)   -6.168    2.970    8.584     0.58153450E+00
BD( 3,13,0.1098)   -6.674    1.523    8.584     0.52594024E+00
BD( 3,14,0.1098)   -6.846   -0.000    8.584     0.44397265E+00
BD( 3,15,0.1098)   -6.674   -1.523    8.584     0.33974254E+00

BD( 3,16,0.1098)   -6.168   -2.970    8.584     0.21847576E+00
BD( 3,17,0.1098)   -5.352   -4.268    8.584     0.86254776E-01
BD( 3,18,0.1098)   -4.268   -5.352    8.584    -0.50292108E-01
BD( 3,19,0.1098)   -2.970   -6.168    8.584    -0.18431687E+00
BD( 3,20,0.1098)   -1.523   -6.674    8.584    -0.30909926E+00
BD( 3,21,0.1098)    0.000   -6.846    8.584    -0.41838264E+00
BD( 3,22,0.1098)    1.523   -6.674    8.584    -0.50668615E+00
BD( 3,23,0.1098)    2.970   -6.168    8.584    -0.56958216E+00
BD( 3,24,0.1098)    4.268   -5.352    8.584    -0.60391653E+00
BD( 3,25,0.1098)    5.352   -4.268    8.584    -0.60796809E+00
BD( 3,26,0.1098)    6.168   -2.970    8.584    -0.58153307E+00
BD( 3,27,0.1098)    6.674   -1.523    8.584    -0.52593803E+00
BD( 4, 0,0.1098)    8.585    0.000    6.846    -0.31135607E+00
BD( 4, 1,0.1098)    8.369    1.910    6.846    -0.25651997E+00
BD( 4, 2,0.1098)    7.734    3.725    6.846    -0.18882084E+00
BD( 4, 3,0.1098)    6.712    5.352    6.846    -0.11165357E+00
BD( 4, 4,0.1098)    5.352    6.712    6.846    -0.28887551E-01
BD( 4, 5,0.1098)    3.725    7.734    6.846     0.55327006E-01
BD( 4, 6,0.1098)    1.910    8.369    6.846     0.13676739E+00
BD( 4, 7,0.1098)   -0.000    8.585    6.846     0.21134979E+00
BD( 4, 8,0.1098)   -1.910    8.369    6.846     0.27533382E+00
BD( 4, 9,0.1098)   -3.725    7.734    6.846     0.32551146E+00
```

Calculated Data for Model #4

	DIPOLE#1	DIPOLE#2	DIPOLE#3	
MOMENT	0.55E-05	0.55E-05	0.55E-05	(AMP*M)
LOCATN	0.066	0.053	0.040	(M FR ORN)

TRANS	1.000 0.000 0.000	0.000 1.000 0.000	0.000 1.000 0.000
MATRIX	0.000 1.000 0.000	-1.000 0.000 0.000	-1.000 0.000 0.000
	0.000 0.000 1.000	0.000 0.000 1.000	0.000 0.000 1.000

THE MEAS SPHERE RADIUS IS 0.1098 M

SPHER DATA POINTS: THETA=T*0.2244; PHI=F*0.2244

BD(T,F,R)	X	Y	Z	FLUX DENS, XEE-11 TESLA
BD(0, 0,0.1098)	0.000	0.000	10.980	0.00000000E+00
BD(1, 0,0.1098)	2.443	0.000	10.705	-0.42410666E+00
BD(1, 1,0.1098)	2.382	0.544	10.705	-0.21413589E+00
BD(1, 2,0.1098)	2.201	1.060	10.705	0.65727420E-02
BD(1, 3,0.1098)	1.910	1.523	10.705	0.22695166E+00
BD(1, 4,0.1098)	1.523	1.910	10.705	0.43594974E+00
BD(1, 5,0.1098)	1.060	2.201	10.705	0.62308735E+00
BD(1, 6,0.1098)	0.544	2.382	10.705	0.77898133E+00
BD(1, 7,0.1098)	-0.000	2.443	10.705	0.89581430E+00
BD(1, 8,0.1098)	-0.544	2.382	10.705	0.96772563E+00
BD(1, 9,0.1098)	-1.060	2.201	10.705	0.99111158E+00
BD(1,10,0.1098)	-1.523	1.910	10.705	0.96479923E+00
BD(1,11,0.1098)	-1.910	1.523	10.705	0.89010805E+00
BD(1,12,0.1098)	-2.201	1.060	10.705	0.77078176E+00
BD(1,13,0.1098)	-2.382	0.544	10.705	0.61280584E+00
BD(1,14,0.1098)	-2.443	-0.000	10.705	0.42410010E+00
BD(1,15,0.1098)	-2.382	-0.544	10.705	0.21412909E+00
BD(1,16,0.1098)	-2.201	-1.060	10.705	-0.65801106E-02
BD(1,17,0.1098)	-1.910	-1.523	10.705	-0.22695762E+00
BD(1,18,0.1098)	-1.523	-1.910	10.705	-0.43595570E+00
BD(1,19,0.1098)	-1.060	-2.201	10.705	-0.62309307E+00
BD(1,20,0.1098)	-0.544	-2.382	10.705	-0.77898550E+00
BD(1,21,0.1098)	0.000	-2.443	10.705	-0.89581704E+00
BD(1,22,0.1098)	0.544	-2.382	10.705	-0.96772736E+00
BD(1,23,0.1098)	1.060	-2.201	10.705	-0.99111187E+00
BD(1,24,0.1098)	1.523	-1.910	10.705	-0.96479762E+00
BD(1,25,0.1098)	1.910	-1.523	10.705	-0.89010495E+00
BD(1,26,0.1098)	2.201	-1.060	10.705	-0.77077711E+00
BD(1,27,0.1098)	2.382	-0.544	10.705	-0.61280006E+00
BD(2, 0,0.1098)	4.764	0.000	9.893	-0.53897387E+00
BD(2, 1,0.1098)	4.645	1.060	9.893	-0.55609001E+00
BD(2, 2,0.1098)	4.292	2.067	9.893	-0.15[illegible]E+00
BD(2, 3,0.1098)	3.725	2.970	9.893	0.53[illegible]E-01
BD(2, 4,0.1098)	2.970	3.725	9.893	0.25905639E+00
BD(2, 5,0.1098)	2.067	4.292	9.893	0.45[illegible]E+00
BD(2, 6,0.1098)	1.060	4.645	9.893	0.62214845E+00
BD(2, 7,0.1098)	-0.000	4.764	9.893	0.76116687E+00
BD(2, 8,0.1098)	-1.060	4.645	9.893	0.86201614E+00
BD(2, 9,0.1098)	-2.067	4.292	9.893	0.91964024E+00
BD(2,10,0.1098)	-2.970	3.725	9.893	0.93114996E+00
BD(2,11,0.1098)	-3.725	2.970	9.893	0.89596778E+00
BD(2,12,0.1098)	-4.292	2.067	9.893	0.81585747E+00
BD(2,13,0.1098)	-4.645	1.060	9.893	0.69483703E+00
BD(2,14,0.1098)	-4.764	-0.000	9.893	0.53897321E+00

```
  BD(13,22,0.1098)    0.544   -2.382 -10.705     -0.52279234E-02
  BD(13,23,0.1098)    1.060   -2.201 -10.705     -0.59444010E-02
  BD(13,24,0.1098)    1.523   -1.910 -10.705     -0.63627958E-02
  BD(13,25,0.1098)    1.910   -1.523 -10.705     -0.64621344E-02
  BD(13,26,0.1098)    2.201   -1.060 -10.705     -0.62374324E-02
  BD(13,27,0.1098)    2.382   -0.544 -10.705     -0.56999549E-02
  BD(14, 0,0.1098)   -0.000    0.000 -10.980     -0.69667045E-08
END OF DATA
```

BD(11,12,0.1098)	-6.168	2.970	-8.585	0.21292880E-01
BD(11,13,0.1098)	-6.674	1.523	-8.585	0.19457854E-01
BD(11,14,0.1098)	-6.846	-0.000	-8.585	0.16647115E-01
BD(11,15,0.1098)	-6.674	-1.523	-8.585	0.13001624E-01
BD(11,16,0.1098)	-6.168	-2.970	-8.585	0.87041594E-02
BD(11,17,0.1098)	-5.352	-4.268	-8.585	0.39702505E-02
BD(11,18,0.1098)	-4.268	-5.352	-8.585	-0.96275867E-03
BD(11,19,0.1098)	-2.970	-6.168	-8.585	-0.58474913E-02
BD(11,20,0.1098)	-1.523	-6.674	-8.585	-0.10438986E-01
BD(11,21,0.1098)	0.000	-6.846	-8.585	-0.14507055E-01
BD(11,22,0.1098)	1.523	-6.674	-8.585	-0.17847657E-01
BD(11,23,0.1098)	2.970	-6.168	-8.585	-0.20293307E-01
BD(11,24,0.1098)	4.268	-5.352	-8.585	-0.21721352E-01
BD(11,25,0.1098)	5.352	-4.268	-8.585	-0.22060193E-01
BD(11,26,0.1098)	6.168	-2.970	-8.585	-0.21292843E-01
BD(11,27,0.1098)	6.674	-1.523	-8.585	-0.19457784E-01
BD(12, 0,0.1098)	4.764	0.000	-9.893	-0.10232415E-01
BD(12, 1,0.1098)	4.645	1.060	-9.893	-0.79920925E-02
BD(12, 2,0.1098)	4.292	2.067	-9.893	-0.53510033E-02
BD(12, 3,0.1098)	3.725	2.970	-9.893	-0.24415914E-02
BD(12, 4,0.1098)	2.970	3.725	-9.893	0.59024827E-03
BD(12, 5,0.1098)	2.067	4.292	-9.893	0.35924902E-02
BD(12, 6,0.1098)	1.060	4.645	-9.893	0.64145885E-02
BD(12, 7,0.1098)	-0.000	4.764	-9.893	0.89150406E-02
BD(12, 8,0.1098)	-1.060	4.645	-9.893	0.10968439E-01
BD(12, 9,0.1098)	-2.067	4.292	-9.893	0.12471836E-01
BD(12,10,0.1098)	-2.970	3.725	-9.893	0.13349853E-01
BD(12,11,0.1098)	-3.725	2.970	-9.893	0.13558436E-01
BD(12,12,0.1098)	-4.292	2.067	-9.893	0.13087146E-01
BD(12,13,0.1098)	-4.645	1.060	-9.893	0.11959597E-01
BD(12,14,0.1098)	-4.764	-0.000	-9.893	0.10232352E-01
BD(12,15,0.1098)	-4.645	-1.060	-9.893	0.79920180E-02
BD(12,16,0.1098)	-4.292	-2.067	-9.893	0.53509139E-02
BD(12,17,0.1098)	-3.725	-2.970	-9.893	0.24415078E-02
BD(12,18,0.1098)	-2.970	-3.725	-9.893	-0.59033651E-03
BD(12,19,0.1098)	-2.067	-4.292	-9.893	-0.35925813E-02
BD(12,20,0.1098)	-1.060	-4.645	-9.893	-0.64146742E-02
BD(12,21,0.1098)	0.000	-4.764	-9.893	-0.89151077E-02
BD(12,22,0.1098)	1.060	-4.645	-9.893	-0.10968495E-01
BD(12,23,0.1098)	2.067	-4.292	-9.893	-0.12471881E-01
BD(12,24,0.1098)	2.970	-3.725	-9.893	-0.13349872E-01
BD(12,25,0.1098)	3.725	-2.970	-9.893	-0.13558425E-01
BD(12,26,0.1098)	4.292	-2.067	-9.893	-0.13087116E-01
BD(12,27,0.1098)	4.645	-1.060	-9.893	-0.11959553E-01
BD(13, 0,0.1098)	2.443	0.000	-10.705	-0.48767217E-02
BD(13, 1,0.1098)	2.382	0.544	-10.705	-0.38089016E-02
BD(13, 2,0.1098)	2.201	1.060	-10.705	-0.25500872E-02
BD(13, 3,0.1098)	1.910	1.523	-10.705	-0.11633986E-02
BD(13, 4,0.1098)	1.523	1.910	-10.705	0.28162310E-03
BD(13, 5,0.1098)	1.060	2.201	-10.705	0.17125262E-02
BD(13, 6,0.1098)	0.544	2.382	-10.705	0.30575558E-02
BD(13, 7,0.1098)	-0.000	2.443	-10.705	0.42492673E-02
BD(13, 8,0.1098)	-0.544	2.382	-10.705	0.52278973E-02
BD(13, 9,0.1098)	-1.060	2.201	-10.705	0.59443824E-02
BD(13,10,0.1098)	-1.523	1.910	-10.705	0.63627884E-02
BD(13,11,0.1098)	-1.910	1.523	-10.705	0.64621381E-02
BD(13,12,0.1098)	-2.201	1.060	-10.705	0.62374435E-02
BD(13,13,0.1098)	-2.382	0.544	-10.705	0.56999773E-02
BD(13,14,0.1098)	-2.443	-0.000	-10.705	0.48766918E-02
BD(13,15,0.1098)	-2.382	-0.544	-10.705	0.38088665E-02
BD(13,16,0.1098)	-2.201	-1.060	-10.705	0.25500439E-02
BD(13,17,0.1098)	-1.910	-1.523	-10.705	0.11633583E-02
BD(13,18,0.1098)	-1.523	-1.910	-10.705	-0.28166780E-03
BD(13,19,0.1098)	-1.060	-2.201	-10.705	-0.17125721E-02
BD(13,20,0.1098)	-0.544	-2.382	-10.705	-0.30575949E-02
BD(13,21,0.1098)	0.000	-2.443	-10.705	-0.42493008E-02

BD(9, 2,0.1098)	8.913	4.292	-4.764	-0.18944908E-01
BD(9, 3,0.1098)	7.734	6.168	-4.764	-0.85801072E-02
BD(9, 4,0.1098)	6.168	7.734	-4.764	0.22149396E-02
BD(9, 5,0.1098)	4.292	8.913	-4.764	0.12898933E-01
BD(9, 6,0.1098)	2.201	9.645	-4.764	0.22936117E-01
BD(9, 7,0.1098)	-0.000	9.893	-4.764	0.31823210E-01
BD(9, 8,0.1098)	-2.201	9.645	-4.764	0.39114501E-01
BD(9, 9,0.1098)	-4.292	8.913	-4.764	0.44444449E-01
BD(9,10,0.1098)	-6.168	7.734	-4.764	0.47545761E-01
BD(9,11,0.1098)	-7.734	6.168	-4.764	0.48262909E-01
BD(9,12,0.1098)	-8.913	4.292	-4.764	0.46559934E-01
BD(9,13,0.1098)	-9.645	2.201	-4.764	0.42522240E-01
BD(9,14,0.1098)	-9.893	-0.000	-4.764	0.36352303E-01
BD(9,15,0.1098)	-9.645	-2.201	-4.764	0.28359499E-01
BD(9,16,0.1098)	-8.913	-4.292	-4.764	0.18944591E-01
BD(9,17,0.1098)	-7.734	-6.168	-4.764	0.85797906E-02
BD(9,18,0.1098)	-6.168	-7.734	-4.764	-0.22152397E-02
BD(9,19,0.1098)	-4.292	-8.913	-4.764	-0.12899242E-01
BD(9,20,0.1098)	-2.201	-9.645	-4.764	-0.22936389E-01
BD(9,21,0.1098)	0.000	-9.893	-4.764	-0.31823464E-01
BD(9,22,0.1098)	2.201	-9.645	-4.764	-0.39114717E-01
BD(9,23,0.1098)	4.292	-8.913	-4.764	-0.44444595E-01
BD(9,24,0.1098)	6.168	-7.734	-4.764	-0.47545835E-01
BD(9,25,0.1098)	7.734	-6.168	-4.764	-0.48262890E-01
BD(9,26,0.1098)	8.913	-4.292	-4.764	-0.46559840E-01
BD(9,27,0.1098)	9.645	-2.201	-4.764	-0.42522088E-01
BD(10, 0,0.1098)	8.584	0.000	-6.846	-0.24935231E-01
BD(10, 1,0.1098)	8.369	1.910	-6.846	-0.19469135E-01
BD(10, 2,0.1098)	7.734	3.725	-6.846	-0.13026774E-01
BD(10, 3,0.1098)	6.712	5.352	-6.846	-0.59311911E-02
BD(10, 4,0.1098)	5.352	6.712	-6.846	0.14617909E-02
BD(10, 5,0.1098)	3.725	7.734	-6.846	0.87814778E-02
BD(10, 6,0.1098)	1.910	8.369	-6.846	0.15660822E-01
BD(10, 7,0.1098)	-0.000	8.584	-6.846	0.21754883E-01
BD(10, 8,0.1098)	-1.910	8.369	-6.846	0.26758041E-01
BD(10, 9,0.1098)	-3.725	7.734	-6.846	0.30419439E-01
BD(10,10,0.1098)	-5.352	6.712	-6.846	0.32555480E-01
BD(10,11,0.1098)	-6.712	5.352	-6.846	0.33059038E-01
BD(10,12,0.1098)	-7.734	3.725	-6.846	0.31904861E-01
BD(10,13,0.1098)	-8.369	1.910	-6.846	0.29150840E-01
BD(10,14,0.1098)	-8.584	-0.000	-6.846	0.24935078E-01
BD(10,15,0.1098)	-8.369	-1.910	-6.846	0.19468952E-01
BD(10,16,0.1098)	-7.734	-3.725	-6.846	0.13026554E-01
BD(10,17,0.1098)	-6.712	-5.352	-6.846	0.59309788E-02
BD(10,18,0.1098)	-5.352	-6.712	-6.846	-0.14620144E-02
BD(10,19,0.1098)	-3.725	-7.734	-6.846	-0.87817051E-02
BD(10,20,0.1098)	-1.910	-8.369	-6.846	-0.15661016E-01
BD(10,21,0.1098)	0.000	-8.584	-6.846	-0.21755066E-01
BD(10,22,0.1098)	1.910	-8.369	-6.846	-0.26758179E-01
BD(10,23,0.1098)	3.725	-7.734	-6.846	-0.30419551E-01
BD(10,24,0.1098)	5.352	-6.712	-6.846	-0.32555524E-01
BD(10,25,0.1098)	6.712	-5.352	-6.846	-0.33059031E-01
BD(10,26,0.1098)	7.734	-3.725	-6.846	-0.31904798E-01
BD(10,27,0.1098)	8.369	-1.910	-6.846	-0.29150739E-01
BD(11, 0,0.1098)	6.846	0.000	-8.585	-0.16647216E-01
BD(11, 1,0.1098)	6.674	1.523	-8.585	-0.13001733E-01
BD(11, 2,0.1098)	6.168	2.970	-8.585	-0.87043047E-02
BD(11, 3,0.1098)	5.352	4.268	-8.585	-0.39703883E-02
BD(11, 4,0.1098)	4.268	5.352	-8.585	0.96261129E-03
BD(11, 5,0.1098)	2.970	6.168	-8.585	0.58473423E-02
BD(11, 6,0.1098)	1.523	6.674	-8.585	0.10438852E-01
BD(11, 7,0.1098)	-0.000	6.846	-8.585	0.14506940E-01
BD(11, 8,0.1098)	-1.523	6.674	-8.585	0.17847568E-01
BD(11, 9,0.1098)	-2.970	6.168	-8.585	0.20293236E-01
BD(11,10,0.1098)	-4.268	5.352	-8.585	0.21721333E-01
BD(11,11,0.1098)	-5.352	4.268	-8.585	0.22060201E-01

BD(6,20,0.1098)	-2.382	-10.436	2.443	-0.79987705E-01
BD(6,21,0.1098)	0.000	-10.705	2.443	-0.10886157E+00
BD(6,22,0.1098)	2.382	-10.436	2.443	-0.13227654E+00
BD(6,23,0.1098)	4.645	-9.645	2.443	-0.14905858E+00
BD(6,24,0.1098)	6.674	-8.369	2.443	-0.15836614E+00
BD(6,25,0.1098)	8.369	-6.674	2.443	-0.15973258E+00
BD(6,26,0.1098)	9.645	-4.644	2.443	-0.15308917E+00
BD(6,27,0.1098)	10.436	-2.382	2.443	-0.13876939E+00
BD(7, 0,0.1098)	10.980	0.000	-0.000	-0.78122199E-01
BD(7, 1,0.1098)	10.705	2.443	-0.000	-0.60571607E-01
BD(7, 2,0.1098)	9.893	4.764	-0.000	-0.39983705E-01
BD(7, 3,0.1098)	8.584	6.846	-0.000	-0.17390829E-01
BD(7, 4,0.1098)	6.846	8.585	-0.000	0.60740449E-02
BD(7, 5,0.1098)	4.764	9.893	-0.000	0.29234361E-01
BD(7, 6,0.1098)	2.443	10.705	-0.000	0.50928745E-01
BD(7, 7,0.1098)	-0.000	10.980	-0.000	0.70069373E-01
BD(7, 8,0.1098)	-2.443	10.705	-0.000	0.85696340E-01
BD(7, 9,0.1098)	-4.764	9.893	-0.000	0.97026169E-01
BD(7,10,0.1098)	-6.846	8.584	-0.000	0.10349071E+00
BD(7,11,0.1098)	-8.585	6.846	-0.000	0.10476571E+00
BD(7,12,0.1098)	-9.893	4.764	-0.000	0.10078728E+00
BD(7,13,0.1098)	-10.705	2.443	-0.000	0.91754973E-01
BD(7,14,0.1098)	-10.980	-0.000	-0.000	0.78121662E-01
BD(7,15,0.1098)	-10.705	-2.443	-0.000	0.60571045E-01
BD(7,16,0.1098)	-9.893	-4.764	-0.000	0.39983004E-01
BD(7,17,0.1098)	-8.584	-6.846	-0.000	0.17390173E-01
BD(7,18,0.1098)	-6.846	-8.585	-0.000	-0.60747452E-02
BD(7,19,0.1098)	-4.764	-9.893	-0.000	-0.29235069E-01
BD(7,20,0.1098)	-2.443	-10.705	-0.000	-0.50929409E-01
BD(7,21,0.1098)	0.000	-10.980	-0.000	-0.70069909E-01
BD(7,22,0.1098)	2.443	-10.705	-0.000	-0.85696757E-01
BD(7,23,0.1098)	4.764	-9.893	-0.000	-0.97026467E-01
BD(7,24,0.1098)	6.846	-8.584	-0.000	-0.10349083E+00
BD(7,25,0.1098)	8.585	-6.846	-0.000	-0.10476571E+00
BD(7,26,0.1098)	9.893	-4.764	-0.000	-0.10078710E+00
BD(7,27,0.1098)	10.705	-2.443	-0.000	-0.91754615E-01
BD(8, 0,0.1098)	10.705	0.000	-2.443	-0.52945185E-01
BD(8, 1,0.1098)	10.436	2.382	-2.443	-0.41222990E-01
BD(8, 2,0.1098)	9.645	4.645	-2.443	-0.27433705E-01
BD(8, 3,0.1098)	8.369	6.674	-2.443	-0.12268774E-01
BD(8, 4,0.1098)	6.674	8.369	-2.443	0.35113776E-02
BD(8, 5,0.1098)	4.645	9.645	-2.443	0.19115403E-01
BD(8, 6,0.1098)	2.382	10.436	-2.443	0.33760943E-01
BD(8, 7,0.1098)	-0.000	10.705	-2.443	0.46713583E-01
BD(8, 8,0.1098)	-2.382	10.436	-2.443	0.57323758E-01
BD(8, 9,0.1098)	-4.645	9.645	-2.443	0.65059483E-01
BD(8,10,0.1098)	-6.674	8.369	-2.443	0.69532812E-01
BD(8,11,0.1098)	-8.369	6.674	-2.443	0.70519507E-01
BD(8,12,0.1098)	-9.645	4.645	-2.443	0.67969978E-01
BD(8,13,0.1098)	-10.436	2.382	-2.443	0.62012229E-01
BD(8,14,0.1098)	-10.705	-0.000	-2.443	0.52944858E-01
BD(8,15,0.1098)	-10.436	-2.382	-2.443	0.41222617E-01
BD(8,16,0.1098)	-9.645	-4.645	-2.443	0.27433231E-01
BD(8,17,0.1098)	-8.369	-6.674	-2.443	0.12268327E-01
BD(8,18,0.1098)	-6.674	-8.369	-2.443	-0.35118437E-02
BD(8,19,0.1098)	-4.645	-9.645	-2.443	-0.19115895E-01
BD(8,20,0.1098)	-2.382	-10.436	-2.443	-0.33761386E-01
BD(8,21,0.1098)	0.000	-10.705	-2.443	-0.46713956E-01
BD(8,22,0.1098)	2.382	-10.436	-2.443	-0.57324048E-01
BD(8,23,0.1098)	4.645	-9.645	-2.443	-0.65059662E-01
BD(8,24,0.1098)	6.674	-8.369	-2.443	-0.69532931E-01
BD(8,25,0.1098)	8.369	-6.674	-2.443	-0.70519507E-01
BD(8,26,0.1098)	9.645	-4.644	-2.443	-0.67969859E-01
BD(8,27,0.1098)	10.436	-2.382	-2.443	-0.62011983E-01
BD(9, 0,0.1098)	9.893	0.000	-4.764	-0.36352538E-01
BD(9, 1,0.1098)	9.645	2.201	-4.764	-0.28359771E-01

```
BD( 4,10,0.1098)   -5.352    6.712    6.846     0.40684360E+00
BD( 4,11,0.1098)   -6.712    5.352    6.846     0.40237278E+00
BD( 4,12,0.1098)   -7.734    3.725    6.846     0.37772536E+00
BD( 4,13,0.1098)   -8.369    1.910    6.846     0.33413684E+00
BD( 4,14,0.1098)   -8.585   -0.000    6.846     0.27379340E+00
BD( 4,15,0.1098)   -8.369   -1.910    6.846     0.19972062E+00
BD( 4,16,0.1098)   -7.734   -3.725    6.846     0.11563307E+00
BD( 4,17,0.1098)   -6.712   -5.352    6.846     0.25747340E-01
BD( 4,18,0.1098)   -5.352   -6.712    6.846    -0.65429389E-01
BD( 4,19,0.1098)   -3.725   -7.734    6.846    -0.15332538E+00
BD( 4,20,0.1098)   -1.910   -8.369    6.846    -0.23353320E+00
BD( 4,21,0.1098)    0.000   -8.585    6.846    -0.30203050E+00
BD( 4,22,0.1098)    1.910   -8.369    6.846    -0.35538232E+00
BD( 4,23,0.1098)    3.725   -7.734    6.846    -0.39091432E+00
BD( 4,24,0.1098)    5.352   -6.712    6.846    -0.40684390E+00
BD( 4,25,0.1098)    6.712   -5.352    6.846    -0.40237248E+00
BD( 4,26,0.1098)    7.734   -3.725    6.846    -0.37772405E+00
BD( 4,27,0.1098)    8.369   -1.910    6.846    -0.33413506E+00
BD( 5, 0,0.1098)    9.893    0.000    4.764    -0.17955577E+00
BD( 5, 1,0.1098)    9.645    2.201    4.764    -0.13567698E+00
BD( 5, 2,0.1098)    8.913    4.292    4.764    -0.84994733E-01
BD( 5, 3,0.1098)    7.734    6.168    4.764    -0.30050620E-01

BD( 5, 4,0.1098)    6.168    7.734    4.764     0.26400227E-01
BD( 5, 5,0.1098)    4.292    8.913    4.764     0.81527352E-01
BD( 5, 6,0.1098)    2.201    9.645    4.764     0.13256645E+00
BD( 5, 7,0.1098)   -0.000    9.893    4.764     0.17695808E+00
BD( 5, 8,0.1098)   -2.201    9.645    4.764     0.21247613E+00
BD( 5, 9,0.1098)   -4.292    8.913    4.764     0.23733979E+00
BD( 5,10,0.1098)   -6.168    7.734    4.764     0.25030208E+00
BD( 5,11,0.1098)   -7.734    6.168    4.764     0.25071317E+00
BD( 5,12,0.1098)   -8.913    4.292    4.764     0.23855257E+00
BD( 5,13,0.1098)   -9.645    2.201    4.764     0.21442974E+00
BD( 5,14,0.1098)   -9.893   -0.000    4.764     0.17955446E+00
BD( 5,15,0.1098)   -9.645   -2.201    4.764     0.13567561E+00
BD( 5,16,0.1098)   -8.913   -4.292    4.764     0.84993124E-01
BD( 5,17,0.1098)   -7.734   -6.168    4.764     0.30049041E-01
BD( 5,18,0.1098)   -6.168   -7.734    4.764    -0.26401792E-01
BD( 5,19,0.1098)   -4.292   -8.913    4.764    -0.81529021E-01
BD( 5,20,0.1098)   -2.201   -9.645    4.764    -0.13256800E+00
BD( 5,21,0.1098)    0.000   -9.893    4.764    -0.17695928E+00
BD( 5,22,0.1098)    2.201   -9.645    4.764    -0.21247697E+00
BD( 5,23,0.1098)    4.292   -8.913    4.764    -0.23734057E+00
BD( 5,24,0.1098)    6.168   -7.734    4.764    -0.25030226E+00
BD( 5,25,0.1098)    7.734   -6.168    4.764    -0.25071317E+00
BD( 5,26,0.1098)    8.913   -4.292    4.764    -0.23855197E+00
BD( 5,27,0.1098)    9.645   -2.201    4.764    -0.21442872E+00
BD( 6, 0,0.1098)   10.705    0.000    2.443    -0.11749262E+00
BD( 6, 1,0.1098)   10.436    2.382    2.443    -0.90323031E-01
BD( 6, 2,0.1098)    9.645    4.645    2.443    -0.58624234E-01
BD( 6, 3,0.1098)    8.369    6.674    2.443    -0.23985893E-01
BD( 6, 4,0.1098)    6.674    8.369    2.443     0.11855263E-01
BD( 6, 5,0.1098)    4.645    9.645    2.443     0.47101982E-01
BD( 6, 6,0.1098)    2.382   10.436    2.443     0.79986811E-01
BD( 6, 7,0.1098)   -0.000   10.705    2.443     0.10886079E+00
BD( 6, 8,0.1098)   -2.382   10.436    2.443     0.13227588E+00
BD( 6, 9,0.1098)   -4.645    9.645    2.443     0.14905816E+00
BD( 6,10,0.1098)   -6.674    8.369    2.443     0.15836596E+00
BD( 6,11,0.1098)   -8.369    6.674    2.443     0.15973258E+00
BD( 6,12,0.1098)   -9.645    4.645    2.443     0.15308958E+00
BD( 6,13,0.1098)  -10.436    2.382    2.443     0.13876998E+00
BD( 6,14,0.1098)  -10.705   -0.000    2.443     0.11749184E+00
BD( 6,15,0.1098)  -10.436   -2.382    2.443     0.90322196E-01
BD( 6,16,0.1098)   -9.645   -4.645    2.443     0.58623135E-01
BD( 6,17,0.1098)   -8.369   -6.674    2.443     0.23984928E-01
BD( 6,18,0.1098)   -6.674   -8.369    2.443    -0.11856399E-01
BD( 6,19,0.1098)   -4.645   -9.645    2.443    -0.47103036E-01
```

BD(2,15,0.1098)	-4.645	-1.060	9.893	0.28316540E+00
BD(2,16,0.1098)	-4.292	-2.067	9.893	0.61380204E-01
BD(2,17,0.1098)	-3.725	-2.970	9.893	-0.16348159E+00
BD(2,18,0.1098)	-2.970	-3.725	9.893	-0.38014710E+00
BD(2,19,0.1098)	-2.067	-4.292	9.893	-0.57774985E+00
BD(2,20,0.1098)	-1.060	-4.645	9.893	-0.74638194E+00
BD(2,21,0.1098)	0.000	-4.764	9.893	-0.87758696E+00
BD(2,22,0.1098)	1.060	-4.645	9.893	-0.96478570E+00
BD(2,23,0.1098)	2.067	-4.292	9.893	-0.10036058E+01
BD(2,24,0.1098)	2.970	-3.725	9.893	-0.99210155E+00
BD(2,25,0.1098)	3.725	-2.970	9.893	-0.93084818E+00
BD(2,26,0.1098)	4.292	-2.067	9.893	-0.82291776E+00
BD(2,27,0.1098)	4.645	-1.060	9.893	-0.67372340E+00
BD(3, 0,0.1098)	6.846	0.000	8.584	-0.39718914E+00
BD(3, 1,0.1098)	6.674	1.523	8.584	-0.26899797E+00
BD(3, 2,0.1098)	6.168	2.970	8.584	-0.12731850E+00
BD(3, 3,0.1098)	5.352	4.268	8.584	0.20745508E-01
BD(3, 4,0.1098)	4.268	5.352	8.584	0.16776884E+00
BD(3, 5,0.1098)	2.970	6.168	8.584	0.30637980E+00
BD(3, 6,0.1098)	1.523	6.674	8.584	0.42962736E+00
BD(3, 7,0.1098)	-0.000	6.846	8.584	0.53133214E+00
BD(3, 8,0.1098)	-1.523	6.674	8.584	0.60639310E+00
BD(3, 9,0.1098)	-2.970	6.168	8.584	0.65104681E+00
BD(3,10,0.1098)	-4.268	5.352	8.584	0.66305465E+00
BD(3,11,0.1098)	-5.352	4.268	8.584	0.64181352E+00
BD(3,12,0.1098)	-6.168	2.970	8.584	0.58838892E+00
BD(3,13,0.1098)	-6.674	1.523	8.584	0.50546032E+00
BD(3,14,0.1098)	-6.846	-0.000	8.584	0.39718533E+00
BD(3,15,0.1098)	-6.674	-1.523	8.584	0.26899403E+00
BD(3,16,0.1098)	-6.168	-2.970	8.584	0.12731367E+00
BD(3,17,0.1098)	-5.352	-4.268	8.584	-0.20749711E-01
BD(3,18,0.1098)	-4.268	-5.352	8.584	-0.16777325E+00
BD(3,19,0.1098)	-2.970	-6.168	8.584	-0.30638385E+00
BD(3,20,0.1098)	-1.523	-6.674	8.584	-0.42963099E+00
BD(3,21,0.1098)	0.000	-6.846	8.584	-0.53133494E+00
BD(3,22,0.1098)	1.523	-6.674	8.584	-0.60639518E+00
BD(3,23,0.1098)	2.970	-6.168	8.584	-0.65104800E+00
BD(3,24,0.1098)	4.268	-5.352	8.584	-0.66305435E+00
BD(3,25,0.1098)	5.352	-4.268	8.584	-0.64181232E+00
BD(3,26,0.1098)	6.168	-2.970	8.584	-0.58838671E+00
BD(3,27,0.1098)	6.674	-1.523	8.584	-0.50545728E+00
BD(4, 0,0.1098)	8.585	0.000	6.846	-0.27379555E+00
BD(4, 1,0.1098)	8.369	1.910	6.846	-0.19972312E+00
BD(4, 2,0.1098)	7.734	3.725	6.846	-0.11563587E+00
BD(4, 3,0.1098)	6.712	5.352	6.846	-0.25750104E-01
BD(4, 4,0.1098)	5.352	6.712	6.846	0.65426707E-01
BD(4, 5,0.1098)	3.725	7.734	6.846	0.15332288E+00
BD(4, 6,0.1098)	1.910	8.369	6.846	0.23353070E+00
BD(4, 7,0.1098)	-0.000	8.585	6.846	0.30202860E+00
BD(4, 8,0.1098)	-1.910	8.369	6.846	0.35538119E+00
BD(4, 9,0.1098)	-3.725	7.734	6.846	0.39091331E+00

Calculated Data for Model #3

	DIPOLE#1	DIPOLE#2	DIPOLE#3	
MOMENT	0.55E-05	0.55E-05	0.55E-05	(AMP*M)
LOCATN	0.066	0.053	0.040	(M FR ORN)
TRANS	1.000 0.000 0.000	0.000 1.000 0.000	0.707 0.707 0.000	
MATRIX	0.000 1.000 0.000	-1.000 0.000 0.000	-0.707 0.707 0.000	
	0.000 0.000 1.000	0.000 0.000 1.000	0.000 0.000 1.000	

THE MEAS SPHERE RADIUS IS 0.1098 M

SPHER DATA POINTS: THETA=T*0.2244; PHI=F*0.2244

BD(T,F,R)	X	Y	Z	FLUX DENS. XEE-11 TESLA
BD(0, 0,0.1098)	0.000	0.000	10.980	0.00000000E+00
BD(1, 0,0.1098)	2.443	0.000	10.705	-0.39150470E+00
BD(1, 1,0.1098)	2.382	0.544	10.705	-0.16483694E+00
BD(1, 2,0.1098)	2.201	1.060	10.705	0.70096433E-01
BD(1, 3,0.1098)	1.910	1.523	10.705	0.30151480E+00
BD(1, 4,0.1098)	1.523	1.910	10.705	0.51781327E+00
BD(1, 5,0.1098)	1.060	2.201	10.705	0.70814663E+00
BD(1, 6,0.1098)	0.544	2.382	10.705	0.86297077E+00
BD(1, 7,0.1098)	-0.000	2.443	10.705	0.97452235E+00
BD(1, 8,0.1098)	-0.544	2.382	10.705	0.10372057E+01
BD(1, 9,0.1098)	-1.060	2.201	10.705	0.10478732E+01
BD(1,10,0.1098)	-1.523	1.910	10.705	0.10060081E+01
BD(1,11,0.1098)	-1.910	1.523	10.705	0.91369218E+00
BD(1,12,0.1098)	-2.201	1.060	10.705	0.77555811E+00
BD(1,13,0.1098)	-2.382	0.544	10.705	0.59853494E+00
BD(1,14,0.1098)	-2.443	-0.000	10.705	0.39149755E+00
BD(1,15,0.1098)	-2.382	-0.544	10.705	0.16482967E+00
BD(1,16,0.1098)	-2.201	-1.060	10.705	-0.70104122E-01
BD(1,17,0.1098)	-1.910	-1.523	10.705	-0.30152106E+00
BD(1,18,0.1098)	-1.523	-1.910	10.705	-0.51781940E+00
BD(1,19,0.1098)	-1.060	-2.201	10.705	-0.70815235E+00
BD(1,20,0.1098)	-0.544	-2.382	10.705	-0.86297494E+00
BD(1,21,0.1098)	0.000	-2.443	10.705	-0.97452497E+00
BD(1,22,0.1098)	0.544	-2.382	10.705	-0.10372066E+01
BD(1,23,0.1098)	1.060	-2.201	10.705	-0.10478783E+01
BD(1,24,0.1098)	1.523	-1.910	10.705	-0.10060062E+01
BD(1,25,0.1098)	1.910	-1.523	10.705	-0.91368854E+00
BD(1,26,0.1098)	2.201	-1.060	10.705	-0.77555287E+00
BD(1,27,0.1098)	2.382	-0.544	10.705	-0.59852856E+00
BD(2, 0,0.1098)	4.764	0.000	9.893	-0.49075735E+00
BD(2, 1,0.1098)	4.645	1.060	9.893	-0.28317207E+00
BD(2, 2,0.1098)	4.292	2.067	9.893	-0.61387379E-01
BD(2, 3,0.1098)	3.725	2.970	9.893	0.16347545E+00
BD(2, 4,0.1098)	2.970	3.725	9.893	0.38014066E+00
BD(2, 5,0.1098)	2.067	4.292	9.893	0.57774431E+00
BD(2, 6,0.1098)	1.060	4.645	9.893	0.74637699E+00
BD(2, 7,0.1098)	-0.000	4.764	9.893	0.87758380E+00
BD(2, 8,0.1098)	-1.060	4.645	9.893	0.96478379E+00
BD(2, 9,0.1098)	-2.067	4.292	9.893	0.10036049E+01
BD(2,10,0.1098)	-2.970	3.725	9.893	0.99210227E+00
BD(2,11,0.1098)	-3.725	2.970	9.893	0.93085104E+00
BD(2,12,0.1098)	-4.292	2.067	9.893	0.82292211E+00
BD(2,13,0.1098)	-4.645	1.060	9.893	0.67372888E+00
BD(2,14,0.1098)	-4.764	-0.000	9.893	0.49075079E+00

```
  BD(13,22,0.1098)    0.544   -2.382 -10.705     -0.53875536E-01
  BD(13,23,0.1098)    1.060   -2.201 -10.705     -0.53317896E-01
  BD(13,24,0.1098)    1.523   -1.910 -10.705     -0.49229065E-01
  BD(13,25,0.1098)    1.910   -1.523 -10.705     -0.41363098E-01
  BD(13,26,0.1098)    2.201   -1.060 -10.705     -0.29945853E-01
  BD(13,27,0.1098)    2.382   -0.544 -10.705     -0.15741441E-01
  BD(14, 0,0.1098)   -0.000    0.000 -10.980     -0.15266519E-07
END OF DATA
```

BD(11,12,0.1098)	-6.168	2.970	-8.585	0.14780160E-01
BD(11,13,0.1098)	-6.674	1.523	-8.585	0.72188787E-02
BD(11,14,0.1098)	-6.846	-0.000	-8.585	-0.23301385E-06
BD(11,15,0.1098)	-6.674	-1.523	-8.585	-0.72192438E-02
BD(11,16,0.1098)	-6.168	-2.970	-8.585	-0.14780771E-01
BD(11,17,0.1098)	-5.352	-4.268	-8.585	-0.22955708E-01
BD(11,18,0.1098)	-4.268	-5.352	-8.585	-0.31907599E-01
BD(11,19,0.1098)	-2.970	-6.168	-8.585	-0.41606180E-01
BD(11,20,0.1098)	-1.523	-6.674	-8.585	-0.52076392E-01
BD(11,21,0.1098)	0.000	-6.846	-8.585	-0.62636435E-01
BD(11,22,0.1098)	1.523	-6.674	-8.585	-0.72291732E-01
BD(11,23,0.1098)	2.970	-6.168	-8.585	-0.79196718E-01
BD(11,24,0.1098)	4.268	-5.352	-8.585	-0.80713630E-01
BD(11,25,0.1098)	5.352	-4.268	-8.585	-0.73976457E-01
BD(11,26,0.1098)	6.168	-2.970	-8.585	-0.57240649E-01
BD(11,27,0.1098)	6.674	-1.523	-8.585	-0.31344850E-01
BD(12, 0,0.1098)	4.764	0.000	-9.893	0.00000000E+00
BD(12, 1,0.1098)	4.645	1.060	-9.893	0.42734672E-01
BD(12, 2,0.1098)	4.292	2.067	-9.893	0.42267874E-01
BD(12, 3,0.1098)	3.725	2.970	-9.893	0.56296357E-01
BD(12, 4,0.1098)	2.970	3.725	-9.893	0.63931704E-01
BD(12, 5,0.1098)	2.067	4.292	-9.893	0.65611124E-01
BD(12, 6,0.1098)	1.060	4.645	-9.893	0.62621891E-01
BD(12, 7,0.1098)	-0.000	4.764	-9.893	0.56503911E-01
BD(12, 8,0.1098)	-1.060	4.645	-9.893	0.48631918E-01
BD(12, 9,0.1098)	-2.067	4.292	-9.893	0.40031988E-01
BD(12,10,0.1098)	-2.970	3.725	-9.893	0.31363733E-01
BD(12,11,0.1098)	-3.725	2.970	-9.893	0.22980921E-01
BD(12,12,0.1098)	-4.292	2.067	-9.893	0.15006138E-01
BD(12,13,0.1098)	-4.645	1.060	-9.893	0.73972131E-02
BD(12,14,0.1098)	-4.764	-0.000	-9.893	-0.23955323E-06
BD(12,15,0.1098)	-4.645	-1.060	-9.893	-0.73976517E-02
BD(12,16,0.1098)	-4.292	-2.067	-9.893	-0.15006606E-01
BD(12,17,0.1098)	-3.725	-2.970	-9.893	-0.22961110E-01
BD(12,18,0.1098)	-2.970	-3.725	-9.893	-0.31364277E-01
BD(12,19,0.1098)	-2.067	-4.292	-9.893	-0.40032586E-01
BD(12,20,0.1098)	-1.060	-4.645	-9.893	-0.48632581E-01
BD(12,21,0.1098)	0.000	-4.764	-9.893	-0.56504447E-01
BD(12,22,0.1098)	1.060	-4.645	-9.893	-0.62622368E-01
BD(12,23,0.1098)	2.067	-4.292	-9.893	-0.65611243E-01
BD(12,24,0.1098)	2.970	-3.725	-9.893	-0.63931406E-01
BD(12,25,0.1098)	3.725	-2.970	-9.893	-0.56297826E-01
BD(12,26,0.1098)	4.292	-2.067	-9.893	-0.42266853E-01
BD(12,27,0.1098)	4.645	-1.060	-9.893	-0.22733336E-01
BD(13, 0,0.1098)	2.443	0.000	-10.705	0.00000000E+00
BD(13, 1,0.1098)	2.382	0.544	-10.705	0.15742343E-01
BD(13, 2,0.1098)	2.201	1.060	-10.705	0.29946566E-01
BD(13, 3,0.1098)	1.910	1.523	-10.705	0.41367500E-01
BD(13, 4,0.1098)	1.523	1.910	-10.705	0.49229046E-01
BD(13, 5,0.1098)	1.060	2.201	-10.705	0.53316389E-01
BD(13, 6,0.1098)	0.544	2.382	-10.705	0.53875644E-01
BD(13, 7,0.1098)	-0.000	2.443	-10.705	0.51443869E-01
BD(13, 8,0.1098)	-0.544	2.382	-10.705	0.46729841E-01
BD(13, 9,0.1098)	-1.060	2.201	-10.705	0.40390074E-01
BD(13,10,0.1098)	-1.523	1.910	-10.705	0.33016574E-01
BD(13,11,0.1098)	-1.910	1.523	-10.705	0.25051929E-01
BD(13,12,0.1098)	-2.201	1.060	-10.705	0.16793463E-01
BD(13,13,0.1098)	-2.382	0.544	-10.705	0.84145465E-02
BD(13,14,0.1098)	-2.443	-0.000	-10.705	-0.27404116E-06
BD(13,15,0.1098)	-2.382	-0.544	-10.705	-0.84150053E-02
BD(13,16,0.1098)	-2.201	-1.060	-10.705	-0.16794018E-01
BD(13,17,0.1098)	-1.910	-1.523	-10.705	-0.25052503E-01
BD(13,18,0.1098)	-1.523	-1.910	-10.705	-0.33017039E-01
BD(13,19,0.1098)	-1.060	-2.201	-10.705	-0.40389858E-01
BD(13,20,0.1098)	-0.544	-2.382	-10.705	-0.46729826E-01
BD(13,21,0.1098)	0.000	-2.443	-10.705	-0.51450506E-01

BD(9, 2,0.1098)	3.913	4.292	-4.764	0.86633623E-01
BD(9, 3,0.1098)	7.734	6.168	-4.764	0.11[illegible]9409E+00
BD(9, 4,0.1098)	6.168	7.734	-4.764	0.11851305E+00
BD(9, 5,0.1098)	4.292	8.913	-4.764	0.11099660E+00
BD(9, 6,0.1098)	2.201	9.645	-4.764	0.97349346E-01
BD(9, 7,0.1098)	-0.000	9.893	-4.764	0.82263139E-01
BD(9, 8,0.1098)	-2.201	9.645	-4.764	0.67794442E-01
BD(9, 9,0.1098)	-4.292	8.913	-4.764	0.54386772E-01
BD(9,10,0.1098)	-6.168	7.734	-4.764	0.41993979E-01
BD(9,11,0.1098)	-7.734	6.168	-4.764	0.30449271E-01
BD(9,12,0.1098)	-8.913	4.292	-4.764	0.19654322E-01
BD(9,13,0.1098)	-9.645	2.201	-4.764	0.96651446E-0[illegible]
BD(9,14,0.1098)	-9.893	-0.000	-4.764	-0.30776280E-06
BD(9,15,0.1098)	-9.645	-2.201	-4.764	-0.9566707[illegible]E-0[illegible]
BD(9,16,0.1098)	-8.913	-4.292	-4.764	-0.19655023E-01
BD(9,17,0.1098)	-7.734	-6.168	-4.764	-0.30449834E-01
BD(9,18,0.1098)	-6.168	-7.734	-4.764	-0.41994567E-01
BD(9,19,0.1098)	-4.292	-8.913	-4.764	-0.54387346E-01
BD(9,20,0.1098)	-2.201	-9.645	-4.764	-0.67795455E-01
BD(9,21,0.1098)	0.000	-9.893	-4.764	-0.82283616E-01
BD(9,22,0.1098)	2.201	-9.645	-4.764	-0.97350180E-01
BD(9,23,0.1098)	4.292	-8.913	-4.764	-0.11099714E+00
BD(9,24,0.1098)	6.168	-7.734	-4.764	-0.11851329E+00
BD(9,25,0.1098)	7.734	-6.168	-4.764	-0.11239320E+00
BD(9,26,0.1098)	8.913	-4.292	-4.764	-0.86631417E-01
BD(9,27,0.1098)	9.645	-2.201	-4.764	-0.45167271E-01
BD(10, 0,0.1098)	8.584	0.000	-6.846	0.00000000E+00
BD(10, 1,0.1098)	8.369	1.910	-6.846	0.40083723E-01
BD(10, 2,0.1098)	7.734	3.725	-6.846	0.73204160E-01
BD(10, 3,0.1098)	6.712	5.352	-6.846	0.93303680E-01
BD(10, 4,0.1098)	5.352	6.712	-6.846	0.99096477E-01
BD(10, 5,0.1098)	3.725	7.734	-6.846	0.94175577E-01
BD(10, 6,0.1098)	1.910	8.369	-6.846	0.83480358E-01
BD(10, 7,0.1098)	-0.000	8.584	-6.846	0.70735455E-01
BD(10, 8,0.1098)	-1.910	8.369	-6.846	0.57973828E-01
BD(10, 9,0.1098)	-3.725	7.734	-6.846	0.46029963E-01
BD(10,10,0.1098)	-5.352	6.712	-6.846	0.35117418E-01
BD(10,11,0.1098)	-6.712	5.352	-6.846	0.25203723E-01
BD(10,12,0.1098)	-7.734	3.725	-6.846	0.16179107E-01
BD(10,13,0.1098)	-8.369	1.910	-6.846	0.78748018E-02
BD(10,14,0.1098)	-8.584	-0.000	-6.846	-0.25376437E-06
BD(10,15,0.1098)	-8.369	-1.910	-6.846	-0.78752823E-02
BD(10,16,0.1098)	-7.734	-3.725	-6.846	-0.16179681E-01
BD(10,17,0.1098)	-6.712	-5.352	-6.846	-0.25204316E-01
BD(10,18,0.1098)	-5.352	-6.712	-6.846	-0.35117798E-01
BD(10,19,0.1098)	-3.725	-7.734	-6.846	-0.46030581E-01
BD(10,20,0.1098)	-1.910	-8.369	-6.846	-0.57974730E-01
BD(10,21,0.1098)	0.000	-8.584	-6.846	-0.70736408E-01
BD(10,22,0.1098)	1.910	-8.369	-6.846	-0.83480477E-01
BD(10,23,0.1098)	3.725	-7.734	-6.846	-0.94176233E-01
BD(10,24,0.1098)	5.352	-6.712	-6.846	-0.99096894E-01
BD(10,25,0.1098)	6.712	-5.352	-6.846	-0.93362786E-01
BD(10,26,0.1098)	7.734	-3.725	-6.846	-0.73202312E-01
BD(10,27,0.1098)	8.369	-1.910	-6.846	-0.40080473E-01
BD(11, 0,0.1098)	6.846	0.000	-8.585	0.00000000E+00
BD(11, 1,0.1098)	6.674	1.523	-8.585	0.31346615E-01
BD(11, 2,0.1098)	6.168	2.970	-8.585	0.57245221E-01
BD(11, 3,0.1098)	5.352	4.268	-8.585	0.73977172E-01
BD(11, 4,0.1098)	4.268	5.352	-8.585	0.80713689E-01
BD(11, 5,0.1098)	2.970	6.168	-8.585	0.79198480E-01
BD(11, 6,0.1098)	1.523	6.674	-8.585	0.72291613E-01
BD(11, 7,0.1098)	-0.000	6.846	-8.585	0.62635779E-01
BD(11, 8,0.1098)	-1.523	6.674	-8.585	0.52076202E-01
BD(11, 9,0.1098)	-2.970	6.168	-8.585	0.41667745E-01
BD(11,10,0.1098)	-4.268	5.352	-8.585	0.31907011E-01
BD(11,11,0.1098)	-5.352	4.268	-8.585	0.22955108E-01

BD(9, 2,0.1098)	8.913	4.292	-4.764	-0.32168325E-01
BD(9, 3,0.1098)	7.734	6.168	-4.764	-0.24101544E-01
BD(9, 4,0.1098)	6.168	7.734	-4.764	-0.14826197E-01
BD(9, 5,0.1098)	4.292	8.913	-4.764	-0.48073940E-02
BD(9, 6,0.1098)	2.201	9.645	-4.764	0.54524504E-02
BD(9, 7,0.1098)	-0.000	9.893	-4.764	0.15438925E-01
BD(9, 8,0.1098)	-2.201	9.645	-4.764	0.24651207E-01
BD(9, 9,0.1098)	-4.292	8.913	-4.764	0.32627348E-01
BD(9,10,0.1098)	-6.168	7.734	-4.764	0.38967434E-01
BD(9,11,0.1098)	-7.734	6.168	-4.764	0.43353509E-01
BD(9,12,0.1098)	-8.913	4.292	-4.764	0.45565665E-01
BD(9,13,0.1098)	-9.645	2.201	-4.764	0.45492958E-01
BD(9,14,0.1098)	-9.893	-0.000	-4.764	0.43139022E-01
BD(9,15,0.1098)	-9.645	-2.201	-4.764	0.38621891E-01
BD(9,16,0.1098)	-8.913	-4.292	-4.764	0.32168072E-01
BD(9,17,0.1098)	-7.734	-6.168	-4.764	0.24101272E-01
BD(9,18,0.1098)	-6.168	-7.734	-4.764	0.14825944E-01
BD(9,19,0.1098)	-4.292	-8.913	-4.764	0.48071072E-02
BD(9,20,0.1098)	-2.201	-9.645	-4.764	-0.54527447E-02
BD(9,21,0.1098)	0.000	-9.893	-4.764	-0.15439216E-01
BD(9,22,0.1098)	2.201	-9.645	-4.764	-0.24651498E-01
BD(9,23,0.1098)	4.292	-8.913	-4.764	-0.32627620E-01
BD(9,24,0.1098)	6.168	-7.734	-4.764	-0.38967643E-01
BD(9,25,0.1098)	7.734	-6.168	-4.764	-0.43353617E-01
BD(9,26,0.1098)	8.913	-4.292	-4.764	-0.45565691E-01
BD(9,27,0.1098)	9.645	-2.201	-4.764	-0.45492906E-01
BD(10, 0,0.1098)	8.584	0.000	-6.846	-0.29663622E-01
BD(10, 1,0.1098)	8.369	1.910	-6.846	-0.26619136E-01
BD(10, 2,0.1098)	7.734	3.725	-6.846	-0.22239853E-01
BD(10, 3,0.1098)	6.712	5.352	-6.846	-0.16745351E-01
BD(10, 4,0.1098)	5.352	6.712	-6.846	-0.10411192E-01
BD(10, 5,0.1098)	3.725	7.734	-6.846	-0.35549663E-02
BD(10, 6,0.1098)	1.910	8.369	-6.846	0.34795215E-02
BD(10, 7,0.1098)	-0.000	8.584	-6.846	0.10339562E-01
BD(10, 8,0.1098)	-1.910	8.369	-6.846	0.16681086E-01
BD(10, 9,0.1098)	-3.725	7.734	-6.846	0.22186175E-01
BD(10,10,0.1098)	-5.352	6.712	-6.846	0.26578754E-01
BD(10,11,0.1098)	-6.712	5.352	-6.846	0.29638540E-01
BD(10,12,0.1098)	-7.734	3.725	-6.846	0.31212129E-01
BD(10,13,0.1098)	-8.369	1.910	-6.846	0.31220622E-01
BD(10,14,0.1098)	-8.584	-0.000	-6.846	0.29663540E-01
BD(10,15,0.1098)	-8.369	-1.910	-6.846	0.26619025E-01
BD(10,16,0.1098)	-7.734	-3.725	-6.846	0.22239670E-01
BD(10,17,0.1098)	-6.712	-5.352	-6.846	0.16745169E-01
BD(10,18,0.1098)	-5.352	-6.712	-6.846	0.10410976E-01
BD(10,19,0.1098)	-3.725	-7.734	-6.846	0.35547570E-02
BD(10,20,0.1098)	-1.910	-8.369	-6.846	-0.34797254E-02
BD(10,21,0.1098)	0.000	-8.584	-6.846	-0.10339763E-01
BD(10,22,0.1098)	1.910	-8.369	-6.846	-0.16681295E-01
BD(10,23,0.1098)	3.725	-7.734	-6.846	-0.22186365E-01
BD(10,24,0.1098)	5.352	-6.712	-6.846	-0.26578881E-01
BD(10,25,0.1098)	6.712	-5.352	-6.846	-0.29638622E-01
BD(10,26,0.1098)	7.734	-3.725	-6.846	-0.31212155E-01
BD(10,27,0.1098)	8.369	-1.910	-6.846	-0.31220585E-01
BD(11, 0,0.1098)	6.846	0.000	-8.585	-0.19835476E-01
BD(11, 1,0.1098)	6.674	1.523	-8.585	-0.17822828E-01
BD(11, 2,0.1098)	6.168	2.970	-8.585	-0.14916483E-01
BD(11, 3,0.1098)	5.352	4.268	-8.585	-0.11262164E-01
BD(11, 4,0.1098)	4.268	5.352	-8.585	-0.70431009E-02
BD(11, 5,0.1098)	2.970	6.168	-8.585	-0.24706742E-02
BD(11, 6,0.1098)	1.523	6.674	-8.585	0.22252561E-02
BD(11, 7,0.1098)	-0.000	6.846	-8.585	0.68098232E-02
BD(11, 8,0.1098)	-1.523	6.674	-8.585	0.11052888E-01
BD(11, 9,0.1098)	-2.970	6.168	-8.585	0.14741715E-01
BD(11,10,0.1098)	-4.268	5.352	-8.585	0.17631344E-01
BD(11,11,0.1098)	-5.352	4.268	-8.585	0.19753340E-01

BD(11,12,0.1098)	-6.168	2.970	-8.585	0.20825788E-01
BD(11,13,0.1098)	-6.674	1.523	-8.585	0.20853449E-01
BD(11,14,0.1098)	-6.846	-0.000	-8.585	0.19835431E-01
BD(11,15,0.1098)	-6.674	-1.523	-8.585	0.17822765E-01
BD(11,16,0.1098)	-6.168	-2.970	-8.585	0.14916368E-01
BD(11,17,0.1098)	-5.352	-4.268	-8.585	0.11262044E-01
BD(11,18,0.1098)	-4.268	-5.352	-8.585	0.70429705E-02
BD(11,19,0.1098)	-2.970	-6.168	-8.585	0.24707355E-02
BD(11,20,0.1098)	-1.523	-6.674	-8.585	-0.22253925E-02
BD(11,21,0.1098)	0.000	-6.846	-8.585	-0.68099536E-02
BD(11,22,0.1098)	1.523	-6.674	-8.585	-0.11053022E-01
BD(11,23,0.1098)	2.970	-6.168	-8.585	-0.14741842E-01
BD(11,24,0.1098)	4.268	-5.352	-8.585	-0.17691407E-01
BD(11,25,0.1098)	5.352	-4.268	-8.585	-0.19753888E-01
BD(11,26,0.1098)	6.168	-2.970	-8.585	-0.20825807E-01
BD(11,27,0.1098)	6.674	-1.523	-8.585	-0.20853437E-01
BD(12, 0,0.1098)	4.764	0.000	-9.893	-0.12203962E-01
BD(12, 1,0.1098)	4.645	1.060	-9.893	-0.10973342E-01
BD(12, 2,0.1098)	4.292	2.067	-9.893	-0.91924742E-02
BD(12, 3,0.1098)	3.725	2.970	-9.893	-0.69506504E-02
BD(12, 4,0.1098)	2.970	3.725	-9.893	-0.43602958E-02
BD(12, 5,0.1098)	2.067	4.292	-9.893	-0.15512977E-02
BD(12, 6,0.1098)	1.060	4.645	-9.893	0.13354912E-02
BD(12, 7,0.1098)	-0.000	4.764	-9.893	0.41553229E-02
BD(12, 8,0.1098)	-1.060	4.645	-9.893	0.67667738E-02
BD(12, 9,0.1098)	-2.067	4.292	-9.893	0.90389140E-02
BD(12,10,0.1098)	-2.970	3.725	-9.893	0.10857802E-01
BD(12,11,0.1098)	-3.725	2.970	-9.893	0.12132239E-01
BD(12,12,0.1098)	-4.292	2.067	-9.893	0.12798298E-01
BD(12,13,0.1098)	-4.645	1.060	-9.893	0.12822609E-01
BD(12,14,0.1098)	-4.764	-0.000	-9.893	0.12203936E-01
BD(12,15,0.1098)	-4.645	-1.060	-9.893	0.10973297E-01
BD(12,16,0.1098)	-4.292	-2.067	-9.893	0.91924034E-02
BD(12,17,0.1098)	-3.725	-2.970	-9.893	0.69505796E-02
BD(12,18,0.1098)	-2.970	-3.725	-9.893	0.43602139E-02
BD(12,19,0.1098)	-2.067	-4.292	-9.893	0.15512137E-02
BD(12,20,0.1098)	-1.060	-4.645	-9.893	-0.13355860E-02
BD(12,21,0.1098)	0.000	-4.764	-9.893	-0.41554011E-02
BD(12,22,0.1098)	1.060	-4.645	-9.893	-0.67668483E-02
BD(12,23,0.1098)	2.067	-4.292	-9.893	-0.90389922E-02
BD(12,24,0.1098)	2.970	-3.725	-9.893	-0.10857854E-01
BD(12,25,0.1098)	3.725	-2.970	-9.893	-0.12132265E-01
BD(12,26,0.1098)	4.292	-2.067	-9.893	-0.127983 9E-01
BD(12,27,0.1098)	4.645	-1.060	-9.893	-0.12822602E-01
BD(13, 0,0.1098)	2.443	0.000	-10.705	-0.58193840E-02
BD(13, 1,0.1098)	2.382	0.544	-10.705	-0.52343346E-02
BD(13, 2,0.1098)	2.201	1.060	-10.705	-0.43868199E-02
BD(13, 3,0.1098)	1.910	1.523	-10.705	-0.33193305E-02
BD(13, 4,0.1098)	1.523	1.910	-10.705	-0.20853961E-02
BD(13, 5,0.1098)	1.060	2.201	-10.705	-0.74688881E-03
BD(13, 6,0.1098)	0.544	2.382	-10.705	0.62907068E-03
BD(13, 7,0.1098)	-0.000	2.443	-10.705	0.19734891E-02
BD(13, 8,0.1098)	-0.544	2.382	-10.705	0.32189409E-02
BD(13, 9,0.1098)	-1.060	2.201	-10.705	0.43029860E-02
BD(13,10,0.1098)	-1.523	1.910	-10.705	0.51712580E-02
BD(13,11,0.1098)	-1.910	1.523	-10.705	0.57802238E-02
BD(13,12,0.1098)	-2.201	1.060	-10.705	0.60993396E-02
BD(13,13,0.1098)	-2.382	0.544	-10.705	0.61126091E-02
BD(13,14,0.1098)	-2.443	-0.000	-10.705	0.58193691E-02
BD(13,15,0.1098)	-2.382	-0.544	-10.705	0.52343123E-02
BD(13,16,0.1098)	-2.201	-1.060	-10.705	0.43867864E-02
BD(13,17,0.1098)	-1.910	-1.523	-10.705	0.33192968E-02
BD(13,18,0.1098)	-1.523	-1.910	-10.705	0.20853553E-02
BD(13,19,0.1098)	-1.060	-2.201	-10.705	0.74684294E-03
BD(13,20,0.1098)	-0.544	-2.382	-10.705	-0.62911375E-03
BD(13,21,0.1098)	0.000	-2.443	-10.705	-0.19735277E-02

```
  BD(13,22,0.1098)    0.544   -2.382 -10.705     -0.32189772E-02
  BD(13,23,0.1098)    1.060   -2.201 -10.705     -0.43030195E-02
  BD(13,24,0.1098)    1.523   -1.910 -10.705     -0.51712804E-02
  BD(13,25,0.1098)    1.910   -1.523 -10.705     -0.57802387E-02
  BD(13,26,0.1098)    2.201   -1.060 -10.705     -0.60993433E-02
  BD(13,27,0.1098)    2.382   -0.544 -10.705     -0.61126053E-02
  BD(14, 0,0.1098)   -0.000    0.000 -10.980     -0.83147178E-08
END OF DATA
```

Calculated Data for Model #5

	DIPOLE#1	DIPOLE#2	DIPOLE#3	
MOMENT	0.11E-04	0.11E-04	0.00E+00	(AMP*M)
LOCATN	0.070	0.070	0.000	(M FR ORN)
TRANS MATRIX	0.906 0.000-0.423 0.000 1.000 0.000 0.423 0.000 0.906	0.000-0.906-0.423 1.000 0.000 0.000 0.000-0.423 0.906	1.000 0.000 0.000 0.000 1.000 0.000 0.000 0.000 1.000	

THE MEAS SPHERE RADIUS IS 0.1098 M

SPHER DATA POINTS: THETA=I*0.2244; PHI=F*0.2244

BD(T,F,R)	X	Y	Z	FLUX DENS, XEE-11 TESLA
BD(0, 0,0.1098)	0.000	0.000	10.980	-0.12354885E-05
BD(1, 0,0.1098)	2.443	0.000	10.705	0.78114372E+00
BD(1, 1,0.1098)	2.382	0.544	10.705	0.11764374E+01
BD(1, 2,0.1098)	2.201	1.060	10.705	0.14506912E+01
BD(1, 3,0.1098)	1.910	1.523	10.705	0.15395555E+01
BD(1, 4,0.1098)	1.523	1.910	10.705	0.14597769E+01
BD(1, 5,0.1098)	1.060	2.201	10.705	0.12703056E+01
BD(1, 6,0.1098)	0.544	2.382	10.705	0.10306473E+01
BD(1, 7,0.1098)	-0.000	2.443	10.705	0.78113908E+00
BD(1, 8,0.1098)	-0.544	2.382	10.705	0.54158998E+00
BD(1, 9,0.1098)	-1.060	2.201	10.705	0.31708521E+00
BD(1,10,0.1098)	-1.523	1.910	10.705	0.10426515E+00
BD(1,11,0.1098)	-1.910	1.523	10.705	-0.10427189E+00
BD(1,12,0.1098)	-2.201	1.060	10.705	-0.31710017E+00
BD(1,13,0.1098)	-2.382	0.544	10.705	-0.54160160E+00
BD(1,14,0.1098)	-2.443	-0.000	10.705	-0.78115535E+00
BD(1,15,0.1098)	-2.382	-0.544	10.705	-0.10306549E+01
BD(1,16,0.1098)	-2.201	-1.060	10.705	-0.12703114E+01
BD(1,17,0.1098)	-1.910	-1.523	10.705	-0.14597826E+01
BD(1,18,0.1098)	-1.523	-1.910	10.705	-0.15395603E+01
BD(1,19,0.1098)	-1.060	-2.201	10.705	-0.14506731E+01
BD(1,20,0.1098)	-0.544	-2.382	10.705	-0.11764164E+01
BD(1,21,0.1098)	0.000	-2.443	10.705	-0.78112715E+00
BD(1,22,0.1098)	0.544	-2.382	10.705	-0.39578557E+00
BD(1,23,0.1098)	1.060	-2.201	10.705	-0.13669676E+00
BD(1,24,0.1098)	1.523	-1.910	10.705	-0.24487235E-01
BD(1,25,0.1098)	1.910	-1.523	10.705	0.24488252E-01
BD(1,26,0.1098)	2.201	-1.060	10.705	0.13672072E+00
BD(1,27,0.1098)	2.382	-0.544	10.705	0.39582533E+00
BD(2, 0,0.1098)	4.764	0.000	9.893	0.82215434E+00
BD(2, 1,0.1098)	4.645	1.060	9.893	0.21332159E+01
BD(2, 2,0.1098)	4.292	2.067	9.893	0.27734528E+01
BD(2, 3,0.1098)	3.725	2.970	9.893	0.26968927E+01
BD(2, 4,0.1098)	2.970	3.725	9.893	0.22320309E+01
BD(2, 5,0.1098)	2.067	4.292	9.893	0.16855755E+01
BD(2, 6,0.1098)	1.060	4.645	9.893	0.12040110E+01
BD(2, 7,0.1098)	-0.000	4.764	9.893	0.82215059E+00
BD(2, 8,0.1098)	-1.060	4.645	9.893	0.52712154E+00
BD(2, 9,0.1098)	-2.067	4.292	9.893	0.29304528E+00
BD(2,10,0.1098)	-2.970	3.725	9.893	0.93917012E-01
BD(2,11,0.1098)	-3.725	2.970	9.893	-0.93924880E-01
BD(2,12,0.1098)	-4.292	2.067	9.893	-0.29305446E+00
BD(2,13,0.1098)	-4.645	1.060	9.893	-0.52713192E+00
BD(2,14,0.1098)	-4.764	-0.000	9.893	-0.82217240E+00

BD(2,15,0.1098)	-4.645	-1.060	9.893	-0.12040234E+01
BD(2,16,0.1098)	-4.292	-2.067	9.893	-0.16855869E+01
BD(2,17,0.1098)	-3.725	-2.970	9.893	-0.22320595E+01
BD(2,18,0.1098)	-2.970	-3.725	9.893	-0.26969309E+01
BD(2,19,0.1098)	-2.067	-4.292	9.893	-0.27734575E+01
BD(2,20,0.1098)	-1.060	-4.645	9.893	-0.21331587E+01
BD(2,21,0.1098)	0.000	-4.764	9.893	-0.82203943E+00
BD(2,22,0.1098)	1.060	-4.645	9.893	0.40216178E+00
BD(2,23,0.1098)	2.067	-4.292	9.893	0.79484451E+00
BD(2,24,0.1098)	2.970	-3.725	9.893	0.37093908E+00
BD(2,25,0.1098)	3.725	-2.970	9.893	-0.37101024E+00
BD(2,26,0.1098)	4.292	-2.067	9.893	-0.79486442E+00
BD(2,27,0.1098)	4.645	-1.060	9.893	-0.40203696E+00
BD(3, 0,0.1098)	6.846	0.000	8.584	0.54570568E+00
BD(3, 1,0.1098)	6.674	1.523	8.584	0.17234449E+01
BD(3, 2,0.1098)	6.168	2.970	8.584	0.22466383E+01
BD(3, 3,0.1098)	5.352	4.268	8.584	0.21011648E+01
BD(3, 4,0.1098)	4.268	5.352	8.584	0.16574821E+01
BD(3, 5,0.1098)	2.970	6.168	8.584	0.11962872E+01
BD(3, 6,0.1098)	1.523	6.674	8.584	0.82277340E+00
BD(3, 7,0.1098)	-0.000	6.846	8.584	0.54570407E+00
BD(3, 8,0.1098)	-1.523	6.674	8.584	0.34272552E+00
BD(3, 9,0.1098)	-2.970	6.168	8.584	0.18806994E+00
BD(3,10,0.1098)	-4.268	5.352	8.584	0.59897874E-01
BD(3,11,0.1098)	-5.352	4.268	8.584	-0.59902992E-01
BD(3,12,0.1098)	-6.168	2.970	8.584	-0.18807518E+00
BD(3,13,0.1098)	-6.674	1.523	8.584	-0.34273338E+00
BD(3,14,0.1098)	-6.846	-0.000	8.584	-0.54571307E+00
BD(3,15,0.1098)	-6.674	-1.523	8.584	-0.82278842E+00
BD(3,16,0.1098)	-6.168	-2.970	8.584	-0.11963129E+01
BD(3,17,0.1098)	-5.352	-4.268	8.584	-0.16575155E+01
BD(3,18,0.1098)	-4.268	-5.352	8.584	-0.21011925E+01
BD(3,19,0.1098)	-2.970	-6.168	8.584	-0.22466230E+01
BD(3,20,0.1098)	-1.523	-6.674	8.584	-0.17234058E+01
BD(3,21,0.1098)	0.000	-6.846	8.584	-0.54564774E+00
BD(3,22,0.1098)	1.523	-6.674	8.584	0.55795938E+00
BD(3,23,0.1098)	2.970	-6.168	8.584	0.86227387E+00
BD(3,24,0.1098)	4.268	-5.352	8.584	0.38374490E+00
BD(3,25,0.1098)	5.352	-4.268	8.584	-0.38382131E+00
BD(3,26,0.1098)	6.168	-2.970	8.584	-0.86230540E+00
BD(3,27,0.1098)	6.674	-1.523	8.584	-0.55787736E+00
BD(4, 0,0.1098)	8.585	0.000	6.846	0.31576139E+00
BD(4, 1,0.1098)	8.369	1.910	6.846	0.85960108E+00
BD(4, 2,0.1098)	7.734	3.725	6.846	0.11287270E+01
BD(4, 3,0.1098)	6.712	5.352	6.846	0.10895306E+01
BD(4, 4,0.1098)	5.352	6.712	6.846	0.88949758E+00
BD(4, 5,0.1098)	3.725	7.734	6.846	0.66184449E+00
BD(4, 6,0.1098)	1.910	8.369	6.846	0.46675396E+00
BD(4, 7,0.1098)	-0.000	8.585	6.846	0.31575996E+00
BD(4, 8,0.1098)	-1.910	8.369	6.846	0.20125645E+00
BD(4, 9,0.1098)	-3.725	7.734	6.846	0.11152965E+00

```
BD(  4,10,0.1098)   -5.352    6.712    6.846     0.35636119E-01
BD(  4,11,0.1098)   -6.712    5.352    6.846    -0.35698503E-01
BD(  4,12,0.1098)   -7.734    3.725    6.846    -0.11153275E+00
BD(  4,13,0.1098)   -8.369    1.910    6.846    -0.20126098E+00
BD(  4,14,0.1098)   -8.585   -0.000    6.846    -0.31576473E+00
BD(  4,15,0.1098)   -8.369   -1.910    6.846    -0.46676153E+00
BD(  4,16,0.1098)   -7.734   -3.725    6.846    -0.66185164E+00
BD(  4,17,0.1098)   -6.712   -5.352    6.846    -0.88950676E+00
BD(  4,18,0.1098)   -5.352   -6.712    6.846    -0.10895329E+01
BD(  4,19,0.1098)   -3.725   -7.734    6.846    -0.11287260E+01
BD(  4,20,0.1098)   -1.910   -8.369    6.846    -0.85957605E+00
BD(  4,21,0.1098)    0.000   -8.585    6.846    -0.31573290E+00
BD(  4,22,0.1098)    1.910   -8.369    6.846     0.19160211E+00
BD(  4,23,0.1098)    3.725   -7.734    6.846     0.35533953E+00
BD(  4,24,0.1098)    5.352   -6.712    6.846     0.16431934E+00
BD(  4,25,0.1098)    6.712   -5.352    6.846    -0.16434389E+00
BD(  4,26,0.1098)    7.734   -3.725    6.846    -0.35535645E+00
BD(  4,27,0.1098)    8.369   -1.910    6.846    -0.19156021E+00
BD(  5, 0,0.1098)    9.893    0.000    4.764     0.18093514E+00
BD(  5, 1,0.1098)    9.645    2.201    4.764     0.38846946E+00
BD(  5, 2,0.1098)    8.913    4.292    4.764     0.50673491E+00
BD(  5, 3,0.1098)    7.734    6.168    4.764     0.51114529E+00

BD(  5, 4,0.1098)    6.168    7.734    4.764     0.44190252E+00
BD(  5, 5,0.1098)    4.292    8.913    4.764     0.34766519E+00
BD(  5, 6,0.1098)    2.201    9.645    4.764     0.25731015E+00
BD(  5, 7,0.1098)   -0.000    9.893    4.764     0.18093342E+00
BD(  5, 8,0.1098)   -2.201    9.645    4.764     0.11867988E+00
BD(  5, 9,0.1098)   -4.292    8.913    4.764     0.67023039E-01
BD(  5,10,0.1098)   -6.168    7.734    4.764     0.21652255E-01
BD(  5,11,0.1098)   -7.734    6.168    4.764    -0.21655604E-01
BD(  5,12,0.1098)   -8.913    4.292    4.764    -0.67024589E-01
BD(  5,13,0.1098)   -9.645    2.201    4.764    -0.11868215E+00
BD(  5,14,0.1098)   -9.893   -0.000    4.764    -0.18093675E+00
BD(  5,15,0.1098)   -9.645   -2.201    4.764    -0.25731307E+00
BD(  5,16,0.1098)   -8.913   -4.292    4.764    -0.34767026E+00
BD(  5,17,0.1098)   -7.734   -6.168    4.764    -0.44190538E+00
BD(  5,18,0.1098)   -6.168   -7.734    4.764    -0.51114577E+00
BD(  5,19,0.1098)   -4.292   -8.913    4.764    -0.50673389E+00
BD(  5,20,0.1098)   -2.201   -9.645    4.764    -0.38846028E+00
BD(  5,21,0.1098)    0.000   -9.893    4.764    -0.18092453E+00
BD(  5,22,0.1098)    2.201   -9.645    4.764     0.12482923E-01
BD(  5,23,0.1098)    4.292   -8.913    4.764     0.92043579E-01
BD(  5,24,0.1098)    6.168   -7.734    4.764     0.47583744E-01
BD(  5,25,0.1098)    7.734   -6.168    4.764    -0.47594365E-01

BD(  5,26,0.1098)    8.913   -4.292    4.764    -0.92043281E-01
BD(  5,27,0.1098)    9.645   -2.201    4.764    -0.12468081E-01
BD(  6, 0,0.1098)   10.705    0.000    2.443     0.10773921E+00
BD(  6, 1,0.1098)   10.436    2.382    2.443     0.18846631E+00
BD(  6, 2,0.1098)    9.645    4.645    2.443     0.23993397E+00
BD(  6, 3,0.1098)    8.369    6.674    2.443     0.24984747E+00
BD(  6, 4,0.1098)    6.674    8.369    2.443     0.22746664E+00
BD(  6, 5,0.1098)    4.645    9.645    2.443     0.18905395E+00
BD(  6, 6,0.1098)    2.382   10.436    2.443     0.14706510E+00
BD(  6, 7,0.1098)   -0.000   10.705    2.443     0.10774022E+00
BD(  6, 8,0.1098)   -2.382   10.436    2.443     0.72882533E-01
BD(  6, 9,0.1098)   -4.645    9.645    2.443     0.42007968E-01
BD(  6,10,0.1098)   -6.674    8.369    2.443     0.13710093E-01
BD(  6,11,0.1098)   -8.369    6.674    2.443    -0.13711330E-01
BD(  6,12,0.1098)   -9.645    4.645    2.443    -0.42010088E-01
BD(  6,13,0.1098)  -10.436    2.382    2.443    -0.72884917E-01
BD(  6,14,0.1098)  -10.705   -0.000    2.443    -0.10774052E+00
BD(  6,15,0.1098)  -10.436   -2.382    2.443    -0.14706743E+00
BD(  6,16,0.1098)   -9.645   -4.645    2.443    -0.18905717E+00
BD(  6,17,0.1098)   -8.369   -6.674    2.443    -0.22746956E+00
BD(  6,18,0.1098)   -6.674   -8.369    2.443    -0.24984837E+00
BD(  6,19,0.1098)   -4.645   -9.645    2.443    -0.23993367E+00
```

```
BD( 6,20,0.1098)   -2.382 -10.436    2.443     -0.18846357E+00
BD( 6,21,0.1098)    0.000 -10.705    2.443     -0.10773463E+00
BD( 6,22,0.1098)    2.382 -10.436    2.443     -0.31478792E-01
BD( 6,23,0.1098)    4.645  -9.645    2.443      0.88720098E-02
BD( 6,24,0.1098)    6.674  -8.369    2.443      0.36687207E-02
BD( 6,25,0.1098)    8.369  -6.674    2.443     -0.86760283E-02
BD( 6,26,0.1098)    9.645  -4.644    2.443     -0.88688098E-02
BD( 6,27,0.1098)   10.436  -2.382    2.443      0.31486176E-01
BD( 7, 0,0.1098)   10.980   0.000   -0.000      0.67436993E-01
BD( 7, 1,0.1098)   10.705   2.443   -0.000      0.10193813E+00
BD( 7, 2,0.1098)    9.893   4.764   -0.000      0.12566465E+00
BD( 7, 3,0.1098)    8.584   6.846   -0.000      0.13306922E+00
BD( 7, 4,0.1098)    6.846   8.585   -0.000      0.12586200E+00
BD( 7, 5,0.1098)    4.764   9.893   -0.000      0.10937601E+00
BD( 7, 6,0.1098)    2.443  10.705   -0.000      0.88783324E-01
BD( 7, 7,0.1098)   -0.000  10.980   -0.000      0.67435741E-01
BD( 7, 8,0.1098)   -2.443  10.705   -0.000      0.46901286E-01
BD( 7, 9,0.1098)   -4.764   9.893   -0.000      0.27599827E-01
BD( 7,10,0.1098)   -6.846   8.584   -0.000      0.90717711E-02
BD( 7,11,0.1098)   -8.585   6.846   -0.000     -0.90730728E-02
BD( 7,12,0.1098)   -9.893   4.764   -0.000     -0.27541153E-01
BD( 7,13,0.1098)  -10.705   2.443   -0.000     -0.46901729E-01

BD( 7,14,0.1098)  -10.980  -0.000   -0.000     -0.67437470E-01
BD( 7,15,0.1098)  -10.705  -2.443   -0.000     -0.88784099E-01
BD( 7,16,0.1098)   -9.893  -4.764   -0.000     -0.10937709E+00
BD( 7,17,0.1098)   -8.584  -6.846   -0.000     -0.12586355E+00
BD( 7,18,0.1098)   -6.846  -8.585   -0.000     -0.13306928E+00
BD( 7,19,0.1098)   -4.764  -9.893   -0.000     -0.12566352E+00
BD( 7,20,0.1098)   -2.443 -10.705   -0.000     -0.10193670E+00
BD( 7,21,0.1098)    0.000 -10.980   -0.000     -0.67435205E-01
BD( 7,22,0.1098)    2.443 -10.705   -0.000     -0.33744399E-01
BD( 7,23,0.1098)    4.764  -9.893   -0.000     -0.11252150E-01
BD( 7,24,0.1098)    6.846  -8.584   -0.000     -0.18648095E-02
BD( 7,25,0.1098)    8.585  -6.846   -0.000      0.18659283E-02
BD( 7,26,0.1098)    9.893  -4.764   -0.000      0.11252858E-01
BD( 7,27,0.1098)   10.705  -2.443   -0.000      0.33747390E-01
BD( 8, 0,0.1098)   10.705   0.000   -2.443      0.44111766E-01
BD( 8, 1,0.1098)   10.436   2.382   -2.443      0.60625095E-01
BD( 8, 2,0.1098)    9.645   4.645   -2.443      0.72468817E-01
BD( 8, 3,0.1098)    8.369   6.674   -2.443      0.77191353E-01
BD( 8, 4,0.1098)    6.674   8.369   -2.443      0.74863911E-01
BD( 8, 5,0.1098)    4.645   9.645   -2.443      0.67224205E-01
BD( 8, 6,0.1098)    2.382  10.436   -2.443      0.56405585E-01
BD( 8, 7,0.1098)   -0.000  10.705   -2.443      0.44111665E-01

BD( 8, 8,0.1098)   -2.382  10.436   -2.443      0.31389307E-01
BD( 8, 9,0.1098)   -4.645   9.645   -2.443      0.18721227E-01
BD( 8,10,0.1098)   -6.674   8.369   -2.443      0.62154047E-02
BD( 8,11,0.1098)   -8.369   6.674   -2.443     -0.62156586E-02
BD( 8,12,0.1098)   -9.645   4.645   -2.443     -0.18721579E-01
BD( 8,13,0.1098)  -10.436   2.382   -2.443     -0.31390764E-01
BD( 8,14,0.1098)  -10.705  -0.000   -2.443     -0.44111930E-01
BD( 8,15,0.1098)  -10.436  -2.382   -2.443     -0.56406613E-01
BD( 8,16,0.1098)   -9.645  -4.645   -2.443     -0.67225516E-01
BD( 8,17,0.1098)   -8.369  -6.674   -2.443     -0.74864149E-01
BD( 8,18,0.1098)   -6.674  -8.369   -2.443     -0.77191234E-01
BD( 8,19,0.1098)   -4.645  -9.645   -2.443     -0.72467923E-01
BD( 8,20,0.1098)   -2.382 -10.436   -2.443     -0.60624787E-01
BD( 8,21,0.1098)    0.000 -10.705   -2.443     -0.44111509E-01
BD( 8,22,0.1098)    2.382 -10.436   -2.443     -0.27162652E-01
BD( 8,23,0.1098)    4.645  -9.645   -2.443     -0.13476871E-01
BD( 8,24,0.1098)    6.674  -8.369   -2.443     -0.38874[illegible]E-02
BD( 8,25,0.1098)    8.369  -6.674   -2.443      0.38[illegible]E-02
BD( 8,26,0.1098)    9.645  -4.644   -2.443      0.13477437E-01
BD( 8,27,0.1098)   10.436  -2.382   -2.443      0.27170665E-01
BD( 9, 0,0.1098)    9.893   0.000   -4.764      0.29726479E-01
BD( 9, 1,0.1098)    9.645   2.261    4.764      0.38497765E-01
```

BD(8, 2,0.1098)	8.913	4.292	-4.764	0.44885464E-01
BD(8, 3,0.1098)	7.734	6.168	-4.764	0.47802657E-01
BD(8, 4,0.1098)	6.168	7.734	-4.764	0.47067493E-01
BD(8, 5,0.1098)	4.292	8.913	-4.764	0.43231566E-01
BD(8, 6,0.1098)	2.201	9.645	-4.764	0.37169155E-01
BD(8, 7,0.1098)	-0.000	9.893	-4.764	0.29726613E-01
BD(8, 8,0.1098)	-2.201	9.645	-4.764	0.21539688E-01
BD(8, 9,0.1098)	-4.292	8.913	-4.764	0.13008311E-01
BD(8,10,0.1098)	-6.168	7.734	-4.764	0.43466352E-02
BD(8,11,0.1098)	-7.734	6.168	-4.764	-0.43467842E-02
BD(8,12,0.1098)	-8.913	4.292	-4.764	-0.13008483E-01
BD(8,13,0.1098)	-9.645	2.201	-4.764	-0.21540105E-01
BD(8,14,0.1098)	-9.893	-0.000	-4.764	-0.29727243E-01
BD(8,15,0.1098)	-9.645	-2.201	-4.764	-0.37169483E-01
BD(8,16,0.1098)	-8.913	-4.292	-4.764	-0.43231428E-01
BD(8,17,0.1098)	-7.734	-6.168	-4.764	-0.47068067E-01
BD(8,18,0.1098)	-6.168	-7.734	-4.764	-0.47802839E-01
BD(8,19,0.1098)	-4.292	-8.913	-4.764	-0.44885617E-01
BD(8,20,0.1098)	-2.201	-9.645	-4.764	-0.38497344E-01
BD(8,21,0.1098)	0.000	-9.893	-4.764	-0.29726479E-01
BD(8,22,0.1098)	2.201	-9.645	-4.764	-0.20210553E-01
BD(8,23,0.1098)	4.292	-8.913	-4.764	-0.11357992E-01
BD(8,24,0.1098)	6.168	-7.734	-4.764	-0.36104757E-02
BD(8,25,0.1098)	7.734	-6.168	-4.764	0.36114759E-02
BD(8,26,0.1098)	8.913	-4.292	-4.764	0.11355050E-01
BD(8,27,0.1098)	9.645	-2.201	-4.764	0.20212054E-01
BD(10, 0,0.1098)	8.584	0.000	-6.846	0.20218913E-01
BD(10, 1,0.1098)	8.369	1.910	-6.846	0.25252517E-01
BD(10, 2,0.1098)	7.734	3.725	-6.846	0.28906986E-01
BD(10, 3,0.1098)	6.712	5.352	-6.846	0.30702375E-01
BD(10, 4,0.1098)	5.352	6.712	-6.846	0.30487780E-01
BD(10, 5,0.1098)	3.725	7.734	-6.846	0.28423835E-01
BD(10, 6,0.1098)	1.910	8.369	-6.846	0.24864648E-01
BD(10, 7,0.1098)	-0.000	8.584	-6.846	0.20218756E-01
BD(10, 8,0.1098)	-1.910	8.369	-6.846	0.14854375E-01
BD(10, 9,0.1098)	-3.725	7.734	-6.846	0.90597197E-02
BD(10,10,0.1098)	-5.352	6.712	-6.846	0.30419084E-02
BD(10,11,0.1098)	-6.712	5.352	-6.846	-0.30424944E-02
BD(10,12,0.1098)	-7.734	3.725	-6.846	-0.90597048E-02
BD(10,13,0.1098)	-8.369	1.910	-6.846	-0.14854565E-01
BD(10,14,0.1098)	-8.584	-0.000	-6.846	-0.20219091E-01
BD(10,15,0.1098)	-8.369	-1.910	-6.846	-0.24864845E-01
BD(10,16,0.1098)	-7.734	-3.725	-6.846	-0.28424110E-01
BD(10,17,0.1098)	-6.712	-5.352	-6.846	-0.30467426E-01
BD(10,18,0.1098)	-5.352	-6.712	-6.846	-0.30702446E-01
BD(10,19,0.1098)	-3.725	-7.734	-6.846	-0.28907005E-01
BD(10,20,0.1098)	-1.910	-8.369	-6.846	-0.25252409E-01
BD(10,21,0.1098)	0.000	-8.584	-6.846	-0.20218737E-01
BD(10,22,0.1098)	1.910	-8.369	-6.846	-0.14866193E-01
BD(10,23,0.1098)	3.725	-7.734	-6.846	-0.85758865E-02
BD(10,24,0.1098)	5.352	-6.712	-6.846	-0.28270278E-02
BD(10,25,0.1098)	6.712	-5.352	-6.846	0.28276916E-02
BD(10,26,0.1098)	7.734	-3.725	-6.846	0.85761137E-02
BD(10,27,0.1098)	8.369	-1.910	-6.846	0.14867202E-01
BD(11, 0,0.1098)	6.846	0.000	-8.585	0.13461083E-01
BD(11, 1,0.1098)	6.674	1.523	-8.585	0.16452022E-01
BD(11, 2,0.1098)	6.168	2.970	-8.585	0.18597163E-01
BD(11, 3,0.1098)	5.352	4.268	-8.585	0.19687738E-01
BD(11, 4,0.1098)	4.268	5.352	-8.585	0.19635744E-01
BD(11, 5,0.1098)	2.970	6.168	-8.585	0.18481102E-01
BD(11, 6,0.1098)	1.523	6.674	-8.585	0.16359571E-01
BD(11, 7,0.1098)	-0.000	6.846	-8.585	0.13461057E-01
BD(11, 8,0.1098)	-1.523	6.674	-8.585	0.99809694E-02
BD(11, 9,0.1098)	-2.970	6.168	-8.585	0.61379597E-02
BD(11,10,0.1098)	-4.268	5.352	-8.585	0.20692083E-02
BD(11,11,0.1098)	-5.352	4.268	-8.585	-0.20695245E-02

BD(11,12,0.1098)	-6.168	2.970	-8.585	-0.61380379E-02
BD(11,13,0.1098)	-6.674	1.523	-8.585	-0.99903233E-02
BD(11,14,0.1098)	-6.846	-0.000	-8.585	-0.13461012E-01
BD(11,15,0.1098)	-6.674	-1.523	-8.585	-0.16359687E-01
BD(11,16,0.1098)	-6.168	-2.970	-8.585	-0.18480867E-01
BD(11,17,0.1098)	-5.352	-4.268	-8.585	-0.19635927E-01
BD(11,18,0.1098)	-4.268	-5.352	-8.585	-0.19687839E-01
BD(11,19,0.1098)	-2.970	-6.168	-8.585	-0.18597011E-01
BD(11,20,0.1098)	-1.523	-6.674	-8.585	-0.16452104E-01
BD(11,21,0.1098)	0.000	-6.846	-8.585	-0.13460964E-01
BD(11,22,0.1098)	1.523	-6.674	-8.585	-0.98970756E-02
BD(11,23,0.1098)	2.970	-6.168	-8.585	-0.60214512E-02
BD(11,24,0.1098)	4.268	-5.352	-8.585	-0.20173045E-02
BD(11,25,0.1098)	5.352	-4.268	-8.585	0.20176684E-02
BD(11,26,0.1098)	6.168	-2.970	-8.585	0.60220733E-02
BD(11,27,0.1098)	6.674	-1.523	-8.585	0.98977834E-02
BD(12, 0,0.1098)	4.764	0.000	-9.893	0.82725994E-02
BD(12, 1,0.1098)	4.645	1.060	-9.893	0.99871606E-02
BD(12, 2,0.1098)	4.292	2.067	-9.893	0.11198934E-01
BD(12, 3,0.1098)	3.725	2.970	-9.893	0.11822347E-01
BD(12, 4,0.1098)	2.970	3.725	-9.893	0.11815470E-01
BD(12, 5,0.1098)	2.067	4.292	-9.893	0.11186182E-01
BD(12, 6,0.1098)	1.060	4.645	-9.893	0.99888593E-02
BD(12, 7,0.1098)	0.000	4.764	-9.893	0.82726665E-02
BD(12, 8,0.1098)	-1.060	4.645	-9.893	0.61686225E-02
BD(12, 9,0.1098)	-2.067	4.292	-9.893	0.38153853E-02
BD(12,10,0.1098)	-2.970	3.725	-9.893	0.12905065E-02
BD(12,11,0.1098)	-3.725	2.970	-9.893	-0.12906599E-02
BD(12,12,0.1098)	-4.292	2.067	-9.893	-0.38155525E-02
BD(12,13,0.1098)	-4.645	1.060	-9.893	-0.61686784E-02
BD(12,14,0.1098)	-4.764	-0.000	-9.893	-0.82729906E-02
BD(12,15,0.1098)	-4.645	-1.060	-9.893	-0.99889860E-02
BD(12,16,0.1098)	-4.292	-2.067	-9.893	-0.11185955E-01
BD(12,17,0.1098)	-3.725	-2.970	-9.893	-0.11815753E-01
BD(12,18,0.1098)	-2.970	-3.725	-9.893	-0.11822529E-01
BD(12,19,0.1098)	-2.067	-4.292	-9.893	-0.11198834E-01
BD(12,20,0.1098)	-1.060	-4.645	-9.893	-0.99869221E-02
BD(12,21,0.1098)	0.000	-4.764	-9.893	-0.82727559E-02
BD(12,22,0.1098)	1.060	-4.645	-9.893	-0.61704963E-02
BD(12,23,0.1098)	2.067	-4.292	-9.893	-0.38024893E-02
BD(12,24,0.1098)	2.970	-3.725	-9.893	-0.12836561E-02
BD(12,25,0.1098)	3.725	-2.970	-9.893	0.12837681E-02
BD(12,26,0.1098)	4.292	-2.067	-9.893	0.38027132E-02
BD(12,27,0.1098)	4.645	-1.060	-9.893	0.61707273E-02
BD(13, 0,0.1098)	2.443	0.000	-10.705	0.39454997E-02
BD(13, 1,0.1098)	2.382	0.544	-10.705	0.47334321E-02
BD(13, 2,0.1098)	2.201	1.060	-10.705	0.52843055E-02
BD(13, 3,0.1098)	1.910	1.523	-10.705	0.55677965E-02
BD(13, 4,0.1098)	1.523	1.910	-10.705	0.55677295E-02
BD(13, 5,0.1098)	1.060	2.201	-10.705	0.52844502E-02
BD(13, 6,0.1098)	0.544	2.382	-10.705	0.47336817E-02
BD(13, 7,0.1098)	0.000	2.443	-10.705	0.39454922E-02
BD(13, 8,0.1098)	-0.544	2.382	-10.705	0.29627180E-02
BD(13, 9,0.1098)	-1.060	2.201	-10.705	0.18836276E-02
BD(13,10,0.1098)	-1.523	1.910	-10.705	0.82207947E-03
BD(13,11,0.1098)	-1.910	1.523	-10.705	-0.62266537E-03
BD(13,12,0.1098)	-2.201	1.060	-10.705	-0.18363777E-02
BD(13,13,0.1098)	-2.382	0.544	-10.705	-0.29628773E-02
BD(13,14,0.1098)	-2.443	-0.000	-10.705	-0.39454285E-02
BD(13,15,0.1098)	-2.382	-0.544	-10.705	-0.47335960E-02
BD(13,16,0.1098)	-2.201	-1.060	-10.705	-0.52843092E-02
BD(13,17,0.1098)	-1.910	-1.523	-10.705	-0.55677205E-02
BD(13,18,0.1098)	-1.523	-1.910	-10.705	-0.55677257E-02
BD(13,19,0.1098)	-1.060	-2.201	-10.705	-0.52842982E-02
BD(13,20,0.1098)	-0.544	-2.382	-10.705	-0.47334991E-02
BD(13,21,0.1098)	0.000	-2.443	-10.705	-0.39454550E-02

```
  BD(13,22,0.1098)    0.544   -2.382 -10.705     -0.29628824E-02
  BD(13,23,0.1098)    1.060   -2.201 -10.705     -0.18363982E-02
  BD(13,24,0.1098)    1.523   -1.910 -10.705     -0.62196306E-03
  BD(13,25,0.1098)    1.910   -1.523 -10.705      0.62210113E-03
  BD(13,26,0.1098)    2.201   -1.060 -10.705      0.18364242E-02
  BD(13,27,0.1098)    2.382   -0.544 -10.705      0.29629306E-02
  BD(14, 0,0.1098)   -0.000    0.000 -10.980     -0.12121944E-06
END OF DATA
```

Appendix D

This section contains the data collected from each of the five multipole conducting sphere experiments.

Experiment Data for Model #1

	X	Y	Flux density (Wb/m²)	Phase, degrees w.r.t. input
00010	0	0	-0.[illegible]	87
00020	1.910	0	-0.[illegible]	85
00030	3.760	0	-0.27290000E 00	83
00040	5.490	0	-0.16200000E 00	80
00050	7.060	0	-0.08700000E 00	78
00060	8.410	0	-0.04500000E 00	76
00070	9.510	0	-0.02300000E 00	74
00080	10.320	0	-0.01200000E 00	77
00090	10.810	0	-0.02100000E 00	78
00100	10.980	0	-0.01700000E 00	80
00110	1.790	0.652	0.13700000E 00	-94
00120	3.530	1.280	0.52400000E 00	-93
00130	5.160	1.880	0.50100000E 00	-93
00140	6.630	2.410	0.37600000E 00	-93
00150	7.900	2.880	0.26100000E 00	-93
00160	8.940	3.250	0.17600000E 00	-93
00170	9.700	3.530	0.12100000E 00	-93
00180	10.160	3.700	0.08400000E 00	-93
00190	10.320	3.760	0.05300000E 00	-93
00200	1.460	1.230	0.83000000E 00	-94
00210	2.880	2.410	1.31300000E 00	-94
00220	4.210	3.530	1.09300000E 00	-94
00230	5.410	4.540	0.76400000E 00	-94
00240	6.440	5.410	0.52400000E 00	-94
00250	7.280	6.110	0.35700000E 00	-94
00260	7.900	6.630	0.24700000E 00	-94
00270	8.280	6.950	0.17900000E 00	-94
00280	8.410	7.060	0.12700000E 00	-94
00290	0.950	1.650	1.23400000E 00	-95
00300	1.880	3.250	1.77500000E 00	-94
00310	2.750	4.750	1.50900000E 00	-94
00320	3.530	6.110	1.08400000E 00	-95
00330	4.210	7.280	0.74100000E 00	-95
00340	4.750	8.240	0.49900000E 00	-95
00350	5.160	8.940	0.35100000E 00	-95
00360	5.410	9.360	0.25200000E 00	-95
00370	5.490	9.510	0.18800000E 00	-95
00380	0.330	1.880	1.55400000E 00	-95
00390	0.650	3.700	2.26200000E 00	-95
00400	0.950	5.410	1.86200000E 00	-95
00410	1.230	6.950	1.23700000E 00	-95
00420	1.460	8.280	0.90700000E 00	-95
00430	1.650	9.360	0.53700000E 00	-95
00440	1.790	10.160	0.41900000E 00	-95

00450	1.880	10.650	0.31000000E 00	-95
00460	1.910	10.810	0.22100000E 00	-94
00470	-0.330	1.880	1.62200000E 00	-95
00480	-0.650	3.700	2.36600000E 00	-95
00490	-0.950	5.410	1.98400000E 00	-95
00500	-1.230	6.950	1.39000000E 00	-95
00510	-1.460	8.280	0.90300000E 00	-95
00520	-1.650	9.360	0.64500000E 00	-95
00530	-1.730	10.160	0.45100000E 00	-96
00540	-1.880	10.650	0.31500000E 00	-95
00550	-1.910	10.810	0.22500000E 00	-95
00560	-0.950	1.650	1.61800000E 00	-95
00570	-1.880	3.250	2.28000000E 00	-95
00580	-2.750	4.750	1.86200000E 00	-95
00590	-3.530	6.110	1.30800000E 00	-95
00600	-4.210	7.280	0.88600000E 00	-95
00610	-4.750	8.240	0.60600000E 00	-95
00620	-5.160	8.940	0.42200000E 00	-95
00630	-5.410	9.440	0.29600000E 00	-95
00640	-5.490	9.510	0.21600000E 00	-95
00650	-1.230	1.460	1.35200000E 00	-96
00660	-2.410	2.880	1.71900000E 00	-95
00670	-3.530	4.210	1.36000000E 00	-95
00680	-4.540	5.410	0.92700000E 00	-95
00690	-5.410	6.440	0.57600000E 00	-95
00700	-6.110	7.280	0.42300000E 00	-95
00710	-6.630	7.900	0.28000000E 00	-95
00720	-6.950	8.280	0.19100000E 00	-95
00730	-7.060	8.410	0.14100000E 00	-95
00740	-1.790	0.650	0.37200000E 00	-96
00750	-3.530	1.280	0.74100000E 00	-95
00760	-5.160	1.880	0.60700000E 00	-95
00770	-6.630	2.410	0.44200000E 00	-95
00780	-7.900	2.880	0.30500000E 00	-95
00790	-8.940	3.250	0.20900000E 00	-95
00800	-9.700	3.530	0.14400000E 00	-95
00810	-10.160	3.700	0.09700000E 00	-95
00820	-10.320	3.760	0.06600000E 00	-95
00830	-1.910	0	-0.82800000E 00	85
00840	-3.760	0	-0.54100000E 00	85
00850	-5.490	0	-0.32700000E 00	84
00860	-7.060	0	-0.19700000E 00	84
00870	-8.410	0	-0.11100000E 00	84
00880	-9.510	0	-0.06300000E 00	83
00890	-10.320	0	-0.03700000E 00	83
00900	-10.810	0	-0.03100000E 00	83
00910	-10.980	0	-0.02300000E 00	82
00920	-1.790	-0.650	-1.86000000E 00	85
00930	-3.530	-1.280	-1.70300000E 00	85
00940	-5.160	-1.880	-1.20200000E 00	85
00950	-6.630	-2.410	-0.78100000E 00	85
00960	-7.900	-2.880	-0.51000000E 00	85
00970	-8.940	-3.250	-0.32700000E 00	85
00980	-9.700	-3.530	-0.23100000E 00	85
00990	-10.160	-3.700	-0.15300000E 00	84
01000	-10.320	-3.760	-0.12700000E 00	85
01010	-1.460	-1.230	-2.75000000E 00	85
01020	-2.880	-2.410	-3.02800000E 00	85
01030	-4.210	-3.530	-2.22700000E 00	85
01040	-5.410	-4.540	-1.58200000E 00	85
01050	-6.440	-5.410	-1.02310000E 00	85
01060	-7.280	-6.110	-0.68700000E 00	85
01070	-8.280	-6.950	-0.32000000E 00	85
01080	-8.410	-7.060	-0.23300000E 00	85
01090	-0.950	-1.650	-2.89000000E 00	85
01100	-1.880	-3.250	-3.58400000E 00	85

[illegible]	[illegible]	[illegible]	[illegible]	85
01120	-3.570	-6.110	-2.63[illegible]E 00	85
01130	-4.210	-7.290	-1.31[illegible]E 00	85
01140	-4.750	-8.240	-0.[illegible]E 00	85
01150	-5.160	-8.940	0.[illegible]E 00	85
01160	-5.410	-9.360	-0.41[illegible]E 00	85
01170	-5.490	-9.510	-0.28400000E 00	85
01180	-0.330	1.230	-2.66[illegible]E 00	85
01190	0.350	0.230	-2.63[illegible]E 00	85
01200	-0.950	-0.430	-3.68000000E 00	85
01210	-1.230	-0.950	-2.14000000E 00	85
01220	-1.460	-3.280	-1.42700000E 00	85
01230	-1.650	-9.360	-0.96200000E 00	85
01240	-1.790	-10.160	-0.56400000E 00	85
01250	-1.880	-10.650	-0.43300000E 00	85
01260	1.910	-10.810	-0.33200000E 00	85
01270	0.530	-1.630	-1.84000000E 00	85
01280	0.650	-3.700	-3.62300000E 00	85
01290	0.350	-5.410	-2.62700000E 00	85
01300	1.230	-6.950	-1.62700000E 00	85
01310	1.460	-8.280	-1.27900000E 00	85
01320	1.650	-9.360	-0.86400000E 00	85
01330	1.790	-10.160	-0.60000000E 00	85
01340	1.880	-10.650	-0.43300000E 00	85
01350	1.910	-10.810	-0.31000000E 00	85
01360	0.950	-1.650	-1.36200000E 00	85
01370	1.880	-3.250	-2.22800000E 00	85
01380	2.750	-4.750	-2.05300000E 00	85
01390	3.530	-6.110	-1.46000000E 00	85
01400	4.210	-7.280	-0.97300000E 00	85
01410	4.750	-8.240	-0.68700000E 00	85
01420	5.160	-8.940	-0.48900000E 00	85
01430	5.410	-9.360	-0.34600000E 00	85
01440	5.490	-9.510	-0.25800000E 00	85
01450	1.460	-1.230	-0.63900000E 00	86
01460	2.880	-2.410	-1.42700000E 00	85
01470	4.210	-3.530	-1.29800000E 00	85
01480	5.410	-4.540	-0.91900000E 00	85
01490	6.440	-5.410	-0.63300000E 00	85
01500	7.280	-6.110	-0.43300000E 00	85
01510	7.900	-6.630	-0.30600000E 00	85
01520	8.280	-6.950	-0.21900000E 00	85
01530	8.410	-7.060	-0.16700000E 00	85
01540	1.790	-6.[illegible]	0.29800000E 00	-98
01550	3.530	-1.[illegible]	-0.45200000E 00	85
01560	5.160	-1.[illegible]	-0.47500000E 00	85
01570	6.440	-2.410	-0.35500000E 00	85
01580	7.300	-2.800	-0.23900000E 00	85
01590	8.040	-3.250	-0.15700000E 00	84
01600	8.20[illegible]	-3.5[illegible]	-0.12000000E 00	84
[illegible]	10.[illegible]	-3.[illegible]	-0.03900000E 00	84
01620	10.[illegible]	-3.75[illegible]	-0.06600000E 00	84
[illegible]	[illegible]			

Experiment Data for Model #2

	X	Y	Flux Density Tesla XE-1	Phase, Degrees w.r.t. input
00010	0	0	-0.52760000E 00	120
00020	1.910	0	0.30460000E 00	-120
00030	3.760	0	0.59480000E 00	-105
00040	5.490	0	0.71360000E 00	-101
00050	7.060	0	0.82780000E 00	-99
00060	8.410	0	0.54860000E 00	-96
00070	9.510	0	0.43800000E 00	-97
00080	10.320	0	0.34860000E 00	-96
00090	10.810	0	0.27100000E 00	-94
00100	10.980	0	0.21260000E 00	-91
00110	1.790	0.650	1.10800000E 00	-106
00120	3.530	1.280	1.81000000E 00	-101
00130	5.160	1.880	1.74000000E 00	-99
00140	6.630	2.410	1.56400000E 00	-99
00150	7.900	2.880	1.25200000E 00	-98
00160	8.940	3.250	0.99000000E 00	-97
00170	9.700	3.530	0.86800000E 00	-97
00180	10.160	3.700	0.60600000E 00	-96
00190	10.320	3.760	0.48400000E 00	-94
00200	1.460	1.230	1.09800000E 00	-102
00210	2.880	2.410	2.54000000E 00	-101
00220	4.210	3.530	2.55800000E 00	-99
00230	5.410	4.540	2.13200000E 00	-99
00240	6.440	5.410	1.77500000E 00	-98
00250	7.280	6.110	1.39500000E 00	-98
00260	7.900	6.630	1.09100000E 00	-97
00270	8.280	6.950	0.85600000E 00	-96
00280	8.410	7.060	0.68400000E 00	-95
00290	0.350	1.650	1.63400000E 00	-106
00300	1.880	3.250	2.97500000E 00	-101
00310	2.750	4.750	3.04500000E 00	-100
00320	3.530	5.110	2.62700000E 00	-99
00330	4.270	7.280	2.08800000E 00	-98
00340	4.750	8.240	1.66200000E 00	-98
00350	5.160	8.940	1.29300000E 00	-97
00360	5.410	9.360	1.01400000E 00	-97
00370	5.490	9.510	0.81400000E 00	-96
00380	0.330	1.880	1.53600000E 00	-107
00390	0.650	3.700	3.02800000E 00	-102
00400	0.950	5.410	3.16700000E 00	-101
00410	1.250	6.950	2.78400000E 00	-100
00420	1.460	8.200	2.24500000E 00	-99
00430	1.650	9.360	1.74000000E 00	-99
00440	1.790	10.160	1.26500000E 00	-98

VITA

First Lieutenant Paul J. De Rego was born on 30 August 1959 in Honolulu, Hawaii. He is the fifth of eight children by Mr. and Mrs. Lawrence S. De Rego. He graduated from Damien Memorial High School, Honolulu, in 1977 and attended the University of Portland from which he received the Bachelor of Science in Electrical Engineering in May 1981. Upon graduation, he received a commission in the USAF through the ROTC program. He served on active duty as an instrumentation flight test engineer at Edwards AFB, California until entering the school of Engineering, Air Force Institude of Technology, in June 1983.

Permanent address: 119 Haokea Dr.
Kailua, Hawaii 96734

14. Kraus, John D. Electromagnetics. New York: McGraw Hill Book Company, 1953.

15. Cohen, Morrel H. Superconductivity in Science and Technology. Chicago and London: University of Chicago Press, 1968.

16. Nolte, John. The Human Brain, An Introduction to its Functional Anatomy. St. Louis: The C.V. Mosby Company, 1981.

17. Hubel, David H. "The Visual Cortex of the Brain," Scientific American, November: 54-62 (1963).

18. Kabrisky, Matthew. A Proposed Model for Visual Information Processing in the Human Brain. Urbana and London: University of Illinois Press, 1966.

19. S.H.E. Corporation. "Operating Instructions, Biomagnetic Probe," San Diego, Calif: 1980.

20. S.H.E. Corporation. "System 330X, Operating Manual," San Diego, Calif: 1980.

21. Kreyszig, Ervin. Advanced Engineering Mathematics. New York: John Wiley and Sons, 1979.

22. S.H.E. Corporation. "Biomagnetic Probe Test Report," San Diego, Calif: Job Number: 140680, January 16, 1984.

23. Maybeck, Peter S. Stochastic Models, Estimation, and Control. New York: Academic Press, 1982.

Bibliography

1. Spence, Alexander P. and Mason, Elliott B. Human Anatomy and Physiology. Menlo Park, Calif: The Benjamin/Cummings Publishing Company, 1979.

2. Guyton, Arthur C. Medical Physiology. Philadelphia: W. B. Saunders Company, 1981.

3. Kennedy, Donald. The Living Cell, Readings from Scientific American. San Francisco: W. H. Freeman and Company, 1965.

4. Kooi, Kenneth A. Fundamentals of Electroencephalography. New York: Harper and Row, 1971.

5. Hayt, William H. Jr. Engineering Electromagnetics. New York: McGraw-Hill Book Company, 1974.

6. Cohen, David. "Magnetoencephalography: Evidence of Magnetic Fields Produced by Alpha-Rhythm Currents," Science, 161: 784-786 (1968).

7. Williamson, Samuel J. et al. Biomagnetism: An Interdisciplinary Approach. New York: Plenum Press, 1982.

8. Ervin Frank R. "On Line Computer Techniques for Analysis of the Visual System," Symposium on the Analysis of Central Nervous System and Cardiovascular Data using Computer Methods, NASA SP-72: 35-51 (1965).

9. Kaufman, Lloyd et al. "On the Relation between Somatic Evoked Potentials and Fields,"International Journal of Neuroscience, 15, 223-229 (1981).

10. Sencaj, Randall W. and Aunon, Jorge I. "Dipole Localization of Average and Single Visual Evoked Potentials," IEEE Transactions on Biomedical Engineering, BME-29: 26-33 (1982).

11. Grynszpan, Flavio. "Relationship Between the Surface Electromagnetic Fields and the Electrical Activity of the Heart," Ph.D. Dissertation, University of Pennsylvania, 1971.

12. Cohen, David and Cuffin, Neil. "Magnetic Fields of a Dipole in Special Volume Conductor Shapes," IEEE Transactions on Biomedical Engineering, 24: 372-381 (1977).

13. Sampson, R. J. Surface II Graphics System. Lawrence, Kansas: Kansas Geological Survey, 1978.

```
01110    -1.880   -3.250      -5.70700000E 00      84
01120    -2.750   -4.750      -6.36300000E 00      85
01130    -3.530   -6.110      -6.22900000E 00      85
01140    -4.210   -7.280      -5.62000000E 00      84
01150    -4.750   -8.240      -3.51500000E 00      84
01160    -5.160   -8.930      -2.14000000E 00      85
01170    -5.410   -9.360      -1.45000000E 00      84
01180    -5.490   -9.510      -1.03400000E 00      84
01190    -0.330   -1.880      -2.19200000E 00      80
01200    -0.650   -3.700      -4.26300000E 00      82
01210    -0.950   -5.410      -6.07300000E 00      83
01220    -1.230   -6.950      -6.14200000E 00      83
01230    -1.460   -8.280      -4.87200000E 00      83
01240    -1.650   -9.360      -3.13200000E 00      83
01250    -1.790  -10.160      -2.00100000E 00      83
01260    -1.880  -10.650      -1.29600000E 00      83
01270    -1.910  -10.810      -0.96000000E 00      83
01280     0.330   -1.880      -1.89700000E 00      77
01290     0.650   -3.700      -2.48800000E 00      77
01300     0.950   -5.410      -2.55800000E 00      77
01310     1.230   -6.950      -2.80100000E 00      78
01320     1.460   -8.280      -2.21000000E 00      79

01330     1.650   -9.360      -1.63200000E 00      79
01340     1.790  -10.160      -1.18700000E 00      80
01350     1.880  -10.650      -0.90100000E 00      81
01360     1.910  -10.810      -0.69300000E 00      81
01370     0.950   -1.650      -1.48200000E 00      73
01380     1.880   -3.250      -2.27900000E 00      74
01390     2.750   -4.750      -1.61800000E 00      70
01400     3.530   -6.110      -1.21800000E 00      69
01410     4.210   -7.280      -0.98800000E 00      72
01420     4.750   -8.240      -0.90800000E 00      72
01430     5.160   -8.940      -0.77100000E 00      77
01440     5.410   -9.360      -0.61100000E 00      78
01450     5.490   -9.510      -0.49800000E 00      79
01460     1.460   -1.230      -0.98800000E 00      69
01470     2.880   -2.410      -3.11500000E 00      77
01480     4.210   -3.530      -3.70600000E 00      79
01490     5.410   -4.540      -2.94100000E 00      79
01500     6.440   -5.410      -1.93100000E 00      79
01510     7.280   -6.110      -1.19200000E 00      78
01520     7.900   -6.630      -0.74800000E 00      78
01530     8.280   -6.950      -0.49900000E 00      78
01540     8.410   -7.060      -0.35700000E 00      77

01550     1.790   -0.650       0.21600000E 00      -7
01560     3.530   -1.280      -2.50600000E 00      78
01570     5.160   -1.880      -4.62800000E 00      81
01580     6.630   -2.410      -4.05400000E 00      82
01590     7.900   -2.880      -2.33200000E 00      82
01600     8.940   -3.250      -1.21300000E 00      81
01610     9.700   -3.530      -0.57400000E 00      80
01620    10.160   -3.700      -0.27500000E 00      77
01630    10.320   -3.760      -0.12400000E 00      74
END OF DATA
```

00450	1.880	10.650	1.11500000E 00	-97
00460	1.910	10.810	0.83900000E 00	-97
00470	-0.330	1.880	1.94900000E 00	-97
00480	-0.650	3.700	3.89800000E 00	-98
00490	-0.950	5.410	3.93200000E 00	-98
00500	-1.230	6.950	3.18400000E 00	-98
00510	-1.460	8.280	2.31400000E 00	-98
00520	-1.650	9.360	1.67600000E 00	-98
00530	-1.790	10.150	1.19200000E 00	-98
00540	-1.880	10.650	0.86800000E 00	-98
00550	-1.910	10.810	0.57000000E 00	-98
00560	-0.950	1.650	1.27500000E 00	-98
00570	-1.880	3.250	2.54000000E 00	-100
00580	-2.750	4.750	2.54000000E 00	-100
00590	-3.530	6.110	2.00100000E 00	-100
00600	-4.210	7.280	1.48900000E 00	-100
00610	-4.750	8.240	1.09100000E 00	-100
00620	-5.160	8.940	0.76600000E 00	-100
00630	-5.410	9.440	0.56300000E 00	-100
00640	-5.490	9.510	0.43200000E 00	-100
00650	-1.230	1.460	0.46100000E 00	-106
00660	-2.410	2.880	0.88400000E 00	-106
00670	-3.530	4.210	1.23700000E 00	-106
00680	-4.540	5.410	0.98800000E 00	-106
00690	-5.410	6.440	0.70600000E 00	-106
00700	-6.110	7.280	0.51900000E 00	-106
00710	-6.630	7.900	0.36700000E 00	-106
00720	-6.950	8.280	0.26100000E 00	-106
00730	-7.060	8.410	0.19100000E 00	-106
00740	-1.790	0.650	-0.47900000E 00	93
00750	-3.530	1.280	-0.27800000E 00	137
00760	-5.160	1.880	-0.23500000E 00	167
00770	-6.630	2.410	-0.18600000E 00	174
00780	-7.900	2.880	-0.13900000E 00	168
00790	-8.940	3.250	-0.10300000E 00	154
00800	-9.700	3.530	-0.08200000E 00	141
00810	-10.160	3.700	-0.06800000E 00	130
00820	-10.320	3.760	-0.06300000E 00	121
00830	-1.910	0	-1.45300000E 00	87
00840	-3.760	0	-1.82700000E 00	91
00850	-5.490	0	-1.67700000E 00	93
00860	-7.060	0	-1.29800000E 00	93
00870	-8.410	0	-0.96700000E 00	93
00880	-9.510	0	-0.72200000E 00	92
00890	-10.320	0	-0.54500000E 00	92
00900	-10.810	0	-0.41400000E 00	91
00910	-10.980	0	-0.32700000E 00	91
00920	-1.790	-0.650	-2.21000000E 00	85
00930	-3.530	-1.280	-3.79305000E 00	87
00940	-5.160	-1.880	-3.93200000E 00	88
00950	-6.630	-2.410	-3.13200000E 00	88
00960	-7.900	-2.880	-2.22700000E 00	88
00970	-8.940	-3.250	-1.62900000E 00	87
00980	-9.700	-3.530	-1.14500000E 00	87
00990	-10.160	-3.700	-0.84000000E 00	87
01000	-10.320	-3.760	-0.64600000E 00	87
01010	-1.460	-1.230	-2.80100000E 00	84
01020	-2.880	-2.410	-5.65500000E 00	86
01030	-4.210	-3.530	-6.10700000E 00	86
01040	-5.410	-4.540	-5.65500000E 00	86
01050	-6.440	-5.410	-4.07200000E 00	86
01060	-7.280	-6.110	-2.64500000E 00	86
01070	-7.900	-6.630	-1.77500000E 00	86
01080	-8.280	-6.950	-1.21800000E 00	86
01090	-8.410	-7.060	-0.91400000E 00	86
01100	-0.950	-1.650	-2.61000000E 00	82

Experiment Data for Model #5

	X	Z	Flux Density Tesla *E-11	Phase, Degrees w.r.t. Input
00010	0	0	-0.[illegible]E 00	38
00020	1.910	0	0.2210000E 00	-65
00030	3.760	0	-0.[illegible]E 00	69
00040	5.490	0	-1.[illegible]E 00	79
00050	7.060	0	-1.3870000E 00	81
00060	8.410	0	-0.6000000E 00	80
00070	9.510	0	-0.0750000E 00	68
00080	10.320	0	0.1480000E 00	-87
00090	10.810	0	0.[illegible]E 00	-81
00100	10.980	0	0.1880000E 00	-92
00110	1.790	0.652	1.1940000E 00	-91
00120	3.530	1.280	2.5930000E 00	-94
00130	5.160	1.880	3.7060000E 00	-96
00140	6.630	2.410	3.5150000E 00	-96
00150	7.900	2.880	2.5750000E 00	-96
00160	8.940	3.250	1.7400000E 00	-96
00170	9.700	3.530	1.1450000E 00	-96
00180	10.160	3.700	0.7760000E 00	-96
00190	10.320	3.760	0.5500000E 00	-96
00200	1.460	1.230	2.0880000E 00	-94
00210	2.880	2.410	5.2900000E 00	-96
00220	4.210	3.530	6.1940000E 00	-97
00230	5.410	4.540	5.4980000E 00	-96
00240	6.440	5.410	4.5590000E 00	-96
00250	7.280	6.110	2.9750000E 00	-97
00260	7.900	6.630	1.8440000E 00	-96
00270	8.280	6.950	1.2270000E 00	-96
00280	8.410	7.060	0.8490000E 00	-96
00290	0.950	1.650	2.4710000E 00	-95
00300	1.880	3.250	5.6720000E 00	-97
00310	2.750	4.750	6.1940000E 00	-97
00320	3.530	6.110	5.8640000E 00	-97
00330	4.210	7.280	4.3850000E 00	-97
00340	4.750	8.240	2.9410000E 00	-97
00350	5.160	8.940	1.8970000E 00	-97
00360	5.410	9.360	1.3170000E 00	-97
00370	5.490	9.510	0.9290000E 00	-97
00380	0.330	1.880	2.3320000E 00	-96
00390	0.650	3.700	5.1160000E 00	-97
00400	0.950	5.410	5.5510000E 00	-97
00410	1.230	6.950	4.6280000E 00	-97
00420	1.460	8.280	2.5230000E 00	-97
00430	1.650	9.360	2.3140000E 00	-97
00440	1.790	10.160	1.6220000E 00	-97

```
01110   -1.880   -3.250      -2.29700000E 00      100
01120   -2.750   -4.750      -1.28100000E 00      107
01130   -3.530   -6.110      -0.70500000E 00      111
01140   -4.210   -7.280      -0.40900000E 00      113
01150   -4.750   -8.240      -0.25900000E 00      110
01160   -5.160   -8.930      -0.17700000E 00      106
01170   -5.410   -9.360      -0.12700000E 00      101
01180   -5.490   -9.510      -0.09200000E 00       99
01190   -0.330   -1.880      -3.67100000E 00       92
01200   -0.650   -3.700      -2.78400000E 00       95
01210   -0.950   -5.410      -1.86200000E 00       97
01220   -1.230   -6.950      -1.22100000E 00       97
01230   -1.460   -8.280      -0.86100000E 00       95
01240   -1.650   -9.360      -0.65100000E 00       93
01250   -1.790  -10.160      -0.52200000E 00       90
01260   -1.880  -10.650      -0.44200000E 00       88
01270   -1.910  -10.810      -0.38800000E 00       85
01280    0.330   -1.880      -3.84500000E 00       91
01290    0.650   -3.700      -3.18400000E 00       92
01300    0.950   -5.410      -2.29700000E 00       92
01310    1.230   -6.950      -1.66200000E 00       92
01320    1.460   -8.280      -1.25500000E 00       90

01330    1.650   -9.360      -1.00900000E 00       88
01340    1.790  -10.160      -0.83700000E 00       86
01350    1.880  -10.650      -0.71900000E 00       85
01360    1.910  -10.810      -0.63700000E 00       83
01370    0.950   -1.650      -3.93200000E 00       90
01380    1.880   -3.250      -3.32300000E 00       90
01390    2.750   -4.750      -2.59300000E 00       89
01400    3.530   -6.110      -1.98400000E 00       88
01410    4.210   -7.280      -1.55400000E 00       87
01420    4.750   -8.240      -1.27200000E 00       86
01430    5.160   -8.940      -1.04600000E 00       85
01440    5.410   -9.360      -0.89300000E 00       83
01450    5.490   -9.510      -0.78300000E 00       82
01460    1.460   -1.230      -3.95000000E 00       89
01470    2.880   -2.410      -3.49700000E 00       88
01480    4.210   -3.530      -2.80100000E 00       88
01490    5.410   -4.540      -2.19200000E 00       87
01500    6.440   -5.410      -1.75700000E 00       86
01510    7.280   -6.110      -1.42000000E 00       85
01520    7.900   -6.630      -1.18300000E 00       84
01530    8.280   -6.950      -1.00100000E 00       84
01540    8.410   -7.060      -0.86800000E 00       83

01550    1.790   -0.650      -3.84500000E 00       88
01560    3.530   -1.280      -3.46300000E 00       87
01570    5.160   -1.880      -2.83600000E 00       86
01580    6.630   -2.410      -2.27900000E 00       85
01590    7.900   -2.880      -1.82100000E 00       85
01600    8.940   -3.250      -1.47700000E 00       84
01610    9.700   -3.530      -1.20600000E 00       84
01620   10.160   -3.700      -1.02700000E 00       83
01630   10.320   -3.760      -0.87900000E 00       82
END OF DATA
```

00450	1.330	10.650	-0.2[illegible]000000E 00	61
00460	1.910	10.810	-0.[illegible]4500[illegible]E 00	63
00470	-0.330	1.380	-1.8972[illegible]0000E 00	86
00480	-0.650	3.700	-0.[illegible]5910[illegible]E 00	33
00490	-0.950	5.410	0.53900000E 00	-61
00500	-1.230	6.950	0.64900000E 00	-70
00510	-1.460	8.280	0.29100000E 00	-72
00520	-1.650	9.360	0.37200000E 00	-71
00530	-1.790	10.160	0.25100000E 00	-68
00540	-1.880	10.650	0.17100000E 00	-62
00550	-1.910	10.810	0.10800000E 00	-47
00560	-0.950	1.650	-1.79200000E 00	87
00570	-1.880	3.250	0.43000000E 00	-56
00580	-2.750	4.750	1.30000000E 00	-78
00590	-3.530	6.110	1.36600000E 00	-81
00600	-4.210	7.280	1.14000000E 00	-83
00610	-4.750	8.240	0.88000000E 00	-85
00620	-5.160	8.940	0.68200000E 00	-85
00630	-5.410	9.440	0.50800000E 00	-85
00640	-5.490	9.510	0.37200000E 00	-84
00650	-1.230	1.460	-1.81000000E 00	90
00660	-2.410	2.880	0.42600000E 00	-68
00670	-3.530	4.210	1.43700000E 00	-80
00680	-4.540	5.410	1.61500000E 00	-82
00690	-5.410	6.440	1.42200000E 00	-85
00700	-6.110	7.280	1.21800000E 00	-87
00710	-6.630	7.900	0.98800000E 00	-89
00720	-6.950	8.280	0.79200000E 00	-90
00730	-7.060	8.410	0.62600000E 00	-90
00740	-1.790	0.650	-2.21000000E 00	92
00750	-3.530	1.280	-0.04900000E 00	98
00760	-5.160	1.880	0.97100000E 00	-80
00770	-6.630	2.410	1.24900000E 00	-82
00780	-7.900	2.880	1.29100000E 00	-84
00790	-8.940	3.250	1.20100000E 00	-88
00800	-9.700	3.530	1.05800000E 00	-90
00810	-10.160	3.700	0.88900000E 00	-92
00820	-10.320	3.760	0.76200000E 00	-93
00830	-1.910	0	-2.50600000E 00	94
00840	-3.760	0	-0.64000000E 00	113
00850	-5.490	0	0.44400000E 00	-104
00860	-7.060	0	0.77800000E 00	-87
00870	-8.410	0	0.91000000E 00	-88
00880	-9.510	0	0.95200000E 00	-90
00890	-10.320	0	0.85400000E 00	-92
00900	-10.810	0	0.82100000E 00	-94
00910	-10.980	0	0.74800000E 00	-96
00920	-1.790	-0.650	-2.74900000E 00	95
00930	-3.530	-1.280	-1.17800000E 00	112
00940	-5.160	-1.880	0.38500000E 00	-171
00950	-6.630	-2.410	0.55000000E 00	-113
00960	-7.900	-2.880	0.61600000E 00	-100
00970	-8.940	-3.250	0.64700000E 00	-97
00980	-9.700	-3.530	0.64400000E 00	-97
00990	-10.160	-3.700	0.54500000E 00	-97
01000	-10.32[illegible]	-3.760	0.58300000E 00	-99
01010	-1.460	-1.230	-3.16700000E 00	95
01020	-2.880	-2.410	-1.71600000E 00	108
01030	-4.210	-3.530	-0.61900000E 00	132
01040	-5.410	-4.540	0.30500000E 00	-179
01050	-6.440	-5.410	0.24900000E 00	-139
01060	-7.280	-6.110	0.25100000E 00	-118
01070	-7.900	-6.630	0.24700000E 00	-109
01080	-8.280	-6.950	0.27000000E 00	-106
01090	-8.410	-7.060	0.26300000E 00	-104
01100	-6.950	-1.650	-3.39300000E 00	94

Experiment Data for Model #4

	X	Y	[illegible]	[illegible] Degrees Input
00010	0	0	[illegible]	80
00020	1.910	0	[illegible]	83
00030	3.760	0	-2.87[illegible]00E 00	83
00040	5.490	0	-2.54000000E 00	83
00050	7.060	0	-2.14000000E 00	83
00060	8.410	0	-1.77500000E 00	83
00070	9.510	0	-1.46000000E 00	83
00080	10.320	0	-1.21300000E 00	83
00090	10.810	0	-1.00400000E 00	83
00100	10.980	0	-0.84900000E 00	84
00110	1.790	0.652	-2.63000000E 00	82
00120	3.530	1.280	-2.59300000E 00	82
00130	5.160	1.880	-2.29700000E 00	82
00140	6.630	2.410	-1.93100000E 00	82
00150	7.900	2.880	-1.59000000E 00	82
00160	8.940	3.250	-1.30700000E 00	82
00170	9.700	3.530	-1.08600000E 00	82
00180	10.160	3.700	-0.90300000E 00	83
00190	10.320	3.760	-0.75500000E 00	83
00200	1.460	1.230	-2.38400000E 00	80
00210	2.880	2.410	-2.14000000E 00	80
00220	4.210	3.530	-1.84400000E 00	80
00230	5.410	4.540	-1.55900000E 00	80
00240	6.440	5.410	-1.29500000E 00	81
00250	7.280	6.110	-1.07400000E 00	81
00260	7.900	6.630	-0.88600000E 00	82
00270	8.280	6.950	-0.69900000E 00	83
00280	8.410	7.060	-0.61100000E 00	83
00290	0.950	1.650	-2.08800000E 00	79
00300	1.880	3.250	-1.49100000E 00	78
00310	2.750	4.750	-1.26500000E 00	78
00320	3.530	6.110	-1.06800000E 00	78
00330	4.210	7.280	-0.89400000E 00	79
00340	4.750	8.240	-0.74300000E 00	80
00350	5.160	8.940	-0.61600000E 00	81
00360	5.410	9.360	-0.51300000E 00	83
00370	5.490	9.510	-0.43200000E 00	85
00380	0.330	1.880	-2.07100000E 00	87
00390	0.650	3.700	-1.01100000E 00	72
00400	0.950	5.410	-0.49200000E 00	50
00410	1.230	6.950	-0.39700000E 00	50
00420	1.460	8.280	-0.33600000E 00	52
00430	1.650	9.360	-0.29600000E 00	56
00440	1.790	10.160	-0.27000000E 00	59

```
01120    -2.750   -4.750      -0.51000000E 00       81
01130    -3.530   -6.110      -0.14400000E 00       76
01140    -4.210   -7.280      -0.01400000E 00       49
01150    -4.750   -8.240       0.00760000E 00      -20
01160    -5.160   -8.930       0.02600000E 00      -87
01170    -5.410   -9.360       0.04960000E 00      -92
01180    -5.490   -9.510       0.08700000E 00      -92
01190    -0.330   -1.880      -3.14900000E 00       85
01200    -0.650   -3.700      -2.47100000E 00       85
01210    -0.950   -5.410      -1.65300000E 00       84
01220    -1.230   -6.950      -1.10100000E 00       85
01230    -1.460   -8.280      -0.79300000E 00       85
01240    -1.650   -9.360      -0.60400000E 00       85
01250    -1.790  -10.160      -0.46500000E 00       85
01260    -1.880  -10.650      -0.34600000E 00       86
01270    -1.910  -10.810      -0.26300000E 00       85
01280     0.330   -1.880      -3.81100000E 00       85
01290     0.650   -3.700      -3.28900000E 00       85
01300     0.950   -5.410      -2.48800000E 00       85
01310     1.230   -6.950      -2.47100000E 00       85
01320     1.460   -8.280      -1.35000000E 00       85
01330     1.650   -9.360      -1.04100000E 00       85

01340     1.790  -10.160      -0.84200000E 00       86
01350     1.880  -10.650      -0.65900000E 00       86
01360     1.910  -10.810      -0.53100000E 00       86
01370     0.950   -1.650      -4.22800000E 00       85
01380     1.880   -3.250      -3.70600000E 00       85
01390     2.750   -4.750      -2.90600000E 00       85
01400     3.530   -6.110      -2.21200000E 00       85
01410     4.210   -7.280      -1.70700000E 00       85
01420     4.750   -8.240      -1.34700000E 00       86
01430     5.160   -8.940      -1.06300000E 00       86
01440     5.410   -9.360      -0.84400000E 00       86
01450     5.490   -9.510      -0.69900000E 00       86
01460     1.460   -1.230      -4.35000000E 00       85
01470     2.880   -2.410      -3.65400000E 00       86
01480     4.210   -3.530      -3.08000000E 00       85
01490     5.410   -4.540      -2.34900000E 00       85
01500     6.440   -5.410      -1.81000000E 00       85
01510     7.280   -6.110      -1.44100000E 00       85
01520     7.900   -6.630      -1.13800000E 00       86
01530     8.280   -6.950      -0.95200000E 00       86
01540     8.410   -7.060      -0.78300000E 00       86
01550     1.790   -0.650      -4.22800000E 00       85

01560     3.530   -1.280      -3.63700000E 00       85
01570     5.160   -1.880      -2.94100000E 00       85
01580     6.630   -2.410      -2.27900000E 00       85
01590     7.900   -2.880      -1.75700000E 00       85
01600     8.940   -3.250      -1.38700000E 00       85
01610     9.700   -3.530      -1.11700000E 00       86
01620    10.160   -3.700      -0.91200000E 00       86
01630    10.320   -3.760      -1.58700000E 00       86
END OF DATA
```

00460	1.910	10.810	-0.07300000E 00	93
00470	-0.330	1.880	-1.61300000E 00	85
00480	-0.650	3.700	-0.45600000E 00	89
00490	-0.950	5.410	0.12200000E 00	-108
00500	-1.230	6.950	0.32400000E 00	-98
00510	-1.460	8.280	0.35000000E 00	-98
00520	-1.650	9.360	0.32000000E 00	-98
00530	-1.790	10.160	0.26600000E 00	-98
00540	-1.880	10.650	0.19700000E 00	-99
00550	-1.910	10.810	0.12500000E 00	-101
00560	-0.950	1.650	-1.60000000E 00	85
00570	-1.880	3.250	-0.23500000E 00	92
00580	-2.750	4.750	0.46100000E 00	-99
00590	-3.530	6.110	0.70800000E 00	-97
00600	-4.210	7.280	0.72400000E 00	-97
00610	-4.750	8.240	0.65400000E 00	-96
00620	-5.160	8.940	0.54300000E 00	-96
00630	-5.410	6.440	0.43300000E 00	-96
00640	-5.490	9.510	0.17900000E 00	-97
00650	-1.230	1.460	-1.54700000E 00	85
00660	-2.410	2.880	-0.14400000E 00	94
00670	-3.530	4.210	0.60400000E 00	-98
00680	-4.540	5.410	0.89100000E 00	-97
00690	-5.410	6.440	0.93800000E 00	-97
00700	-6.110	7.280	0.87500000E 00	-96
00710	-6.630	7.900	0.74600000E 00	-96
00720	-6.950	8.280	0.62100000E 00	-96
00730	-7.060	8.410	0.48500000E 00	-96
00740	-1.790	0.650	-1.61500000E 00	84
00750	-3.530	1.280	-0.19100000E 00	83
00760	-5.160	1.880	0.56600000E 00	-96
00770	-6.630	2.410	0.89400000E 00	-96
00780	-7.900	2.880	1.00200000E 00	-96
00790	-8.940	3.250	0.94300000E 00	-95
00800	-9.700	3.530	0.84600000E 00	-95
00810	-10.160	3.700	0.70300000E 00	-95
00820	-10.320	3.760	0.58100000E 00	-95
00830	-1.910	0	-1.75700000E 00	-84
00840	-3.760	0	-0.36000000E 00	-82
00850	-5.490	0	0.51900000E 00	-94
00860	-7.060	0	0.93400000E 00	-94
00870	-8.410	0	1.04100000E 00	-95
00880	-9.510	0	0.93800000E 00	-94
00890	-10.320	0	0.86300000E 00	-95
00900	-10.810	0	0.72700000E 00	-94
00910	-10.980	0	0.63000000E 00	-94
00920	-1.790	-0.650	-1.98400000E 00	84
00930	-3.530	-1.280	-0.64200000E 00	81
00940	-5.160	-1.880	0.42100000E 00	-87
00950	-6.630	-2.410	0.90800000E 00	-92
00960	-7.900	-2.880	0.97100000E 00	-93
00970	-8.940	-3.250	0.81600000E 00	-93
00980	-9.700	-3.530	0.73800000E 00	-94
00990	-10.160	-3.700	0.62100000E 00	-94
01000	-10.320	-3.760	0.55000000E 00	-94
01010	-1.460	-1.230	-1.42200000E 00	84
01020	-2.880	-2.410	-0.13100000E 00	69
01030	-4.210	-3.530	0.63900000E 00	-92
01040	-5.410	-4.540	0.82800000E 00	-93
01050	-6.440	-5.410	0.74300000E 00	-94
01060	-7.280	-6.110	0.61200000E 00	-94
01070	-7.900	-6.630	0.47700000E 00	-94
01080	-8.280	-6.950	0.40900000E 00	-93
01090	-8.410	-7.060	0.41800000E 00	-93
01100	-0.950	-1.650	-2.29700000E 00	84
01110	-1.830	-3.250	-1.30500000E 00	83

Experiment Data for Model #3

	X	Y	Flux Density Tesla XEE-11	Phase, Degrees w.r.t. input
[illegible]	0	0	-2.71400000E 00	82
[illegible]	1.910	0	-3.25400000E 00	84
[illegible]	3.760	0	-3.08000000E 00	84
[illegible]	5.430	0	-2.57500000E 00	84
[illegible]	7.060	0	-2.03600000E 00	85
[illegible]	8.410	0	-1.61000000E 00	85
[illegible]	9.510	0	-1.28200000E 00	85
[illegible]	10.320	0	-1.00100000E 00	85
[illegible]	10.380	0	-0.66300000E 00	86
00110	1.790	0.652	-2.85400000E 00	84
00120	3.530	1.280	-2.50600000E 00	85
00130	5.160	1.880	-2.03600000E 00	85
00140	6.630	2.410	-1.59000000E 00	85
00150	7.900	2.880	-1.24400000E 00	85
00160	8.940	3.250	-0.99900000E 00	85
00170	9.700	3.530	-0.78600000E 00	86
00180	10.160	3.700	-0.63300000E 00	86
00190	10.320	3.760	-0.53800000E 00	87
00200	1.460	1.230	-2.48800000E 00	85
00210	2.880	2.410	-1.91400000E 00	85
00220	4.210	3.530	-1.47900000E 00	86
00230	5.410	4.540	-1.15400000E 00	86
00240	6.440	5.410	-0.88700000E 00	86
00250	7.280	6.110	-0.70300000E 00	86
00260	7.900	6.630	-0.55300000E 00	86
00270	8.280	6.950	-0.45600000E 00	86
00280	8.410	7.060	-0.39300000E 00	87
00290	0.950	1.650	-2.26200000E 00	85
00300	1.880	3.250	-1.47700000E 00	86
00310	2.750	4.750	-1.02000000E 00	86
00320	3.530	6.110	-0.66600000E 00	86
00330	4.210	7.280	-0.56600000E 00	86
00340	4.750	8.240	-0.43300000E 00	86
00350	5.160	8.940	-0.34600000E 00	86
00360	5.410	9.360	-0.29100000E 00	87
00370	5.490	9.510	-0.26400000E 00	87
00380	0.330	1.880	-1.93100000E 00	85
00390	0.650	3.700	-0.96200000E 00	86
00400	0.950	5.410	-0.43500000E 00	87
00410	1.230	6.950	-0.21200000E 00	89
00420	1.460	8.280	-0.10600000E 00	90
00430	1.650	9.360	-0.06300000E 00	93
00440	1.790	10.160	-0.04700000E 00	97
00450	1.880	10.650	-0.05400000E 00	95

01110	-1.380	-3.250	-4.71500000E 00	83
01120	-2.750	-4.750	-4.69800000E 00	83
01130	-3.530	-6.110	-3.98500000E 00	83
01140	-4.210	-7.280	-3.20200000E 00	83
01150	-4.750	-8.240	-2.48800000E 00	83
01160	-5.160	-8.930	-1.89700000E 00	83
01170	-5.410	-9.360	-1.52800000E 00	84
01180	-5.490	-9.510	-1.24200000E 00	84
01190	-0.330	-1.880	-2.95800000E 00	84
01200	-0.650	-3.700	-4.59400000E 00	83
01210	-0.950	-5.410	-4.71400000E 00	83
01220	-1.230	-6.950	-4.07200000E 00	83
01230	-1.460	-8.280	-3.23600000E 00	83
01240	-1.650	-9.360	-2.52300000E 00	83
01250	-1.790	-10.160	-1.93100000E 00	84
01260	-1.880	-10.650	-1.50700000E 00	84
01270	-1.910	-10.810	-1.23200000E 00	84
01280	0.330	-1.880	-2.54000000E 00	85
01290	0.650	-3.700	-3.82800000E 00	84
01300	0.950	-5.410	-4.00200000E 00	84
01310	1.230	-6.950	-3.39300000E 00	84
01320	1.460	-8.280	-2.76700000E 00	84
01330	1.650	-9.360	-2.10500000E 00	84
01340	1.790	-10.160	-1.65000000E 00	84
01350	1.880	-10.650	-1.28600000E 00	84
01360	1.910	-10.810	-1.04700000E 00	84
01370	0.950	-1.650	-1.91400000E 00	85
01380	1.880	-3.250	-2.94100000E 00	84
01390	2.750	-4.750	-2.85400000E 00	84
01400	3.530	-6.110	-2.52300000E 00	84
01410	4.210	-7.280	-2.01800000E 00	84
01420	4.750	-8.240	-1.57600000E 00	84
01430	5.160	-8.940	-1.21300000E 00	84
01440	5.410	-9.360	-0.94800000E 00	84
01450	5.490	-9.510	-0.76600000E 00	84
01460	1.460	-1.230	-1.13500000E 00	88
01470	2.880	-2.410	-1.68600000E 00	85
01480	4.210	-3.530	-1.64300000E 00	84
01490	5.410	-4.540	-1.37600000E 00	84
01500	6.440	-5.410	-1.08600000E 00	84
01510	7.280	-6.110	-0.84900000E 00	84
01520	7.900	-6.630	-0.64900000E 00	84
01530	8.280	-6.950	-0.51900000E 00	84
01540	8.410	-7.060	-0.41400000E 00	84
01550	1.790	-0.650	-0.35300000E 00	99
01560	3.530	-1.280	-0.43000000E 00	91
01570	5.160	-1.880	-0.39300000E 00	88
01580	6.630	-2.410	-0.30600000E 00	87
01590	7.900	-2.880	-0.02300000E 00	86
01600	8.940	-3.250	-0.16900000E 00	85
01610	9.700	-3.530	-0.12200000E 00	83
01620	10.160	-3.700	-0.08900000E 00	81
01630	10.320	-3.760	-0.07000000E 00	80

END OF DATA

00450	1.330	10.650	1.06300000E 00	-97
00460	1.910	10.810	0.84700000E 00	-96
00470	-0.330	1.880	1.35400000E 00	-110
00480	-0.650	3.700	2.76700000E 00	-104
00490	-0.950	5.410	2.35300000E 00	-102
00500	-1.230	6.950	2.55800000E 00	-101
00510	-1.460	8.280	2.07100000E 00	-100
00520	-1.650	9.360	1.60800000E 00	-99
00530	-1.790	10.160	1.25100000E 00	-99
00540	-1.880	10.650	0.95700000E 00	-98
00550	-1.910	10.810	0.76900000E 00	-97
00560	-0.950	1.650	1.65800000E 00	-122
00570	-1.880	3.250	1.31000000E 00	-108
00580	-2.750	4.750	2.12300000E 00	-106
00590	-3.530	6.110	1.93100000E 00	-104
00600	-4.210	7.280	1.54900000E 00	-103
00610	-4.750	8.240	1.22700000E 00	-102
00620	-5.160	8.940	0.94000000E 00	-100
00630	-5.410	6.440	0.69900000E 00	-39
00640	-5.490	9.510	0.42500000E 00	-97
00650	-1.230	1.460	0.33800000E 00	-128
00660	-2.410	2.880	0.79700000E 00	-122
00670	-3.530	4.210	1.02500000E 00	-117
00680	-4.540	5.410	0.94500000E 00	-113
00690	-5.410	6.440	0.77100000E 00	-109
00700	-6.110	7.280	0.59700000E 00	-106
00710	-6.630	7.900	0.43000000E 00	-103
00720	-6.950	8.280	0.33200000E 00	-101
00730	-7.060	8.410	0.24500000E 00	-98
00740	-1.790	0.650	-1.20800000E 00	91
00750	-3.530	1.280	-0.80900000E 00	99
00760	-5.160	1.880	-0.52200000E 00	104
00770	-6.630	2.410	-0.34600000E 00	105
00780	-7.900	2.880	-0.22600000E 00	101
00790	-8.940	3.250	-0.16000000E 00	95
00800	-9.700	3.530	-0.13100000E 00	89
00810	-10.160	3.700	-0.11500000E 00	84
00820	-10.320	3.760	-0.11000000E 00	80
00830	-1.910	0	-2.24500000E 00	86
00840	-3.760	0	-2.34900000E 00	84
00850	-5.490	0	-2.01800000E 00	82
00860	-7.060	0	-1.52600000E 00	81
00870	-8.410	0	-1.13400000E 00	80
00880	-9.510	0	-0.90800000E 00	81
00890	-10.320	0	-0.71300000E 00	81
00900	-10.810	0	-0.57900000E 00	82
00910	-10.980	0	-0.48000000E 00	82
00920	-1.790	-0.650	-2.90600000E 00	85
00930	-3.530	-1.280	-3.08000000E 00	85
00940	-5.160	-1.880	-2.52300000E 00	85
00950	-6.630	-2.410	-1.96600000E 00	85
00960	-7.900	-2.880	-1.57300000E 00	84
00970	-8.940	-3.250	-1.32900000E 00	84
00980	-9.700	-3.530	-1.13300000E 00	84
00990	-10.160	-3.700	-0.95200000E 00	84
01000	-10.320	-3.760	-0.82000000E 00	84
01010	-1.460	-1.230	-3.20200000E 00	84
01020	-2.880	-2.410	-4.17600000E 00	84
01030	-4.210	-3.530	-3.93200000E 00	83
01040	-5.410	-4.540	-3.16700000E 00	83
01050	-6.440	-5.410	-2.61000000E 00	83
01060	-7.280	-6.110	-2.07100000E 00	83
01070	-7.900	-6.630	-1.65300000E 00	83
01080	-8.280	-6.950	-1.34200000E 00	84
01090	-8.410	-7.060	-1.08600000E 00	84
01100	-6.950	-1.650	-3.11500000E 00	84

UNCLASSIFIED

SECURITY CLASSIFICATION OF THIS PAGE

REPORT DOCUMENTATION PAGE

1a. REPORT SECURITY CLASSIFICATION UNCLASSIFIED	1b. RESTRICTIVE MARKINGS
2a. SECURITY CLASSIFICATION AUTHORITY	3. DISTRIBUTION/AVAILABILITY OF REPORT Approved for public release; distribution unlimited
2b. DECLASSIFICATION/DOWNGRADING SCHEDULE	
4. PERFORMING ORGANIZATION REPORT NUMBER(S) AFIT/GE/ENG/84D-23	5. MONITORING ORGANIZATION REPORT NUMBER(S)
6a. NAME OF PERFORMING ORGANIZATION School of Engineering 6b. OFFICE SYMBOL (*If applicable*) AFIT/ENG	7a. NAME OF MONITORING ORGANIZATION
6c. ADDRESS (*City, State and ZIP Code*) Air Force Institute of Technology Wright-Patterson AFB, Ohio 45433	7b. ADDRESS (*City, State and ZIP Code*)
8a. NAME OF FUNDING/SPONSORING ORGANIZATION 8b. OFFICE SYMBOL (*If applicable*)	9. PROCUREMENT INSTRUMENT IDENTIFICATION NUMBER
8c. ADDRESS (*City, State and ZIP Code*)	10. SOURCE OF FUNDING NOS. PROGRAM ELEMENT NO. / PROJECT NO. / TASK NO. / WORK UNIT NO.
11. TITLE (*Include Security Classification*) See Box 19	
12. PERSONAL AUTHOR(S) Paul J. De Rego, B.S., 1st Lt, USAF	
13a. TYPE OF REPORT MS Thesis 13b. TIME COVERED FROM _____ TO _____	14. DATE OF REPORT (*Yr., Mo., Day*) 1984 December 15. PAGE COUNT 151
16. SUPPLEMENTARY NOTATION	

17. COSATI CODES		
FIELD	GROUP	SUB. GR.
06	02	

18. SUBJECT TERMS (*Continue on reverse if necessary and identify by block number*)

Magnetoencephalograms, Dipoles, Electromagnetic Fields, Cerebral Cortex, Models

19. ABSTRACT (*Continue on reverse if necessary and identify by block number*)

Title: A MULTIPLE MODEL OF THE OBSERVED CEREBRAL CORTEX MAGNETIC FIELD

Approved for public release: IAW AFR 190-17

Thesis Chairman: Matthew Kabrisky
Assistant for Advanced Research and
Associate Professor of Electrical Engineering

20. DISTRIBUTION/AVAILABILITY OF ABSTRACT UNCLASSIFIED/UNLIMITED ☒ SAME AS RPT. ☐ DTIC USERS ☐	21. ABSTRACT SECURITY CLASSIFICATION UNCLASSIFIED
22a. NAME OF RESPONSIBLE INDIVIDUAL Matthew Kabrisky	22b. TELEPHONE NUMBER (*Include Area Code*) 513-255-5276 22c. OFFICE SYMBOL AFIT/ENG

DD FORM 1473, 83 APR EDITION OF 1 JAN 73 IS OBSOLETE.

UNCLASSIFIED

SECURITY CLASSIFICATION OF THIS PAGE

A Multipole model of magnetic field sources in the cerebral cortex was developed as an expansion of Grynszpan's single dipole model. Both computer simulation and actual conducting sphere experiments were used to generate field plots in five separate dipole configurations. These include one case of a single dipole, three cases of three dipoles on a single radial, and one case of two dipoles on independent radials.

The results show that dipoles oriented on a single radial do not produce multiple flux peaks, but rather a twisted version of the single dipole field. Sufficiently distant dipoles on independent radials, however, do produce multiple peaks. The largest field distortions occurred when nonconducting masses were in close proximity to the active dipoles.

END

FILMED

5-85

DTIC